New Macrocyclic Reagents for Heavy Metals

Thesis submitted by

Ioana Monica Vasilescu B.Sc. (Hons) M.Sc.

January 2010

For the Degree of Doctor of Philosophy

School of Pharmacy and Molecular Sciences

James Cook University

Townsville, Queensland, Australia

Statement of Access

I, the undersigned, the author of this thesis, understand that James Cook University will make this work available for use within the University Library and, *via* the Australian Digital Theses network, for use elsewhere.

I understand that, as an unpublished work, a thesis has significant protection under the Copyright Act and all users consulting this thesis will have to sign the following statement:

> "In consulting this thesis I agree not to copy or closely paraphrase it in whole or in part without the written consent of the author, and to make proper written acknowledgement for any assistance which I have obtained from it."

Beyond this, I do not wish to place any further restriction on access to this work.

_____

Ioana M. Vasilescu

January 2010

Statement of Sources

I declare that this thesis is my own work and has not been submitted in any form for another degree or diploma at any university or other institution of tertiary education. Information derived from the published or unpublished work of others has been acknowledged in the text and a list of references is given.

_____

Ioana M. Vasilescu

January 2010

FOR

FATHER

Statement of Contribution of Others

The work reported in this thesis was conducted under the supervision of Prof. George V. Meehan (School of Pharmacy and Molecular Sciences at James Cook University) and Prof. Leonard F. Lindoy (School of Chemistry at the University of Sydney).

Dr. Ken R. Adam (School of Pharmacy and Molecular Sciences at James Cook University) is acknowledged for expert advice and supervision with respect to the computer modeling study presented in this thesis.

Dr. Anthony J. Leong and Dr. Feng Li assisted with the thermodynamic studies.

A/Prof. Bruce F. Bowden (School of Pharmacy and Molecular Sciences at James Cook University) provided training to the candidate on the use of the nuclear magnetic resonance instruments and their software as well as assistance with the interpretation of a number of spectra.

X-ray crystallography was in the most part conducted by Dr. Jack Clegg (School of Chemistry at the University of Sydney). Other contributors to X-ray crystallography include Dr. Brian J. McCool (School of Pharmacy and Molecular Sciences at James Cook University).

Dr. David Bourne at the Defence Science Technology Organisation (DSTO) Melbourne collected the high resolution electrospray mass spectra for many samples reported in this thesis. Other contributors to mass spectrometry results included Mr Rick Willis at the Australian Institute of Marine Sciences (AIMS).

Acknowledgements

I would like to extend a very special thank you to my supervisors Prof. G. V. Meehan and Prof. L. F. Lindoy for their guidance and enthusiastic support over the past years.

Thanks are also due to Prof. F. R. Keene as Head of Department for allowing this work to be carried out and also to the past Head of School A/Prof. M. J. Ridd for his support.

I would like to extend a very special thank you to Dr. David Bourne (DSTO) for his valuable contribution to the high resolution mass spectrometry results presented in this thesis.

Thanks are also due to my colleagues in the Chemistry Department: Dr. K. R. Adam, Dr B. McCool, Dr. M. Davies and Dr. C. Glasson for helpful discussions.

A special thank you goes to all the technical and office staff in the Chemistry Department and also to Mr. D. Mylrea for his help with IT support.

Finally, but certainly not least, thanks are due to my family and friends for their support and encouragement throughout the course of this study.

Abstract

A series of potentially pentadentate, unsymmetrical, mixed donor systems of type **I**, based on the corresponding 'symmetrical' macrocycles synthesised over many years in the author's laboratory, have been synthesised during the course of this project. Chapter 1 includes a review of these latter ligands along with aspects of their metal ion chemistry towards Co(II), Ni(II), Cu(II), Zn(II), Cd(II), Ag(I) and Pb(II) and serves as a background for the author's (related) results presented in subsequent chapters of the thesis.

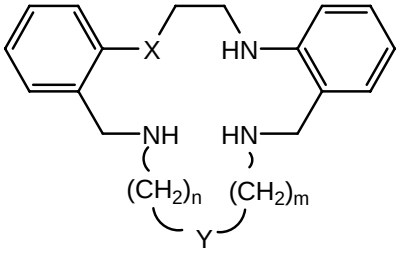

X = S or O

Y = NH, S or O

n = 2 or 3

m = 2 or 3

I

The synthesis of the new unsymmetrical macrocycles involved, in each case, the Schiff-base condensation between the appropriate linear di- or tri-amine and unsymmetrical dialdehyde precursors, followed by *in situ* reduction of the resulting diimine. The preparation of the unsymmetrical dialdehyde precursors is also described. The extensive organic ligand synthetic studies resulted in successful isolation and characterisation of a range of 17- and 18-membered, unsymmetrical, mixed-donor rings which are described in Chapter 2.

Selected crystalline Ni(II), Cu(II), Cd(II) and Ag(I) complexes of the new 17-membered mixed donor macrocycles suitable for X-ray diffraction analysis were isolated: [Ni**L**Cl]$^{-}$Cl·3H_2O (**L** = **138**), [Ni**L**Cl]Cl·0.125CH_3CN·3.75H_2O (**L** = **142**), [Cu**L**Cl_2]·CH_3CN (**L** = **138**), [Cu**L**Cl_2]·CH_3CN (**L** = **142**), [Cu**L**Cl]Cl·2.375H_2O (**L** = **141**), [Cd**L**$(NO_3)_2$]·CH_3OH (**L** = **138**), [Cd**L**(NO_3)] (NO_3)·CH_3CH_2OH (**L** = **132**), [Ag**L**]PF_6 (**L** = **132**) and [Ag**L**]PF_6 (**L** = **141**) as well as the metal-free diprotonated nitrate salt (**L**H_2)$(NO_3)_2$ (**L** = **137**). The

results of the corresponding X-ray studies, presented in Chapter 3, revealed that the Ni(II) species display distorted octahedral geometries, with the respective macrocycles acting as pentadentate ligands. Cu(II) yields both five and six coordinate complexes in which the respective macrocycles act as both tridentate and pentadentate ligands; the coordination geometries vary from close to square pyramidal to distorted square pyramidal and distorted octahedral - largely reflecting the different affinities of the macrocyclic donors for this metal ion in each case. In the Cd(II) complexes the metal is seven-coordinate and binds to all the ligand donors with nitrate groups completing the coordination sphere. Ag(I) yielded complexes of two different structural types: in the first of these, the coordination geometry around silver can be described as close to square pyramidal, with the central metal coordinating to all five donors of the macrocyclic ring, while in the second, a one-dimensional coordination polymer was obtained.

The thermodynamic stabilities of the above unsymmetrical 17-membered rings were investigated with respect to their Co(II), Ni(II), Cu(II), Zn(II), Cd(II), Ag(I) and Pb(II) complexation in 95 percent methanol. The stabilities for these systems were found to follow the Irving-Williams order. The magnitude of the log *K* values obtained is strongly influenced by the number of nitrogen donors present in the macrocyclic donor set. The results confirmed previous observations that metal ion recognition can be ‘tuned’ by changing both the available donor set and the spatial arrangement of the respective donors for a given donor set in the macrocyclic backbone. Thus, for example, ligand **I** (X = Y = S, n = m = 2) showed very good discrimination for Ag(I) over Pb(II) relative to the other systems investigated, with a difference between the log *K* values of the respective complexes of 7.5.

The development of a simple procedure for modeling the metal complex stability constants of Co(II), Ni(II), Cu(II), Zn(II), Cd(II), Ag(I) and Pb(II) complexes of dibenzo-substituted, 17-membered mixed-donor macrocycles of both symmetrical and unsymmetrical derivatives of the present type is described in Chapter 4. In general, quite good agreement with the experimentally determined log *K* values was obtained across the ligand series investigated. In addition, the results provide a means for predicting log *K*

values for complexes of other systems of type **I** (n = m = 2) for which experimental data is not yet available.

Finally, previously documented ligand design strategies for achieving Ag(I) discrimination were successfully applied to the design and synthesis of a new N-benzylated S_3N_2-donor macrocycle, which was demonstrated to show enhanced selectivity for Ag(I) over Co(II), Ni(II), Cu(II), Zn(II), Cd(II) and Pb(II) in both log *K* and bulk membrane transport studies. The silver complex is at least 10^5 more stable than any of the remaining complexes investigated. Suitable crystals for X-ray diffraction analysis were isolated for this complex. The structure of the complex cation (see **II)** shows that all macrocyclic donors coordinate to the Ag(I) centre, with the latter adopting a distorted square pyramidal geometry.

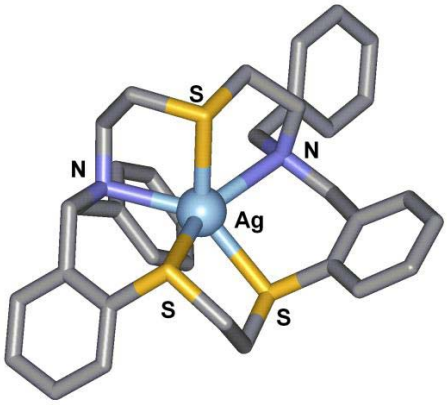

II

The current study demonstrates the structural diversity and metal ion discrimination behaviour that is possible from the use of potentially pentadentate ligands of general type **I** containing different donor set combinations – with different metal ion affinities – when reacted with transition and post-transition ions of the type mentioned above.

Table of Contents

Chapter 1 – Introduction

Chapter 2 – Synthesis of macrocyclic ligands

Chapter 3 – Interaction of the new potentially pentadentate macrocyclic ligands with selected transition and post-transition metal ions

Chapter 5 – Rational ligand design for metal ion recognition. Synthesis of an N-benzylated S_3N_2-donor macrocycle for enhanced Ag(I) discrimination

Appendix

Chapter 1 – Introduction

1. Background and historical perspective

1.1 Some preliminaries

Macrocycles can broadly be defined as polydentate ligands containing a minimum of three donor atoms incorporated in or, in some cases attached to, a cyclic backbone consisting of at least nine atoms. Fundamental biological processes such as electron transfer reactions, oxygen transport and storage, oxygen reduction, oxygenation of organic substrates and reduction of peroxides depend on metal ion complexes of tetrapyrrolic macrocycles.[1] Early interest in the chemistry of metal-binding macrocycles can be, in part, attributed to the recognition that macrocyclic ligand complexes play a central role in such crucial processes.[2-5]

The first *synthetic* macrocyclic systems to be investigated were the phthalocyanines. Structurally related to the natural porphyrins, the blue copper phthalocyanine pigment (see later) contained the first new chromophore of commercial importance developed in the first quarter of the 20th century.[6] Subsequently in the 1960s, the work of Curtis,[7, 8] Busch[9] and Jäger[10] on polyazamacrocycles and later Pedersen's first crown ethers[11] provided the cornerstones of modern macrocyclic chemistry.[12]

The study of these early synthetic macrocyclic ligands revealed principles that have broad areas of application, from catalysis to medicine, and provided a basis for rationalising some of the behaviour of metal ions in heme proteins and metal-containing enzymes. These studies also led to the development of metal complexes tailored for use as models for biochemical processes, the development of new families of synthetic macrocycles and of new metal compounds of interest in their own right that revealed the unusual properties frequently associated with cyclic ligand complexes.

1.2 Natural macrocycles

Some of the best known natural macrocyclic ligands are the tetrapyrroles such as the porphyrin ring **1** of the iron-containing heme proteins. The study of porphyrin chemistry

can be said to have started more than a century ago, with Hoppe-Seyler's isolation in 1880 of hematoporphyrin from hemin **2** (a product of hemoglobin denaturation).[13]

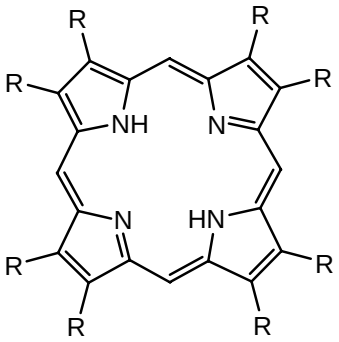

1

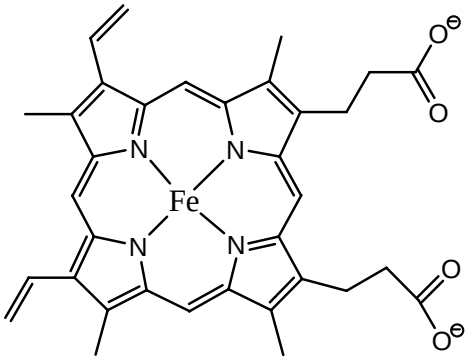

2

This ring system occurs in hemoglobin, myoglobin, catalase, most peroxidases, the b-type cytochromes and the cytochromes P-450.[1] The versatility of the heme centre is best illustrated by the latter group since they are involved in catalysing a wide variety of chemical reactions such as hydroxylation, epoxidation, dehydrogenation, sulphoxydation, dehalogenation and N-, S-, and O-dealkylation.[1, 14] Following loss of the pyrrole protons, porphyrins can quite readily form complexes with a variety of metal ions. While the conjugated macrocyclic nature of the ligand results in the nitrogen to centre of the ring distance being to some degree 'fixed', the molecule is not completely rigid and the effect is to limit the degree that the ring expands or contracts to accommodate the metal ion.[4, 15] Thus, the metal-nitrogen bond distances for the metalloporphyrins do undergo modest changes as the size of the metal ion changes and can vary, for example, from 2.10 Å in the ferric porphyrins to 1.95 Å in the nickel porphyrins.

The magnesium-binding chlorin **3** is the fundamental chromophore of the chlorophylls. It differs from porphyrin in having one pyrrole ring reduced at the *β*-position.[3, 16] Naturally occurring chlorins contain a full complement of substituents at the *β*-pyrrolic positions of the macrocycle. Recent studies into the effects of substituents on the chlorin spectral properties have revealed a potential for a number of applications that range from light harvesting and artificial photosynthesis to photomedicine.[17, 18]

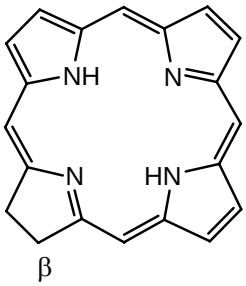

3

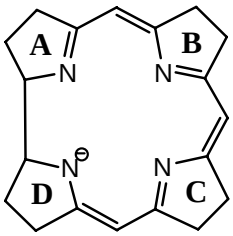

4

Coenzyme B12 (**Figure 1.1**)[19] contains the corrin ring **4** which incorporates a cobalt ion.[20, 21] The corrins differ from other tetrapyrroles in that the planarity of the ring is destroyed by the presence of a direct link between rings A and D. This also creates

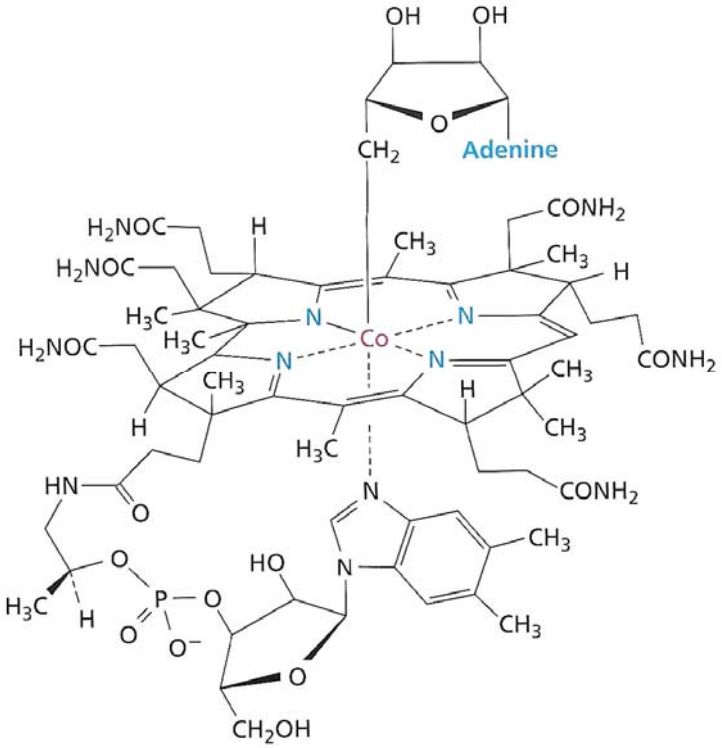

Figure 1.1 Coenzyme B_{12} – Adenosylcobalamin

a smaller central cavity for the metal.[20] Eschenmoser had postulated that 'self-assembly' of the A – D link may be a consequence of the relatively small ionic radius of the Co(III) ion.[22] The Co(III) is bound to the four nitrogens of the corrin ring and a nitrogen from the axial dimethylbenzimidazole ligand. The sixth ligand binds via a carbon atom making

B12 and its derivatives rare examples of naturally occurring bio-organometallic compounds.[23] The homolytic cleavage of the Co–C bond is the first step of all rearrangement reactions catalysed by the B12-dependent enzymes.[24]

The macrocyclic antibiotics of microbial origin such as valinomycin **5** represent another class of natural macrocycles. This category readily forms complexes with alkali metals and is capable of increasing the corresponding cation permeability of biological membranes; physiological processes such as the excitation of nerve membranes rely on such a phenomenon.[25] Valinomycin is a cyclic dodecadepsipeptide, containing 12 residues of alternating ester and peptide linkages, which selectively transports potassium

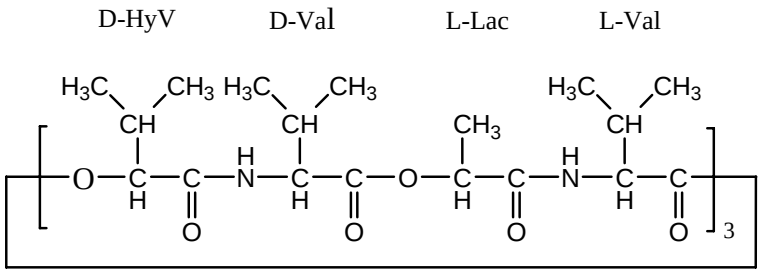

5

ions across membranes.[26] On complexation, the potassium ion is coordinated to the carbonyl oxygen of each of the six valine residues, with the structure being further stabilised by six intramolecular hydrogen bonds.[27] The methyl and isopropyl groups project outwards, giving the exterior of the complex a hydrophobic character, while the centre is hydrophilic. This aids the molecule to function as an ionophore. Valinomycin binds potassium more strongly than sodium, with the log *K* values in methanol being 4.90 and 0.67 respectively.[28] Such selectivity is significant given the physiological importance of these ions; mammalian cells typically have concentrations of K^+ in the 140 mM range within the cell and 5 – 10 mM outside it, while the Na^+ concentrations are 5 – 10 mM inside and 140 – 150 mM outside.[29]

The macrotetrolide antibiotics nonactin **6** and monactin **7** are 32-membered ring systems which incorporate four ether and four ester groups. They also bind alkali metals and the

kinetics of complex formation is remarkably fast: for example, the sodium complex of **6** has a rate of formation of 10^8 $M^{-1}sec^{-1}$ in methanol.[30]

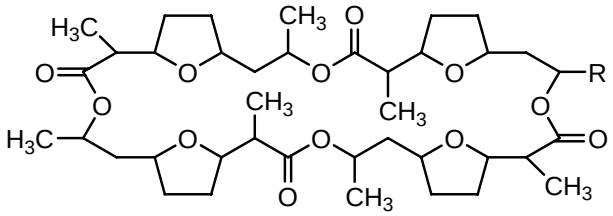

6 R = CH_3

7 R = CH_2CH_3

Once again, these ionophores preferentially bind potassium ions in the presence of sodium ions. The selectivity sequence for the macrotetrolides is $K^+ \geq Rb^+ > Cs^+ > Na^+$; in methanol, at 30 ˚C, the potassium complex of monactin exhibits a stability constant of 2.5 x 10^5 M^{-1} while the value for the sodium derivative is 1.1 x 10^3 M^{-1}.[30, 31] On coordination, the potassium ion is bound to four ether and four carbonyl oxygen atoms, with the conformation of the macrocycle backbone resembling the seam of a tennis ball.[32] The naturally occurring macrotetrolide homologues are derived by sequential substitution of ethyl groups for methyl groups on the macrocyclic backbone. These derivatives exhibit a wide range of activities. The differences in activity follow the differences in K^+ binding affinity. Increasing the alkyl substitution leads to a more rigid structure and lowers the entropy penalty for ion binding.[33, 34] Thus the homologue containing two ethyl groups has an association constant for its K^+ complex that is 7-fold greater than for the parent nonactin.[28, 34]

1.3 Synthetic macrocycles

As mentioned already, phthalocyanine **8** and its derivatives represent the first category of synthetic macrocycles to be developed.[6] Copper phthalocyanine and its substituted derivatives are used extensively as both blue and blue-green pigments and dyes and are remarkably stable towards heat as well as to the presence of acids and alkalis. Phthalocyanine incorporates four nitrogen donors in a similar manner to the porphyrins,

but the meso carbon atoms between the five-membered rings in the latter are replaced by nitrogen atoms in phthalocyanine and there are fused benzene rings on the pyrroles.

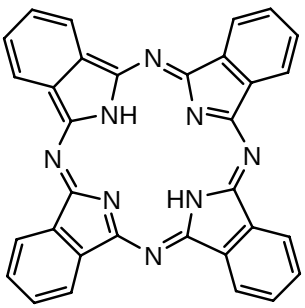

8

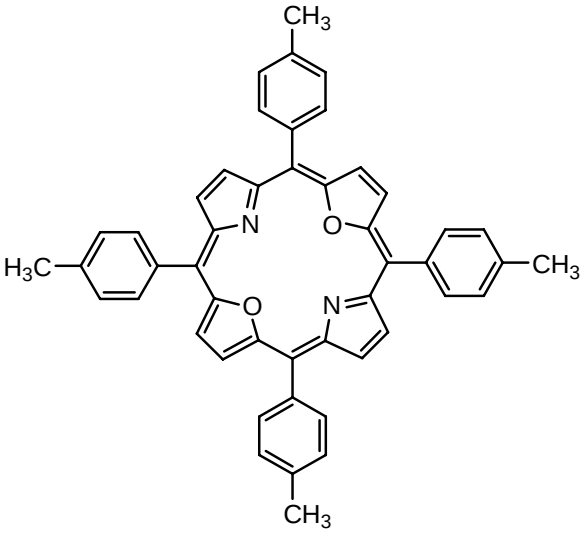

9

By the early 1960s, a large number of synthetic porphyrins and their complexes with a variety of metal ions had also appeared in the literature.[35-38] Later work included inner-core modified porphyrins where some of the nitrogens are replaced by other donor atoms. An early example of such a derivative, in which two nitrogens were replaced by oxygens, is compound **9** which was shown to yield a stable high-spin Ni(II) complex.[39]

Following the early work on phthalocyanines and porphyrins, as mentioned earlier, the study of structurally simpler polyazamacrocyclic systems was initiated by the pioneering work of Curtis,[7] Busch[9] and Jäger.[40] Thus, in 1962, Curtis reported an example of a synthetic macrocyclic tetradentate ligand, **10**, containing imine linkages, obtained from the reaction of acetone with the tris(ethylenediamine)nickel cation.[7, 41] The preparation of the macrocyclic complex was considered to be an example of a metal ion template reaction, given that the corresponding reaction of acetone with ethylenediamine produced tarry polymeric material. Curtis also noted that the macrocyclic ligand formed was stabilised by metal coordination since removal of the nickel ion produced a mixture of ethylenediamine and mesityl oxide under the conditions employed.[42]

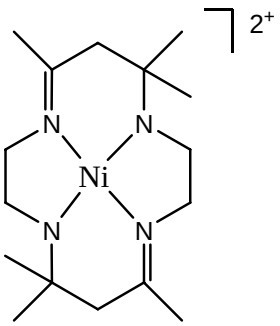

10

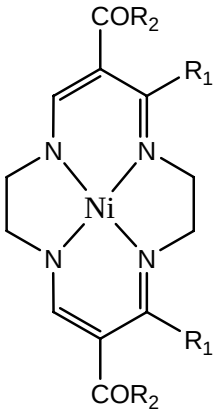

11

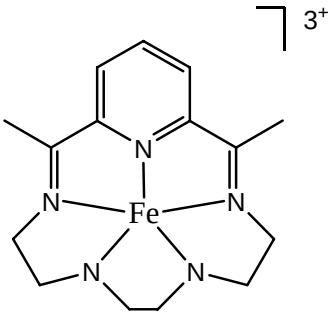

12

In turn, Jäger synthesised a series of analogous tetraaza macrocycles such as **11**[40] while other early workers in the area, Busch and Curry, reported the Fe(III) complex **12** containing a synthetic pentaaza macrocycle – the first example of a cyclic pentadentate ligand.[9]

In the late 1960's Pedersen synthesised a range of crown ethers of which **13** (dibenzo-18-crown-6) is a typical example.[11] These then highly novel compounds were shown to form stable complexes with alkali and alkaline earth metal ions.

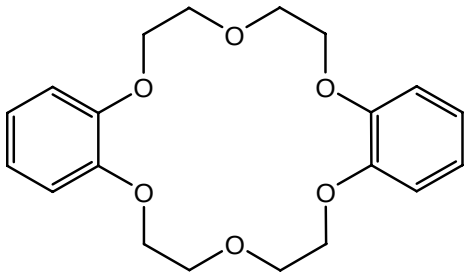

13

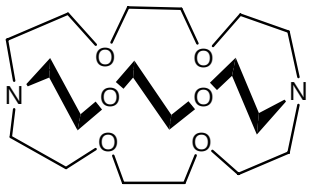

14

A further significant development came in 1969 with the development by Lehn and co-workers of a new class of compounds, the macrobicyclic cryptands, of which **14** is an example.[43] This three dimensional system is able to completely encapsulate a coordinated

metal ion. Complex formation demonstrated both enhanced specificity and stability towards individual metal ions.[44]

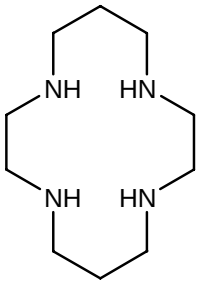

15

The above reports coupled with the development of new or improved synthetic procedures for further macrocyclic ligand types such as cyclam **15**,[45] resulted in rapidly increased interest in the metal ion chemistry of synthetic macrocycles. This was further fuelled by the widespread realisation that there is often a significant enhancement in stability for metal ion complexes of cyclic ligands compared with the corresponding complexes of their open chain analogues – the so-called *macrocyclic effect*.

1.4 The macrocyclic effect

Early studies directed toward elucidating the properties of macrocyclic complexes revealed that the ligand field strengths of a number of macrocyclic ligands appeared to be unusually high.[46, 47] In addition, synthetic and stereochemical studies suggested that many macrocyclic complexes are unusually inert towards dissociation of the ligands, even under strong acidic or alkaline conditions,[8] and display enhanced thermodynamic stability over the corresponding open-chain ligand complexes. In a pioneering study Cabbiness and Margerum proposed the existence of the 'macrocyclic effect'[48, 49] to explain the increased stability (by a factor of 10^7 in 6.1 M HCl) of the Cu(II) complex of **16** compared to the related complex of the open-chain tetramine **17**. This led to a number of studies aimed at understanding the nature of the macrocyclic effect.

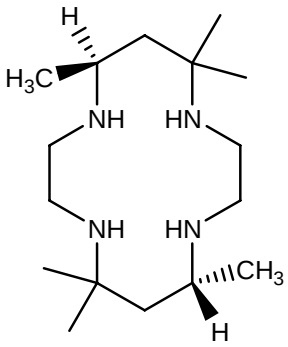

16

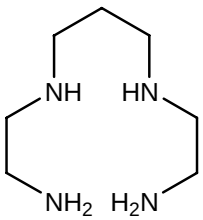

17

It is now clear that, in the simplest case, the thermodynamic stability constant (K) for a complex at equilibrium involving a given ligand (L) is related to the rates of complex formation and dissociation, as shown below, where k_f is the second order formation rate constant and k_d is the first order dissociation rate constant.

$$M + L \underset{k_d}{\overset{k_f}{\rightleftharpoons}} ML$$

$$K_{ML} = \frac{[ML]}{[M]\,[L]} = k_f/k_d$$

Comparison of the observed first-order dissociation rate constants of the Cu(II) complexes of **16** and **17** revealed large differences in the values for the two ligands, with the rate of dissociation of the macrocyclic complex of **16** being much slower than for the open-chain complex of **17**.[49] The higher K value for the complex of **16** was considerably more than could be rationalised from the simple presence of one additional chelate ring and hence the increased stability was considered to reflect the operation of the macrocyclic effect.

It needs to be noted that early studies into the thermodynamic origins of the macrocyclic effect, especially involving complexes of tetraaza ligands, were contradictory with regards to the relative importance of the entropy and enthalpy terms. For certain systems the additional stability was attributed either entirely to entropy factors[50, 51] or wholly to

enthalpy factors.[52] Subsequent investigations carried out on tetraaza macrocycles showed that both the entropic and enthalpic terms may contribute to the macrocyclic effect.[53-55] While generally the entropy term tends to be favourable (less rotational and translational freedom in cyclic ligands results in lower relative 'ordering' upon coordination), the enthalpy values can be quite variable and even unfavourable.[44, 56] In particular cases, a favourable contribution to the enthalpy term has been postulated to be associated with less ligand desolvation being necessary for formation of the macrocyclic complex but this in turn may be partially compensated by a less favourable entropic term.[53, 55]

The thermodynamic parameters relating to the formation of the high-spin Ni(II) complex of cyclam **15** and its open-chain analogue **17** clearly show (**Table 1.1**) that for this system the observed considerable macrocyclic effect is a reflection of both a favourable entropy term and a favourable enthalpy term.[56]

Table 1.1 Thermodynamic parameters illustrating the macrocyclic effect for the high-spin Ni(II) complex for the reaction:[a,b]

$[NiL_{non\text{-}cyclic}]^{2+} + L_{cyclic} \rightleftharpoons [NiL_{cyclic}]^{2+} + L_{non\text{-}cyclic}$

Ligand	ΔG/kJ mol^{-1}	ΔH/kJ mol^{-1}	$T\Delta S$/kJ mol^{-1}
17/**15**	-33.67	-20.5	13.2

[a]Where $\Delta G = \Delta H - T\Delta S$; [b]aqueous solution, 25 ˚C

Further insight into the nature of the macrocyclic effect was provided by studies involving macrocycles containing only thioether donor atoms. These ligands are not highly solvated and are free of protonation concerns, making it possible to examine directly any configurational contributions to the macrocyclic effect. In addition, the Cu(II) complexes are generally sufficiently weak to enable the values for both k_f and k_d to be obtained from direct measurements.[57, 58] In general, such complexes show a much

smaller macrocyclic effect compared to the tetraamine systems (where a 10^6-fold enhancement is sometimes observed).[59] For example, the Cu(II) complex of the S_4-macrocyclic analogue of cyclam is only about a hundred times more stable in water than the corresponding open-chain ligand complex; however, in methanol/water mixtures this difference is somewhat enhanced.[58]

1.5 Representative macrocyclic systems

1.5.1 Single ring macrocycles

While a range of examples of this ligand type has already been described in this chapter, further examples, with emphasis on systems that relate to the results presented in later chapters of this thesis, now follow.

1.5.1.1 Nitrogen donor systems

Nitrogen-containing macrocycles generally form quite stable complexes with transition and post-transition metal ions such as Co(II), Co(III), Ni(II), Cu(II), Zn(II), or Cd(II). A number of reviews acknowledge the large interest that has traditionally been shown in the metal ion chemistry of this ligand category.[60-64] It is not surprising that a very large number of studies have involved complexes of polyazamacrocycles since reliable procedures for their synthesis have long been established as well as methods for their modification, in particular N-substitution, have been well documented. Individual ligands of this type have been of particular interest with regard to their use in a number of applications.[64] These include as models that mimic metal ion–macrocycle reactions in a range of biological systems.[28]

The work of Richman and Atkins represented a major advance in the synthesis of a range of cyclic amines of medium to large ring size (3-6 nitrogen atoms and 12-18 membered rings) without requiring either high dilution or the presence of a template.[65] One member of this series, 1,4,8,11-tetraazacyclotetradecane, [14]aneN_4 (cyclam) **15**, has already been mentioned and has been the subject of many investigations over the past several decades. This 14-membered macrocycle provides an appropriately sized cavity for the planar

coordination of a range of 3*d* transition metals. It also forms a favourable symmetrical sequence of 5,6,5,6-chelate rings on coordination to a central metal.

For ligands with the same size macrocyclic cavities but a different sequence of chelate rings, as is the case in cyclam **15** and isocyclam **18**, the enthalpies of formation of the Cu(II) complexes have been shown to favour **15** with its symmetrical 5,6,5,6-sequence.[66] It has been suggested that in the case of **18**, where the two six-membered chelate rings are adjacent, steric repulsions may induce some distortion in the macrocyclic framework resulting in the displacement of the nitrogen donors from the planar coordination sites often preferred by Cu(II) and, as a consequence, the presence of weaker Cu–N interactions is expected to be reflected in less exothermic complexation of **18** relative to **15**.[67]

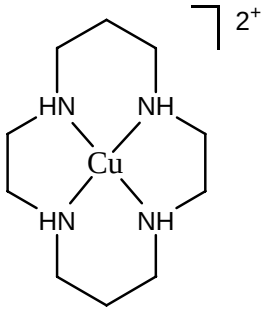

15

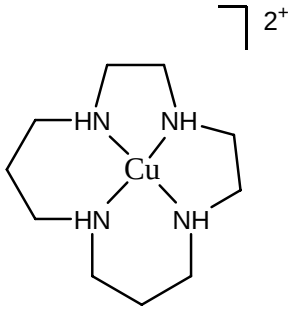

18

The various preferred geometric requirements of different metal ions will also influence the above situation.[68] The match of the macrocyclic cavity for the diameter of the metal ion is clearly important and more favourable formation enthalpies are expected when the match is good.[44, 69] Nevertheless, it is noted that the most stable conformation for a macrocyclic metal complex is not necessarily the one in which the metal ion occupies the centre of the cavity.[70]

Many of the earlier studies were motivated by interest in finding ways to control the thermodynamic stabilities of metal complexes through macrocyclic ring size variation in order that metal-ion specificity for particular transition ions might be achieved. For

example, the study of the stability of Zn(II) and Cd(II) complexes with the 14 – 16-membered, dibenzo-substituted, N_4-donor macrocycles **19** – **21** revealed (**Figure 1.2)** that the 15-membered macrocycle displays marked recognition/discrimination for Zn(II) in the presence of Cd(II).[71] Such discrimination, termed 'dislocation discrimination',[72] occurs along a series of closely related macrocyclic ligands when an abrupt change in coordination behaviour (the dislocation) is induced towards one metal ion relative to another, for example, as the ring size is progressively altered. At the point of dislocation, adjacent complexes in the series may show major differences in their coordination geometries and/or their ligand conformations.[73] As a consequence, enhanced discrimination between metal ions may result.

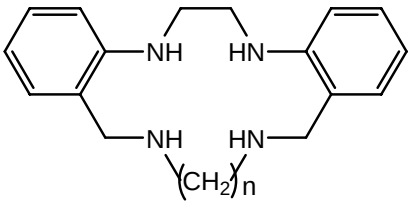

19 n = 2

20 n = 3

21 n = 4

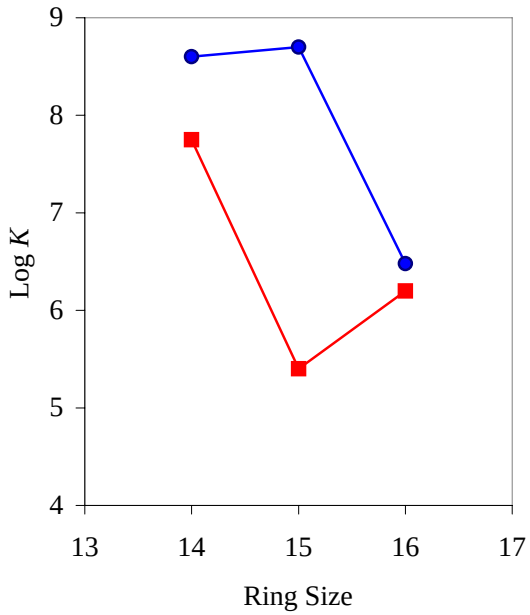

Figure 1.2 Log *K* values for formation of Zn(II) and Cd(II) complexes with **19** – **21**; ● Zn(II), ■ Cd(II).

It is noted that this type of discrimination does not necessarily depend on the match of the radius of the metal ion to the available macrocyclic ligand cavity.[74] Rather, such behaviour may be a consequence of steric strain differences between individual complexes along the respective complex series.

Dioxocyclam **22,** in which two of the four amine groups are replaced by two amide groups, has also been extensively studied and demonstrated to form a range of stable complexes with both transition and post-transition metal ions.[75-77] A new family of related ring systems, the chiral dioxocyclams of type **23**, has also been reported.[78] These enantiomerically pure derivatives form stable complexes with Cu(II) and preliminary experiments reveal that they act as catalysts for the cyclopropanation of olefins.

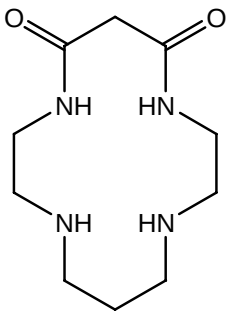

22

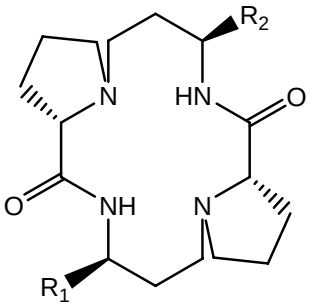

23

In a recent study Cu(II) has also been used as a template in the formation of new examples of mixed amine/imine macrocycles of type **24**. Once again the complexes are resistant to demetallation by acid (but are oxidized by nitric acid and slowly degraded in alkaline solution).[79]

The 21-membered ring macrocycle **25** incorporating a rigid phenanthroline moiety has been demonstrated to exhibit somewhat unusual binding and spectral properties.[80] This ligand forms 1:1 complexes at low pH (0.4 – 2.0) while at pH values greater than 2.0 a 2:1 metal ion:macrocycle complex prevails.[81] Both the 1:1 and 2:1 Cu(II) complexes are stable at relatively high acidities.

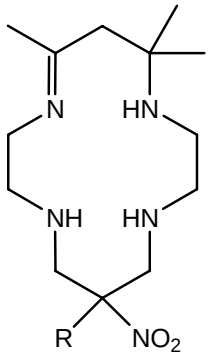

24

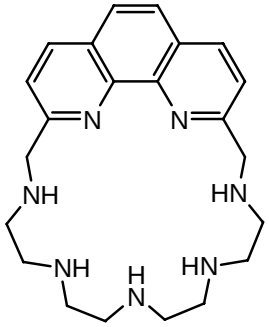

25

1.5.1.2 Oxygen donor systems

Oxygen donor macrocycles are best exemplified by the crown ethers. These ligands preferentially form stable complexes with alkali and alkaline-earth cations although a wide range of other metal complexes are also known.[11] Although literature references to cyclic polyethers predate Pedersen's work, none mentioned the formation of stable complexes with salts of the alkali and alkaline earth elements.[11] In his initial publication, Pedersen reported a range of new 'crowns', ranging from 9- to 60-membered rings incorporating between 3 and 20 oxygen atoms (for example, dicyclohexyl-30-crown-10 **26**).[11]

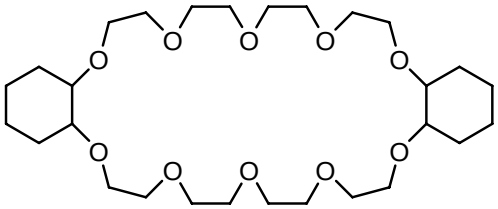

26

Crown ethers of type **27** incorporating a fluorescent chromophore such as xanthone have also been synthesised for potential use in determining the binding coefficients of sodium, potassium and caesium via spectrofluorimetric (and conductimetric) methods.[82]

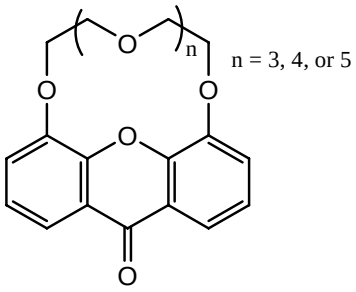

27

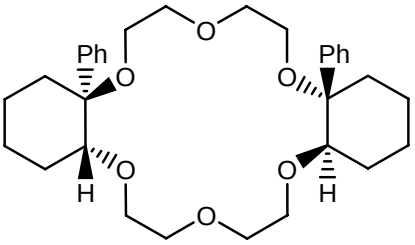

28

Cram and coworkers have reported a number of optically active crown ethers.[83, 84] Such compounds have potential for separating suitable organic enantiomers and studies of this type increasingly became an important part of the host – guest chemistry area. For example, chiral crown ethers such as **28** were shown to recognise neutral chiral amines.[85] For this system it was expected that the cyclohexane moiety incorporated in the 18-crown-6 framework would reduce conformational flexibility of the crown ether, while the bulky phenyl groups, which extend perpendicularly above and below the face of the crown ring, might act as a chiral barrier and improve enantiomer recognition ability in particular instances.

1.5.1.3 Sulfur donor systems

Macrocycles containing sulfur atoms coordinate well to soft metal ions [such as Ag(I), Cu(I), Pd(II), or Hg(II)] which tend to be large and often less strongly solvated. Complexes with a number of borderline metals such as Co(II) and Cu(II) are also well known.[86, 87] Ligands of this type also exhibit a number of properties which may influence the study of complex formation in solution: complexation is not complicated by competing protonation equilibria (as occurs with amine systems), the uncomplexed macrocycles tend to have limited solubility in water and many transition metal complexes of such ligands absorb strongly in the visible region, facilitating spectrophotometric monitoring.[88]

An early crystal structure of [14]aneS_4 revealed that the free ligand exists in the exodentate conformation illustrated by **29**, with the lone pairs of the four sulfur atoms

pointing outward from the macrocyclic cavity.[89] However, in the corresponding Cu(II) and Ni(II) complexes the macrocycle converts to an endodentate configuration (see **30)**

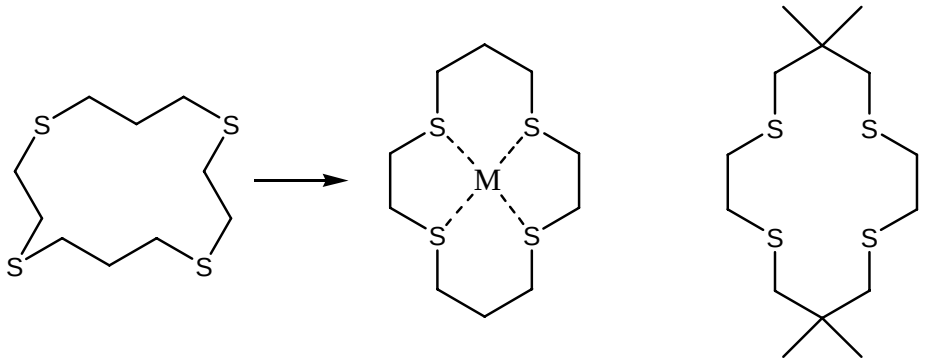

29 **30** **31**

which necessitates a complete conformational rearrangement to turn the donor atoms 'right side in'. This process costs energy, explaining why complexes of [14]aneS_4 tend to show only a small macrocyclic effect.[90] The exodentate orientation of the donors in free [14]aneS_4 contrasts with the more commonly seen endodentate conformation that occurs in related oxa and aza macrocycles. It has been suggested that on complexation, it is the major conformational reorganisation during second bond formation in the case of [14]aneS_4 (**29**) that will lead to a reduction in the complexation rate,[89] with further coordination of the remaining donors being expected to be little affected. This observation is in agreement with earlier work on the macrocyclic effect for Cu(II) complexes of cyclic tetrathiaethers which supported second-bond formation as the rate-determining step.[57] Addition of gem-dimethyl groups to the central carbon of the propylene segments in **29** causes all sulfur atoms to adopt endodentate configurations as shown in **31,** resulting in this species exhibiting enhanced metal ion binding.[91]

A series of substituted derivatives of [14]aneS_4 has been prepared in order to examine the influence of backbone substituents on the coordination properties of ring systems of this type.[92-94] The two-carbon bridges were replaced by 1,2-benzene or *cis*- or *trans*-1,2-cyclohexane rings. The resulting stability constants (in 80% methanol) with Cu(II) were enhanced by approximately 10 to 10^4 times relative to the values obtained using the

unsubstituted (parent) ligand. The Cu(II) complex of *syn-cis,cis*-dicyclohexyl-[14]aneS_4 **32** has the highest stability constant while the stability constant for the *anti-cis,cis* analogue **33** is 10^3-fold smaller. This was in part attributed to the different orientation of the electron lone pairs on the sulfur donor atoms in these two complexes.[92]

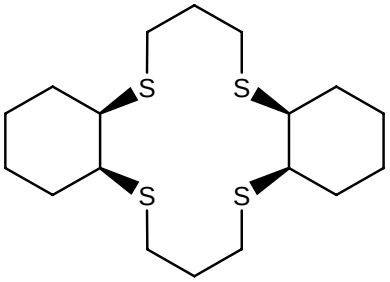

32

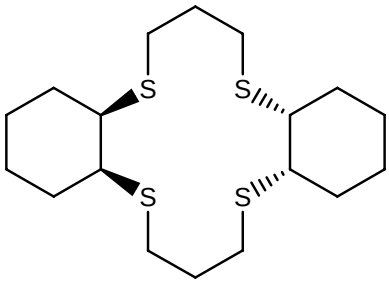

33

In contrast, the incorporation of a single benzo group into the ligand structure (as shown in **34**) causes a decrease in the stability of the Cu(II) complex of approximately 5 orders of magnitude relative to the corresponding monocyclohexyl derivative, presumably, at least in part, reflecting the negative inductive effect of the benzene ring upon the coordinating ability of the sulfur donor atoms. Although it was not possible to obtain quantitative data for **35**, the presence of a second benzo group appeared to inhibit complex formation even further.[92]

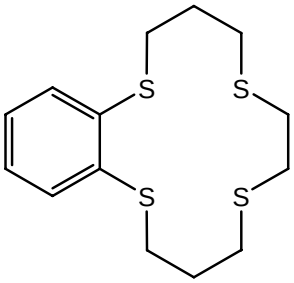

34

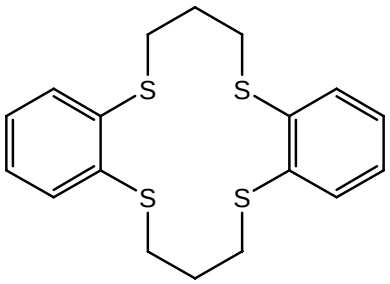

35

More recently, a related series of macrocyclic ligands has been reported in which, for the first time, 1,2-cyclopentane groups were systematically substituted for both two-carbon bridges in [14]aneS_4.[95] The Cu(II) complex of the *syn-cis,cis* ligand **36** exhibited (in 80% methanol) the largest k_f and smallest k_d values of all the cyclopentane substituted ligands

investigated. This behaviour was explained in relation to the crystal structure of the free ligand which shows that the lone-pair electrons for all the sulfur atoms tend to be oriented out of the macrocyclic cavity and toward the same side of the plane through the macrocyclic ring. The greater rigidity of the cyclopentane rings was reflected in a general decrease in the stability constants relative to values for the corresponding 1,2-cyclohexane substituted ligands.

Thiophene, (a poor coordinating group) has also been incorporated into macrocycle rings (such as **37**) in an attempt to induce endodentate coordination behaviour towards Cu(I); the X-ray structure of the product showed that the thiophene group does not bind to this metal ion in the solid state structure.[96]

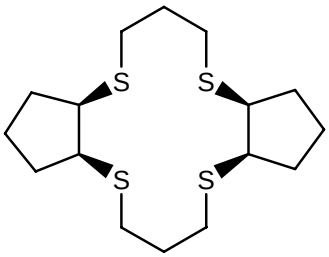

36

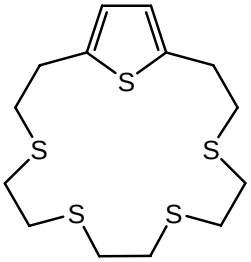

37

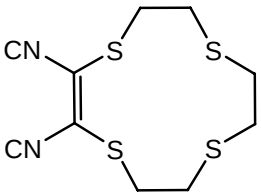

38

Twelve-membered S_4-donor macrocycles are too small to completely accommodate a transition or post-transition metal ion in their macrocyclic cavities and recent work aimed at preorganisation of these ligands for sandwich complexation has involved the incorporation of a rigid maleonitrile unit into the ligand backbone.[97] The resulting macrocycle **38** forms a 2:1 complex with Ag(I); this was both the first reported sandwich complex of a tetrathiacrown ether and the first complex with an octa(thioether) coordination sphere.

1.5.1.4 Other donor systems

Relative to the ligand categories so far discussed, a much lower number of polyphospha- and polyarsa-containing macrocycles have been reported.[98, 99] On complex formation, arsenic ligands act as weaker σ-donors and π-acceptors than their corresponding

phosphine derivatives. Further, the stereochemically active lone pair of the trigonal pyramidal arsenic atom can act as a site for additional structural functionalisation.[100] A more recent study describes the synthesis of the arsenic-containing macrocycle **39**, via a lithium template.[101] The lithium complex displays a long arsenic to lithium bond of 3.16 Å. Reaction of **39** with yttrium chloride through a metathesis type procedure, produced the first yttrium complex reported to contain a Y–As bond.[101]

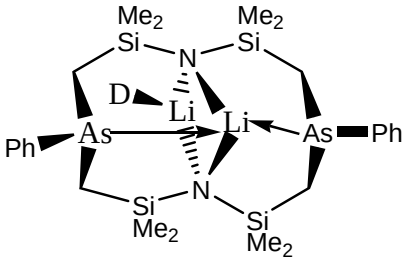

D = 1,4-dioxane

39

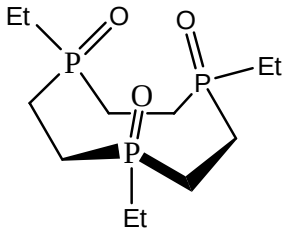

40

The smaller number of phosphorus macrocycles can, in part, be attributed to the lack of appropriate precursors for cyclisation, as well as synthetic difficulties arising from the air-sensitivity of many tervalent phosphorus species.[102] Fe(II) was used as a template to synthesise 1,4,7-triphosphacyclononane [12]aneP_3 derivatives such as the tris-phosphinoxide **40**.[102]

Examples of selenium- and tellurium-donor macrocycles include **41** and **42** respectively.[103, 104]

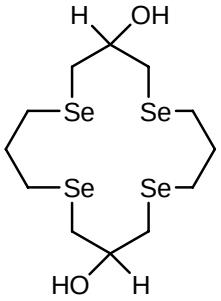

41

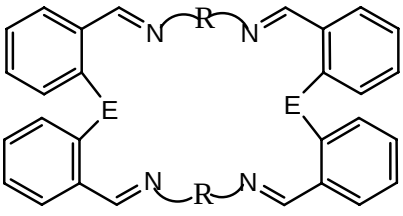

E = Se or Te

42

Generally, this group of macrocycles shows particular affinity for transition as well as other heavy metal ions; however, investigations using such ligand systems have tended to be somewhat restricted by the lack of convenient synthetic methods.[55]

A series of unsaturated selenium analogues of crown ether compounds with varying ring sizes was reported in 2005.[105] Silver ion complexation studies for these unsaturated derivatives have been carried out. Thus, studies involving ligands of type **43** showed the formation of 1:1 complexes at low metal ion concentrations. However, at higher concentrations, additional complexation occurs for the 7- and 8-donor atom rings with a 2:1 Ag^{+}/macrocycle ratio being observed. At the time of this study no other unsaturated selenacrown ethers containing carbon-carbon double bonds had been previously reported.[105]

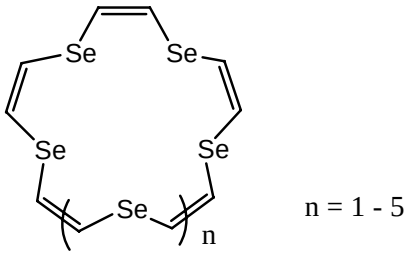

43

1.5.1.5 Mixed N, S and/or O donor systems

Early work involving crown ethers showed that the selectivity towards different alkali metal cations varied with the crown ether ring size with, at least for the smaller rings, the most favourable binding occurring when the size of the cation matched the hole size of the macrocyclic cavity.[106] For sodium, potassium and caesium the optimum ring sizes for maximum binding were found to be 15 – 18, 18 and 18 – 21 respectively, depending on the particular crown investigated.

The solution behaviour of the Ni(II) complexes with the 12- to 16-membered unsubstituted tetra-aza macrocycles revealed that the most exothermic complexation occurs with the 14-membered cyclam ring (**15**) and this ring was thus proposed to

provide the best fit for this ion.[107] However, there are limitations associated with the 'ion in the hole' concept of metal-ion discrimination. For example, as the number of ring atoms increases so does the conformational flexibility of the macrocycle and defining the cavity diameter unambiguously becomes more difficult.[28, 44] Hole-size effects will tend to be more dominant when the macrocyclic system involved is fairly rigid.[44] In this respect, the introduction of unsaturation can be helpful in reducing the number of available conformations.[55]

The advantage of combining donor atoms with different bonding preferences in a given ligand framework has often resulted in complexes exhibiting less common coordination behaviour, including the observation of new metal ion selectivity.[55] Substitution of oxygen by nitrogen in crown ethers such as 18-crown-6 and dibenzo-18-crown-6 results in lower affinity for potassium compared to the parent macrocycle but increased *K* values for Ag(I) complexation. Substituting sulfur for oxygen in crown ethers also induces major changes in the resulting cation-ligand affinities; in general, the stabilities of Ag(I) and Hg(II) complexes are increased while those of harder metal ions such as K^+ or Pb(II) are reduced.[28]

In early studies, the Ni(II) binding properties of a series of related 14- to 17-membered macrocycles (**44** – **47**) incorporating O_2N_2-donor sets has been investigated.[108] The presence of the dibenzo groups is advantageous since such ligand systems display intermediate flexibility, resulting in a restricted number of possible conformations able to be adopted by the coordinated ligand.[109]

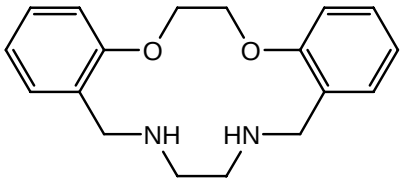

44

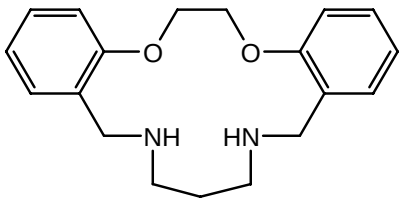

45

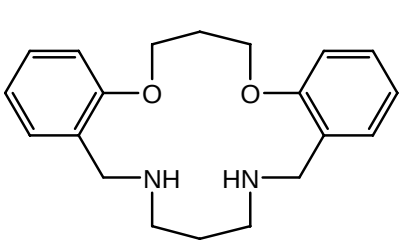

46

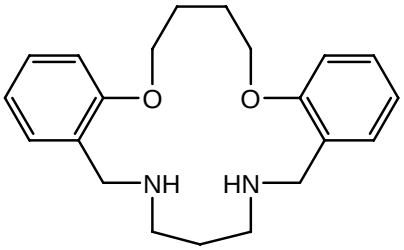

47

The log *K* variation illustrated in **Figure 1.3** shows that the stabilities of the nickel complexes follow the macrocyclic ring size sequence 14 < 15 < 16 > 17 (that is **44** < **45** < **46** > **47**).

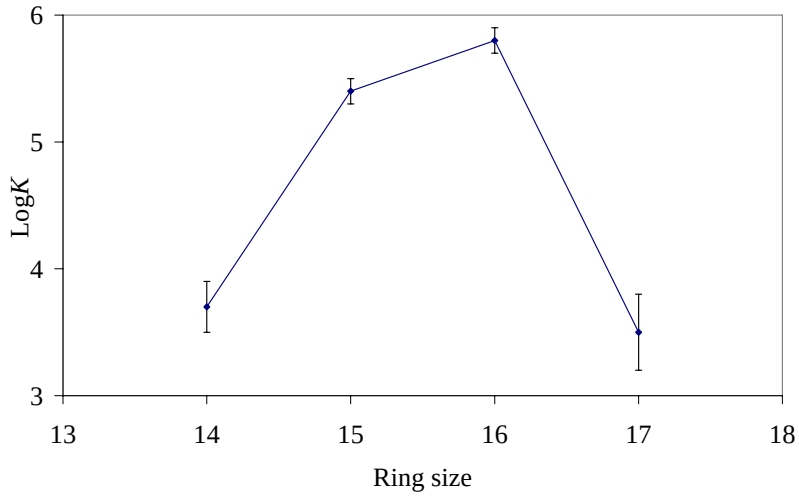

Figure 1.3 Log *K vs* ring size for Ni(II) complexes.

While hole size 'fit' is clearly important along this series, it needs to be noted that changes in the chelate ring sizes will also contribute to the observed behaviour. In particular, the formation of a 7-membered chelate ring in the complex of **47** will also likely contribute to the observed drop in stability for this complex. Likewise, a study of the dissociation kinetics involving the Ni(II) complexes of the above ligands demonstrated the dependence of the dissociation rate on the macrocyclic ring size. The labilities followed the ring size sequence 14 > 15 > 16 < 17 with the nickel complex of **46** (the 16-membered ring) showing the slowest rate.[110, 111] This clearly demonstrates how,

for a series of related Ni(II) complexes, small changes in macrocycle hole diameter (of the order of 0.05 – 0.1 Å between successive members of the 14- to 17-membered rings) can markedly influence their kinetic and thermodynamic properties.[108] Calculations based on X-ray structural data indicate that the fit of high-spin nickel for the 16-membered ring **46** is near ideal.[112]

More recently, a series of related N_2O_2 and N_2O_3 dibenzo-substituted macrocycles incorporating one or two xylyl groups has also been reported,[113] as well as examples of mixed oxygen-nitrogen macrocycles incorporating dibenzofuran **48** and pyrrole **49** units.[114] In 1:1 methanol:water **48** showed unusual selectivity for Cd(II) over Co(II), Ni(II) and Zn(II), but not Cu(II). The complexation behaviour as well as competitive membrane transport experiments using a series of pyrrole azacrown ethers such as **49** has been reported.[115] A marked preference for the selective transport of Pb(II) was observed.

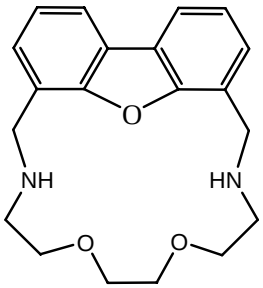

48

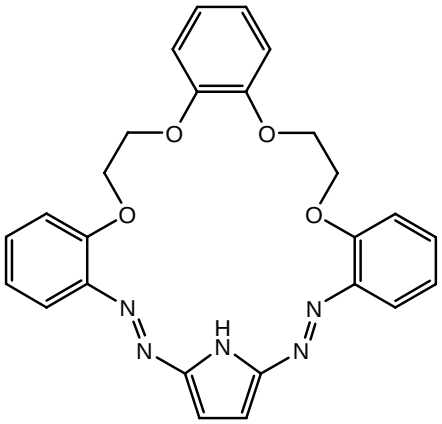

49

A 34-membered N_6O_4-donor macrocycle (**Figure 1.4**) was reported and investigated as potential solvent extractant for cation/anion binding studies.[116] Under appropriate pH conditions this ligand acts as both a metal ion and anion extractant. It was shown to be an especially efficient extractant towards Ag(I) (100% at pH 6.1 under the conditions employed) and Zn(II) (82% at pH 7.2).

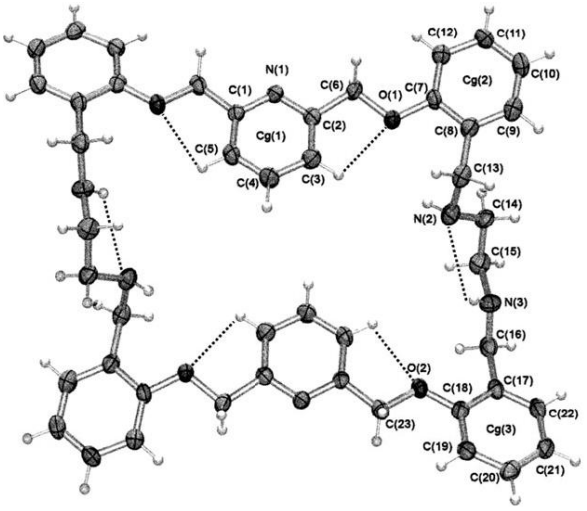

Figure 1.4 ORTEP plot of the N_6O_4-donor macrocycle. Dashed lines indicate intramolecular hydrogen bonds.

Ligands containing both nitrogen and sulfur donors typically exhibit a range of properties which, not surprisingly, often lie between those of the macrocyclic polythiaethers and the macrocyclic polyamines.[117] Early examples of aza-thioether macrocycles have been used for metal complexation studies and also for investigations into the thermodynamic origins of the macrocyclic effect. The stabilities of the Cu(II) complexes of the 16-membered N_2S_2 isomers **50** and **51**, which upon complexation give rise to all 6-membered chelate rings, do not vary much even though they incorporate *cis* and *trans* arrangements of the heteroatoms respectively.[118]

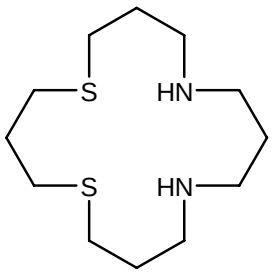

50

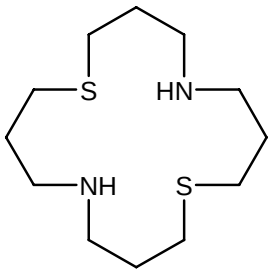

51

Comparison of thermodynamic data for the Cu(II) complexes of **52** ([14]aneN_2S_2) (the *cis* N_2S_2 analogue of cyclam) and the open-chain analogue **53** showed the presence of a large

macrocyclic effect ($\Delta \log K = 4.55$) that was mainly due to a favourable entropic term ($T\Delta S = 17.6$ kJmol^{-1}) and only partially due to the enthalpic term ($-\Delta H = 8.4$ kJmol^{-1}).[118]

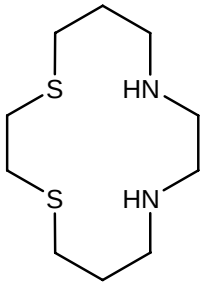

52

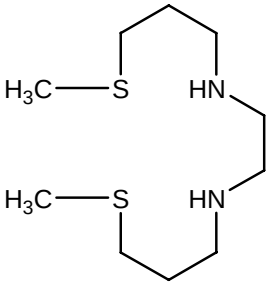

53

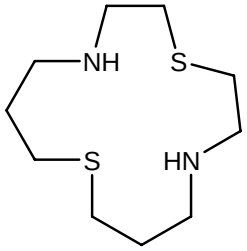

54

For the Ni(II) complexes of the 14-membered N_2S_2 ligands, the stability of the complex of the *cis* isomer **52** is higher than that of the unsymmetrical *trans* isomer **54**. The proposed rationale for this (and also for the corresponding Cu(II) case) is that the higher stability arises from the presence of strongly binding 5-membered chelate rings incorporating two nitrogens which are present in the metal complexes of **52** but absent in the complexes of **54**.[118]

In a later study of Cu(II) complexes involving the 14-membered N_2S_2 macrocyclic ligands **52**, **55** and **56** with three possible arrangements of the donor atoms (but identical sequence of chelate rings), it was established that complexes of both **55** ([14]aneNSSN) and **56** ([14]aneNSNS) dissociate quite rapidly in acid ($\geq$ 1.0 M) while the complex of **52** requires several weeks for similar dissociation to occur.[117]

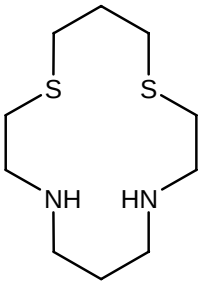

55

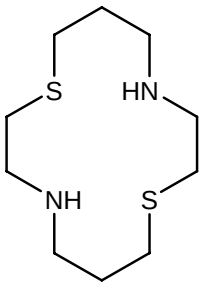

56

The large ring N_2S_4-donor macrocycle **57** is a recent example of a macrocyclic ligand containing both nitrogen and sulfur donor atoms. It was reported to show high selectivity for Ag(I) and Hg(II) over Cd(II), Zn(II), Cu(II), Ni(II), Mn(II), Co(II) and Pb(II).[119]

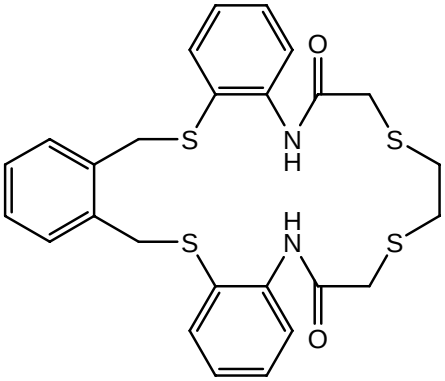

57

While less common, there are a number of examples of ligands containing mixed oxygen and sulfur donors. For example, the S_2O_2-donor macrocycle **58** interacts with K_2PtCl_4 to afford a bridged dimer complex of the type $[Pt_2\mathbf{L}_2Cl_4]$ (**L** = **58**).[120]

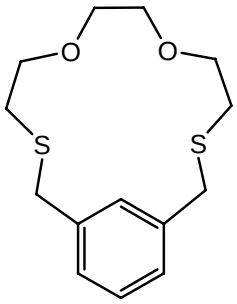

58

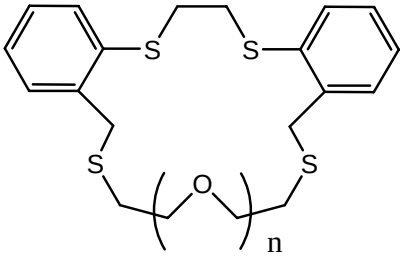

59 n = 1

60 n = 2

The tetrathiaoxa-dibenzo macrocycles **59** and **60** were synthesised in an attempt to generate new Tl(I)- and Ag(I)-selective ionophores.[121] The crystal structure of **59** indicates that the macrocycle exists in a non-folded configuration with two exodentate benzyl sulfur donors separated as far apart as possible, at the corners of a pseudo-rectangular plane. Attempts to obtain crystal structures of the Ag(I) or Tl(I) complexes of

59 were not successful. The crystal structure for **60** was also not obtained; however, an electrode based on this macrocycle showed remarkable potentiometric sensing ability for Tl^+ and Ag^+ ions. The crystal structure of the Tl(I) complex with **60** shows that the macrocycle adopts a baseball-glove-like conformation with the thallium ion lying 1.815 Å above the mean S_2O_2-donor plane.

Pentadentate macrocyclic ligands with mixed nitrogen, oxygen and sulfur in the same ligand backbone have also been somewhat less studied.[122] Early examples of such ligands were used in studies aimed at investigating the dependence of the macrocyclic effect on the nature of the metal-ion (as illustrated by the complexation behaviour of the mixed pentadentate ON_2S_2-donor macrocycle **61**). The Cu(II) complex of this ligand shows a substantial increase in stability when compared to that of the open-chain ligand **63**, and only a slightly less increase when compared to its pentaamine macrocyclic analogue.[123]

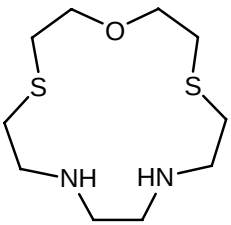

61

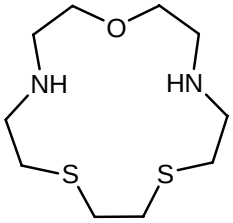

62

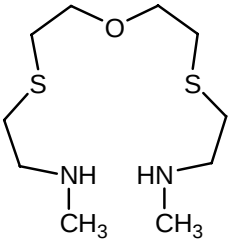

63

For this system large macrocyclic effects occur with Co(II), Ni(II) and Cu(II) but only moderate ones with Cd(II) and Ag(I). However, no macrocyclic effect was observed for Zn(II) and Pb(II), perhaps reflecting substantially different coordination geometries between the macrocyclic and reference complexes for these metals.[44, 123] The origin of the macrocyclic effect in the case of Cu(II) was shown to be equally enthalpic and entropic while in the case of Pb(II) both these contributions were found to be negligible.[123]
On the other hand, the Pb(II) complex of the pentaamine analogue displayed a strong macrocyclic effect due entirely to a large favourable entropic term, while the enthalpic contribution was found to be close to zero.[123] The results of further studies also confirmed the general trends just discussed.[123-125]

With respect to the above, comparison of the overall complex formation constants with Cu(II) showed that **61** forms a complex which is 50 times more stable than that of **62**. For Ag(I), the complex of **61** is about 10 times more stable than that of **62**, while for Ni(II) the stabilities are similar.[123] Later examples include [15]aneNO_2S_2 **64** and [15]aneN_2O_2S **65** which were investigated for their cadmium binding properties.[122] The X-ray crystal structures were among the first structurally characterised examples of medium-ring crown aza-oxa-thioether complexes of Cd(II).

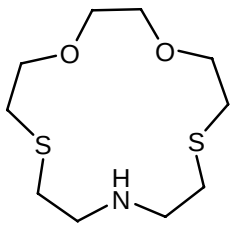

64

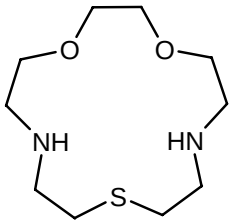

65

In the case of **64** the central Cd(II) ion is eight coordinate being bound to five macrocyclic donor atoms, one bidentate nitrato ligand and one monodentate nitrato ligand (**Figure 1.5**). The combined steric and conformational demands of the sulfur centers result in a 'butterfly' configuration of the macrocycle with the plane of the ring folded at

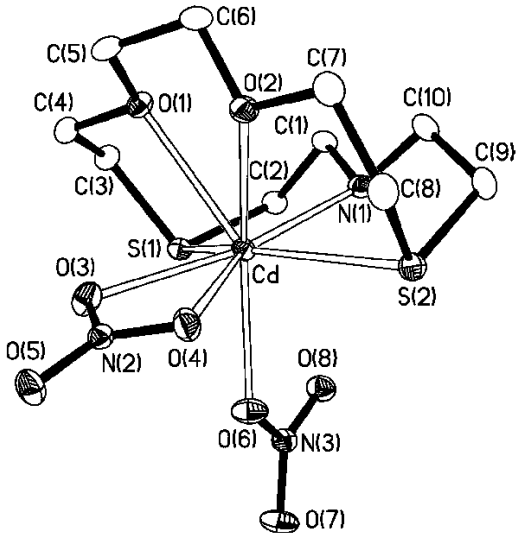

Figure 1.5 Structure of [Cd$(NO_3)_2$**64**] (Hydrogens have been omitted for clarity).

each sulfur atom. Macrocycle **65** on the other hand coordinates to the metal in an essentially flat conformation with all five macrocyclic donor atoms bound to Cd(II) and only one nitrato anion bound (which coordinates in a bidentate manner).

The five-donor macrocycle **66** was found to form exclusively square planar complexes with Pd(II) and Cu(II) in which the metal ion coordinates to the pyridine nitrogen, two sulfur atoms and one chloro ligand.[126] The oxygen atoms are oriented away from the metal centre and, in accordance with the 'hard-soft acid-base' principle, the hard donors do not interact with the metal. The ligand thus coordinates in a tridentate fashion.

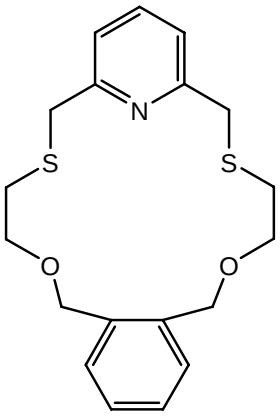

66

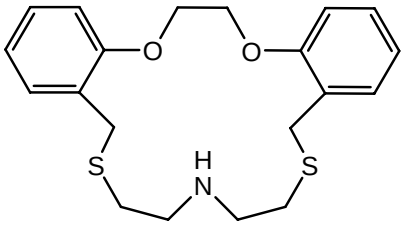

67

The dibenzo substituted macrocycle **67** was synthesised and investigated for its metal binding behaviour towards Cd(II) and Hg(II). In its cadmium complex the macrocycle coordinates as a tridentate ligand, binding *exo*-fashion *via* its nitrogen and two sulfur donors. The remaining coordination sites are filled by two bidentate nitrate ions such that, overall, the cadmium is seven-coordinate.[127] The complex afforded by the reaction of **67** with $Hg(ClO_4)_2$ exhibited a highly distorted octahedral coordination geometry with the O_2S_2-donors from the macrocyclic ring defining the equatorial plane while the axial positions are occupied by the ring nitrogen and an oxygen from a monodentate perchlorato ion.

1.5.2 Compartmental and di- or polynuclear macrocyclic systems

These are cyclic ligands which usually bind two or more metal ions, often in close proximity. The resulting complexes display interesting properties, some of which appear relevant to those characteristic of particular metalloproteins.[128] The classic example of a binucleating ligand is Robson's N_4O_2-system **68** whose macrocyclic framework places two metals at a close separation.[129] This system was also the first example of such a macrocycle that shares donor atoms between adjacent metal-binding sites. On coordination, **68** loses the phenolic protons and the phenoxide oxygens bridge between metal ions. A series of related mixed donor macrocycles of type **69** were shown to form dinuclear complexes with both Ni(II) and Cd(II), with the conformations adopted dependent on the particular metal ion radius as well as on the level of ligand N-alkylation present.[130]

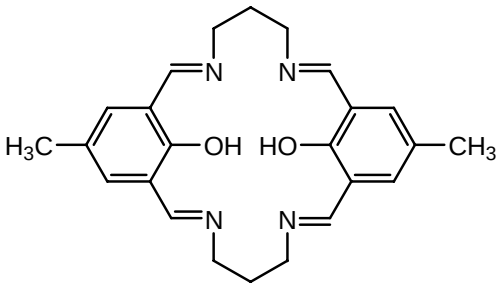

68

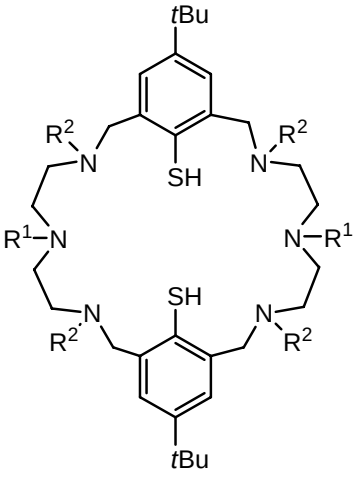

69

Recently, a category of dinucleating macrocyclic Schiff base ligands incorporating between 34- and 52-membered rings has been synthesised in the presence of Ca(II), Ba(II) and Mn(II) as 'transient' metal templates.[131] The free macrocycles react with Zn(II) acetate in methanol to produce dinuclear Zn(II) complexes such as illustrated by **70**.

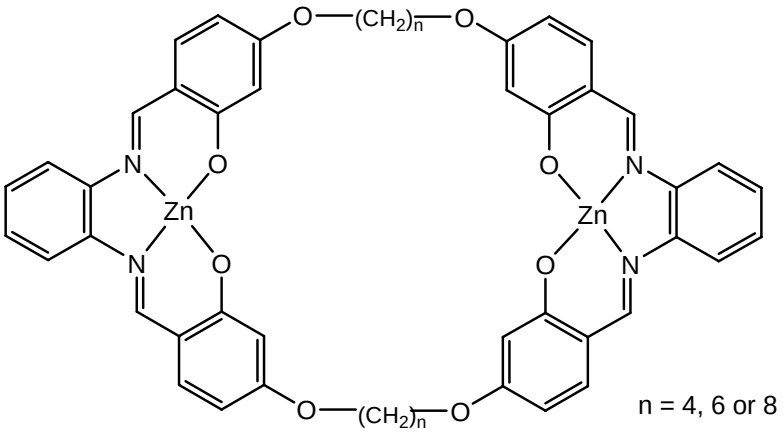

70

1.5.3 Linked di- or polynuclear macrocyclic systems

These are linked macrocyclic rings which typically simultaneously bind two or more metal ions, with the resulting complexes sometimes displaying unusual electronic, catalytic and/or redox properties.[132] A prototypical example of this type is the bicyclam derivative **71**; this compound has been extensively studied for its anti-HIV activity and, even though it only advanced to stage II clinical trials due to cardiac side-effects, interest in this compound continues due to its ability to mobilise stem cells, its potential use in transplant therapy and its enhanced co-receptor binding strength upon Zn(II) complexation.[133, 134] It is also noted that there is considerable interest in systems which incorporate mixed donor sets such as **72**[135] or less common multi-component structures containing heteromacrocyclic rings such as **73**.[136] It was expected that ligand systems such as **73** will promote the binding of different metal ions in sterically defined spatial and electronic environments.

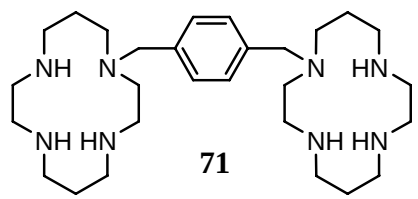

71

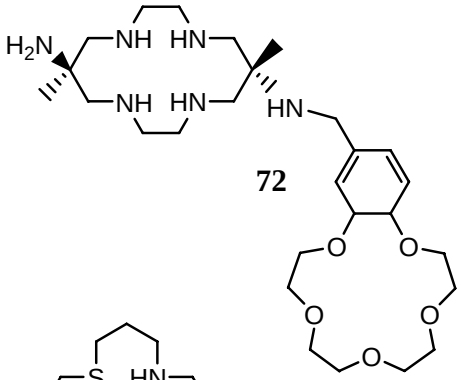

72

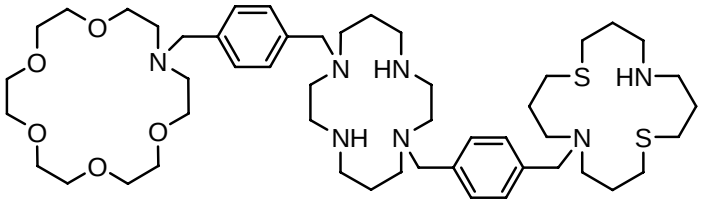

73

More recently, tri-linked *trans* N_2S_2-donor 16-membered macrocycles (see **51**) were reported to form complexes of formula $[Cu_3L](PF_6)_3$ with Cu(I).[137]

Direct linking of the monomeric NO_2S_2 macrocycle **67** through a xylyl bridge gives rise to **74**.[138] The reaction of this bridged analogue with two molar equivalents of $AgClO_4$ yields a dinuclear complex of formula $[Ag_2(\mathbf{L})](ClO_4)_2$ (**L** = **74**) whereas the reaction with Cu(I) iodide affords a one dimensional coordination polymer of formula $[Cu_4(\mathbf{L})I_4]_n$, (**L** = **74**).

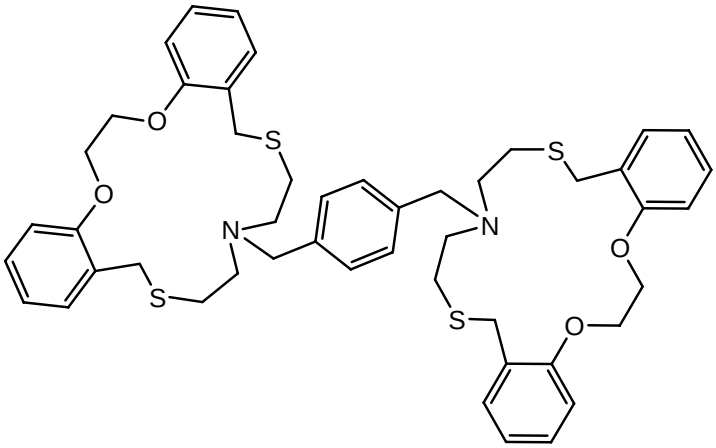

74

Dendritic structures incorporating macrocyclic ligand units have received increasing attention over recent years. For example, a second generation dendrimer **75**, incorporating nine S_2N_2-donor macrocycles, was shown via spectrophotometric titration to bind nine Pd(II) cations.[139]

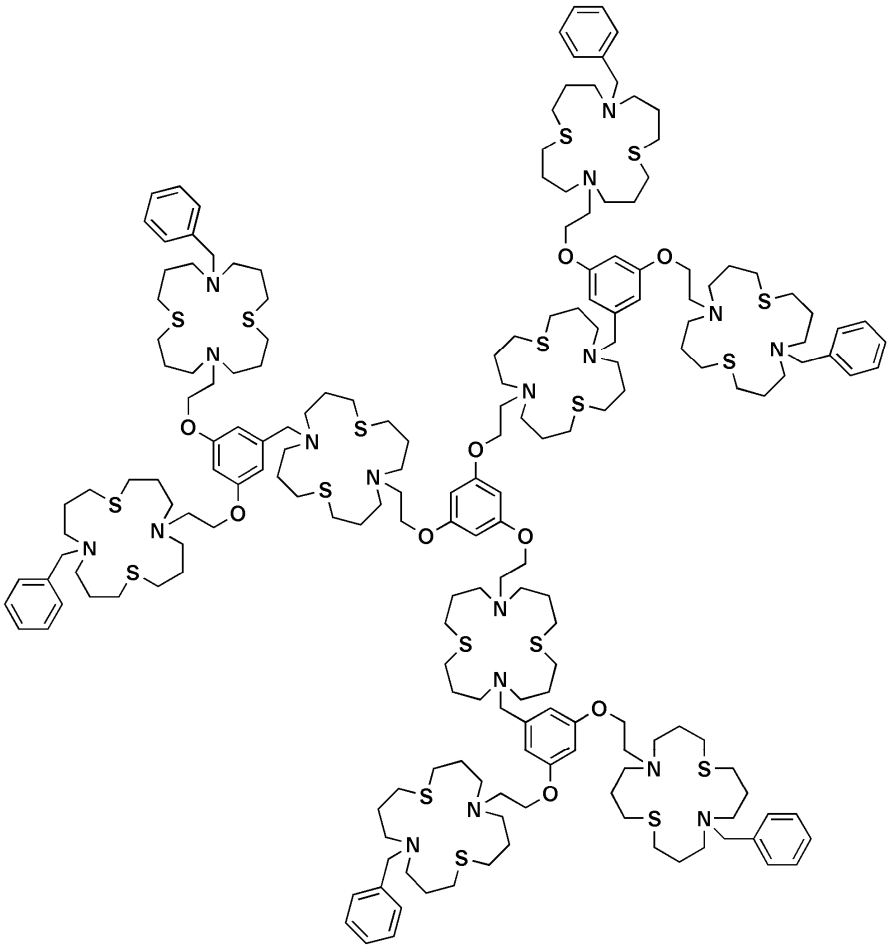

75

1.5.4 Cryptands

As mentioned already, in 1969 Lehn reported the first synthesis and investigation of the three dimensional cryptands (see structure **14**). These macrobicyclic ligands are able to completely encapsulate metal ions inside their molecular cavities.[43, 140] The resulting metal complexes (cryptates) are virtually always characterised by higher stabilities than their two-dimensional macrocyclic counterparts (the cryptate effect); they also tend to show higher selectivity towards particular metal ions.[141, 142]

The octaamine cryptand **76** has been shown to accommodate two Cu(II) ions,[143] while **77** exhibited, at the time of its publication, the longest separation (19.6 Å) between the two bridgehead nitrogen atoms in Schiff base complexes (and their corresponding reduced polyaza) cryptands so far reported.[144] The silver complex of **77** incorporates two Ag(I) ions, with each of them bound to three secondary amine nitrogen atoms and one bridgehead nitrogen atom.

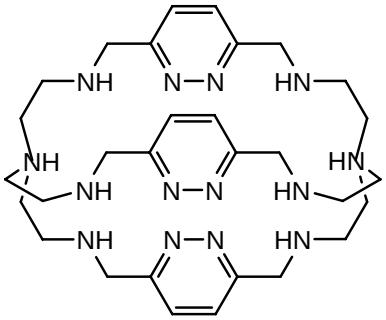

76

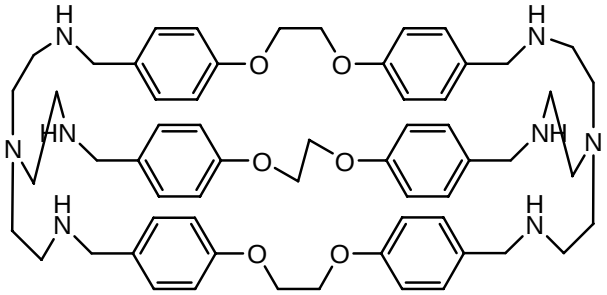

77

1.5.5 Pendant arm macrocycles

These are single ring ligands which contain appended side chains incorporating additional donor functions and are therefore structurally related to both macrocyclic and open-chain ligand systems.[44]

The mixed donor pendant arm macrocycle **78** bearing four thioether groups was prepared by Mäcke *et al.*[145] It forms an extremely stable silver complex, with the Ag(I) ion coordinated to all four ring nitrogens and to two of the pendant thioether groups. This Ag(I) complex has one of the highest stability constants (log K = 19.63) so far reported for this ion.[146]

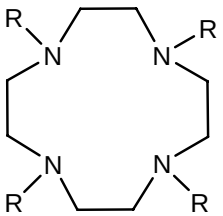

R = CH_2-CH_2-S-CH_3

78

A series of pendant arm mixed donor macrocycles derived from [12]aneS_3N, [12]ane S_2ON, [15]aneS_2ON_2 and [15]aneS_3N_2 containing hydrogen-bonding amide functionalities has also been synthesised.[147] Liquid membrane and liquid-liquid extraction studies have shown that these systems are highly selective for Ag(I) over Co(II), Ni(II), Cu(II), Zn(II), Cd(II) and Pb(II).

1.6 Mixed donor ligand systems of direct relevance to the present investigation

The design and synthesis of macrocyclic ligands that are able to recognise one metal ion in the presence of others has been a topic of considerable interest over the years.[72, 86, 148-151] An approach to attaining such metal ion recognition (and hence discrimination) has been to 'tune' the structural and electronic features of a ligand type towards the binding of a metal ion of interest. For example, the macrocyclic ring size, the number, type and arrangement of donor atoms present, the electronic and structural nature of the macrocyclic backbone and the number and size of the chelate rings formed on metal binding are all able to be varied in order to promote such recognition. In the case of transition metal ions, contributions from crystal field effects may also need to be considered.

Early studies in the author's laboratory were directed towards the synthesis of cyclic ligands of type **79** that are structurally intermediate between the crown cyclic polyethers and the tetradentate macrocycles containing four nitrogen atoms.[152-154] However, when coordinated, there was a tendency for these macrocycles to undergo hydrolysis of their imine functions which rendered them less suitable for solution studies, including the determination of their metal ion binding constants. Consequently derivatives of type **80**

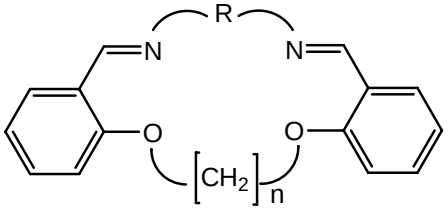

n = 2 or 3
R = -CH_2CH_2-
R = -$CH_2CH_2CH_2$-
R = -$CH_2CH(CH_3)$-

79

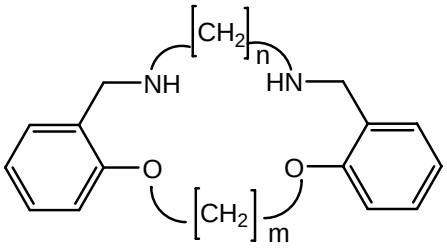

m = 2 or 3
n = 2 or 3

80

were employed instead; in these, the imine functions have been reduced to secondary amines. Subsequently a range of closely related macrocycles was obtained, which enabled the effects of minor ligand changes on metal-ion complexation to be evaluated (as previously illustrated by the 14- to 17-membered macrocycles **44** – **47**[108] discussed in section **1.5.1.5**)

Particular attention has been given to mixed donor macrocyclic systems tailored for the recognition (if only one metal is used) and/or discrimination (if two or more metals are present) of ions within the following industrially important groups: Co(II)/Ni(II)/Cu(II), Zn(II)/Cd(II) and Ag(I)/Pb(II).[155] Expansion of the initial synthetic program involved extending the ligand series to include 16- to 20-membered pentadentate macrocycles of type **81** in which systematic variation in donor-atom pattern, ring size and substitution occurs.

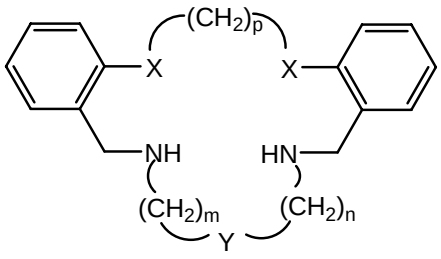

m = 2, 3 or 4
n = 2 or 3
p = 1, 2, 3 or 4

81

The diverse structural chemistry for complexes of this ligand type is exemplified in a recent study involving the complexation behaviour of Ag(I), Cd(II), Hg(II) and Pd(II) with a 17-membered N_3O_2-donor macrocycle of type **81** (X = O, Y = N, m = n = p = 2).[156] A range of structural types was obtained, including both mononuclear and dinuclear species; the effect of anion variation on the resulting structures was also investigated. For Ag(I) five related 2:2 (metal:ligand) complexes were obtained with metal salts incorporating different anions (NO_3^-, ClO_4^-, PF_6^-, OTf^- and CN^-); each silver centre binds to two N atoms from one ligand and one N atom from a second, with the ether oxygen donors uncoordinated. A weak Ag···Ag contact between adjacent silver ions is also present. The $[Ag_2\mathbf{L}_2(\mu\text{-CN})][Ag(CN)_2]\cdot H_2O$ complex (**L** = **81**, X = O, Y = N, m = n = p = 2) (**Figure 1.6**) represents a rare example of a discrete binuclear silver complex incorporating a two-electron μ2-κC:κC bridging cyanide group.

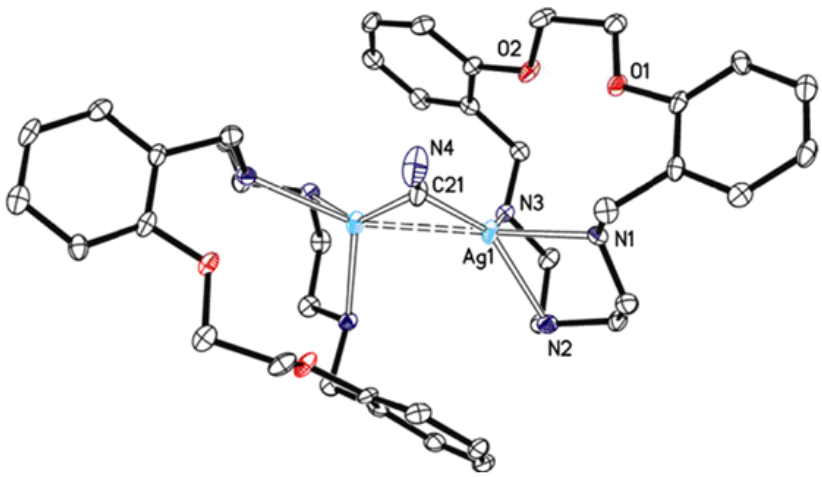

Figure 1.6 Dimeric structure of $[Ag_2\mathbf{L}_2(\mu\text{-CN})][Ag(CN)_2]\cdot H_2O$. Hydrogens, non-coordinating anions and non-coordinating solvent molecules are omitted.

In the cadmium complex $[Cd\mathbf{L}_2](ClO_4)_2\cdot CH_3CN$ (**L** = **81**, X = O, Y = N, m = n = p = 2) two macrocyclic units coordinate to the Cd(II) centre *via* a facial arrangement of the nitrogen donors (**Figure 1.7**) to form a distorted octahedral array of six N atoms; the ether oxygens do not coordinate. This contrasts with the distorted pentagonal-bipyramidal

coordination geometry of the related 1:1 complex [Cd**L**$(NO_3)_2$] (**L** = **81**, X = O, Y = N, m = n = p = 2) reported previously.[73] In this complex all macrocyclic donors coordinate, with the Cd(II) ion lying in the macrocyclic cavity; two monodentate nitrate groups occupy the axial sites such that the Cd(II) centre achieves a seven-coordinate geometry. This presumably also reflects the effect of anion (and perhaps solvent) variation on the structural type generated in the case of Cd(II) complexes.

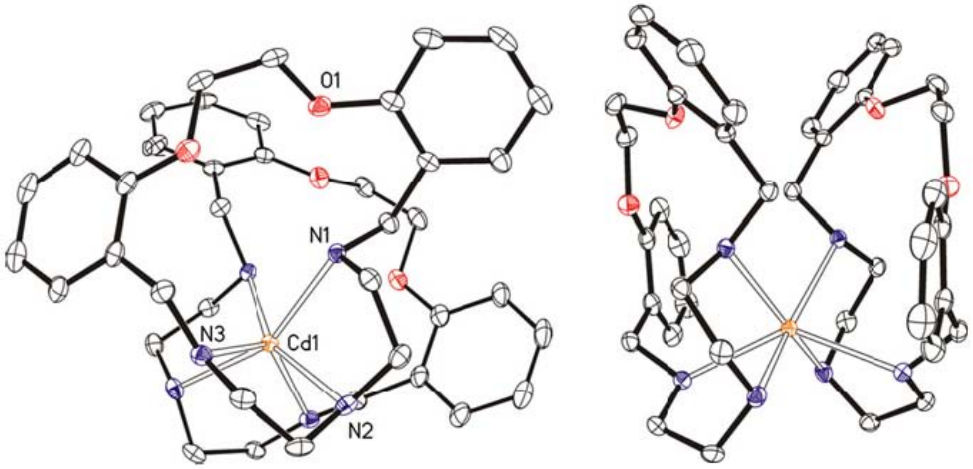

Figure 1.7 Structure of [Cd**L**$_2$]$(ClO_4)_2$·CH_3CN (top and side views). Hydrogen atoms and non-coordinating anions are omitted.

In the Pd(II) complexes reported the ether oxygens, once again, do not coordinate. For [Pd**L**Cl]Cl·H_2O and [Pd**L**(NO_3)](NO_3)·CH_3OH (**L** = **81**, X = O, Y = N, m = n = p = 2) both palladium centres attain a square-planar coordination geometry *via* binding to three N donors from the ligand and a chloro or nitrato group in the remaining site. Both structures in this case are analogues of the previously reported acetate-containing complex [Pd**L**(OAc)]OAc·H_2O (**L** = **81**, X = O, Y = N, m = n = p = 2).[157]

Mercury forms 1:1 (M:**L**) complexes of type [Hg**L**$(ClO_4)_2$] and [Hg**L**$(SCN)_2$]·CH_3CN (**L** = **81**, X = O, Y = N, m = n = p = 2). In the first of these the Hg(II) ion coordinates to all

macrocyclic donors and two monodentate perchlorato ligands, thus achieving an overall coordination geometry of seven while in the latter case the mercury ion is five-coordinate, being bound to three N donors from the ligand and two S atoms from the thiocyanato groups (**Figure 1.8**).

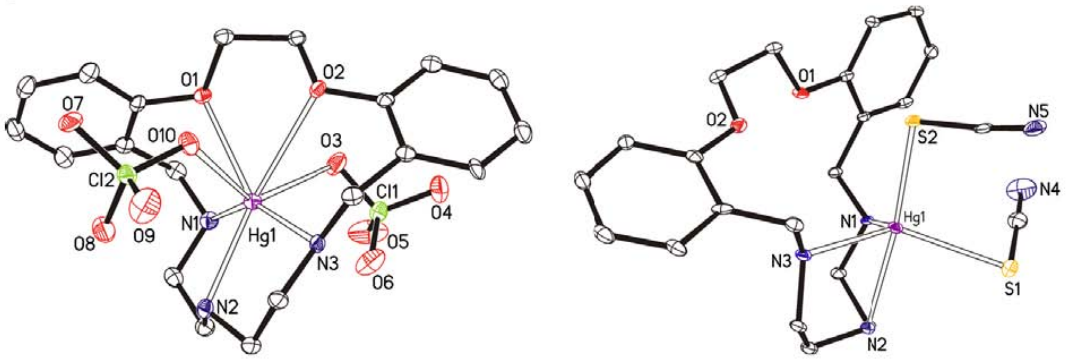

a **b**

Figure 1.8 Structure of (**a**) [Hg**L**$(ClO_4)_2$] and (**b**) [Hg**L**$(SCN)_2$]·CH_3CN. Hydrogen atoms and non-coordinating anions are omitted.

Hg(II) also yields a further two structural types. In [Hg_2**L**$_2$](HgI_4) (**L** = **81**, X = O, Y = N, m = n = p = 2) each mercury has a distorted tetrahedral geometry, being bound to three ligand nitrogens with a mercury-mercury bond occupying the fourth position, resulting in a 2:2 dinuclear complex. Finally, [Hg**L**$_2$]$(NO_3)_2$·$2CH_3OH$ (**L** = **81**, X = O, Y = N, m = n = p = 2) can be described as having a distorted octahedral geometry where each of the two ligands coordinates to the metal centre *via* three nitrogens; the macrocycle oxygens and the nitrate anions remain uncoordinated.

1.6.1 Donor atom set variation

In situations where the consecutive increments in ionic radii are not so different, (such as across the latter first row transition metal ions), it becomes difficult to achieve discrimination relying exclusively on the cation-cavity 'best fit' approach.[158] Indeed, it is the number, kind and arrangement of donor atoms in the macrocyclic ring that will also

usually play a significant role in achieving any observed metal ion selectivity.[159] For example, the donor atom pattern present may have a dramatic effect on complex stability. This is illustrated by the log *K* values for the Cu(II) complexes of the series of nine 17-membered macrocyclic ligands of type **82** in which the donor atom set (N, O and S) is systematically varied.[160] On variation of the donor type at three of the five potential donor sites, the log *K* values (in 95% methanol, 25˚C) ranged from 6.4 for the complex with an N_2O_3 set (X = Y = O) to ~16.3 for that of the complex with the N_5-donor set (X = Y = NH) – a stability difference of close to ten orders of magnitude across the series.

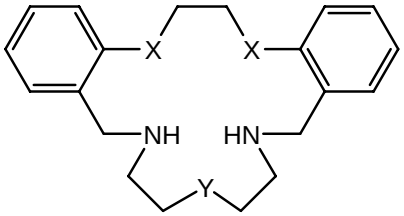

82

The stabilities of the Cu(II) complexes are uniformly high (log *K* > 14) whenever Y = NH (such that an aliphatic N_3-donor backbone is present). A further observation from the above study was that the contribution of the various donor atom types to the overall copper complex stability falls in the order NH(aliphatic) > NH(anilino) > S > O, a not unexpected order.[28, 159, 160]

Apart from the considerable stability differential for complexes of a given metal ion which results from donor atom variation, such behaviour has often been employed to achieve discrimination between individual metal ions. For example, the systematic variation of the X and Y donors in the ligand series given by **82** has led to exceptional discrimination for silver over lead (metals which occur together in nature) (**Table 1.2**).[161, 162] Comparison of the log *K* values for both silver and lead with the N_5-donor (X = Y = NH) and the O_2N_3-donor (X = O, Y = NH) rings shows a stability difference between the respective complexes of less than a factor of 10; the fact that the former yields the higher

absolute log *K* value with each metal, no doubt reflects the relatively poorer coordinating ability of ether oxygen donors towards both metals.

Table 1.2 Log *K* data for formation of 1:1 complexes of Ag(I) and Pb(II) with macrocycles of type **82** (95% methanol, 25 ˚C).

Donor set	Ag(I)	Pb(II)	Δlog *K*
X = NH, Y = NH	10.3	9.4	0.9
X = NH, Y = O	9.8	6.7	3.1
X = NH, Y = S	10.8	5.9	4.9
X = O, Y = NH	8.7	8.1	0.6
X = O, Y = O	7.1	5.5	1.6
X = O, Y = S	8.6	4.5	4.1
X = S, Y = NH	11.7	8.0	3.7
X = S, Y = O	10.3	~3.0	~7.3
X = S, Y = S	12.4	~3.0	~9.4

Overall, the most stable Pb(II) complexes in this series are those formed by those ligands which contain a secondary amine in the Y position (to yield an aliphatic N_3 backbone). Finally, the macrocycle containing the S_2N_2S-donor set (X = S, Y = S) yields the highest discrimination amongst the members of the series of approximately 10^9 in favour of silver.

A recent structural investigation of the effect of varying the single donor X in the 17-membered O_2S_2X macrocycle of type **83** showed that this can result in dramatic changes in the coordination geometry of the resulting Ag(I) complexes.[163]

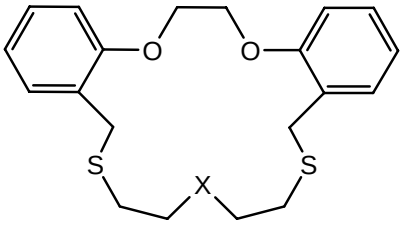

83

Four complexes with different topologies were isolated. A sandwich complex of type $[Ag(\mathbf{L})_2](ClO_4)$ (**L** = **83**) was obtained in the case where X = S (to give an O_2S_3 donor sequence). For X = O the results were solvent dependent: in the presence of acetonitrile the complex crystallised in a cofacial dimeric form (**Figure 1.9**), with two $[Ag\mathbf{L}(CH_3CN)]$ (**L** = **83**) units connected by an argentophilic Ag–Ag interaction at 3.33 Å, while a one-dimensional coordination polymer consisting of $[Ag_4(\mathbf{L})_2(CH_3OH)_2](ClO_4)_4$ (**L** = **83**) units was obtained in the presence of methanol (**Figure 1.10**).

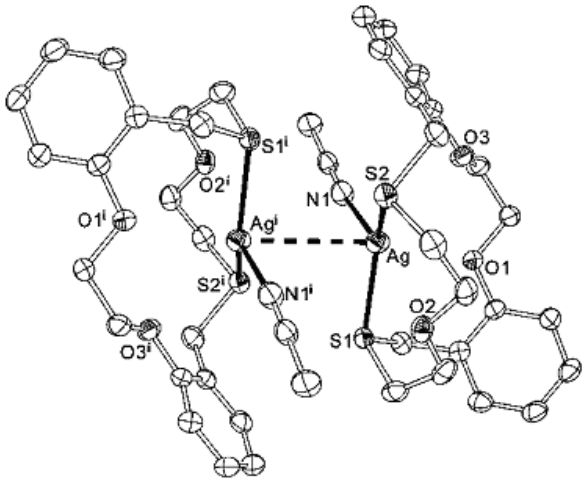

Figure 1.9 The dimeric structure of $\{[Ag\mathbf{L}(CH_3CN)](ClO_4)\}_2$. Hydrogen atoms and non-coordinating anions are omitted.

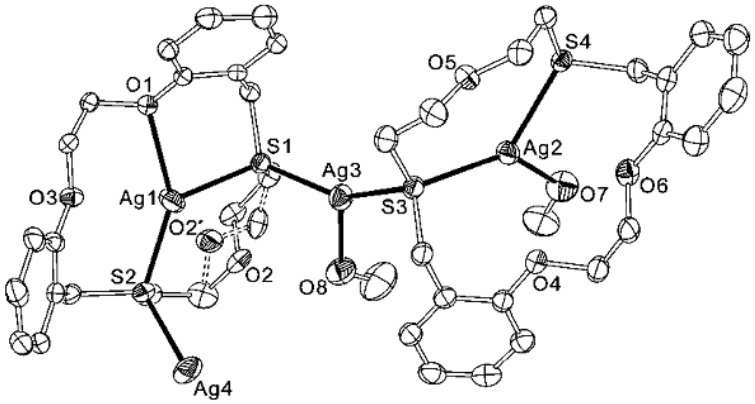

Figure 1.10 The one-dimensional polymeric structure of $\{[Ag_4(\mathbf{L})_2(CH_3OH)_2](ClO_4)_4\}_n$. Hydrogen atoms and non-coordinating anions are omitted.

Finally, in the case where X = NH a tetrameric bowl-type complex of composition $[Ag_4(\mathbf{L})_4(\mu\text{-}ClO_4)_2](ClO_4)_2$ (**L** = **83**) was obtained in which the overall geometry around each silver atom is distorted tetrahedral.

1.6.2 Ring size variation

In terms of selectivity, the match between the macrocycle cavity dimensions and the cation is particularly evident (as previously mentioned) in small preorganised ligands such as cryptands or porphyrins where limited conformational change is possible upon complexation.[159]

For the macrocyclic systems of direct interest to the work presented later in this thesis, the incorporation of dibenzo groups has tended to be advantageous since this yielded ligands of intermediate flexibility and consequently has restricted the number of conformations that the coordinated ligand could adopt. In addition, the ligand systems have generally involved 17 – 19-membered macrocyclic ring sizes and were found to favour 1:1 (metal:ligand) complexation, thus aiding the interpretation of solution results.[72] However, in many instances it is noted that the metal ion was not contained in the macrocyclic ring and factors such as chelate ring size rather than the cation and macrocycle cavity dimensions may control both the stabilities of complex formation and hence also the selectivities for particular metal ions.[159]

A study of the interaction of Cu(II) with a series of closely related 16- to 19-membered pentadentate macrocyclic ligands of type **84** provided further insight into the effect of macrocyclic ring size (and concomitant chelate ring size) variation on the stability of the resulting complexes.[164]

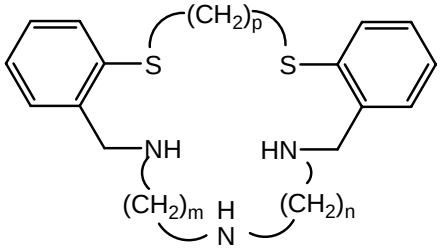

84

The stability of the Cu(II) complex with the 16-membered ring (m = n = 2, p = 1) is significantly less than that of the 17-membered ligand (m = n = p = 2), while that for the corresponding 19-membered ring complex (m = n = 3, p = 2) was lower by almost five

orders of magnitude. This complex stability order thus follows that expected from chelate ring size considerations, where 5-membered rings form more stable complexes than 4- or 6-membered rings.

For the system of the type **81** with an N_5 donor set (**81**, X = Y = NH), complexes of the larger rings tend to be less stable than for the 'parent' 17-membered macrocycle.[74] Thus, the 20-membered ring (m = n = p = 3) yields zinc and cadmium complexes which are more than 6 orders of magnitude less stable than the corresponding complexes of the 17-membered macrocycle – again attributable to the presence of additional 6-membered chelate rings in the former case.

Finally, in terms of macrocyclic ring-size discrimination, a study of thermodynamic stabilities of the Zn(II) and Cd(II) complexes of a series of O_2N_3-donor macrocycles of type **85** (**Figure 1.11**) revealed the effect that minor changes, such as varying the number of methylene linkages in the NNN-donor string (while the remainder of the ring remains unaltered), can have.[73, 165] For the 17- and 18-membered ligands of this type the stability trends for each of the above metal ion complexes parallel each other, as 5-memberd chelate rings are replaced by 6-membered ones. However, there is a larger than expected decrease in stability for the Cd(II) complex with the 19-membered ring, now $10^2 - 10^3$ less stable than the corresponding 18-membered complex, and also of lower stability than the Zn(II) analogues. This 'dislocation' appears to reflect the non-coordination of the ether oxygens in solution, as shown to occur in the solid state by X-ray diffraction.

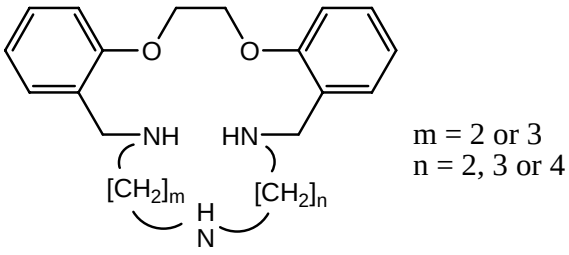

85

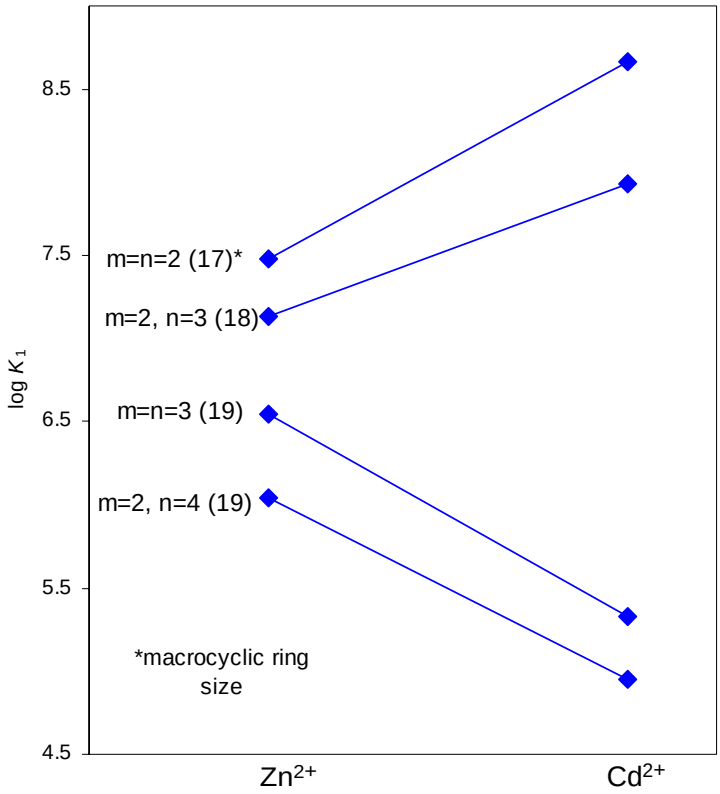

Figure 1.11 Log *K* values for the Zn(II) and Cd(II) complexes of O_2N_3-donor macrocycles of type **85** (95% methanol, 25 ˚C).

Thus, in the solid state of the 17-membered ring complex cadmium displays an overall coordination number of 7 with a distorted pentagonal-bipyramidal coordination geometry. The Cd(II) ion lies in the cavity of the five 'equatorial' donor atoms of the macrocycle with monodentate nitrate groups occupying the 'axial' sites. It is noted that the bonds to the two ether oxygen atoms are long (2.614 and 2.732 Å). It was proposed that if a similar coordination geometry is maintained in the 18-membered ring, these bonds would likely be even weaker. The corresponding 19-membered ring cadmium complex contains an approximately planar CdN_3 unit, with (as expected) the ether donors outside bonding distance. The overall coordination number of the Cd(II) is now 5 with two monodentate nitrates completing the coordination shell. Similar behaviour was predicted to occur for the second 19-membered ring complex shown in **Figure 1.11**.[73, 74]

1.6.3 Effects of N-alkylation

A number of studies have investigated the effects of N-alkylation on the metal binding properties of both open chain and cyclic ligands.[166-168] In general, N-alkylation resulted in a decrease in thermodynamic stability of the resulting metal complexes when compared to that of the corresponding unsubstituted ligands, in many cases largely ascribed to the steric influence of the particular bulky N-substituents present. The effect of appending N-alkyl substituents on the 17-membered macrocycle **86** on its metal ion discrimination behaviour is summarised in **Table 1.3**.[72]

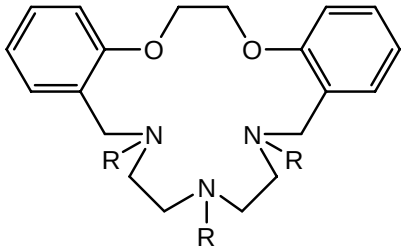

86

Table 1.3 Effect of N-substituents on the stability constants for the metal complexes of type **86** (95% methanol, 25 ˚C).

Substituent	Co(II)	Ni(II)	Cu(II)	Zn(II)	Cd(II)	Ag(I)	Pb(II)
R = H	7.6	10.0	14.4	7.5	8.7	8.7	8.1
R = CH_3	<3.5	<3.5	-[a]	5.1	6.1	10.3	6.6
R = $CH_2C_6H_5$	<3.5	<3.5	-[a]	~3.5	~3.5	9.3	4.3

[a]Data not obtained due to precipitation.

As expected, the presence of substituents on the nitrogen donors in general resulted in the formation of weaker complexes than those for the unsubstituted macrocycle [the exception is with Ag(I)]. As just mentioned, such a decrease has been largely attributed to steric hindrance from the ‘R’ groups inhibiting complex formation; the greatest effect is

usually seen for bulky substituents such as benzyl groups. However, for Ag(I) the log *K* values remain consistently high; in the case of the tribenzylated derivative (**86**, R = $CH_2C_6H_5$) the value is even slightly higher than that of the parent macrocycle.

N-alkylation of tetraazalkane ligands (both linear and cyclic) has been shown by Meyerstein *et al.* to favour stabilisation of low valent transition metal complexes.[168-170] A number of factors has been proposed to account for such behaviour, with solvation effects suggested to be dominant. Behaviour of this type would favour Ag(I) relative to the +2 oxidation state of the other metals listed in **Table 1.3**. [72]

Similar effects have been observed for other ligand systems; for example, following N-methylation and N-benzylation of the diaza-crown macrocycle **87**.[171] The log *K* values

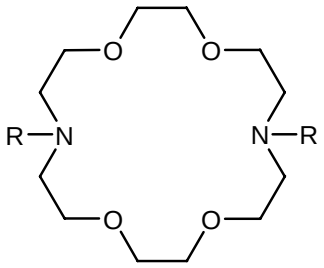

87

(**Table 1.4**) confirm that the parent N_2O_4-ring (**87**, R = H) forms moderately strong complexes with Cu(II), Cd(II), Ag(I) and Pb(II) relative to those of Co(II), Ni(II) and Zn(II). The highest affinity is shown for Ag(I) while the value for Pb(II) is only slightly lower. The bis-methylated analogue (**87**, R = CH_3) maintains the selectivity for Ag(I) and Pb(II), with the affinity for the latter ion, interestingly, slightly increased over the log *K* value for when R = H. The data clearly show that the dibenzylated macrocycle (**87**, R = $CH_2C_6H_5$) shows quite good selectivity for these two ions over the other metal ions investigated. In particular it is noted that N-benzylation has only a minor effect on the stability of the Ag(I) complex while the affinity of the ring is significantly 'detuned' for all the other ions except Pb(II) [for which, in the case of **87** (R = $CH_2C_6H_5$), only modest 'detuning' is apparent].

Table 1.4 Effect of N-substituents on the stability constants of the metal complexes of **87** (R = H, CH_3, $CH_2C_6H_5$) (95% methanol, 25 ˚C).

Substituent	Co(II)	Ni(II)	Cu(II)	Zn(II)	Cd(II)	Ag(I)	Pb(II)
R = H	<4	<4	7.6	~4.0	7.11	9.79	9.10
R = CH_3	<4	<4	6.96	<4	5.74	9.15	10.12
R = $CH_2C_6H_5$	<4	<4	~5.4	<4	<4	9.62	8.4

More recent work on the interaction of the metal ions mentioned above with a series of dibenzo-substituted mixed donor macrocycles containing O_2N_2- (**45**), O_3N_2- (**88**), and O_2N_3-(**86**) donor sets as well as pyridinyl-containing, oxygen-nitrogen mixed

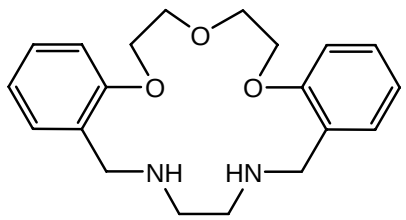

88

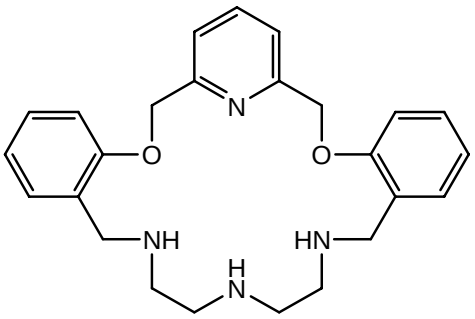

89

donor macrocycles (for example **89**) in general show related behaviour to that just described.[172, 173] Invariably the results indicate that the N-benzylation of the secondary amine donor groups on the parent macrocyclic ring leads to enhanced selectivity for Ag(I) relative to the other six metals investigated.

A comparative investigation involving the parent unsubstituted macrocycle **86** (R = H), the monobenzylated macrocycle **90**, the related O_3N_2-donor dibenzyl substituted ring **91** and the O_2N_3-donor tribenzyl derivative **92** and the above metal ions has been carried

out.[174] Monobenzylation resulted in a marginally enhanced stability for silver, with the log *K* values for all other metal ions being reduced (**Table 1.5**), even though the Cu(II) complex still displayed the highest overall stability. The experimental data show that increasing ring N-benzylation affects the ligand affinity for Ag(I) only moderately while the binding strengths towards the remaining metal ions are collectively 'detuned'. As a consequence of this, high selectivity for silver has been achieved in the case of the tribenzylated macrocycle **92**.

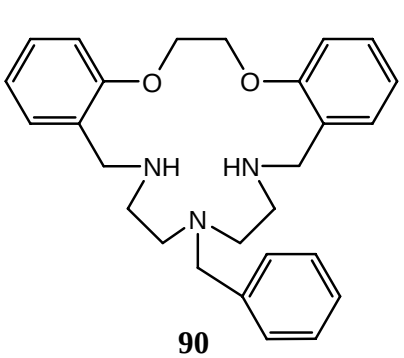

90

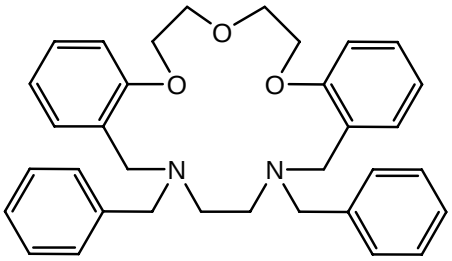

91

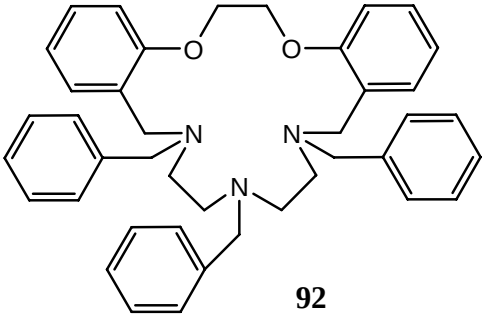

92

Table 1.5 Effect of N-benzylation on the log *K* values for the metal complexes of **86** (R=H), **90**, **91** and **92** (95% methanol, 25 ˚C).

Ligand	Co(II)	Ni(II)	Cu(II)	Zn(II)	Cd(II)	Ag(I)	Pb(II)
86(R=H)	7.7	10.0	14.2	7.5	8.7	8.7	8.1
90	5.7	<6	11.85	6.5	6.3	9.2	6.2
91	<4	<4	5.4	<4	<4	8.9	4.4
92	<4	<4	-[a]	<4	<4	9.3	4.3

[a]Data not obtained due to precipitation.

1.7 Summary of stability data for complexes of the five-donor dibenzo substituted macrocycles

While, in general terms, recognition for a particular metal ion of interest is achieved when the properties of the macrocyclic ligand best match the steric and electronic nature of the metal, selectivity depends on achieving a difference in the binding constants for respective metal cations of interest. Namely, it is the difference in the log *K* values rather than their absolute magnitude that is of primary interest.[72] As a result, the respective stability constant values provide a useful resource for monitoring and controlling ligand synthesis for achieving metal ion discrimination. Starting from a particular macrocyclic ligand chosen on the basis of its likelihood to give rise to discrimination, the synthesis of related derivatives is then carried out using the respective log *K* values as a monitor such that a systematic 'tuning up' process of any discrimination observed occurs.[148]

Largely involving a strategy of the above type, an extended series of related (potentially) pentadentate, mixed donor, dibenzo-substituted rings of the type mentioned above has been prepared previously in the author's laboratory and their interaction with selected transition and post-transition metal ions investigated (**Table 1.6**).[72-74, 160-162, 164, 172, 174-184] What follows is a full summary of these ligands together with their corresponding log *K* data in order to provide a background for the author's results presented in subsequent chapters of this thesis.

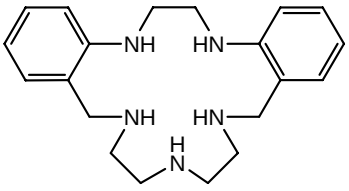

93

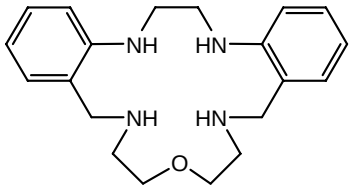

94

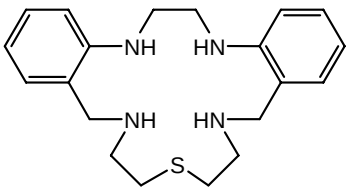

95

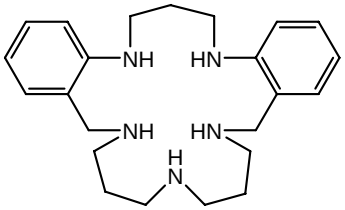

96

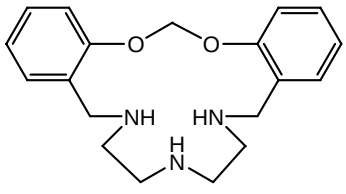

97

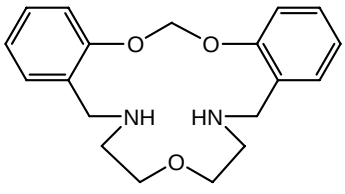

98

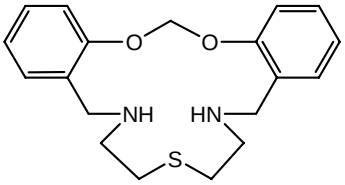

99

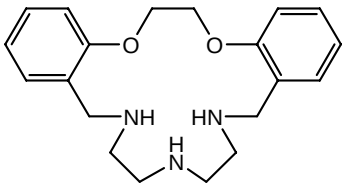

100

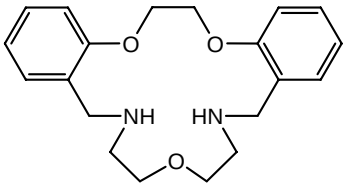

101

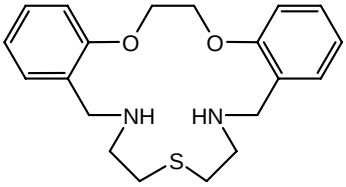

102

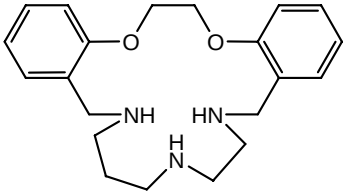

103

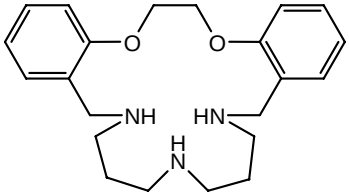

104

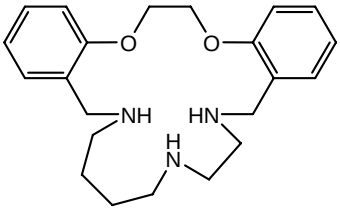

105

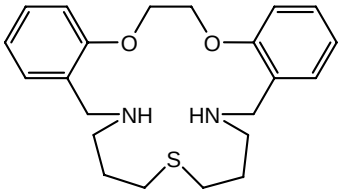

106

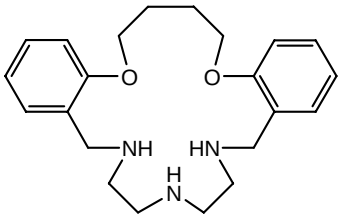

107

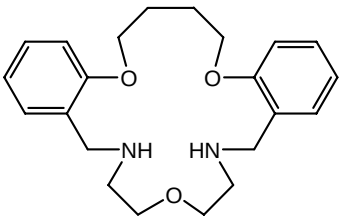

108

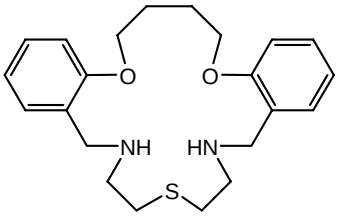

109

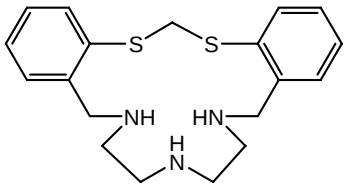

110

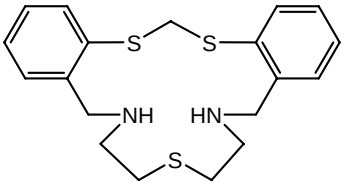

111

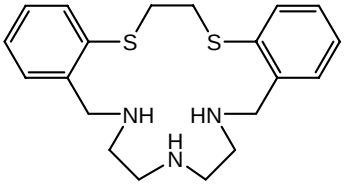

112

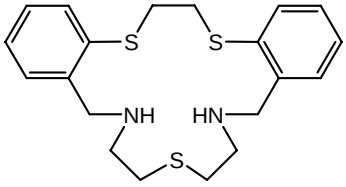

113

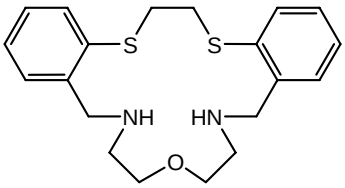

114

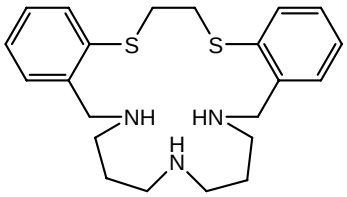

115

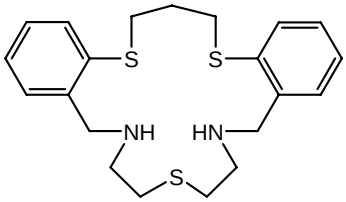

116

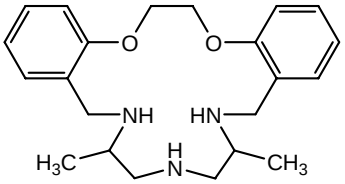

117

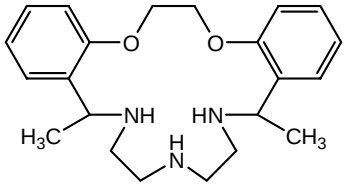

118

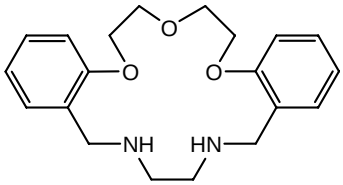

88

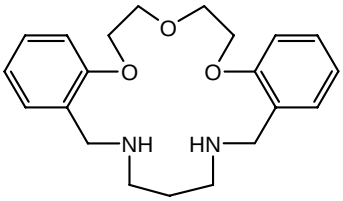

119

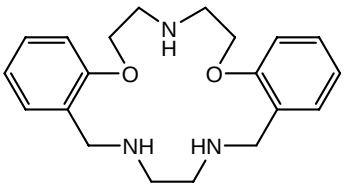

120

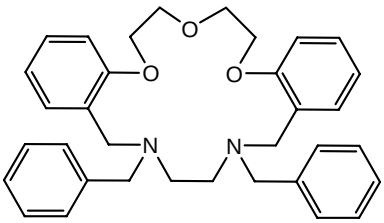

91

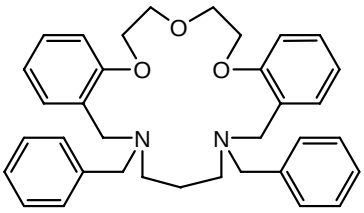

121

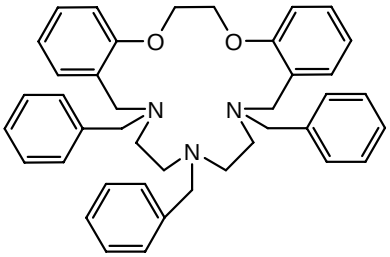

92

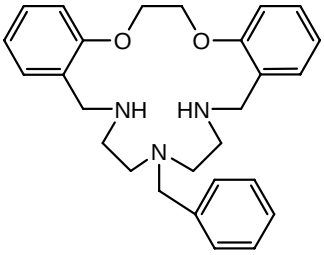

90

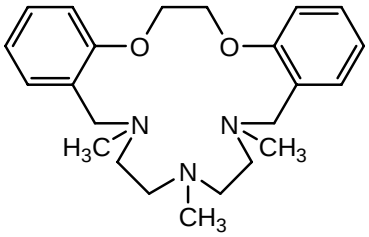

122

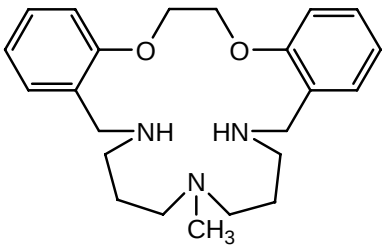

123

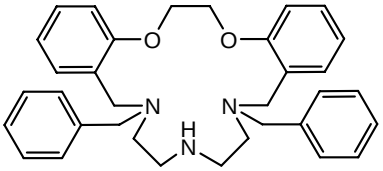

124

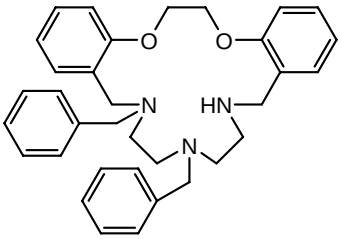

125

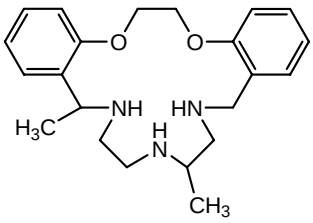

126

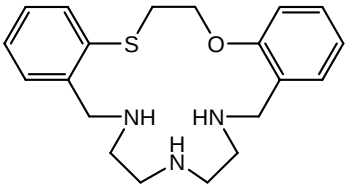

127

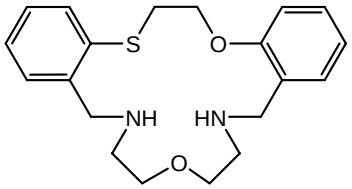

128

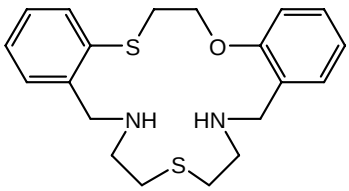

129

Table 1.6 Metal stability constants (ML^{n+}) for **88**, **90** – **129** (95% methanol, 25 ˚C).

Ligand	Co(II)	Ni(II)	Cu(II)	Zn(II)	Cd(II)	Ag(I)	Pb(II)
93	-	-	16.3[a]	11.9[b]	12.1[b]	10.3[c]	9.4[c]
94	-	-	14.5[a]	7.8[b]	10.0[b]	9.8[c]	6.7[c]
95	-	-	14.5[a]	8.9[b]	9.2[b]	10.8[c]	5.9[c]
96	-	-	13.9[d]	5.6[b]	5.8[b]	-	-
97	6.1[k]	8.3[k]	14.9[d]	6.5[b]	7.3[b]	7.7[c]	7.8[c]
98	<3.5[k]	<3.5[k]	~7.0[d]	*p*[b]	3.5[b]	-	-
99	*p*[k]	~3.0[k]	~6.9[d]	*p*[b]	*p*[b]	7.7[c]	4.6[c]
100	7.7[f]	10.0[f]	14.4[e]	7.5[b]	8.7[b]	8.7[c]	8.1[c]
101	<3.5[k]	<3.5[k]	6.5[a]	<3.5[b]	5.3[b]	7.1[c]	5.5[c]
102	~3.0[k]	5.5[k]	7.4[a]	<3.5[b]	4.4[b]	8.6[c]	4.5[c]

Table 1.6 Metal stability constants (ML^{n+}) for **88**, **90** – **129** (95% methanol, 25˚C) (Continued).

Ligand	Co(II)	Ni(II)	Cu(II)	Zn(II)	Cd(II)	Ag(I)	Pb(II)
103	7.3[f]	9.8[f]	14.0[e]	7.1[b]	7.9[b]	8.8[c]	7.9[c]
104	5.1[f]	6.4[f]	11.0[f]	6.6[b]	5.3[b]	*p*[c]	7.6[c]
105	<5[f]	5.1[f]	10.5[f]	6.0[b]	5.0[b]	-	-
106	~3.4[k]	<3.5[k]	~7.8[d]	<3.5[b]	<3.5[b]	~8.5[c]	*p*[c]
107	7.3[k]	9.7[k]	14.0[d]	7.3[b]	7.2[b]	7.2[c]	7.5[c]
108	~3.5[k]	3.5[k]	7.0[d]	3.8[b]	<3.5[b]	*p*[c]	6.2[c]
109	~3.4[k]	*p*[k]	~7.2[d]	3.6[b]	3.8[b]	7.8[c]	5.9[c]
110	5.5[k]	8.4[k]	14.3[d]	5.6[b]	6.6[b]	10.9[c]	7.0[c]
111	<3.5[k]	*p*[k]	6.3[d]	*p*[b]	~3.3[b]	11.0[c]	3.1[c]
112	*p*[k]	9.5[k]	15.6[a]	6.3[b]	7.8[b]	11.7[c]	8.0[c]
113	<3.5[k]	<3.5[k]	8.1[a]	*p*[b]	~3.3[b]	12.4[c]	~3[c]
114	<3.5[k]	~3.4[k]	6.9[a]	*p*[b]	4.4[b]	10.3[c]	~3[c]
115	~3.4[k]	5.7[k]	11.0[d]	5.4[b]	4.6[b]	-	-
116	<3.5[k]	-	7.3[d]	*b*[b]	<3.5[b]	10.9[c]	~3.5[c]
117	5.5[f]	6.9[f]	14.3[e]	5.6[l]	7.9[l]	-	-
118	5.6[g]	8.0[g]	13.5[g]	6.4[g]	7.6[g]	-	7.8[g]
88	4.6[h]	6.5[f]	9.7[h]	4.7[m]	5.2[m]	6.7[m]	4.9[m]
119	<4.2[h]	4.8[f]	7.7[h]	<5[m]	4.1[m]	6.0[m]	6.1[m]
120	5.8[h]	8.2[h]	14.2[h]	7.6[m]	10.2[m]	10.6[m]	5.7[m]
91	<4[i]	<4[i]	5.4[i]	<4[i]	<4[i]	8.9[i]	4.4[i]

Table 1.6 Metal stability constants (ML^{n+}) for **88**, **90** – **129** (95% methanol, 25˚C) (Continued).

Ligand	Co(II)	Ni(II)	Cu(II)	Zn(II)	Cd(II)	Ag(I)	Pb(II)
121	<4[i]	<4[i]	5.3[i]	<4[i]	<4[i]	5.1[i]	~4.4[i]
92	<4[i]	<4[i]	*p*[i]	<4[i]	<4[i]	9.3[i]	4.3[i]
90	5.7[j]	<6[j]	11.85[j]	6.5[j]	6.3[j]	9.2[j]	6.2[j]
122	<3.5[n]	<3.5[n]	*p*[f]	5.1[l]	6.1[l]	10.3[n]	6.6[n]
123	-	<6.4[f]	*p*[f]	5.9[l]	4.7[l]	-	-
124[o]*	-	-	-	-	-	-	-
125[o]*	-	-	-	-	-	-	-
126[q]*	-	-	-	-	-	-	-
127	7.2[r]	~9.3[r]	13.9[r]	7.0[s]	8.1[s]	~10.8[s]	7.8[s]
128	<3.5[r]	<3.5[r]	6.1[r]	<4.0[s]	4.9[s]	9.3[s]	4.5[s]
129	<3.5[r]	-	7.4[r]	<4.0[s]	~4.0[s]	11.1[s]	~3.8[s]

[a] From ref. 160. [b] From ref. 74. [c] From ref. 162. [d] From ref. 164. [e] From ref. 181. [f] From ref. 175. [g] From ref. 179. [h] From ref. 178. [i] From ref. 172. [j] From ref. 174. [k] From ref. 176. [l] From ref. 73. [m] From ref. 177. [n] From ref. 72. [o]* From ref. 182. [q]* From ref. 180. [r] From ref. 183. [s] From ref. 184. *These ligands were included for completeness. A '-' means no literature value was available; *p* means that precipitation or competing hydrolysis prevented determination of a log *K* value. Where the value is shown as approximate, this corresponds to a mean value determined from a limited number of data points – often giving rise to duplicate or triplicate determinations whose individual results differed by 0.3 – 0.4 log *K* units.

1.8 The present study

A major aim of the project was to extend the mixed donor macrocycle discrimination work just discussed, with emphasis on the development of unsymmetrical donor ligand systems. While a large number of symmetrical mixed-donor macrocyclic ligands have been synthesised over the past 40 years, systems with unsymmetrical arrangements of their donor atoms remain quite rare. One goal was to prepare a range of such unsymmetrical systems that were based on the corresponding ‘symmetrical’ macrocycles of type **81** synthesised over many years in the author's laboratory and to undertake an investigation of their metal binding affinities. In particular, it was of interest to probe the metal ion specificity of the new derivatives for the following (industrially important) transition and post-transition ions Co(II), Ni(II), Cu(II), Zn(II), Cd(II), Ag(I) and Pb(II). Following a description of the extensive organic ligand synthetic studies performed as a (major) part of the project in Chapter 2, the interactions of the respective ligands with the above metal ions are presented in Chapters 3 and 4. Based in part on the results obtained in the above studies, the final chapter presents an extension of the above studies aimed at achieving enhanced discrimination for Ag(I) via means of rational ligand design.

1.9 References

1. S. K. Chapman, S. Daff and A. W. Munro, *Struct. Bond.*, 1997, **88**, 39.
2. H. Fischer, A. Treibs and G. Hummel, *Z. Phys. Chem.*, 1929, **185**, 33.
3. E. M. Dietz and T. H. Werner, *J. Am. Chem. Soc.*, 1934, **56**, 2180.
4. E. B. Fleischer, *Acc. Chem. Res.*, 1970, **3**, 105.
5. B. F. Burnham and J. J. Zuckerman, *J. Am. Chem. Soc*., 1970, **92**, 1547.
6. M. A. Dahlen, *Ind. Eng. Chem* 1939, **31**, 839.
7. M. M. Blight and N. F. Curtis, *J. Chem. Soc.*, 1962, 3016.
8. N. F. Curtis, *Chem. Commun.*, 1966, 881.
9. J. D. Curry and D. H. Busch, *J. Am. Chem. Soc.*, 1964, **86**, 592.
10. E.-G. Jaeger, *Z. Anorg. Allg. Chem.*, 1969, **364**, 177.
11. C. J. Pedersen, *J. Am. Chem. Soc*., 1967, **89**, 7017.
12. D. E. Fenton, *Chem. Soc. Rev.*, 1999, **28**, 159 and references therein.
13. D. Ostfeld and M. Tsutsui, *Acc. Chem. Res.*, 1974, **7**, 52.
14. L.-L. Wong, A. C. G. Westlake and D. P. Nickerson, *Struct. Bond.*, 1997, **88**, 175-207.
15. L. J. Hoard, *Science*, 1971, **174**, 1295.
16. J. B. Conant and C. F. Bailey, *J. Am. Chem. Soc.*, 1933, **55**, 795.
17. J. K. Laha, C. Muthiah, M. Taniguchi, B. E. McDowell, M. Ptaszek and J. S. Lindsey, *J. Org. Chem.*, 2006, **71**, 4092.
18. C. Muthiah, M. Taniguchi, T. M. Nguien, K. M. Flack and J. S. Lindsey, *J. Org. Chem.*, 2007, **72**, 7736.
19. J. E. McMurry and T. P. Begley, *The Organic Chemistry of Biological Pathways*, Roberts and Company, Colorado, 2005.
20. J. M. Pratt, *Pure and Appl. Chem.*, 1993, **65**, 1513.
21. M. K. Geno and J. Halpern, *J. Am. Chem. Soc.*, 1987, **109**, 1238.
22. A. Eschenmoser, *Angew. Chem. Int. Ed.*, 1988, **27**, 5.
23. P. P. Power, C. W. Kirby and N. J. Taylor, *J. Am. Chem. Soc.*, 1998, **120**, 9428.
24. Rovira, C., K. Kunc, J. Hutter and M. Parrinello, *Inorg. Chem.*, 2001, **40**, 11.
25. P. B. Chock, F. Eggers, M. Eigen and R. Winkler, *Biophys. Chem.*, 1977, **6**, 239.
26. D. F. Mayers and D. W. Urry, *J. Am. Chem. Soc.*, 1972, **94**, 77.

27. M. Pinkerton, L. K. Steinrauf and P. Dawkins, *Biochem. Biophys. Res. Commun.*, 1969, **35**, 512.
28. R. M. Izatt, J. S. Bradshaw, S. A. Nielsen, J. D. Lamb and J. J. Christensen, *Chem. Rev.*, 1985, **85**, 271.
29. W. G. Gokel and M. M. Dasch, *Coord. Chem. Rev.*, 2008, **252**, 886.
30. H. Diebler, M. Eigen, G. Ilgenfritz, G. Maaß and R. Winkler, *Pure & Appl. Chem.*, 1969, **20**, 93.
31. C. U. Zust, P. U. Fruh and W. Simon, *Helv. Chim. Acta*, 1973, **56**, 495.
32. M. Dobler, J. D. Dunitz and B. T. Kilbourn, *Helv. Chim. Acta*, 1969, **52**, 2573.
33. J. W. Lee and N. D. Priestley, *Bioorg. Med. Chem. Lett.*, 1998, **8**, 1725.
34. M. E. Nelson and N. D. Priestley, *J. Am. Chem. Soc.*, 2002, **124**, 2894.
35. D. W. Thomas and A. E. Martell, *J. Am. Chem. Soc.*, 1959, **81**, 5111.
36. E. B. Fleischer, *Inorg. Chem.*, 1962, **1**, 493.
37. M. Tsutsui, M. Ichikawa, F. Vohwinkel and K. Suzuki, *J. Am. Chem. Soc.*, 1966, **88**, 854.
38. P. Hambright, *Coord. Chem. Rev.*, 1971, **6**, 247.
39. Z. Gross, I. Saltsman, R. P. Pandian and C. M. Barzilay, *Tetrahedron Lett.*, 1997, **38**, 2383.
40. E.-G. Jaeger, *Z. Chem.*, 1964, **4**, 437.
41. M. M. Blight and N. F. Curtis, *J. Chem. Soc.*, 1962, 1204.
42. N. F. Curtis, *J. Chem. Soc.*, 1964, 2644.
43. B. Dietrich, J. M. Lehn and J. P. Sauvage, *Tet. Lett.*, 1969, **34**, 2885.
44. L. F. Lindoy, *The Chemistry of Macrocyclic Ligand Complexes*, Cambridge University Press, Cambridge 1989.
45. B. Bosnich, C. K. Poon and M. L. Tobe, *Inorg. Chem.*, 1965, **4**, 1102.
46. G. R. Brubaker and D. H. Busch, *Inorg. Chem.*, 1966, **5**, 2114.
47. D. H. Busch, *Acc. Chem. Res.*, 1978, **11**, 392.
48. D. K. Cabbiness and D. W. Margerum, *J. Am. Chem. Soc.*, 1969, **91**, 6540.
49. D. K. Cabbiness and D. W. Margerum, *J. Am. Chem. Soc.*, 1970, **92**, 2151.
50. M. Kodama and E. Kimura, *J. Chem. Soc., Dalton Trans.*, 1976, 116.
51. M. Kodama and E. Kimura, *J. Chem. Soc., Dalton Trans.*, 1976, 2341.

52. F. P. Hinz and D. W. Margerum, *Inorg. Chem.*, 1974, **13**, 2941.
53. R. M. Clay, M. Micheloni, P. Paoletti and W. V. Steele, *J. Am. Chem. Soc.*, 1979, 4119.
54. M. Micheloni and P. Paoletti, *Inorg. Chim. Acta*, 1980, **43**, 109.
55. E. C. Constable, *Coordination Chemistry of Macrocyclic Compounds*, Oxford University Press, 1999.
56. M. Micheloni, P. Paoletti and A. Sabatini, *J. Chem. Soc., Dalton Trans.*, 1983, 1189.
57. T. E. Jones, L. L. Zimmer, L. L. Diaddario, D. B. Rorabacher and L. A. Ochrymowycz, *J. Am. Chem. Soc.*, 1975, **97**, 7163.
58. L. L. Diaddario, L. L. Zimmer, T. E. Jones, L. S. W. L. Sokol, R. B. Cruz, E. L. Yee, L. A. Ochrymowycz and D. B. Rorabacher, *J. Am. Chem. Soc.*, 1979, **101**, 3511.
59. L. S. W. L. Sokol, L. A. Ochrymowycz and D. B. Rorabacher, *Inorg. Chem.*, 1981, **20**, 3189.
60. S. L. W. McWhinnie, *Annu. Rep. Prog. Chem., Sect. A: Inorg. Chem.*, 1991, **88**, 303.
61. S. L. W. McWhinnie, *Annu. Rep. Prog. Chem., Sect. A: Inorg. Chem.*, 1993, **90**, 313.
62. S. L. W. McWhinnie, *Annu. Rep. Prog. Chem., Sect. A: Inorg. Chem.*, 1995, **91**, 351.
63. S. J. Archibald, *Annu. Rep. Prog. Chem., Sect. A: Inorg. Chem.*, 2006, **102**, 332.
64. S. J. Archibald, *Annu. Rep. Prog. Chem., Sect. A: Inorg. Chem.*, 2007, **103**, 264.
65. J. E. Richman and T. J. Atkins, *J. Am. Chem. Soc.*, 1974, **96**, 2268.
66. L. Fabbrizzi, M. Micheloni and P. Paoletti, *J. Chem. Soc., Chem. Comm.*, 1978, 833.
67. L. Fabbrizzi, M. Micheloni and P. Paoletti, *J. Chem. Soc., Dalton Trans.*, 1979, 1581.
68. L. Fabbrizzi, M. Micheloni and P. Paoletti, *J. Chem. Soc., Dalton Trans.*, 1980, 134.

69. A. Anichini, L. Fabbrizzi, P. Paoletti and R. M. Clay, *J. Chem. Soc., Dalton Trans.*, 1978, 577.
70. A. E. Martell and R. D. Hancock, *Coordination Chemistry - A Century of Progress*, American Chemical Society, 1994.
71. K. R. Adam, C. W. G. Ansell, K. P. Dancey, L. A. Drummond, A. J. Leong, L. F. Lindoy and P. A. Tasker, *J. Chem. Soc., Chem. Commun.*, 1986, 1011.
72. L. F. Lindoy, *Pure & Appl. Chem.*, 1997, **69**, 2179.
73. K. R. Adam, K. P. Dancey, A. J. Leong, L. F. Lindoy, B. J. McCool, M. McPartlin and P. A. Tasker, *J. Am. Chem. Soc.*, 1988, **110**, 8471.
74. K. R. Adam, S. P. H. Arshad, D. S. Baldwin, P. A. Duckworth, A. J. Leong, L. F. Lindoy, B. J. McCool, M. McPartlin, B. A. Tailor and P. A. Tasker, *Inorg. Chem.*, 1994, **33**, 1194.
75. M. Kodama and E. Kimura, *J. Chem. Soc., Dalton Trans.*, 1979, 325.
76. T. R. Wagler, Y. Fang and C. J. Burrows, *J. Org. Chem.*, 1989, **54**, 1584.
77. K.-C. Song, M. H. Kim, H. J. Kim and S.-K. Chang, *Tet. Lett.*, 2007, **48**, 7464 and references within.
78. M. Achmatowicz, A. Szumna, T. Zielinski and J. Jurczak, *Tetrahedron*, 2005, **61**, 9031.
79. N. F. Curtis and H. Puschmann, *Polyhedron*, 2006, **25**, 1204.
80. C. Bazzicalupi, A. Bencini, V. Fusi, C. Giorgi, P. Paoletti and B. Valtancoli, *Inorg. Chem.*, 1998, **37**, 941.
81. T. Biver, D. Lombardi, F. Secco, M. R. Tine, M. Venturini, A. Bencini, A. Bianchi and B. Valtancoli, *Dalton Trans.*, 2006, 1524.
82. B. G. Cox, T. V. Hurwood, L. Prodi, M. Montalti, F. Bolletta and C. I. F. Watt, *J. Chem. Soc., Perkin Trans. 2*, 1999, 289.
83. E. P. Kyba, M. G. Siegel, L. R. Sousa, G. D. Y. Sogah and D. J. Cram, *J. Am. Chem. Soc.*, 1973, **95**, 2691.
84. E. B. Kyba, K. Koga, L. R. Sousa, M. G. Siegel and D. J. Cram, *J. Am. Chem. Soc.*, 1973, **95**, 2962.
85. K. Naemura, Y. Tobe and T. Kaneda, *Coord. Chem. Rev.*, 1996, **148**, 199.
86. R. D. Hancock and A. E. Martell, *Chem. Rev.*, 1989, **89**, 1875.

87. J. S. Bradshaw and R. M. Izatt, *Acc. Chem. Res.*, 1997, **30**, 338.
88. H. Elias, *Coord. Chem. Rev.*, 1999, **187**, 37.
89. R. E. DeSimone and M. D. Glick, *J. Am. Chem. Soc.*, 1976, **98**, 762.
90. S. R. Cooper, *Acc. Chem. Res.*, 1988, 141.
91. J. M. Desper and S. H. Gellman, *J. Am. Chem. Soc.*, 1990, **112**, 6732.
92. L. Aronne, B. C. Dunn, J. R. Vyvyan, C. W. Souvignier, M. J. Mayer, T. A. Howard, C. A. Salhi, S. N. Goldie, L. A. Ochrymowycz and D. B. Rorabacher, *Inorg. Chem.*, 1995, **34**, 357.
93. L. Aronne, Q. Yu, L. A. Ochrymowycz and D. B. Rorabacher, *Inorg. Chem.*, 1995, **34**, 1844.
94. C. A. Salhi, Q. Yu, M. J. Heeg, N. M. Villeneuve, K. L. Juntunen, R. R. Schroeder, L. A. Ochrymowycz and D. B. Rorabacher, *Inorg. Chem.*, 1995, **34**, 6053.
95. S. H. Kakos, L. T. Dressel, J. D. Buschendorf, C. P. Kotarba, P. Wijetunge, C. P. Kulatilleke, M. McGillivary, P., G. Chaka, M. J. Heeg, L. A. Ochrymowycz and D. B. Rorabacher, *Inorg. Chem.*, 2006, **45**, 923.
96. H. Meliani, C. Vinas, F. Teixidor, R. Sillanpaa and R. Kivekas, *Polyhedron*, 2001, **20**, 2517.
97. H.-J. Holdt, H. Muller, M. Potter, A. Kelling, U. Schilde, I. Starke, M. Heydenreich and E. Kleinpeter, *Eur. J. Inorg. Chem.*, 2006, 2377.
98. M. Ciampolini, *Pure & Appl. Chem.*, 1986, **58**, 1429.
99. P. G. Kerr, P.-H. Leung and S. B. Wild, *J. Am. Chem. Soc.*, 1987, **109**, 4321.
100. W. J. Vickarious, E. R. Healey, O. B. Berryman and D. W. Johnson, *Inorg. Chem.*, 2005, **44**, 9247.
101. C. D. Carmichael and M. D. Fryzuk, *Dalton Trans.*, 2005, 452.
102. P. G. Edwards, R. Haig, D. Li and P. D. Newman, *J. Am. Chem. Soc.*, 2006, **128**, 3818.
103. R. J. Batchelor, F. W. B. Einstein, I. D. Gay, J.-H. Gu, S. Mehta, B. M. Pinto and X.-M. Zhou, *Inorg. Chem.*, 2000, **39**, 2558.
104. S. Panda, H. B. Singh and R. J. Butcher, *Inorg. Chem.*, 2004, **43**, 8532.

105. T. Schimizu, M. Kawaguchi, T. Tsuchia, K. Hirabayashi and N. Kamigata, *J. Org. Chem.*, 2005, **70**, 5036.
106. H. K. Frensdorff, *J. Am. Chem. Soc.*, 1971, **93**, 600.
107. L. Fabbrizzi, *Adv. Mol. Rel.*, 1980, **18**, 109.
108. G. Anderegg, A. Ekstrom, L. F. Lindoy and R. J. Smith, *J. Am. Chem. Soc.*, 1980, **102**, 2670.
109. L. F. Lindoy, *Chem. in Aust.*, 1991, 157.
110. A. Ekstrom, L. F. Lindoy and R. J. Smith, *J. Am. Chem. Soc.*, 1979, **101**, 4014.
111. A. Ekstrom, L. F. Lindoy and R. J. Smith, *Inorg. Chem.*, 1980, **19**, 724.
112. H. J. Goodwin, K. Henrick, L. F. Lindoy, M. McPartlin and P. A. Tasker, *Inorg. Chem.*, 1982, **21**, 3261.
113. J. Kim, L. F. Lindoy, T.-H. Ahn and G.-S. Choi, *Synth. Commun.*, 2004, **34**, 3653.
114. F. Li, R. Delgado, M. G. B. Drew and V. Felix, *Dalton Trans.*, 2006, 5396.
115. E. Luboch, E. Wagner-Wysiecka, M. Feinerman-Melnicova, L. F. Lindoy and J. F. Biernat, *Supramol. Chem.*, 2006, **18**, 593.
116. M. Wenzel, K. Gloe, K. Gloe, G. Bernhard, J. K. Clegg, X.-K. Ji and L. F. Lindoy, *New J. Chem.*, 2008, **32**, 132.
117. B. C. Westerby, K. L. Juntunen, G. H. Leggett, V. B. Pett, M. J. Koenigbauer, M. D. Purgett, M. J. Taschner, L. A. Ochrymowycz and D. B. Rorabacher, *Inorg. Chem.*, 1991, **30**, 2109.
118. M. Micheloni, P. Paoletti, L. Siegfried-Hertli and T. A. Kaden, *J. Chem. Soc., Dalton Trans.*, 1985, 1169.
119. H. Alp, Z. Biykhoglu, M. Ocak, U. Ocak, H. Kantekin and G. Dilber, *Sep. Sci. Technol.*, 2007, **42**, 835.
120. J. Seo, I. Yoon, J.-E. Lee, M. R. Song, S. Y. Lee, S. H. Park, T. H. Kim, K.-M. Park, B. G. Kim and S. S. Lee, *Inorg. Chem. Commun.*, 2005, **8**, 916.
121. K.-M. Park, Y. H. Lee, Y. Jin, J. Seo, I. Yoon, S. C. Lee, S. B. Park, M.-S. Gong, M. L. Seo and S. S. Lee, *Supramol. Chem.*, 2004, **16**, 51.
122. M. W. Glenny, L. G. A. van de Water, W. L. Driessen, J. Reedijk, A. J. Blake, C. Wilson and M. Schroeder, *Dalton Trans.*, 2004, 1953.

123. F. Arnaud-Neu, M.-J. Schwing-Weill, R. Louis and R. Weiss, *Inorg. Chem.*, 1979, **18**, 2956.
124. A. Bianchi, L. Bologni, P. Dapporto, M. Micheloni and P. Paoletti, *Inorg. Chem.*, 1984, **23**, 1201.
125. V. J. Thom, M. S. Shaikjee and R. D. Hancock, *Inorg. Chem.*, 1986, **25**, 2992.
126. M. Vetrichelvan, Y.-H. Lai and K. F. Mok, *Inorg. Chim. Acta*, 2004, **357**, 1397.
127. Y. Jin, I. Yoon, J. Seo, J.-E. Lee, S.-T. Moon, J. Kim, S. W. Han, K.-M. Park, L. F. Lindoy and S. S. Lee, *Dalton Trans.*, 2005, 788.
128. A. J. Atkins, D. Black, A. J. Blake, A. Martin-Becerra, S. Parsons, L. Kuiz-Ramirez and M. Schroeder, *Chem. Commun.*, 1996, 457.
129. N. H. Pilkington and R. Robson, *Aust. J. Chem.*, 1970, **23**, 2225.
130. M. Gressenbuch and B. Kersting, *Eur. J. Inorg. Chem.*, 2007, 90.
131. Z.-L. Yuan, Q.-L. Zhang, X. Liang, B.-X. Zhu, L. F. Lindoy and G. Wei, *Polyhedron*, 2008, **27**, 344.
132. L. F. Lindoy, *Coord. Chem. Rev.*, 1998, **174**, 327.
133. X. Liang and P. J. Sadler, *Chem. Soc. Rev.*, 2004, **33**, 246.
134. F. Liang, S. Wan, Z. Li, X. Xiong, L. Yang, X. Zhou and C. Wu, *Current Medicinal Chemistry*, 2006, **13**, 711.
135. P. V. Bernhardt and E. J. Hayes, *Inorg. Chem.*, 2002, **41**, 2892.
136. J. D. Chartres, L. F. Lindoy and G. V. Meehan, *Tetrahedron*, 2006, **62**, 4173.
137. A. M. Groth, L. F. Lindoy, G. V. Meehan, B. W. Skelton and A. H. White, *Inorg. Chem. Comm.*, 2007, **10**, 1070.
138. H. J. Kim, Y. Jin, J. Seo, J.-E. Lee, J. Y. Lee and S. S. Lee, *Inorg. Chem. Comm.*, 2006, **9**, 1040.
139. I. M. Atkinson, J. D. Chartres, A. M. Groth, L. F. Lindoy, M. P. Lowe and G. V. Meehan, *Chem. Commun.*, 2002, 2428.
140. B. Dietrich, J. M. Lehn and J. P. Sauvage, *Tetrahedron*, 1973, **29**, 1647.
141. J. M. Lehn and J. P. Sauvage, *J. Am. Chem. Soc.*, 1975, **97**, 6700.
142. J. M. Lehn, *Acc. Chem. Res.*, 1978, **11**, 49.
143. S. Brooker, J. D. Ewing, T. K. Ronson, C. J. Harding, J. Nelson and D. J. Speed, *Inorg. Chem.*, 2003, **42**, 2764.

144. Z. Ma and R. Cao, *J. Mol. Struct.*, 2005, **738**, 137.
145. T. Gyr, H. R. Macke and M. Hennig, *Angew. Chem., Int. Ed. Engl.*, 1997, **36**, 2786.
146. T. A. Kaden, *Dalton Trans.*, 2006, 3617.
147. M. W. Glenny, M. Lacombe, J. B. Love, A. J. Blake, L. F. Lindoy, R. C. Luckay, K. Gloe, B. Antonioli, C. Wilson and M. Schroeder, *New J. Chem.*, 2006, **30**, 1755.
148. L. F. Lindoy, *Pure & Appl. Chem.*, 1989, **61**, 1575.
149. R. D. Hancock, *J. Chem. Ed.*, 1992, **69**, 615.
150. B. P. Hay and R. D. Hancock, *Coord. Chem. Rev.*, 2001, **212**, 61.
151. P. Comba and W. Schiek, *Coord. Chem. Rev.*, 2003, **238**, 21.
152. L. G. Armstrong and L. F. Lindoy, *Inorg. Chem.*, 1975, **14**, 1322.
153. L. F. Lindoy, H. C. Lip, L. F. Power and J. H. Rea, *Inorg. Chem.*, 1975, **15**, 1724.
154. L. G. Armstrong, P. G. Grimsley, L. F. Lindoy, H. C. Lip, V. A. Norris and R. J. Smith, *Inorg. Chem.*, 1978, **17**, 2350.
155. L. F. Lindoy, *Prog. Macrocyclic Chem.*, 1987, **3**, 53.
156. J.-E. Lee, J. Y. Lee, J. Seo, S. Y. Lee, H. J. Kim, S. B. Park, K.-M. Park, L. F. Lindoy and S. S. Lee, *Polyhedron*, 2008, **27**, 3004.
157. S. Bilge, Z. Kilic, T. Hokelek and B. Erdogan, *J. Mol. Struct.*, 2004, **691**, 85.
158. V. Alexander, *Chem. Rev.*, 1995, **95**, 273.
159. R. M. Izatt, K. Pawlak, J. S. Bradshaw and R. L. Bruening, *Chem. Rev.*, 1995, **95**, 2529.
160. K. R. Adam, D. S. Baldwin, P. A. Duckworth, A. J. Leong, L. F. Lindoy, M. McPartlin and P. A. Tasker, *J. Chem. Soc., Chem. Commun.*, 1987, 1124.
161. K. R. Adam, D. S. Baldwin, A. Bashall, L. F. Lindoy, M. McPartlin and H. R. Powell, *J. Chem. Soc., Dalton Trans.*, 1994, 237.
162. K. R. Adam, D. S. Baldwin, P. A. Duckworth, L. F. Lindoy, M. McPartlin, A. Bashall, H. R. Powell and P. A. Tasker, *J. Chem. Soc., Dalton Trans.*, 1995, 1127.
163. I. Yoon, J. Seo, J.-E. Lee, M. R. Song, S. Y. Lee, K. S. Choi, O.-S. Jung, K.-M. Park and S. S. Lee, *Dalton Trans.*, 2005, 2352.

164. K. R. Adam, M. Antolovich, D. S. Baldwin, P. A. Duckworth, A. J. Leong, L. F. Lindoy, M. McPartlin and P. A. Tasker, *J. Chem. Soc., Dalton Trans.*, 1993, 1013.

165. K. R. Adam, K. P. Dancey, B. A. Harrison, A. J. Leong, L. F. Lindoy, M. McPartlin and P. A. Tasker, *J. Chem. Soc., Chem. Commun.*, 1983, 1351.

166. R. M. Izatt, K. Pawlak, J. S. Bradshaw and R. L. Bruening, *Chem. Rev.*, 1991, **91**, 1721.

167. R. D. Hancock, *Coord. Chem. Rev.*, 1994, **133**, 39.

168. D. Meyerstein, *Coord. Chem. Rev.*, 1999, **185-186**, 141.

169. G. Golub, H. Cohen, P. Paoletti, A. Bencini, L. Messory, I. Bertini and D. Meyerstein, *J. Am. Chem. Soc.*, 1995, **117**, 8353.

170. T. Clark, M. Hennemann, R. van Eldik and D. Meyerstein, *Inorg. Chem.*, 2002, **41**, 2927.

171. T. W. Hambley, L. F. Lindoy, J. R. Reimers, P. Turner, G. Wei and A. N. Widmer-Cooper, *J. Chem. Soc., Dalton Trans.*, 2001, 614.

172. J. Kim, T.-H. Ahn, M. Lee, A. J. Leong, L. F. Lindoy, B. R. Rumbel, B. W. Skelton, T. Strixner, G. Wei and A. H. White, *J. Chem. Soc., Dalton Trans.*, 2002, 3993.

173. J. R. Price, M. Feinerman-Melnicova, D. E. Fenton, K. Gloe, L. F. Lindoy, T. Rambush, B. W. Skelton, P. Turner, A. H. White and K. Wichmann, *Dalton Trans.*, 2004, 3715.

174. M. Feinerman-Melnicova, A. Nezhadali, G. Rounaghi, J. C. McMurtrie, J. Kim, K. Gloe, M. Langer, S. S. Lee, L. F. Lindoy, T. Nishimura, K.-M. Park and J. Seo, *Dalton Trans.*, 2004, 122.

175. K. R. Adam, A. J. Leong, L. F. Lindoy, H. C. Lip, B. W. Skelton and A. H. White, *J. Am. Chem. Soc.*, 1983, **105**, 4645.

176. K. R. Adam, M. Antolovich, D. S. Baldwin, L. G. Brigden, P. A. Duckworth, L. F. Lindoy, A. Bashall, M. McPartlin and P. A. Tasker, *J. Chem. Soc., Dalton Trans.*, 1992, 1869.

177. C. A. Davis, A. J. Leong, L. F. Lindoy, J. Kim and S.-H. Lee, *Aust. J. Chem.*, 1998, **51**, 189.

178. C. A. Davis, P. A. Duckworth, A. J. Leong, L. F. Lindoy, A. Bashall and M. McPartlin, *Inorg. Chim. Acta*, 1998, **273**, 372.

179. I. M. Atkinson, K. A. Byriel, P. S. K. Chia, C. H. L. Kennard, A. J. Leong, L. F. Lindoy, M. P. Lowe, S. Mahendran, G. Smith and G. Wei, *Aust. J. Chem.*, 1998, **51**, 985.

180. K. R. Adam, A. J. Leong, L. F. Lindoy, B. J. McCool, A. Ekstrom, I. Liepa, P. A. Harding, K. Henrick, M. McPartlin and P. A. Tasker, *J. Chem. Soc., Dalton Trans.*, 1987, 2537.

181. K. R. Adam, L. F. Lindoy, H. C. Lip, J. H. Rea, B. W. Skelton and A. H. White, *J. C. S. Dalton*, 1981, 74.

182. K. J. Park, J.-H. Kim, G. V. Meehan, T. Nishimura, L. F. Lindoy, S. S. Lee, K.-M. Park and I. Yoon, *Aust. J. Chem.*, 2002, **55**, 773.

183. D. S. Baldwin, PhD Thesis, unpublished work, James Cook University, 1987.

184. K. R. Adam, D. S. Baldwin, L. F. Lindoy, G. V. Meehan, I. M. Vasilescu and G. Wei, *Inorg. Chim. Acta*, 2003, **352**, 46.

Chapter 2 – Synthesis of macrocyclic ligands

2.1 Introductory remarks

Over recent years there has been increased interest in both the synthesis and potential of unsymmetrical ligands for use in a number of applications. For example, unsymmetrically substituted Schiff-base ligands,[1] porphyrins,[2] ferrocenes,[3] and 1,3-diketimines,[4] have all been investigated with respect to the influence of the dissymmetry on their reaction behaviour. In particular, Schiff-base ligands are extremely versatile and their widespread use reflects their important role as metal coordination reagents[5, 6] and in supramolecular chemistry.[7] In addition, Schiff-bases are of considerable interest in dynamic combinatorial chemistry,[8] as components for molecular motors[9] as well as for numerous biological and medical applications.

A number of comprehensive reviews have been published covering the design and development of synthetic procedures for the preparation of mono-, di- and poly-nuclear Schiff-base complexes as well as for the introduction of asymmetry into such ligands.[10-15]

The synthetic procedure employed to prepare the macrocycles in the present study has, in each case, involved Schiff-base formation as an intermediate step in the overall reaction sequence. In view of this, a treatment of Schiff-base systems has been given some emphasis in the discussion that follows.

2.2 Synthetic procedures

The procedures for synthesising macrocyclic Schiff-base ligands can be broadly divided into two major categories. The first of these involves the use of a metal ion as a ‘template’ to promote the cyclisation reaction. Alternatively, the macrocycle can be prepared by conventional multi-step organic synthesis procedures. Irrespective of the method chosen, the priority is to maximise the yield of the desired product by selecting strategies which inhibit competing reactions such as linear polymerisation.[16]

2.2.1 Metal-ion template synthesis

The first *rational* syntheses of macrocycles around metal ion templates were demonstrated in the early 1960s by the Busch group. Thus, Schiff-base ligands derived from α-diketones and β-mercaptoethylamine were stabilised by metal complexation (structure **130**)[17] and then reacted further with difunctional alkylating agents such as α,α′-dibromo-*o*-xylene to produce macrocyclic ligands of type **131** (**Figure 2.1**).[18] Since then, numerous other synthetic procedures have been developed involving the use of a metal-ion template for the synthesis of macrocyclic and macrobicyclic ligands, as well as for the preparation of interlocked structures.[12, 13, 19]

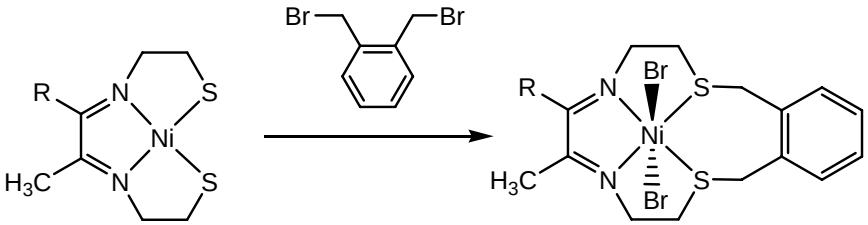

130 **131**

Figure 2.1 An early rational metal-ion template synthetic procedure for obtaining Schiff-base macrocyclic ligand complexes of type **131**.

Thompson and Busch have delineated two possible roles for the metal ion during this type of synthesis: to stabilise the macrocycle once formed (*equilibrium displacement* or *thermodynamic template effect*) or to direct, through coordination, the steric course of the condensation reaction (*kinetic template effect*).[17, 18, 20] While examples of the operation of both these effects have been documented, for a given reaction, the role of the metal ion may be quite complex and, for example, involve some aspects of both the above-mentioned effects.[21]

The formation of [1 + 1] and [2 + 2] Schiff-base macrocycles in the presence of a metal-ion template is very often a multistep process (**Scheme 2.1**).[22] For example, following the initial condensation between a dicarbonyl compound and a diamine, the reaction can further proceed via an intramolecular condensation to give the [1 + 1] product or by a second intermolecular condensation to yield the [2 + 2] ring.

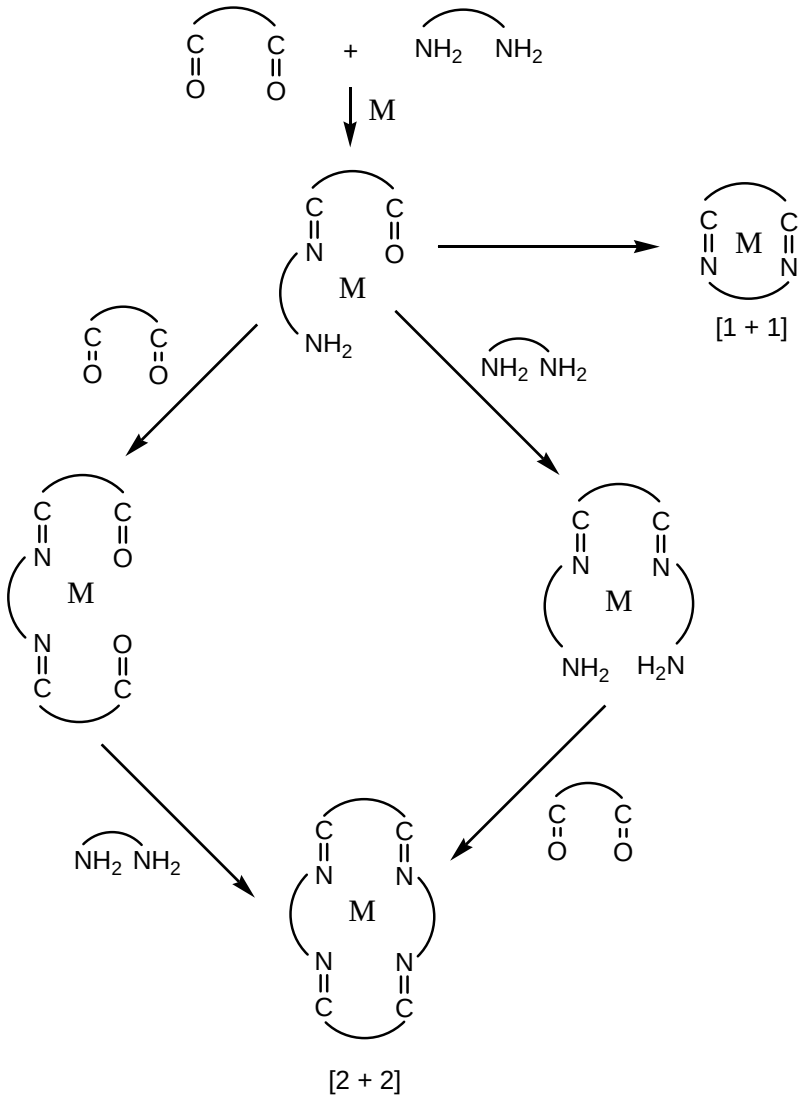

Scheme 2.1 Possible mechanistic pathways for the multistep template synthesis of a tetraimine macrocycle. (Adapted from [22]).

Finally, it needs to be noted that the synthesis of metal complexes of macrocyclic ligands using the 'template' approach in many cases has limitations with respect to the metal to be employed, and sometimes does not allow the isolation of the macrocycle free of its metal ion.[23, 24] With respect to the above, it needs to be noted that in the absence of a metal template, reactions between dicarbonyl and diamine compounds may generate a wide range of products including polycondensation products.[15]

2.2.2 Direct macrocycle synthesis

There are numerous documented examples of Schiff base macrocycles prepared in reasonable yields in the absence of a metal template[15, 25] and also cases where the presence of a metal ion template did not improve the yield.[26]

In order to inhibit linear polymerisation reactions, many macrocyclisation reactions have traditionally been performed under high dilution conditions (10^{-2} – 10^{-3} M and lower),[16] with the starting compounds being added slowly to the reaction solution in stoichiometric ratios. Nevertheless, there are also reports of Schiff-base macrocycle syntheses carried out at higher concentrations,[25] for example at 0.1 M.[27]

However, overall, the *direct* synthesis of *cyclic* Schiff bases remains a challenge since different condensation products (acyclic, cyclic or polymeric in nature) often readily result from the use of di- or poly-functional precursors (see for example **Scheme 2.2**) and the formation of a variety of by-products (including hydrolysis or solvolysis products) can result in the purification of the designed macrocycle being difficult and may lead to a considerably reduced yield.[12]

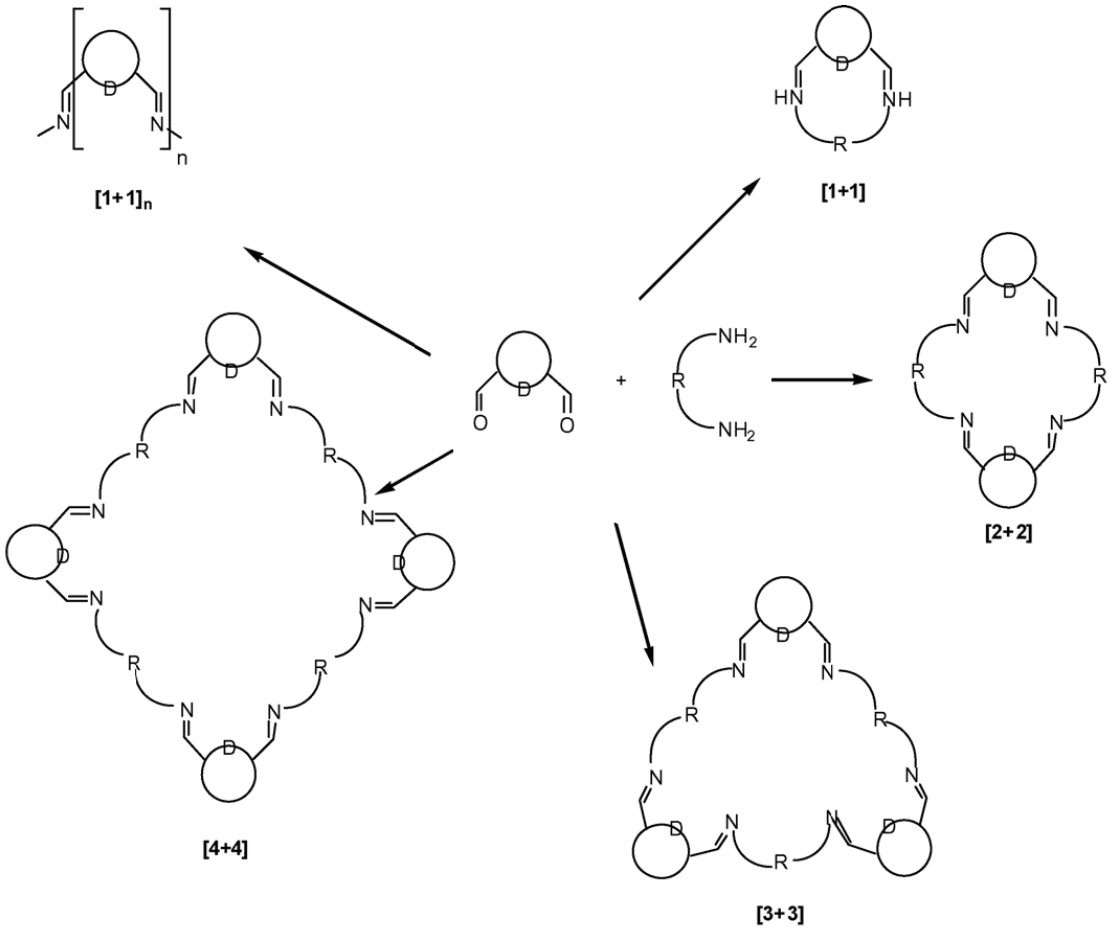

Scheme 2.2 Possible condensation products from a representative Schiff base synthesis.[12]

2.3 The present study: potentially pentadentate macrocyclic ligands with unsymmetrically positioned heteroatoms

As discussed in Chapter 1, previous synthetic studies in the author's laboratory have produced an extended series of potentially pentadentate mixed donor macrocycles with a symmetrical arrangement of their donor atoms (see **90** – **126**), but only three examples of corresponding unsymmetrical ligands (**127** – **129**) have been synthesised due, in part, to the relatively laborious nature of such preparations. The present chapter describes the synthesis, or attempted synthesis, of the related unsymmetrical systems, **132** – **144**, along with their corresponding precursors.

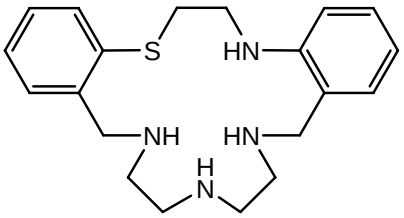

132

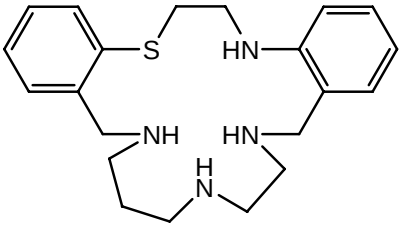

133

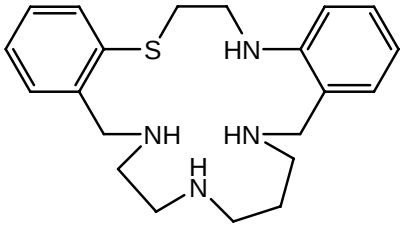

134

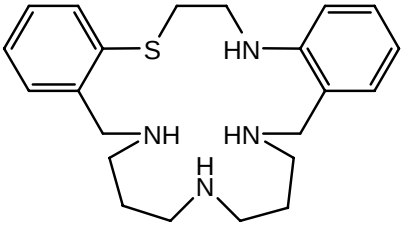

135

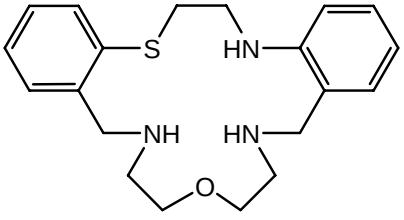

136

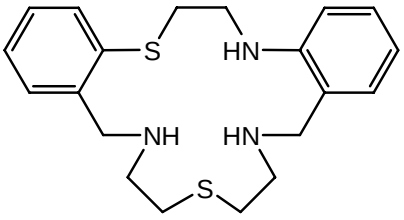

137

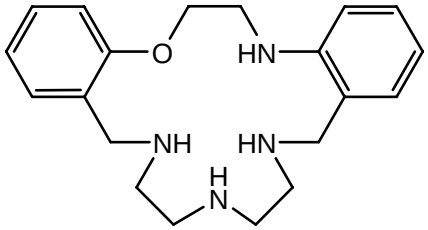

138

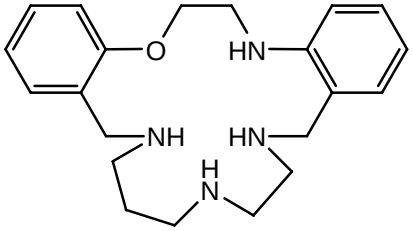

139

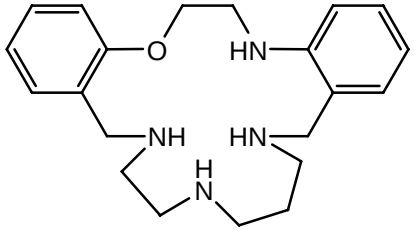

140

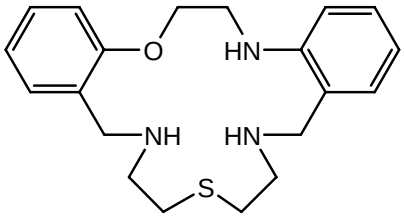

141

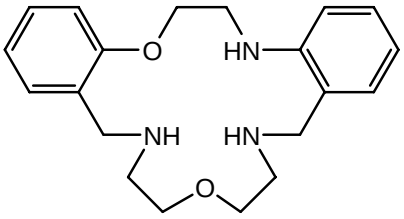

142

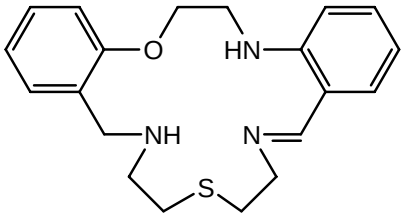

143

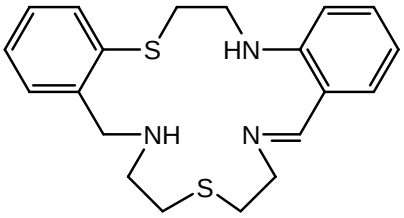

144

2.4 Macrocyclisation reactions

2.4.1 Preparation of unsymmetrical dialdehyde precursors

The unsymmetrical dialdehydes employed in the present study have the mesylate **147** as a common precursor. This was obtained *via* a two step synthesis involving the reaction (at low temperature) of ethylene oxide with methyl anthranilate (**145**) in glacial acetic acid[28] to yield the corresponding alcohol **146**. The intermediate **146** was then converted to **147** by reaction with methanesulfonyl chloride in the presence of triethylamine (**Scheme 2.3**). The mesylate **147** was prepared in yields of up to 80%; however, it was found necessary to remove the purified product from the recrystallisation solvent as soon as possible and store it under nitrogen in the absence of light if degradation was to be avoided.

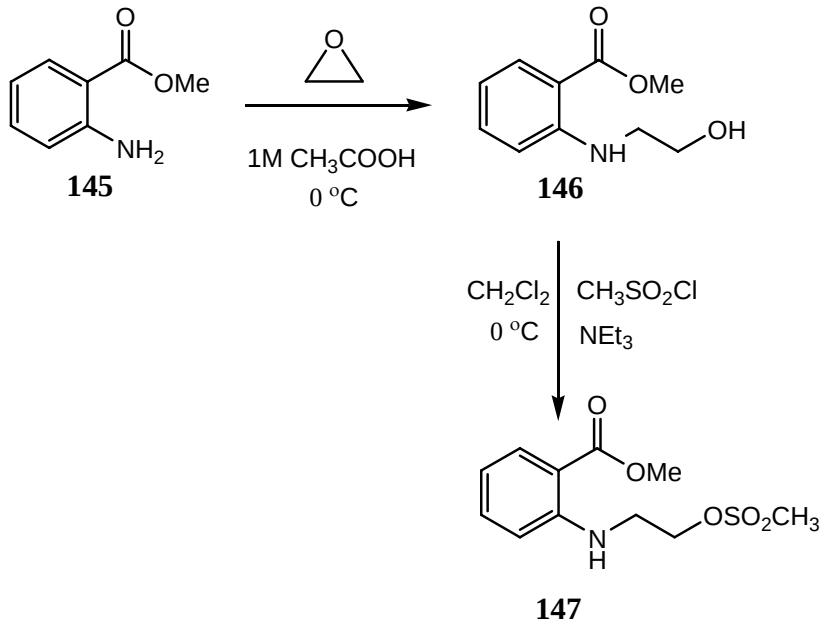

Scheme 2.3 Synthesis of the mesylate precursor **147**

The dialdehydes incorporating either an SN- or an ON-donor sequence were then prepared by the methods outlined in **Schemes 2.4** and **2.5** respectively, with each of the intermediates shown in these schemes requiring purification by either recrystallisation or

chromatography (or a combination of both) prior to being utilised for the subsequent condensation step.

For the synthesis of the SN-dialdehyde (**Scheme 2.4**), thiosalicylic acid (**148**) was esterified with ethanol under acid catalysis[29] and the resulting ethyl ester **149** was alkylated with **147** in the presence of potassium carbonate (K_2CO_3) to give the SN-diester **150** in yields varying between 27 – 64% from repeated preparations. The ^{1}H and ^{13}C NMR spectra for the crude diester were in accord with those expected for **150**. Thus, in addition to the signals corresponding to eight aromatic protons, the ^{1}H NMR spectrum contained the methyl ester singlet at δ 3.86 and the ethyl ester quartet and triplet at δ 4.44 and δ 1.41 respectively. The spectrum also showed two-proton multiplets at δ 3.56 and δ 3.22, assigned to the methylene groups adjacent to the secondary amine and the thioether respectively. Recrystallisation of the initial product from a mixture of ethanol and chloroform afforded pure **150** in 74% yield. Subsequent reduction of the diester with lithium aluminium hydride ($LiAlH_4$) in dry tetrahydrofuran (THF) gave the diol **151** as a pale yellow oil. The ^{1}H NMR spectrum of this product lacked signals corresponding to the ester functionalities of **150** and instead contained two-proton singlets at δ 4.46 and δ 4.65, consistent with the presence of methylene protons adjacent to the OH groups as required for **151**. Purification of this product was carried out by column chromatography followed by recrystallisation. The SN-diol **151** was obtained in yields up to 90%.

The most efficient approach for generating the SN-dialdehyde **152** was found to be the selective oxidation of **151** using barium manganate ($BaMnO_4$). This reagent was chosen for its selective and mild oxidation properties; it was prepared in good yield using the literature method.[30] Oxidation of **151** was carried out in freshly distilled dichloromethane (DCM) due to the susceptibility of the oxidising agent to decomposition under acidic conditions. The progress of the reaction was followed by thin layer chromatography;

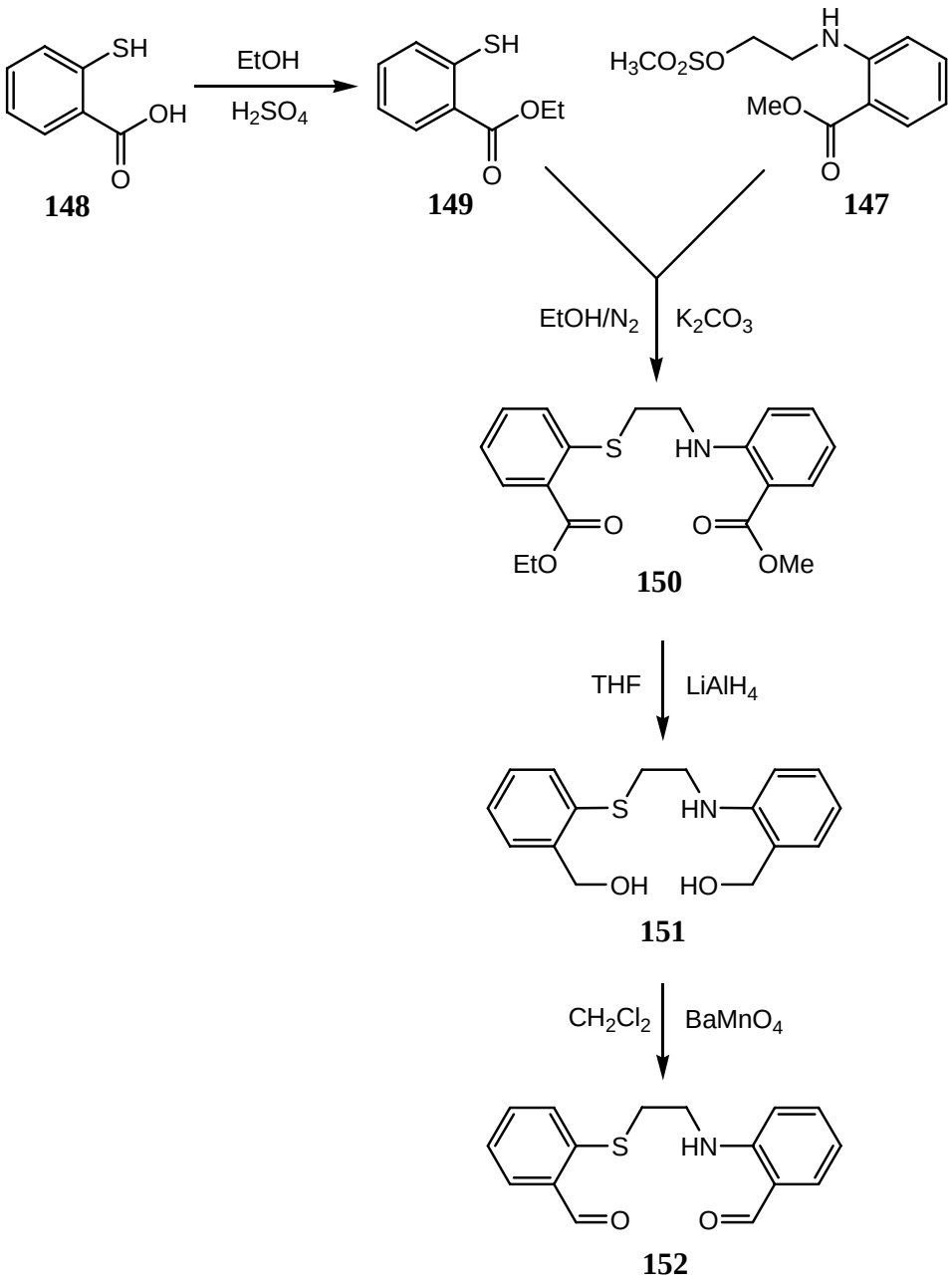

Scheme 2.4 Synthesis of the dialdehyde **152** incorporating a thioether group.

further $BaMnO_4$ additions were occasionally required in order to achieve complete oxidation. Gravity filtration through a small plug of celite or silica gel successfully separated the DCM solution containing **152** from the solid remaining in the reaction solution. It proved necessary to wash the reagent 'cake' repeatedly in order to ensure

efficient recovery of the product. The recovered yield was also improved when the preparation of the dialdehyde was carried out in multiple small batches rather than on a large scale. Under these conditions yields of up to 75% were obtained. Almost invariably, the crude product required chromatography prior to recrystallisation. In the ^{1}H NMR spectrum of the purified **152**, the two-proton singlets at δ 4.46 and δ 4.65 present in the ^{1}H NMR spectrum of **151** were no longer observed and were replaced by two one-proton singlets at δ 9.81 and δ 10.42, as expected for the target dialdehyde.

The possibility of using other oxidation reagents in the above procedure was also investigated, however, the results in each case were not satisfactory. For example, small scale attempts to oxidise **151** to the corresponding dialdehyde with tetra-n-butyl ammonium dichromate and also with pyridinium chlorochromate were not successful, each resulting in a mixture of products which seemed to be a combination of partially oxidised materials. Very low yields of the dialdehyde **152** were observed in each case and no further effort was made to separate and identify any of the remaining products.

The ON-dialdehyde (**156**), incorporating secondary amine and ether functionalities in its backbone, was obtained using a parallel procedure (**Scheme 2.5**) to that just described, starting from salicylaldehyde **153** and mesylate **147**, which afforded the ester **154**. In addition to the expected eight aromatic protons, the ^{1}H NMR spectrum of **154** contained signals for the aldehyde and methyl ester functionalities at δ 10.52 and δ 3.86 respectively, as well as a two-proton triplet at δ 4.33 corresponding to the methylene group adjacent to the ether functionality and a second (broad) two-proton triplet at δ 3.73 characteristic of the methylene neighboring the secondary amine.

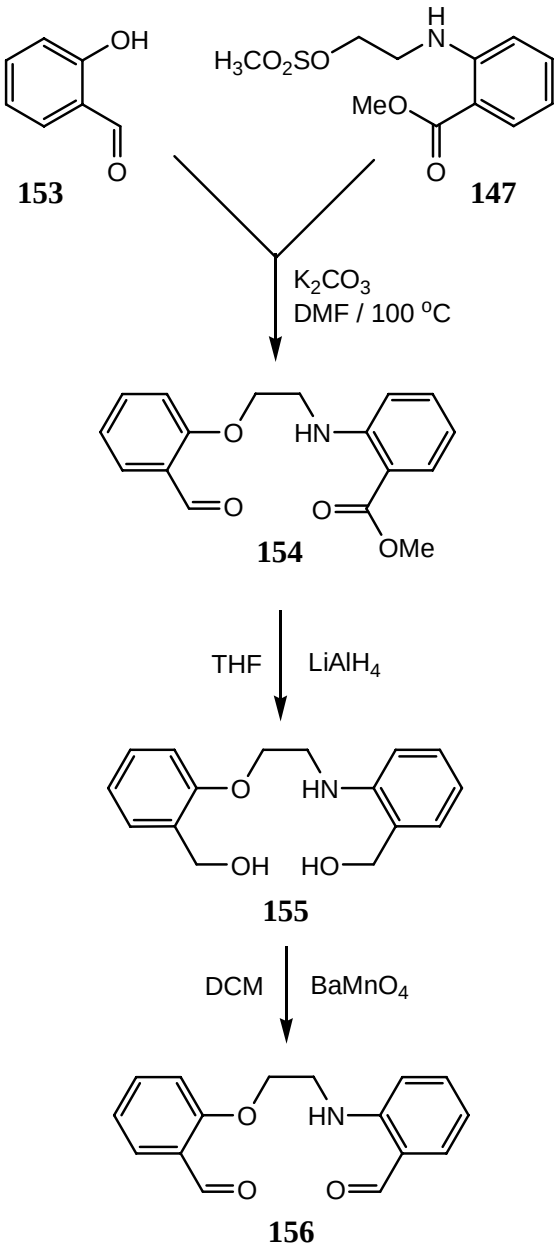

Scheme 2.5 Synthesis of the dialdehyde **156** incorporating an ether oxygen.

Reduction of **154** with $LiAlH_4$ in dry THF under a nitrogen atmosphere afforded the diol **155**. The ^1H NMR spectrum of the crude product lacked the singlets at δ 10.52 and δ 3.86 present in **154**; instead it contained a four proton singlet at δ 4.59, corresponding to the two methylene groups adjacent to alcohol functionalities in **155**. Column

chromatography on silica gel with DCM as solvent followed by recrystallisation from a DCM/hexane mixture afforded pure **155** in yields as high as 85%. Selective oxidation of **155** with $BaMnO_4$ resulted in **156**. The ^1H NMR of this product showed the appearance of two one-proton singlets at δ 9.80 and δ 10.52, indicative of dialdehyde formation; the four proton singlet at δ 4.59 (present in the spectrum of **155**) was absent.

2.4.2 Reductive amination reactions

The synthesis of the new unsymmetrical macrocycles in each case involved two reductive amination steps. That is, it involved the Schiff-base condensation between the appropriate linear di- or tri-amine and unsymmetrical dialdehyde precursors followed by *in situ* reduction of the resulting diimine with sodium borohydride ($NaBH_4$). (**Scheme 2.6**).

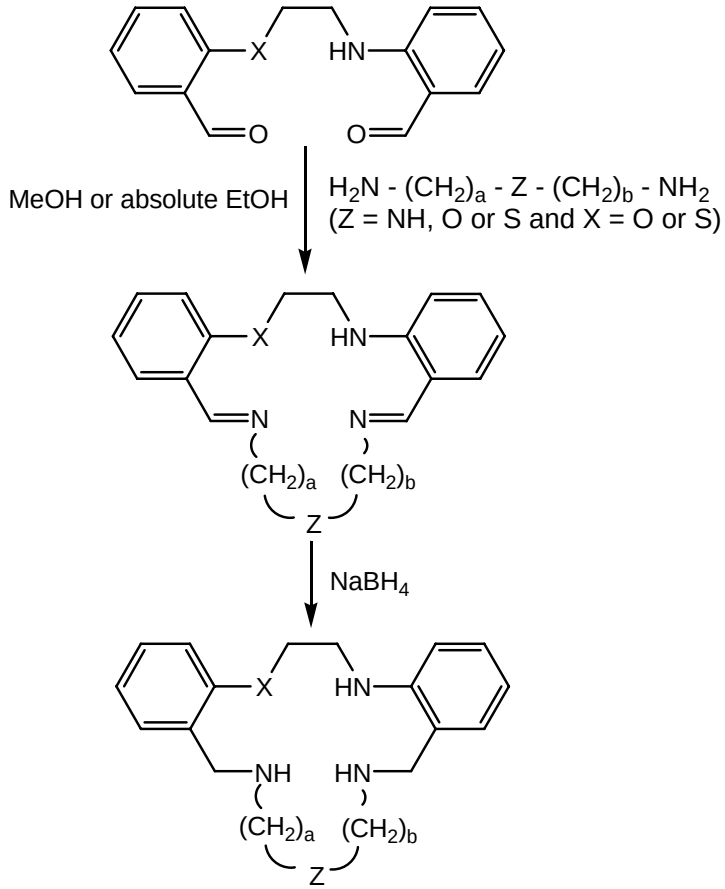

Scheme 2.6 The double reductive amination reaction employed for preparation of **132** – **144**.

Isolation of the diimine (or aminal) intermediate prior to reduction was found to be unnecessary. In each case the ^{1}H and ^{13}C NMR spectra of the purified products confirmed the absence of imine functions.

Moderate-dilution techniques were employed for these syntheses in an attempt to aid cyclisation over linear polymerisation and yields between 30 – 80% were obtained following various reaction conditions and work-up procedures; the latter included chromatography and/or recrystallisation, with no uniform purification procedure being applicable to all ligands prepared. Each macrocycle was typically synthesised several times, providing the opportunity to optimise the synthesis and work-up conditions in order to improve the yields. In all cases the progress of the respective reactions was followed through the use of thin layer chromatography (TLC) as well as by ^{1}H NMR spectroscopy.

Structural elucidation of the new macrocycles was initially carried out using 1D and 2D NMR experiments. Initial emphasis was placed on NMR structural elucidation, with X-ray crystallography data for selected compounds being obtained at a later stage. The proposed structures were also supported by microanalysis data. In addition, in all cases the mass spectra of the purified ligands did not contain peaks at *m/z* values greater than those expected for monomeric [1 + 1] condensation products.

Attempts to prepare (and isolate) the 19-membered SN_4 macrocycle **135** were inhibited by the presence of large amounts of polymeric material and possibly other by-products. However ^{1}H NMR spectra indicated that a small amount of **135** was present in the reaction mixture; nevertheless, after several tries, attempts to isolate this macrocycle were not pursued.

The initial success (see pages 86 – 87) in synthesising and separating the isomeric macrocyclic products **133** and **134** prompted the attempted synthesis of their ON-analogues **139** and **140**. However, in these cases the NMR data for the crude reaction

products indicated the presence of mainly polymeric material and no further effort was made to isolate these ligands.

2.4.3 Specific macrocycle syntheses

132 (17-membered SN/NNN)

Reaction of the unsymmetrical SN-dialdehyde **152** with di(2-aminoethyl)amine followed by *in situ* reduction with $NaBH_4$ afforded **132**. The ^{1}H and ^{13}C NMR spectra of the purified ligand established the absence of imine functions while the mass spectral and microanalysis data confirmed the macrocycle was a [1 + 1] condensation product. 2D NMR spectroscopy was employed to aid proton and carbon chemical shift assignments as well as long-range atom connectivities for structural determination (**Figures 2.2** and **2.3**). Selected NMR spectra for **132** are included in **Appendix A**.

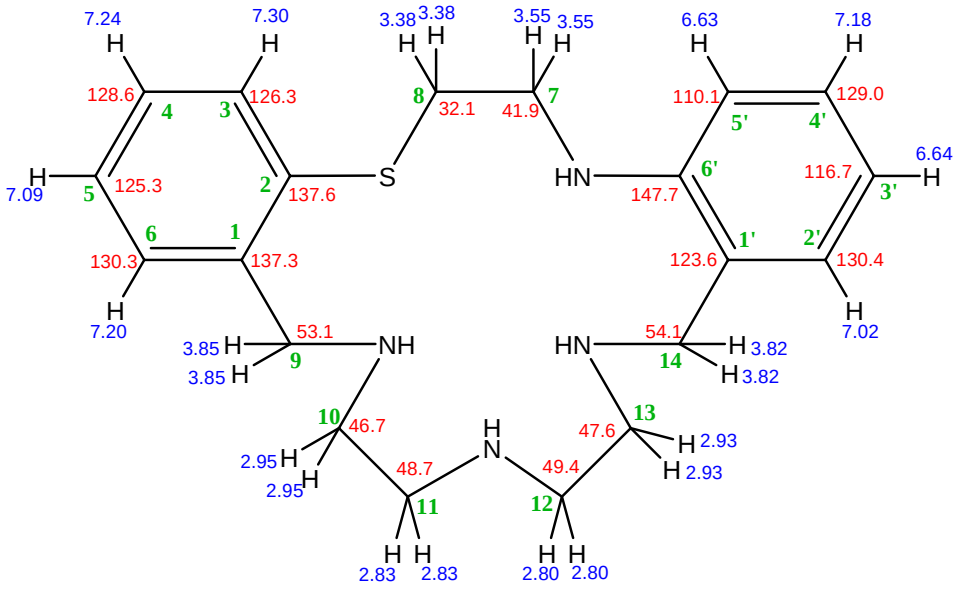

Figure 2.2 ^{1}H and ^{13}C NMR (HSQC, J =140 Hz) assignments for **132** (non-systematic atom numbering employed for ease of discussion).

The conformational flexibility of the macrocyclic backbone portion which includes the NNN-donor string is reflected in the equivalence of the benzylic methylene hydrogens which appear as two-proton singlets at δ 3.85 and δ 3.82.

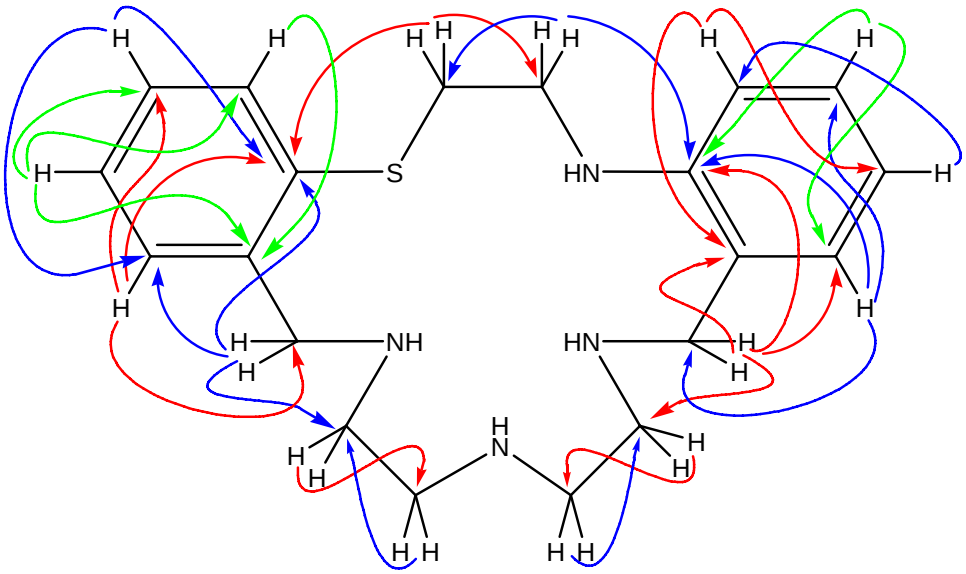

Figure 2.3 Long range NMR (HMBC, J = 8 Hz) correlations* for **132**.

The benzylic methylene signal at δ 3.82 (H14) showed long range correlations to the aromatic carbon atoms of the N-substituted ring at 147.6, 123.6 and 130.4 ppm (carbons 6′, 1′ and 2′ respectively) as well as, across the nitrogen, to the signal at 47.6 ppm (C13). The low-field position of the quaternary carbon signal at 147.6 ppm provided evidence for N-substitution.[32] The benzylic methylene protons at δ 3.85 (H9) correlated with the signals at 137.6, 130.3 and 46.7 ppm (C2, C6 and C10 respectively). The assignment for C2 was made on the basis of a correlation from the methylene group at δ 3.38 (H8). The same methylene signal showed a strong correlation to the carbon at 41.9 ppm (C7). Correlations observed from H7 (δ 3.55) to the carbons at 32.1 ppm (C8) and 147.6 ppm (C 6′), in conjunction with the chemical shifts of C7 and C8, indicative of attachment to N and S respectively, were used to assign the atom connectivity in the upper part of the macrocyclic backbone. In the N-substituted aromatic ring, correlations were observed from the proton at δ 7.01 (H2′) to C6′, C4′ and C14. The proton at δ 6.63 (H5′) showed correlations to the carbon at 123.6 ppm (C1′) and the signal at 116.6 ppm

*It should be noted that in this figure, as well as in subsequent diagrams displaying long-range NMR correlation arrows, there is no significance attached to the colour of these arrows; the different colours are used for clarity only. In addition, for consistency, correlations originating from one set of proton signals have been assigned the same colour.

(C3′), while the signal at δ 6.64 (H3′) correlated to the carbons at 123.6 and 110.0 ppm (C1′ and C5′ respectively). The multiplicities (dd and dt respectively) of the signals assigned to H5′ and H3′ are as expected. The assignment of the remaining proton signal at δ 7.18 (H4′) was confirmed by correlations to C1′ and C3′. The S-substituted aromatic ring was assigned in a similar fashion, as illustrated by the correlation arrows given in **Figure 2.3**.

Crystals of **132** suitable for X-ray study were obtained from acetonitrile. The X-ray structure obtained for this macrocycle, as do all the remaining X-ray structures described in this chapter, confirmed the atom connectivity assigned from the NMR studies. The conformation adopted by **132** in the solid state is shown in **Figure 2.4**.

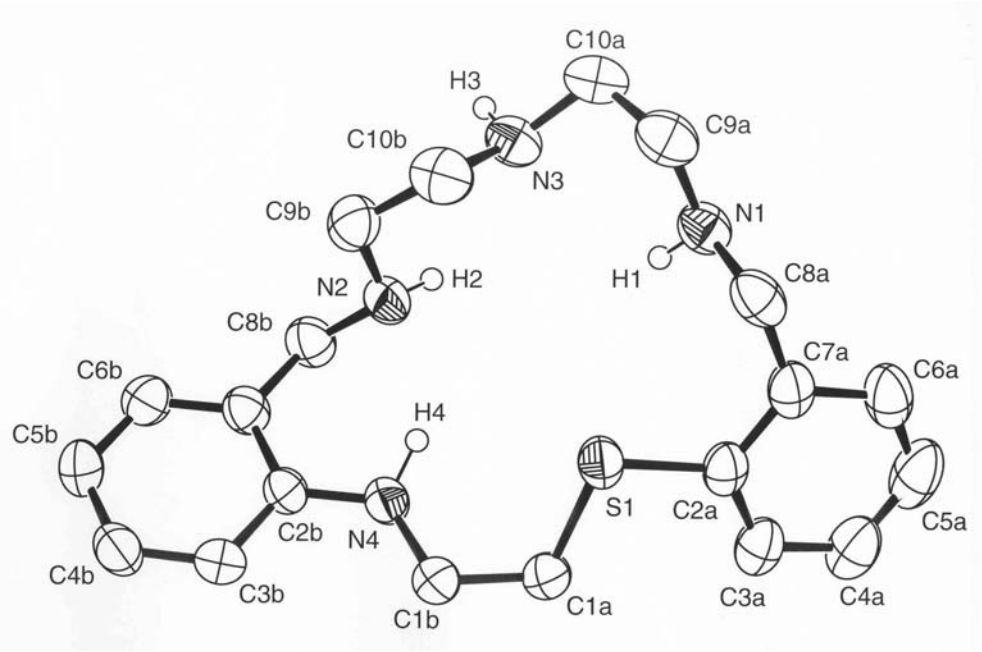

Figure 2.4 The X-ray crystal structure of **132**

Crystal data and a summary of data collection for **132** as well as non-hydrogen bond lengths and bond angles are shown in **Appendix B**, **Tables B.1** – **B.3**.

Macrocycles **133** and **134** (18-membered SN/NNN)

As expected, reaction of N-(2-aminoethyl)-1,3-propanediamine with the unsymmetrical SN-dialdehyde **152** yielded a mixture of two isomeric macrocyclic products **133** and **134**. Due to the similar polarity of these products, repeated chromatography on silica gel in chloroform with increasing amounts of triethylamine (0 – 20%) proved necessary to achieve reasonable separation. The isomers differ in the orientation within the macrocyclic ring of the fragment derived from N-(2-aminoethyl)-1,3-propanediamine. Isomer **133**, in which the 1,3-diaminopropane unit is orientated on the same side as the thioether group, was eluted first. The proton and carbon chemical shifts of this isomer are as shown in **Figure 2.5**. Here too, a non-systematic atom numbering system is employed for ease of discussion.

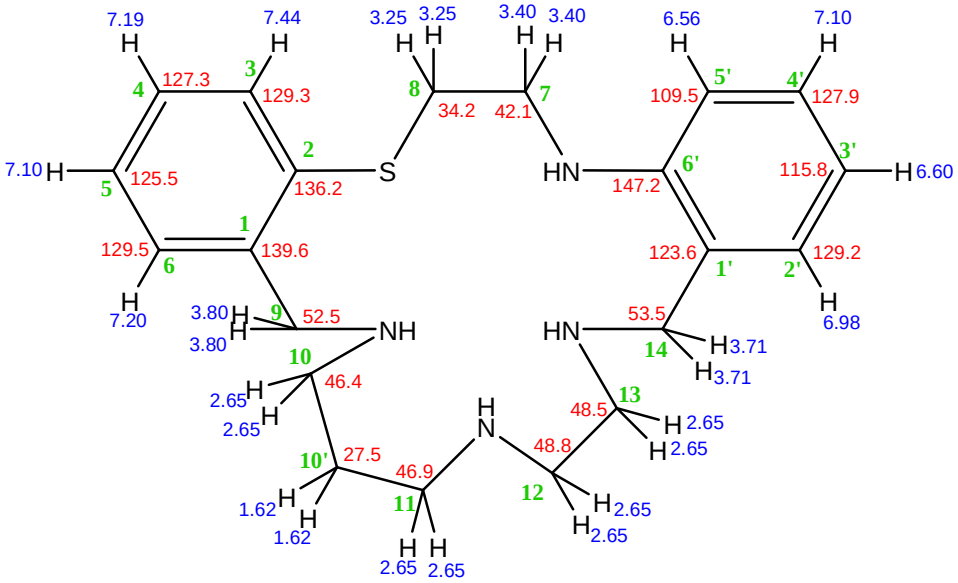

Figure 2.5 ^{1}H and ^{13}C NMR (HSCORR, J = 140 Hz) assignments for **133**.

The orientation of the N-(2-aminoethyl)-1,3-propanediamine fragment in **133** was assigned on the basis of the observed long range correlations shown in **Figure 2.6**.

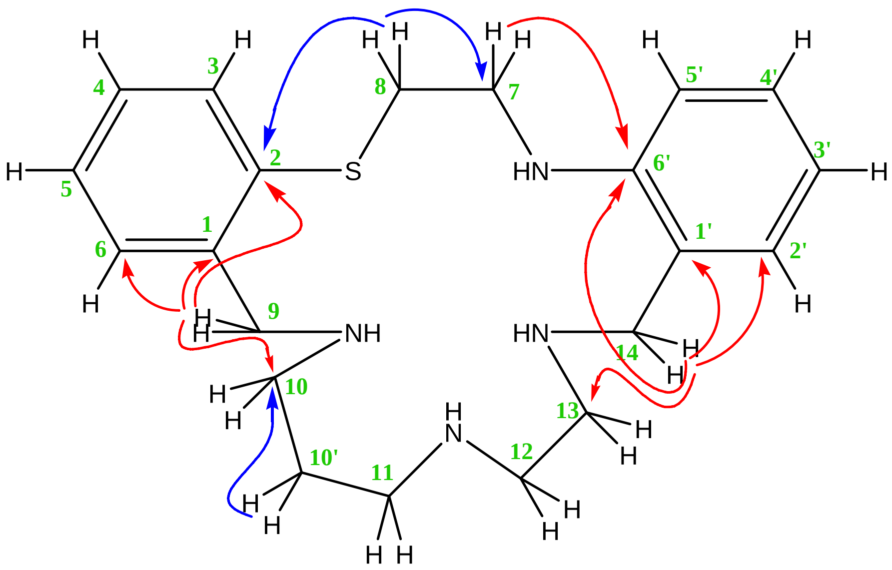

Figure 2.6 Long range NMR (COLOC, J = 10 Hz) correlations for **133**.

The benzylic protons at δ 3.71 (H14) correlated with the ethylenediamine carbon (C13) at δ 48.5 ppm and also to the aromatic carbon atoms at 123.6, 129.2 and 147.2 ppm. These were assigned to carbons 1′, 2′ and 6′ of the N-substituted aromatic ring, using the low-field position (147.2 ppm) of the C6′ signal as evidence for N-substitution. This assignment was further supported by the upfield chemical shifts of H5′ and H3′ (δ 6.56 and 6.60, respectively). The benzylic protons at δ 3.80 (H9) correlated with C10 (46.4 ppm). The assignment of C10 was made on the basis of a correlation from H10′ (δ 1.62), the central protons of the 1,3-diaminopropane unit. The same benzylic protons (δ 3.80, H9) also showed correlations to the aromatic carbon signals at δ 129.5, 136.2, and 139.6, which were assigned to carbons 6, 2 and 1 respectively of the S-substituted aromatic ring. Furthermore, the methylene protons at δ 3.40 (H7) correlated with the signal at 147.2 ppm (C6′), while the methylene protons at δ 3.25 (H8) correlated with the signal at 136.2 ppm (C2). The chemical shifts of C7 and C8 are also diagnostic of attachment to N and S, respectively. The NMR assignments for **134** were made by analogy with those obtained for isomer **133** as just discussed. Unfortunately, attempts to produce suitable crystals for X-ray studies from a variety of solvent mixtures were unsuccessful for both these isomers.

135 (19-membered SN/NNN)

The reaction of **152** with di(3-aminopropyl)amine was, as mentioned above, not successful in producing the desired macrocycle **135** in significant yield compared to other side products. Due to the relative difficulty in obtaining the SN-dialdehyde, the preparation of this macrocyclic ring was not pursued further.

Synthesis of **136** (SN/NON)

Reductive amination involving the SN-dialdehyde **152** and di(2-aminoethyl)ether dihydrochloride afforded the unsymmetrical macrocycle **136** which contained the SN-donor pattern in the 'upper' bridge and an NON-donor string in the 'lower' bridge. Following the reaction work-up, the still crude product was chromatographed on silica gel with 20% methanol (MeOH) in DCM to yield the pure product in 53% yield.

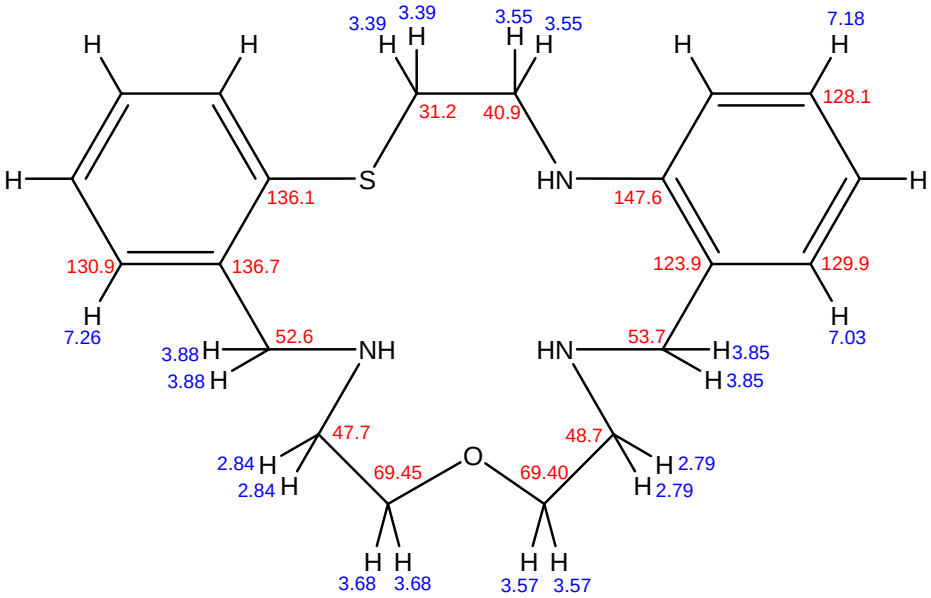

Figure 2.7 ^{1}H and ^{13}C NMR (HSQC, J =140 Hz) assignments for **136**.

The microanalysis data for the above product was consistent with the structure proposed on the basis of the NMR data. In this macrocycle also, the benzylic methylene protons are equivalent, appearing as two-proton singlets at δ 3.88 and δ 3.85, again indicating flexibility in the lower portion of the macrocyclic ring (**Figure 2.7**). Long range proton-

carbon correlations are shown in **Figure 2.8** and are also consistent with the proposed structure. Thus, the benzylic protons at δ 3.85 correlated with the ethylene carbon in the lower bridge at δ 48.7 ppm (adjacent to the secondary amine) and also to the aromatic carbon atoms at δ 123.9, 129.9 and 147.6 ppm. These were again assigned to carbons of the N-substituted aromatic ring, using the low-field position at δ 147.6 ppm as evidence for N-substitution. At the same time the ethylene protons at δ 2.79 (ethylene carbon at 48.7 ppm) in the 'lower' bridge showed correlations to the benzylic carbon at 53.7 ppm as well as the carbon at 69.40 ppm adjacent to the ether oxygen in the 'lower' bridge. For the opposite side of the molecule, the connectivity was confirmed on the basis of correlations from the benzylic protons at δ 3.88 to the aromatic carbon signals at 130.9, 136.7, and 136.1 ppm of the S-substituted ring. The assignment of the carbon at 136.1 ppm was made on the basis of a correlation from the upper bridge methylene protons at δ 3.39 (carbon at 31.2 ppm, diagnostic of attachment to S[32]).

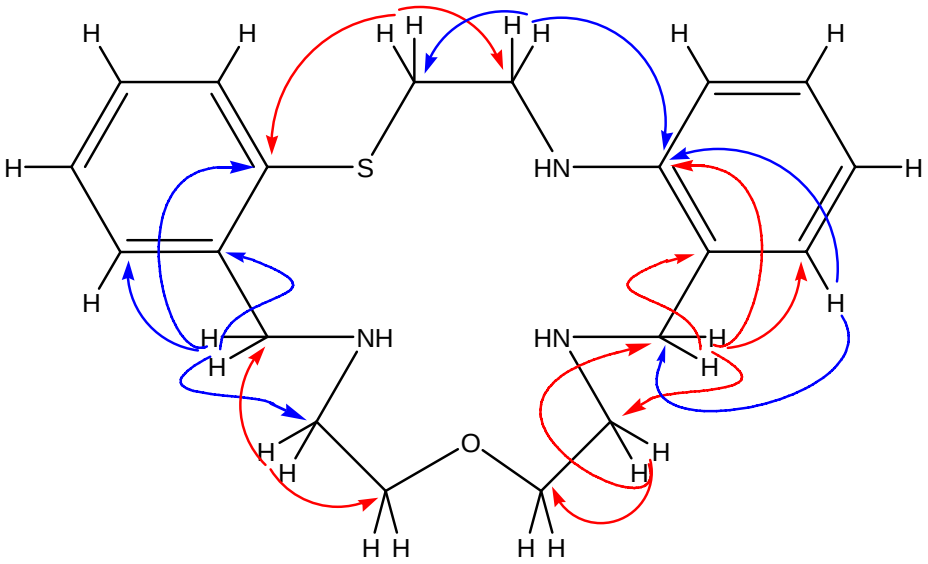

Figure 2.8 Long range NMR (HMBC, J = 8 Hz) correlations for **136**.

Recrystallisation from acetonitrile afforded crystals suitable for an X-ray study which confirmed the atom connectivity deduced from NMR experiments. The molecule adopts the conformation shown in **Figure 2.9** in the solid state.

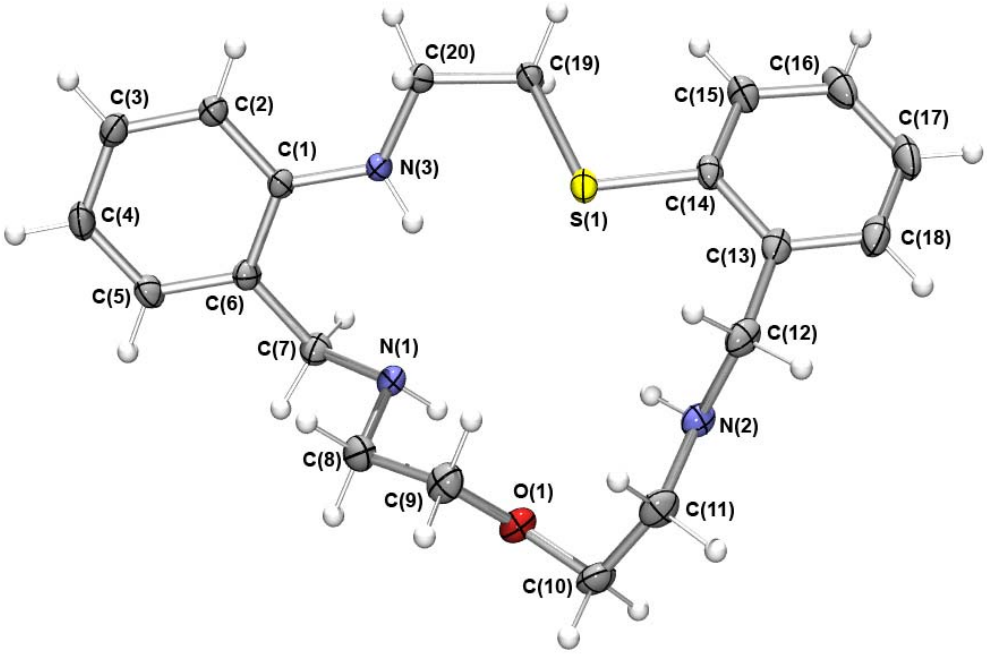

Figure 2.9 The X-ray crystal structure of **136**.

Crystal data and a summary of data collection as well as non-hydrogen bond lengths and bond angles for **136** are shown in **Appendix B**, **Tables B.4** – **B.6**.

Synthesis of **137** (SN/NSN)

Di(2-aminoethyl)sulfide was required for the synthesis of the above macrocycle and was prepared by the author *via* a modification of the previously reported preparation of 2-aminoethyl 3-aminopropyl sulfide.[33] Reaction of di(2-aminoethyl)sulfide with the SN-dialdehyde (**152**), followed by $NaBH_4$ reduction yielded the required S_2N_3-donor macrocycle **137**. Several attempts were made to produce this ligand using both absolute ethanol and methanol as reaction solvents, as well as employing $NaBH_3CN$ as the reducing agent in one instance (see **159**). The most favourable result was obtained using HPLC grade MeOH and $NaBH_4$ as the reducing agent. Even under these conditions problems were experienced in reducing both imine functions (see **144**) and, the target macrocycle (**137**) needed to be separated by chromatography (on silica gel with 3%

MeOH in DCM as solvent) from other by-products, including partially reduced products. The 1D and 2D NMR spectral data for the purified product are consistent with the proposed structure; the ^{1}H and ^{13}C assignments are given in **Figure 2.10**. It must be emphasised that, with the exception of the benzylic methylene protons at δ 3.78 and δ 3.92, which are equivalent and appear as two-proton singlets in the ^{1}H NMR spectrum of **137**, all other methylene protons appear as multiplets, centred on the chemical shift values given in **Figure 2.10**.

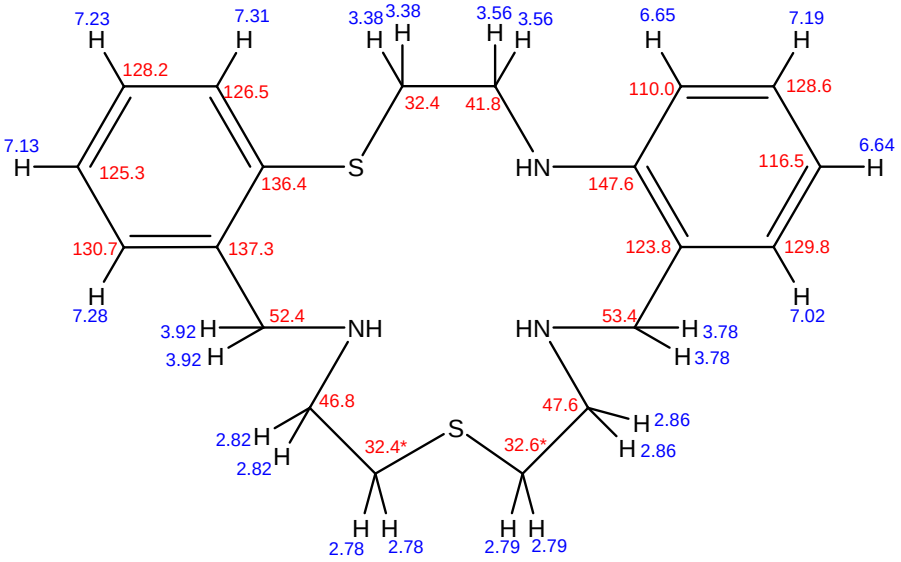

Figure 2.10 ^{1}H and ^{13}C NMR (HSQC, J =140 Hz) assignments for **137**.

The long range proton-carbon correlations used to elucidate the ligand structure are shown in **Figure 2.11**. Crystals suitable for an X-ray diffraction study were obtained from a mixture of DCM/hexane/diethyl ether.

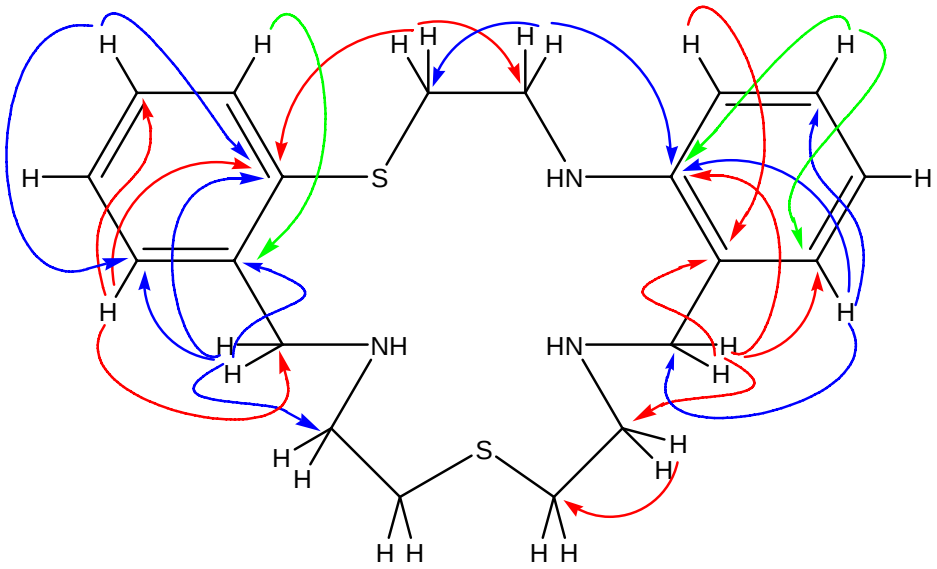

Figure 2.11 Long range NMR (HMBC, J = 8 Hz) correlations for **137**.

The conformation adopted by the ring in solid state is illustrated in **Figure 2.12**. Once again the X-ray results confirmed the atom connectivity inferred from the NMR experiments. Crystal data and a summary of data collection for **137** as well as non-hydrogen bond lengths and bond angles are shown in **Appendix B**, **Tables B.7** – **B.9**.

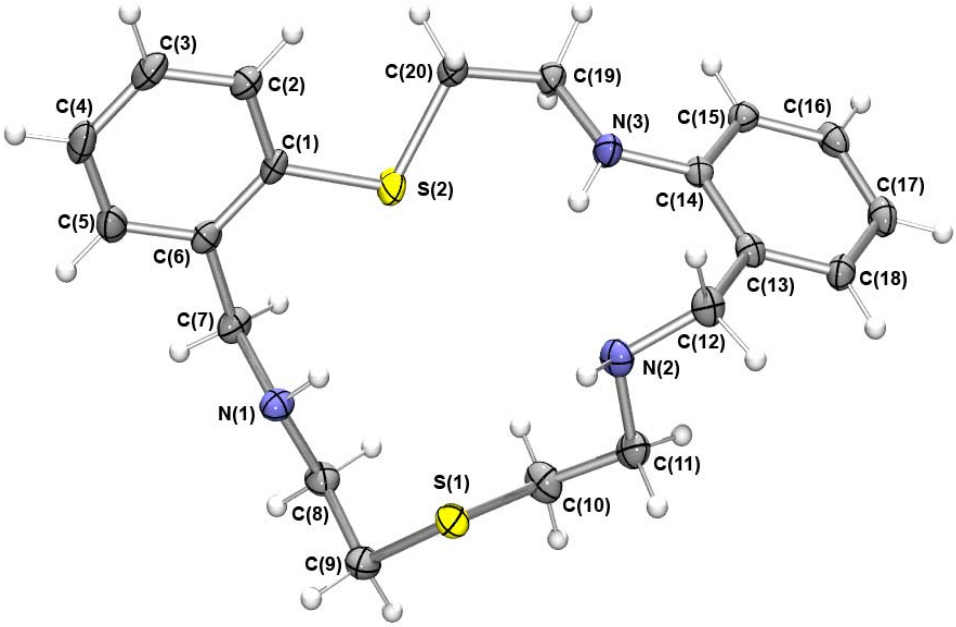

Figure 2.12 The X-ray crystal structure of **137**.

138 (17-membered ON/NNN)

Reductive amination involving di(2-aminoethyl)amine and the unsymmetrical ON-dialdehyde **156** afforded the 17-membered macrocycle **138** in yields up to 80%, depending on the method employed (see **Experimental** section). The ^{1}H and ^{13}C NMR spectral data once again confirmed the absence of the imine functions while the microanalysis data confirmed the purity of the product.

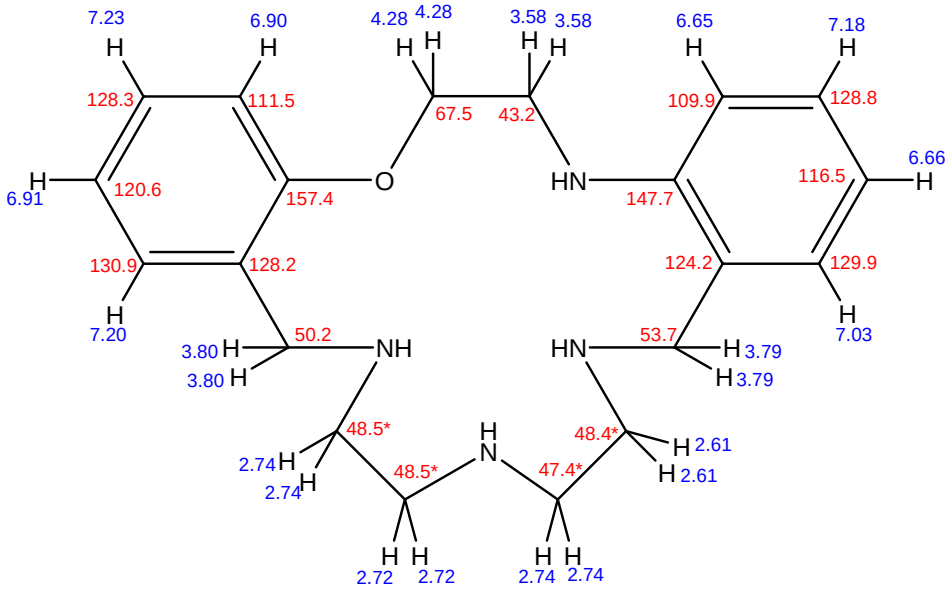

Figure 2.13 ^{1}H and ^{13}C NMR (HSCORR, J = 140 Hz) assignments for **138** (*interchangeable values).

2D NMR experiments similar to those discussed so far enabled assignment of the proton and carbon chemical shifts (**Figure 2.13**). The conformational flexibility of the ligand backbone segment which includes the NNN-donor string is again reflected in the equivalence of the benzylic methylene hydrogens which appear as two-proton singlets at δ 3.80 and δ 3.79. The methylene signal at δ 3.58 correlated with the carbon atoms at 147.7 and 67.5 ppm, while the methylene protons at δ 4.28 correlated with the signals at 157.4 and 43.2 ppm (**Figure 2.13**). The chemical shifts of these two methylene carbons at 43.2 and 67.5 ppm are also diagnostic of attachment to N and O respectively[32] and, as a

result, they were assigned to the ‘upper’ bridge portion of the macrocycle. In addition, the broad appearance of the signal at δ 3.58 is indicative of coupling to the NH proton. There was a high degree of overlap in the aliphatic region of the ^{1}H NMR spectrum for this ligand and, as a consequence, the signals corresponding to the NNN-donor string in the ‘lower bridge’ could not be assigned unequivocally. In **Figure 2.13**, the symbol ‘*’ indicates that the chemical shift values for these atoms are interchangeable. However, the signals in the aromatic region showed less overlap and allowed for a more detailed assignment of their chemical shifts.

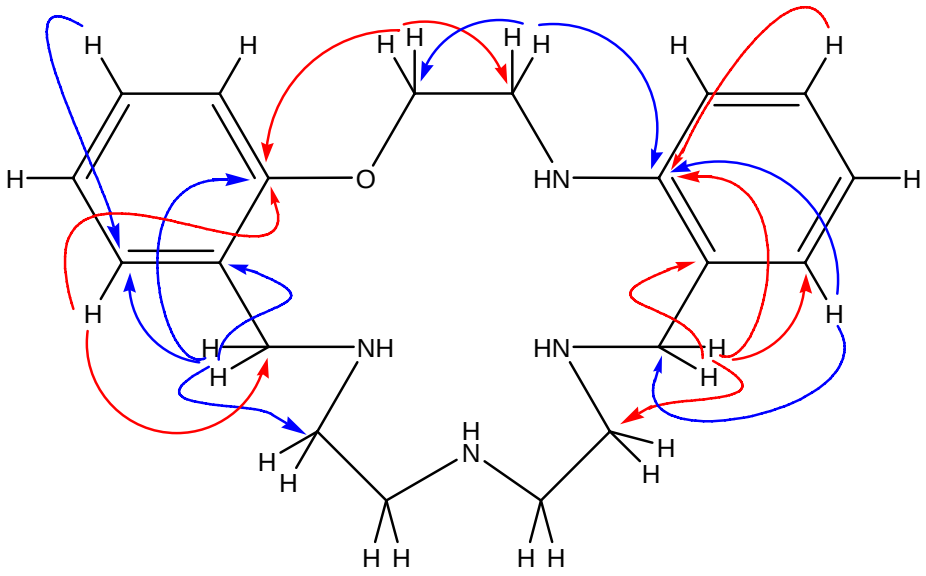

Figure 2.14 Long range NMR (COLOC, J = 10 Hz) correlations for **138**

The peaks for the two ‘halves’ of the macrocyclic ring were assigned on the basis of observed correlations shown in **Figure 2.14**. Thus, long range correlations were observed from the benzylic methylene hydrogens δ 3.79 to the aromatic carbons at 147.7, 124.4 and 129.9 ppm (of the N-substituted aromatic ring) as well as the carbon signal at 48.4 ppm, while from the benzylic methylene hydrogens at δ 3.80, correlations were observed to the carbons at 157.4, 128.8 and 130.9 ppm (of the O-substituted aromatic ring) as well as to the signal at 48.5 ppm. Crystals suitable for an X-ray diffraction study were obtained from acetonitrile; the conformation adopted by **138** in the solid state is

illustrated in **Figure 2.15**. Crystal data and a summary of data collection as well as non-hydrogen bond lengths and angles for **138** are shown in **Appendix B**, **Tables B.1** – **B.3**.

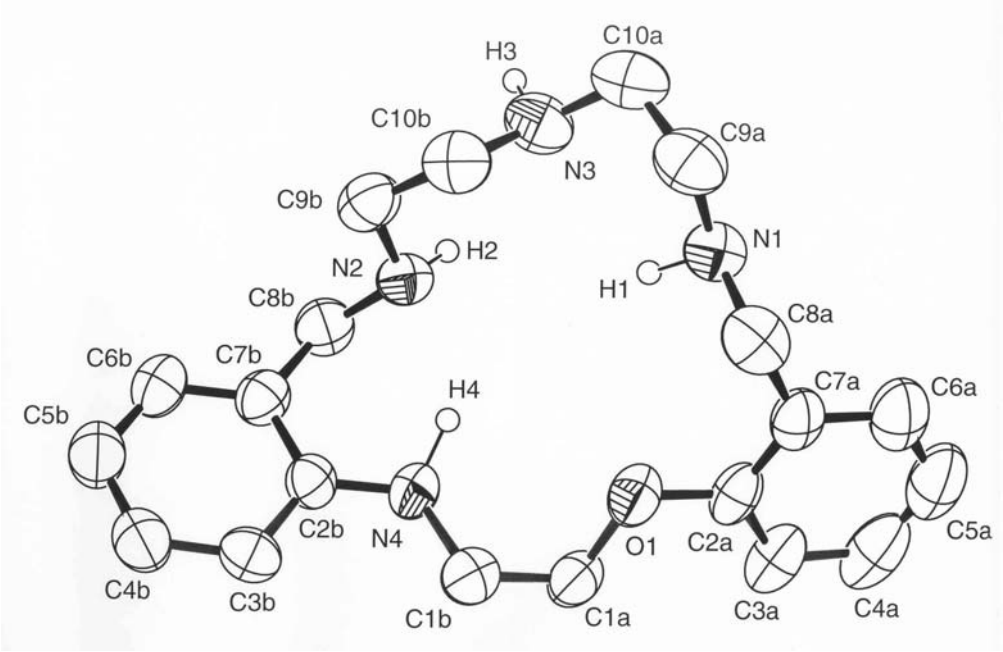

Figure 2.15 The X-ray crystal structure of **138**.

Comparison of the crystal structure of **138** (**Figure 2.15**) with that of the SN-analogue **132** (**Figure 2.4**) reveals that both structures are similar, with close agreement between chemically equivalent bond lengths and angles. Closely related geometries are adopted by these two macrocycles even though there are significant differences in bond lengths and angles occurring about the S(1) and O(1) heteroatoms in the respective structures.

Macrocycles **139** and **140** (18-membered ON/NNN)

A single attempt was made to synthesise the two possible isomers with the above donor atom pattern. Inspection of the ^{1}H NMR spectrum of the crude reaction mixture revealed the presence of only a very small amount of either of the desired products and, for the reasons mentioned previously, the preparation of these ligands was not pursued further.

Synthesis of **141** (ON/NSN)

The ON/NSN macrocycle **141** was obtained by reduction of the condensation product of **156** and di(2-aminoethyl)sulfide using $NaBH_4$. Addition of excess reducing agent failed to completely reduce the imine functions, as indicated by the ^1H NMR spectrum of the reaction mixture. This behaviour parallels the similar difficulty encountered during the synthesis of **137**. Work-up of the reaction mixture followed by chromatography with MeOH/DCM and recrystallisation from acetonitrile afforded **141** in 45% yield.

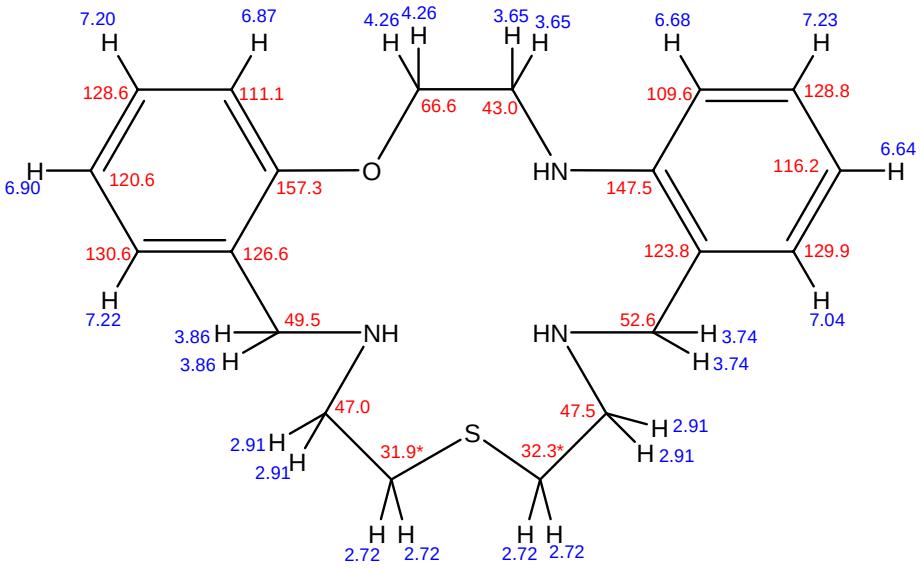

Figure 2.16 ^1H and ^{13}C NMR (HSQC, J =140 Hz) assignments for **141**.

The correlations observed in the 2D NMR spectra once again allowed chemical shift assignment and connectivity to be established for most of the atoms in the molecule including those in the aromatic region (**Figures 2.16** and **2.17**).

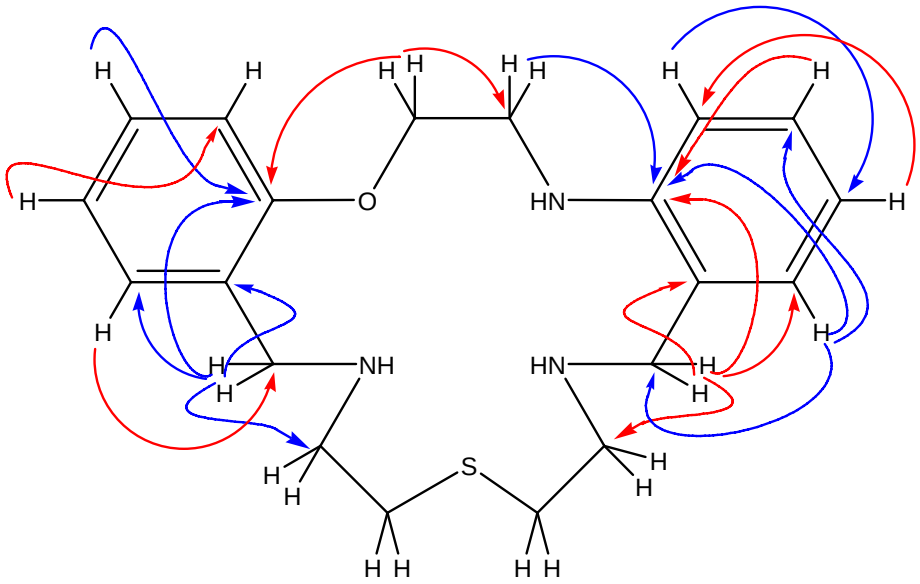

Figure 2.17 Long range NMR (HMBC, J = 8 Hz) correlations for **141**.

Attempts to obtain crystals suitable for X-ray diffraction using a variety of solvent combinations were not successful in this case. However, the crystal structures of metal complexes incorporating **141** obtained subsequently (see Chapter 3) served to confirm the structure of this macrocycle derived from NMR experiments.

As an aside, several repeat preparations of this macrocycle resulted in a corresponding number of ^{1}H NMR spectra being recorded; this in turn, led to the observation that the change in chemical shift values ($\Delta\delta$) with concentration (not an unexpected phenomenon) was considerably more for one benzylic methylene signal than for the other. The results of a small scale experiment to document this variation in δ values with concentration are shown in **Figure 2.18**.

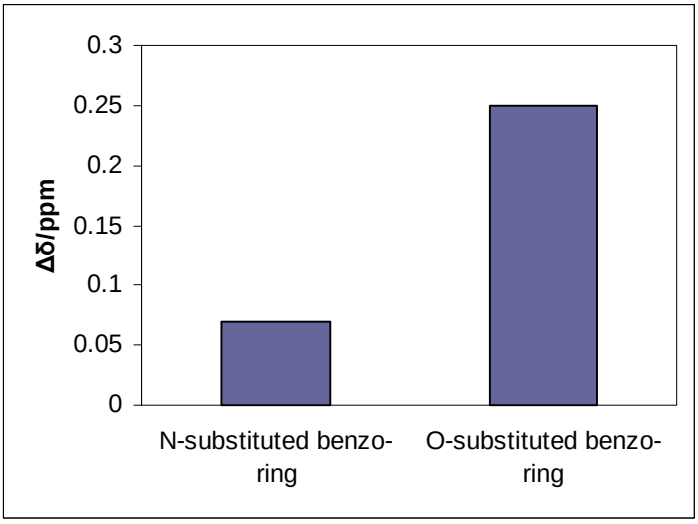

Figure 2.18 Relative chemical shift variation (Δδ) of the benzylic methylene proton signal of the N-substituted benzo-ring compared to that of the O-substituted benzo-ring with increasing concentration from 0.013 M to 0.190 M.

The chemical shifts were measured in $CDCl_3$ at two concentrations: 0.013 M and 0.190 M (that is almost 15x more concentrated in the latter case). In the case of the benzylic methylene hydrogens of the N-substituted benzo-ring, the peak shifted upfield by 0.07ppm, from δ 3.81 to δ 3.74, while the benzylic methylene protons of the O-substituted benzo-ring experienced a much greater upfield shift of 0.25ppm, from 4.11 to 3.86 reflecting the increase in concentration. These observations most likely reflect intermolecular π-stacking with increased concentration of the macrocycle. The greater effect on the benzylic protons of the O-substituted benzo-ring is less easily rationalised; in the absence of additional data further speculation is inappropriate.

Synthesis of **142** (ON/NON)

The reaction of **156** with di(2-aminoethyl)ether dihydrochloride, followed by reduction with $NaBH_4$, produced the O_2N_3-donor unsymmetrical macrocycle **142**. The chemical shift assignments and atom connectivity for this ring were obtained in similar fashion to those described previously and the results are shown in **Figure 2.19** and **Figure 2.20**, respectively.

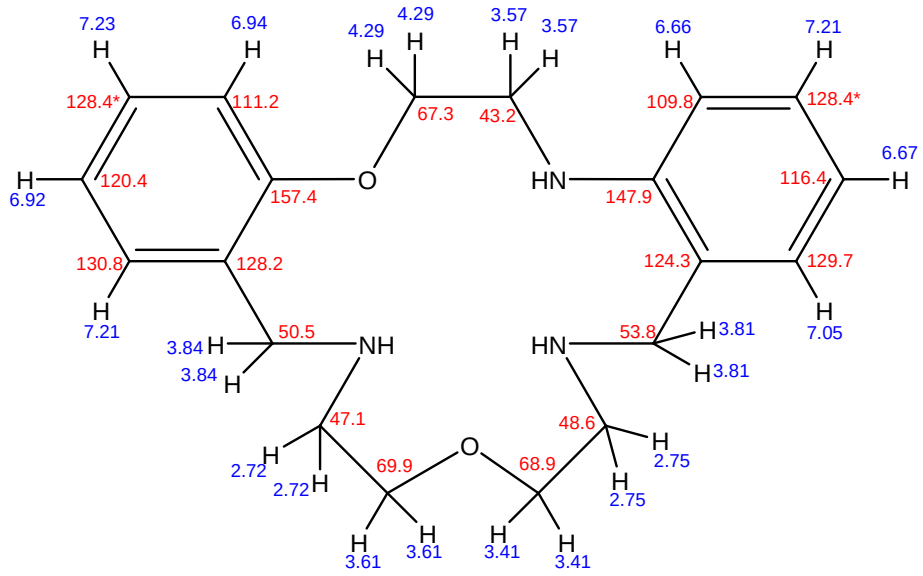

Figure 2.19 ^{1}H and ^{13}C NMR (HSQC, J =140 Hz) assignments for **142**.

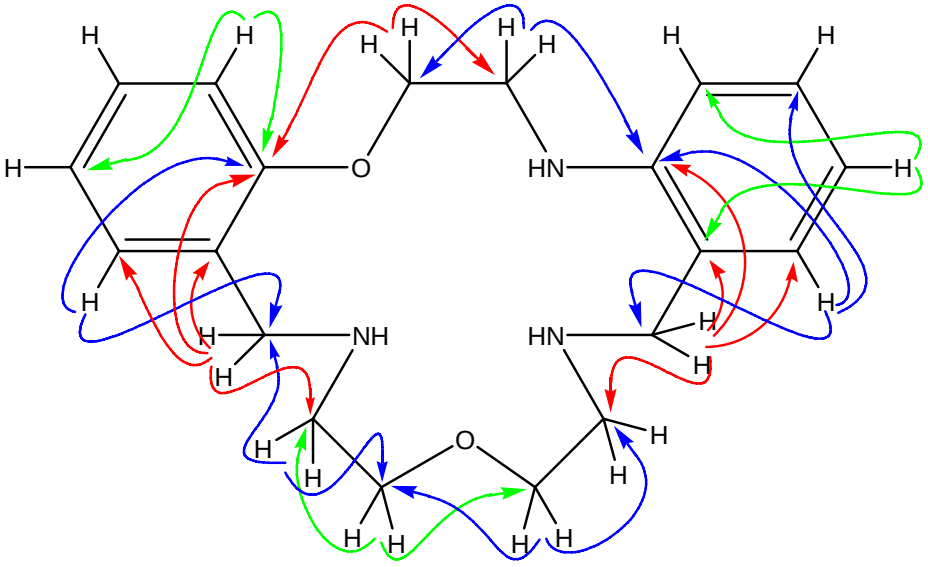

Figure 2.20 Long range NMR (HMBC, J = 8 Hz) correlations for **142**.

A mixture of methanol and acetonitrile yielded crystals of **142** suitable for X-ray diffraction, with the solid state conformation shown in **Figure 2.21**.

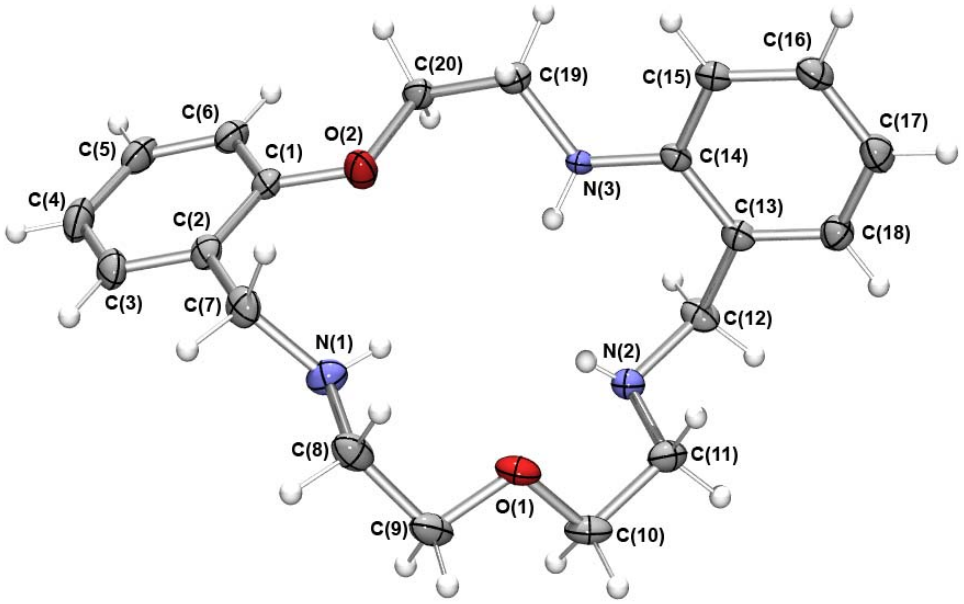

Figure 2.21 The X-ray crystal structure of **142**.

Crystal data and a summary of data collection as well as non-hydrogen bond lengths and bond angles for **142** are shown in **Appendix B**, **Tables B.10** – **B.12**.

The mono-imines **143** and **144**

Slow addition of di(2-aminoethyl)sulfide to the ON-dialdehyde **156**, followed by heating at reflux for 12 hours, produced the corresponding diimine, based on the ^{1}H NMR spectrum of the product. Addition of reducing agent, even in vast excess, once again failed to completely reduce both imine functions in the corresponding macrocyclic ring, There appeared to be almost half of the macrocyclic product being present as the corresponding mono-imine derivative. The presence in the ^{1}H NMR spectrum of only one imine proton, indicated that the reaction mixture did not contain a mixture of partially reduced intermediates, rather it indicated preferential reduction of only one of the imine groups. Following the appropriate reaction work-up, column chromatography on silica gel with increasing amounts of MeOH (0 – 40%) in DCM successfully separated the less polar mono-imine **143** from the fully reduced product.

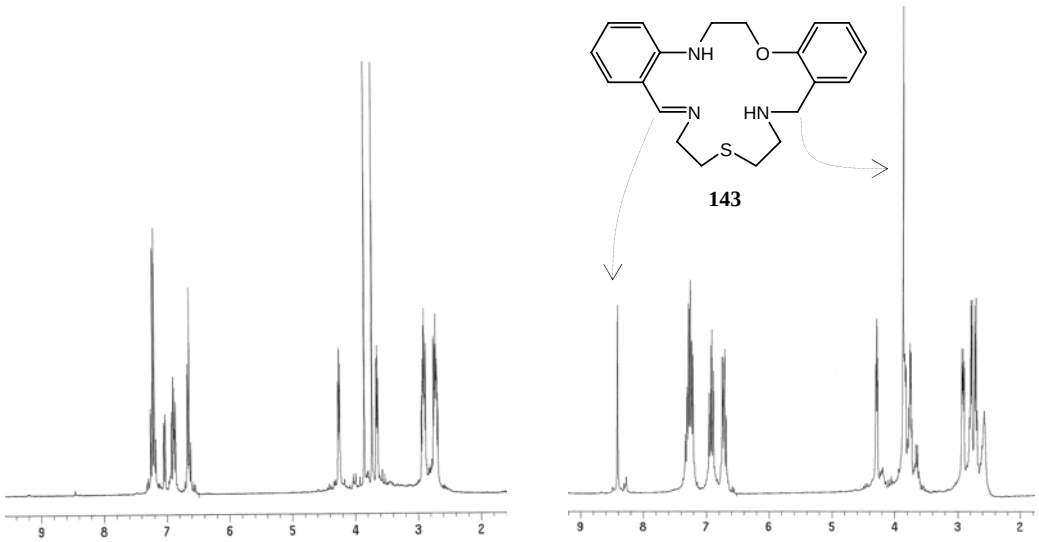

Figure 2.22 ^{1}H NMR spectra of **141** (a) and **143** (b).

The NMR data for **143** are characterised by the appearance of a one-proton singlet at δ 8.34 and a carbon resonance at 164.9 ppm, consistent with the presence of an imine functionality, with the ^{1}H NMR spectrum (**Figure 2.22** b) containing only one two-proton singlet at δ 3.87. Comparison with the data for **141** reveals that this signal corresponds to the benzylic methylene hydrogens adjacent to the O-substituted benzo-ring, and indicates the imine adjacent to the N-substituted benzo-ring was not reduced. The conformational flexibility of this portion of the macrocyclic ring is maintained, given the signal for the benzylic methylene protons again appears as a singlet. 2D NMR studies were not carried out for **143** and, as a result, the chemical shift values were not assigned in this case. Addition of excess $NaBH_4$ to a MeOH solution of **143** resulted in 100% conversion to the ON/NSN macrocycle **141**. It is possible that the mono-imine corresponding to the O-containing 'half' of the macrocyclic ring was also present in the reaction mixture, however if so, it would be only there as a very minor component (< 5%) since its presence was not detected by NMR.

In similar fashion, the mono-imine **144** was isolated as a result of incomplete reduction of the diimine corresponding to the SN/NSN macrocycle **137**. Chemical shift assignment and atom connectivity for **144** were established on the basis of correlations observed in the 2D NMR spectra as shown in **Figure 2.23** and **Figure 2.24**, respectively.

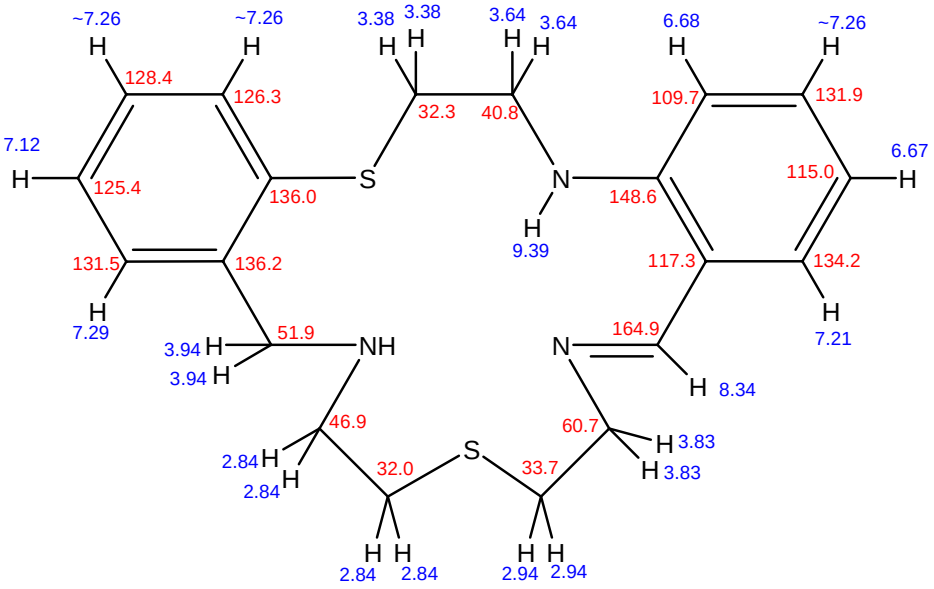

Figure 2.23 ^{1}H and ^{13}C NMR (HSQC, J =140 Hz) assignments for the mono-imine derivative **144**.

Once more the conformational flexibility of the NSN-portion of the macrocyclic ring is maintained, as suggested by the appearance of a singlet for the benzylic methylene protons despite of the presence of the imine group. In addition, the methylene hydrogens in the NSN-fragment at δ2.84 (see **Figure 2.23**) appear as a broad four-proton singlet, as further evidence for flexibility in this portion of the ring.

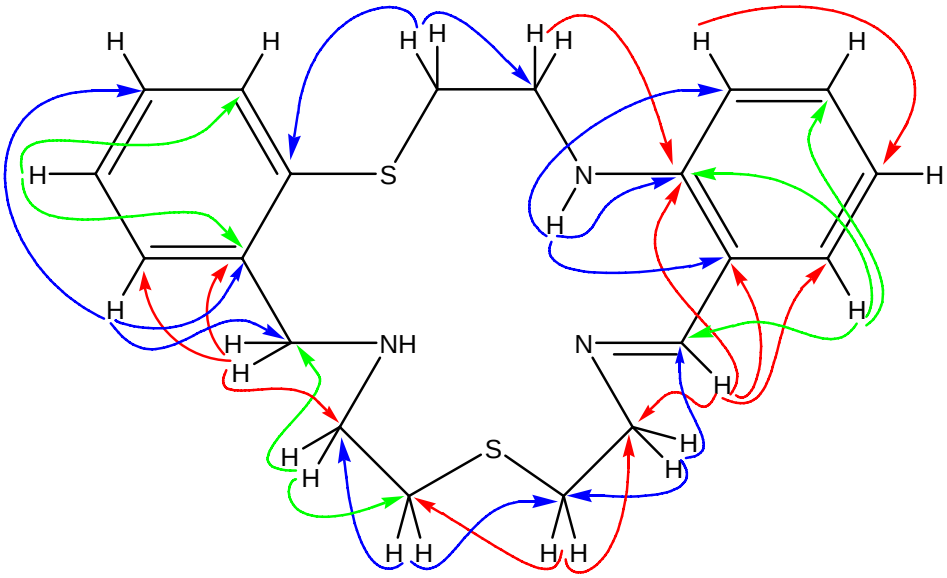

Figure 2.24 Long range NMR (HMBC, J = 8 Hz) correlations for **144**.

2.4.4 By-products of macrocycle syntheses

As expected, various by-products were obtained during the macrocyclic syntheses discussed above. Three of these by-products (**157** – **159**) were obtained in sufficiently high yields to allow isolation, purification and structural elucidation. The bicyclic product **157** was obtained during the synthesis of **133**/**134** while the alcohol **158** was obtained during the preparation of **141**. The reductive amination reaction intended for the production of macrocycle **137** and carried out in the presence of $NaBH_3CN$ *in situ*, resulted instead in the isolation of the open chain [2 + 1] condensation product **159**.

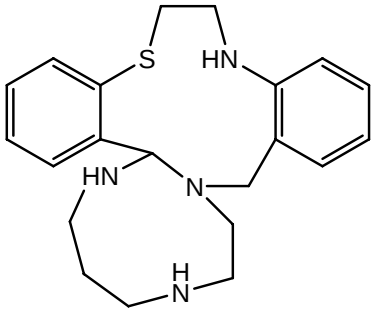

157

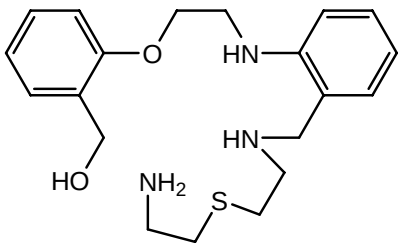

158

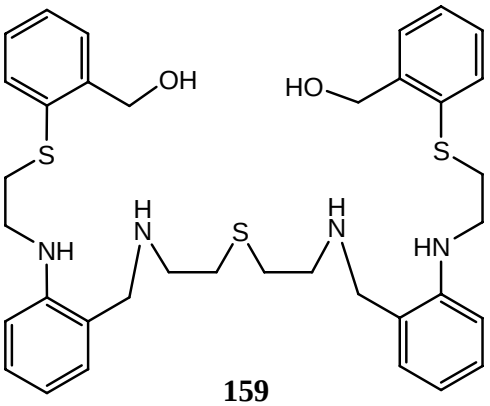

159

Bicyclic product **157**

Slow addition of N-(2-aminoethyl)-1,3-propanediamine to a dilute solution of the SN-dialdehyde **152** in dry methanol followed by overnight reflux resulted in a mixture of products that appeared largely polymeric in nature (as indicated by TLC and the ^{1}H NMR spectrum). A small amount of what appeared to be one of the expected diimine species (by ^{1}H NMR) was also present. Nevertheless, rapid addition of $NaBH_4$ to the reaction solution produced virtually no yield of the expected macrocyclic isomers **133**/**134**. The major component able to be separated by column chromatography was the bicyclic product **157**. Ring contractions are known to occur in Schiff-base macrocycles as a consequence of the susceptibility of the C=N group to nucleophilic attack.[34] In many examples of such intramolecular processes, the addition of a secondary amine in the ring across a proximate imine bond is usually stabilised by metal coordination of the latter.[35-37] There are also (less common) reports of ring contractions occurring in the absence of a metal template (see **Scheme 2.7**) with the ring-contracted form (**161**) in this case crystallising from the organic reaction mixture.[38] ^{1}H NMR spectra ($CDCl_3$) analysis revealed that the ring-contracted form **161** also persists in solution.[38]

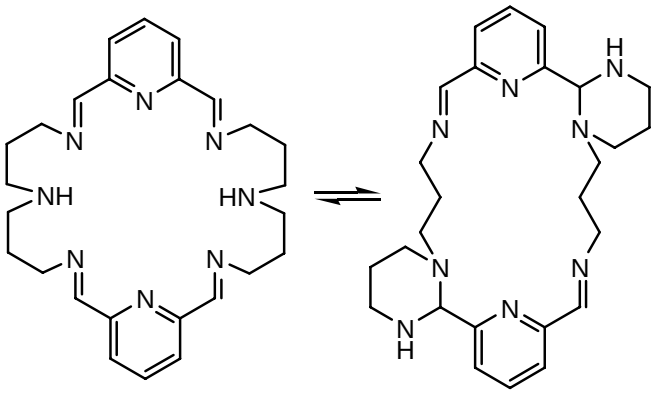

160 **161**

Scheme 2.7 [2:2] Condensation products of pyridine-2,6-dicarbaldehyde and 4-azaheptane-1,7-diamine in acetonitrile[38]

The size of the two aliphatic rings in the case of the bicyclic product **157** (9- and 11-membered) is a little surprising. In literature precedents, these intramolecular processes involve an imine and an adjoining secondary amine (see **Scheme 2.7**) such that 5- or 6-membered rings are formed on closure. It is possible that during the author's reaction, such typical ring contraction did occur, for instance involving the central amine in the NNN-donor string and the imine adjacent to the S-substituted benzo-ring. However, if so, the yields were too low to be observed in the ^{1}H NMR analysis of the chromatography fractions.

The structure for **157** was assigned from an investigation of its 1D and 2D NMR spectra as shown in **Figure 2.25** and **Figure 2.26**.

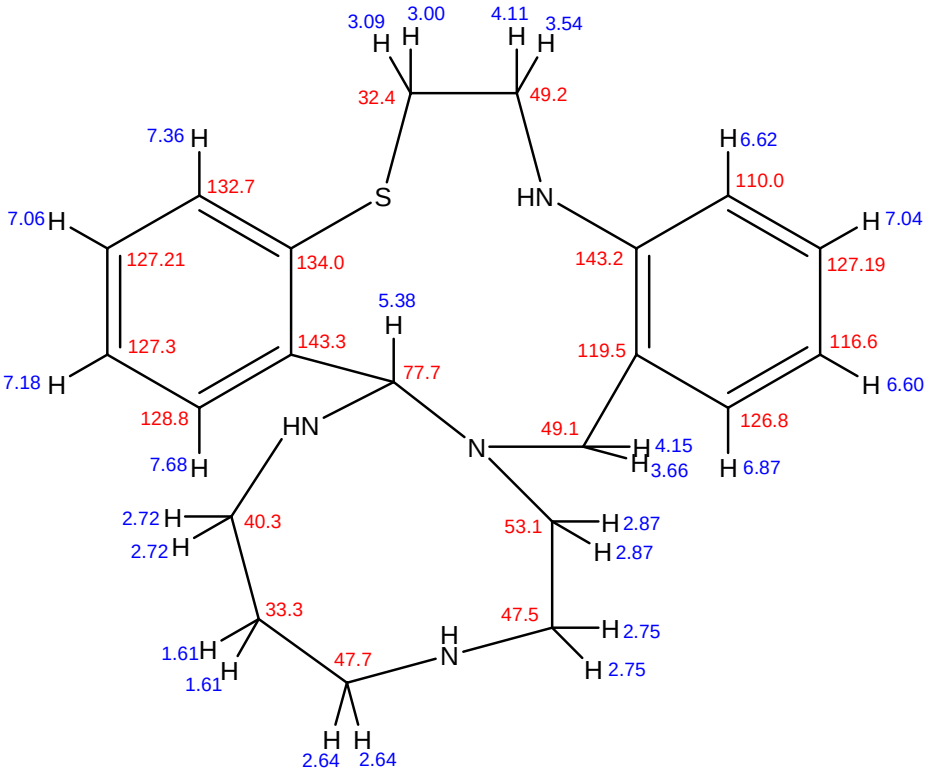

Figure 2.25 ^{1}H and ^{13}C NMR (HSQC, J =140 Hz) assignments for **157**.

Long range correlations were observed from the bridgehead proton at δ 5.38 to the S-substituted ring carbons at 134.0, 143.3 and 128.9 ppm as well as across the nitrogen to the benzylic methylene carbon at 49.1 ppm and the carbon at 53.1 ppm of the N-(2-aminoethyl)-1,3-propanediamine fragment. The ring contraction resulted in loss of the flexibility in the lower portion of the ring as indicated by the benzylic methylene protons now appearing as two separate doublets at δ 3.66 and δ 4.15. The benzylic methylene protons showed, as expected, long range correlations to the carbons on the N-substituted ring at 143.2 and 126.8 ppm and more importantly to the bridgehead carbon at 77.7 ppm. This latter correlation as well as that from the bridgehead proton at δ5.38 to the carbon at 49.1 ppm would not be observed if the ring contraction had, for example, involved the central nitrogen of the NNN-donor string as this would imply a long-range correlation across 6 bonds!

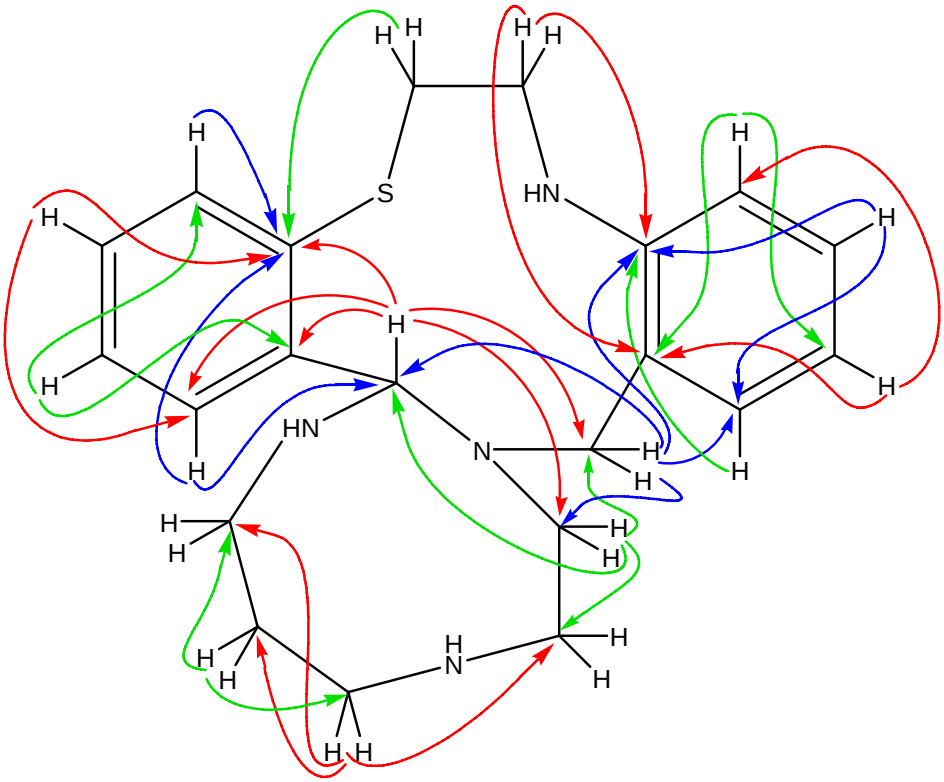

Figure 2.26 Long range NMR (HMBC, J = 8 Hz) correlations for **157** (Dashed lines represent correlations to nitrogen atoms).

The orientation of the N-(2-aminoethyl)-1,3-propanediamine fragment was assigned on the basis of long range correlations from both the bridgehead proton and the benzylic methylene protons to the carbon at 53.1 ppm. In the absence of suitable crystals for an X-ray diffraction study, the long range correlations observed to the nitrogen atoms in **157** (as indicated by dashed lines in **Figure 2.26**) also confirmed the expected atom connectivities.

Benzylic alcohol **158**

One attempted preparation of **141** resulted instead in the formation of **158**. In this case the addition of the diamine was carried out as before and, after no remaining unreacted ON-dialdehyde **156** could be detected by TLC, the reaction mixture was heated at reflux

overnight – a time considered adequate for diimine formation based on the author's experience with related condensation reactions. Due to instrumental problems at the time, it was not possible to obtain an NMR spectrum of the crude reaction mixture. Following addition of an excess of $NaBH_4$ and reaction work-up, column chromatography afforded a small amount of macrocycle **141**. The major fraction, while somewhat similar by ^1H NMR to **141**, lacked the benzylic methylene signal at δ 3.86 and contained a new two proton singlet at δ 4.68, characteristic of a C**H**$_2$OH signal (*c.f.* the alcoholic methylene chemical shift for the diol **155**). The ^1H and ^{13}C NMR assignments and long range 2D correlations for **158** are shown in **Figures 2.27** and **2.28** respectively.

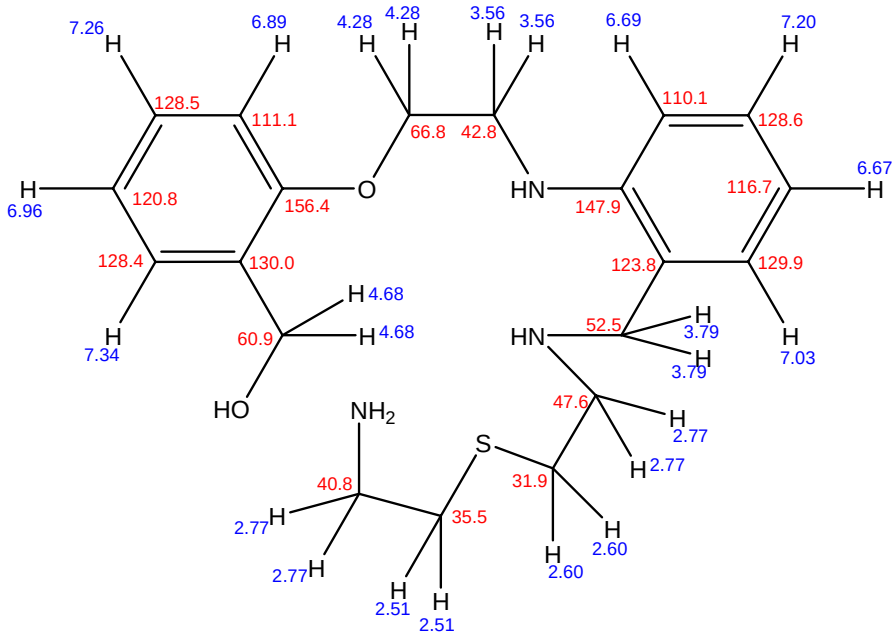

Figure 2.27 ^1H and ^{13}C NMR (HSQC, J =140 Hz) assignments for **158**.

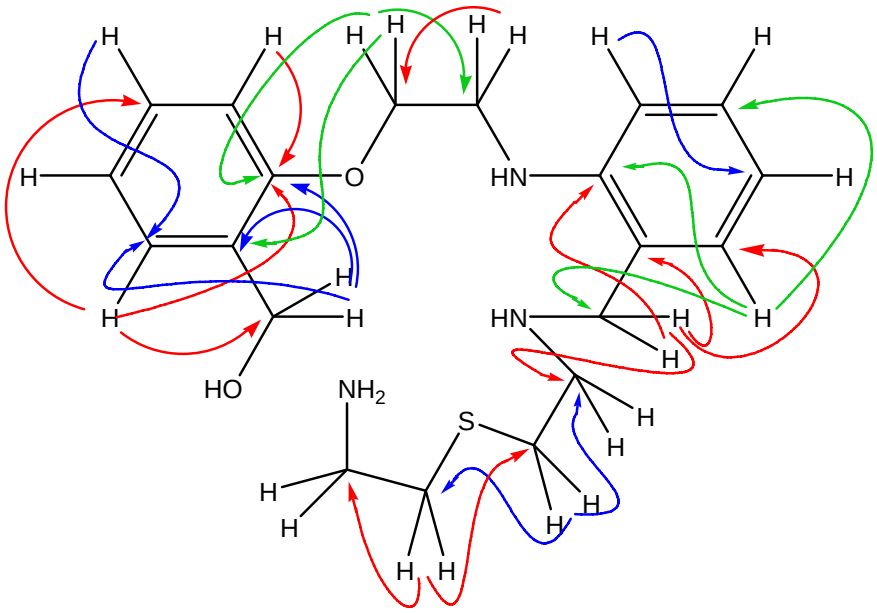

Figure 2.28 Long range NMR (HMBC, J = 8 Hz) correlations for **158**.

The lack of long range correlations from the methylene protons at δ 4.68 to any of the carbon atoms in the NSN-donor portion and also from any of the protons at δ 2.77 to the carbon at 60.9 ppm, is consistent with the acyclic structure proposed.

[2 + 1] condensation product **159**

An attempt was made to improve the synthesis of **137** (SN/NSN*)* by replacing $NaBH_4$ with $NaBH_3CN$ as the *in situ* reducing agent, but this proved less successful. Following reaction workup (including column chromatography with 2% MeOH in DCM), a small amount of the SN-diol **151** was isolated, together with the [2 + 1] diol **159**.

The ^{1}H and ^{13}C NMR assignments and long range 2D correlations for **159** are shown in **Figures 2.29** and **2.30** respectively.

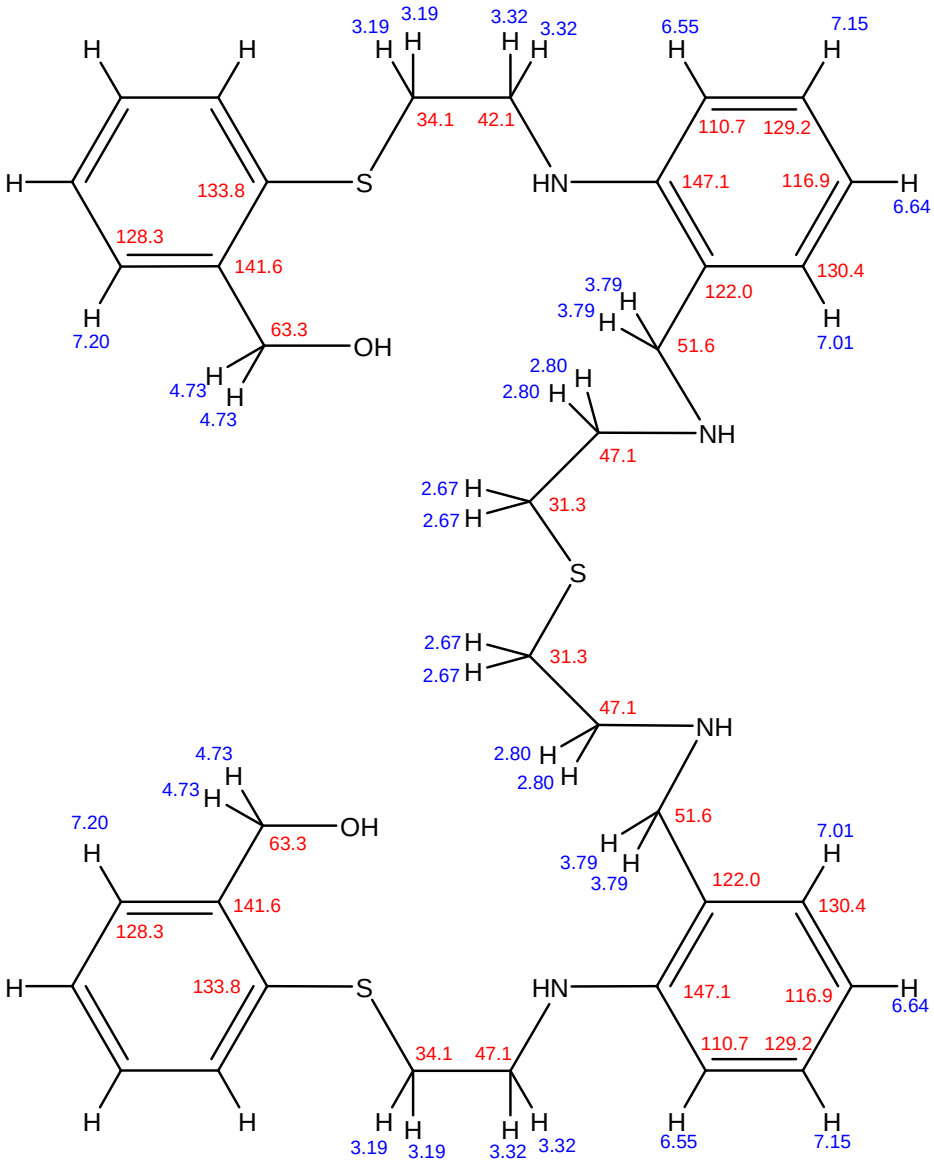

Figure 2.29 ^{1}H and ^{13}C NMR (HSQC, J =140 Hz) assignments for **159**.

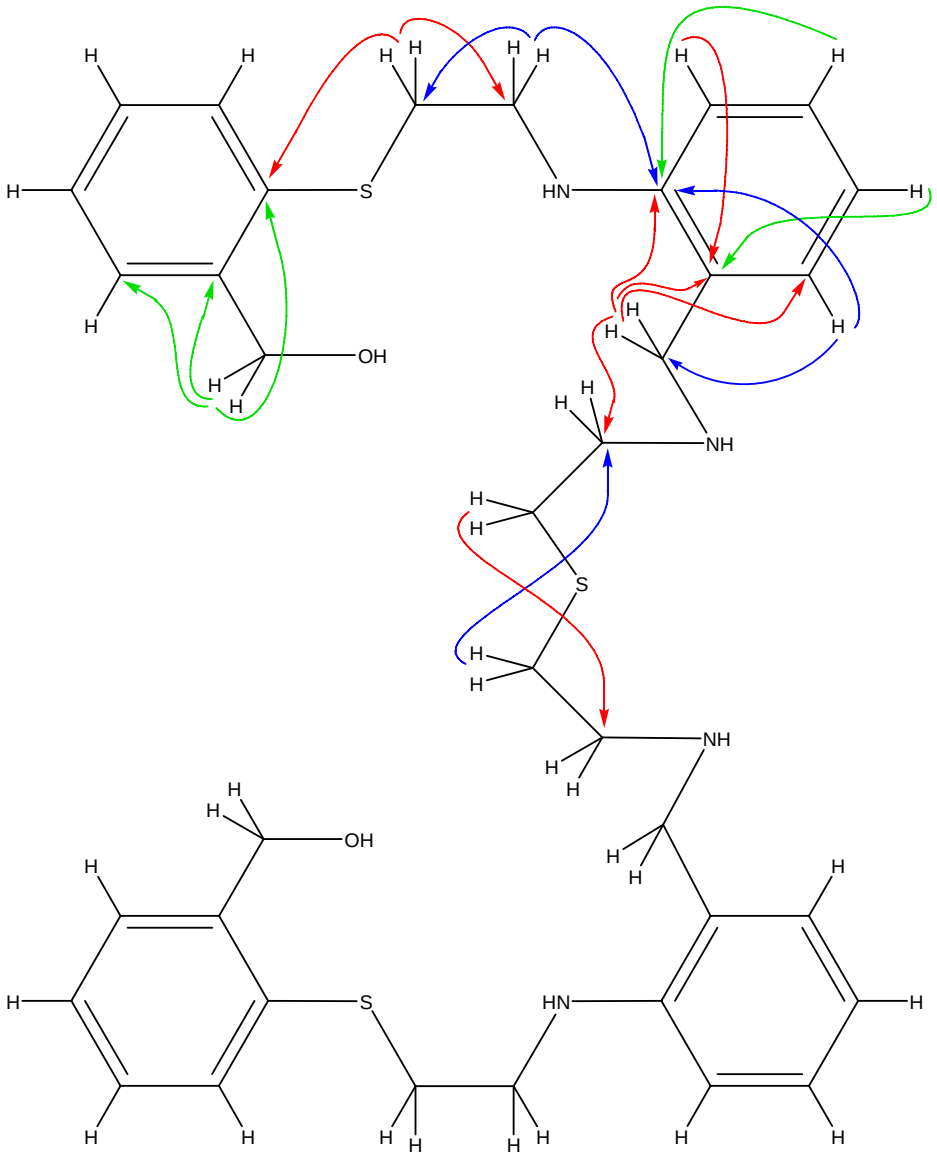

Figure 2.30 Long range NMR (HMBC, J = 8 Hz) correlations for **159**.

The absence of correlations from the alcoholic methylene protons at δ 4.73 to any carbon signals other than the aromatic carbons of the S-substituted benzo-ring (as shown in **Figure 2.30**) is consistent with the acyclic structure proposed for **159**; further, the integral for the ^{1}H NMR spectrum (see the Experimental section) is in agreement with the presence of a [2 + 1] condensation product.

2.5 Experimental

2.5.1 General

Solvents and reagents

Dry tetrahydrofuran (THF) was obtained by an initial distillation from sodium wire, followed by a second distillation in the presence of sodium benzophenone ketyl under a positive atmosphere of dry nitrogen, immediately prior to use. Dry N,N-dimethylformamide (DMF) was prepared by distillation under reduced pressure onto 4A molecular sieves for temporary storage; this procedure was repeated immediately prior to use. Chromatography solvents were distilled through a 1 metre fractionation column packed with glass helices. Dichloromethane (DCM) was distilled from calcium hydride. The saturated ammonia solution used for chromatography was prepared by bubbling dry NH_3 through chilled water. The solution was stored in a sealed glass container at 4 ˚C. Analytical grade triethylamine (NEt_3) was used as supplied. N-(2-aminoethyl)-1,3-propanediamine was dried over 4A molecular sieves prior to use.

$BaMnO_4$ was prepared according to literature methods.[30]

Di(2-aminoethyl)sulfide was prepared via a modification of the previously reported preparation of 2-aminoethyl 3-aminopropyl sulfide.[33] Di(2-aminoethyl)ether was generated *in situ* from commercially available di(2-aminoethyl)ether dihydrochloride by dissolving it in absolute ethanol (EtOH) followed by addition of the required amount of sodium hydroxide.

All other reagents were of analytical grade where available and used as supplied.

Chromatography

Reaction progress was monitored by thin layer chromatography (TLC) on commercial plates (Merck, DC-Plastickfolien Kieselgel 60 F_{254}) and viewed under UV light. Rapid column chromatography was carried out using TLC grade silica gel (Merck, Kieselgel 60H) dry packed under vacuum into a glass column fitted with a sintered glass disk. The content of the chromatography fractions was also monitored using TLC.

Nuclear Magnetic Resonance (NMR) Spectroscopy and Mass Spectrometry (MS)

^{1}H NMR spectra were recorded using a Bruker AM-300 spectrometer (300.133 MHz) or a Bruker AM-600 spectrometer at 298 K. Chemical shifts are quoted as δ values relative to the solvent used. In particular, for $CDCl_3$ the values are reported relative to the residual solvent proton at δ 7.26. Signal multiplicity is designated as singlet (s), doublet (d), triplet (t), quartet (q), multiplet (m), broad (br). Aromatic protons are designated (Ar). Coupling constants (*J*) are reported in Hertz (Hz). The signals are reported in the text in the following format: δ value, multiplicity, coupling constant(s), integral, assignment. In cases where NH or OH proton signals were not clearly observed, they are omitted from the reported spectral assignment.

^{13}C NMR spectra were recorded using a Bruker AM-300 spectrometer (75MHz), unless otherwise stated. ^{1}H decoupled spectra were recorded and the chemical shifts are reported as δ values relative to $CDCl_3$ (δ 77.0 ppm).

Electrospray (ES) fourier transform ion cyclotron resonance high resolution mass spectra (FTICR-MS) were obtained on a Bruker BioApex 47e and were recorded by Mr. R. Willis at the Australian Institute of Marine Science, Cape Cleveland, Townsville.

X-ray Structures

X-ray diffraction studies for macrocycles **132** and **138** were carried out by Dr B. McCool, School of Pharmacy and Molecular Sciences, James Cook University, Townsville. The data was collected at room temperature on an Enraf Nonius CAD4 diffractometer and was solved by direct methods using SHELXS97[39] and refined with SHELXL97[39] using WINGX as the graphical interface.[40] No absorption corrections were applied. All non-hydrogen atoms were refined anisotropically. Except for those on the amine nitrogen atoms, all hydrogen atoms were placed at calculated positions (riding model) and their parameters were not refined. Those hydrogen atoms attached to the nitrogens were located with a Fourier difference map and were refined isotropically. Crystal data and details of the refinement are given in **Appendix B**; selected bond lengths and bond angles are also presented in **Appendix B**.

The X-ray studies for **136**, **137** and **142** as well as the metal complexes presented in later chapters were performed by Dr J. Clegg, School of Chemistry, University of Sydney; some preliminary data collection was also carried out by Dr. Feng Li also at the University of Sydney. Data for **136**, **137** and **142** were collected on a Bruker-Nonius APEX2-X8-FR591 diffractometer employing graphite-monochromated Mo-Kα radiation generated from a rotating anode (0.71073 Å) with ω and ψ scans to approximately 56° 2θ at 150(2) K [Bruker-Nonius (2003). APEX v2.1, SAINT v.7 and XPREP v.6.14. Bruker AXS Inc. Madison, Wisconsin, USA.]. Data integration and reduction were undertaken with SAINT and XPREP [Bruker (1995), SMART, SAINT and XPREP. Bruker Analytical X-ray Instruments Inc., Madison, Wisconsin, USA]. Subsequent computations were carried out using the WinGX-32 graphical user interface.[41] Structures were solved by direct methods using SIR97.[42] Multi-scan empirical absorption corrections, when applied, were applied to the data sets using the programs TWINABS or SADABS.[43] Data were refined and extended with SHELXL-97.[44] In general, non-hydrogen atoms with occupancies greater than 0.5 were refined anisotropically. Carbon-bound hydrogen atoms were included in idealised positions and refined using a riding model. Oxygen and nitrogen bound hydrogen atoms were first located in the difference Fourier map before refinement. Where these hydrogen atoms could not be located, they were not modelled. Disorder was modelled, and twinning where present accounted for, using standard crystallographic methods including constraints, restraints and rigid bodies where necessary. Queries regarding crystallography can be directed to Dr Jack K. Clegg, School of Chemistry, F11, The University of Sydney, NSW, 2006, Australia.

Crystal data and summaries of data collection for **132**, **136** – **138** and **142** as well as non-hydrogen bond lengths and bond angles are presented in **Appendix B**.

2.5.2 Synthesis of macrocyclic precursors

Synthesis of intermediate **146**

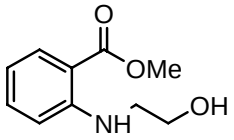

Ethylene oxide (100 ml, 2.0 mol) was added to a solution of methyl anthranilate (124 g, 0.82 mol) in 1 M acetic acid at 0 ˚C.[28] The reaction mixture was stirred for 3 days (and monitored daily by ^{1}H NMR). The aqueous phase was decanted and the residual oil was washed quickly with 10% sodium hydroxide (200 ml) and then water (3 x 200 ml). The oil was then dissolved in DCM and the solution dried over anhydrous sodium sulfate. The product **146** crystallised as white needles upon the addition of cyclohexane (110 g, 68%). (Found (ES): $[M + H]^+$, 196.0958. $C_{10}H_{13}NO_3$ requires $[M + H]^+$, 196.0968). ^{1}H NMR ($CDCl_3$) δ 3.36, t, *J* 6.0 Hz, 2H, NHC**H**$_2$; 3.81, s, 3H, OC**H**$_3$; 3.84, t, *J* 6.0 Hz, 2H, C**H**$_2$OH; 6.59, ddd, *J* 8.0, 7.0, 0.9 Hz, 1H, Ar; 6.69, br d, *J* 8.5 Hz, 1H, Ar; 7.33, ddd, *J* 8.5, 7.1, 1.7 Hz, 1H, Ar; 7.88, dd, *J* 8.0, 1.7 Hz, 1H, Ar. ^{13}C NMR ($CDCl_3$) δ 44.9, 51.4, 60.9, 110.2, 111.3, 114.8, 131.6, 134.5, 150.9, 168.9.

Synthesis of mesylate **147**

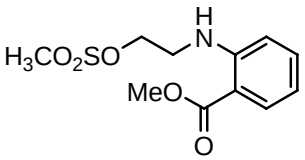

A solution of the alcohol **146** (65.7 g, 0.34 mol) and NEt_3 (34.1 g) in DCM (200 ml) was cooled in ice and methanesulfonyl chloride (44 g, 0.38 mol) was added dropwise with stirring. A white precipitate formed during the addition. The mixture was stirred for 1 h at room temperature (r. t.) and water (700 ml) was added. The organic layer was separated and washed with 1M hydrochloric acid (200 ml), water (200 ml) and 5% sodium hydroxide (200 ml), and then dried over anhydrous sodium sulfate. Removal of DCM under reduced pressure yielded a white solid, which was recrystallised from boiling EtOH to give **147** as white needles (56.2 g, 61%). (Found: C, 48.1; H, 5.7; N, 5.1%. $C_{11}H_{15}NO_5S$ requires C, 48.3; H, 5.5; N, 5.1%). ^{1}H NMR ($CDCl_3$) δ 3.02, s, SO_2C**H**$_3$; 3.62, t, 2H, *J* 5.7 Hz, NC**H**$_2$; 3.86, s, 3H, OC**H**$_3$; 4.41, t, *J* 5.5 Hz, 2H, C**H**$_2$OS; 6.67, dd, *J* 7.2, 8.1 Hz, 1H, Ar; 6.73, br d, *J* 8.4 Hz, 1H, Ar; 7.38, dt, *J* 8.4, 0.9 Hz, 1H, Ar; 7.92, dd, *J* 7.8, 1.5 Hz, 1H, Ar; 7.97, br s, 1H (exchanges with D_2O), N**H**. ^{13}C NMR ($CDCl_3$) δ 37.6, 42.0, 51.7, 67.6, 110.9, 111.1, 115.8, 131.8, 134.6, 149.7, 168.7.

Synthesis of ethyl thiosalicylate **149**

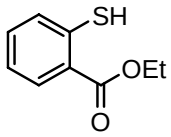

Thiosalicylic acid (77 g, 0.5 mol) was dissolved in absolute EtOH (500 ml) and concentrated H_2SO_4 (20 ml) added slowly with stirring.[29] The mixture was refluxed overnight then cooled to room temperature. The EtOH was partly removed and the residue poured into water (500 ml). The aqueous phase was decanted and the organic layer washed with water (2 x 250 ml) then dissolved in DCM (250 ml) washed again with water and dried with anhydrous sodium sulfate. Removal of the DCM under vacuum afforded **149** as an orange-brown oil (81.4 g, 88%). Due care is necessary during the initial removal of EtOH so that the temperature in the flask does not rise too much (50 ˚C) causing side products to form. In addition, it was necessary to remove a small amount of yellow powdery material by filtration, probably due to some unreacted thiosalicylic acid. ^{1}H NMR ($CDCl_3$) δ 1.41, t, *J* 6.0 Hz, 3H, C**H**$_3$CH$_2$O; 4.39, q, *J* 6.0 Hz, 2H, CH$_3$C**H**$_2$O; 4.69, s, 1H, S**H**; 7.16, m, 1H, Ar; 7.30 – 7.32, m, 2H, Ar; 8.03, brd, *J* 9.0 Hz, 1H, Ar.

Synthesis of the SN diester **150**

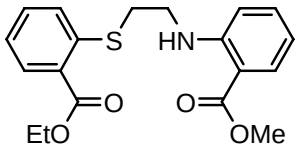

Ethyl thiosalicylate **149** (28.7 g, 0.15 mol), the mesylate **147** (43.05 g, 0.15 mol) and K_2CO_3 (43.53 g, 0.32 mol) were added to absolute EtOH (700 ml) and the mixture was heated at the reflux under nitrogen for 3 h. The reaction mixture was then cooled, poured into water (2 l) and the crude product was removed by filtration and washed with water. The diester **150**, was chromatographed with 30% DCM in hexane as eluent and recrystallised from EtOH:$CHCl_3$ (5:1) to afford fine white needles (36.2 g, 64%). (Found (ES): $[M + Na]^+$, 382.1093. $C_{19}H_{21}SO_4$ requires $[M + Na]^+$, 382.1083). ^{1}H NMR ($CDCl_3$) 1.41, t, *J* 7.1 Hz, 3H, C**H**$_3$CH$_2$O; 3.22, m, 2H, SC**H**$_2$; 3.56, m, 2H, NC**H**$_2$; 3.86, s, 3H, OC**H**$_3$; 4.40, q, *J* 7.1 Hz, 2H, CH$_3$C**H**$_2$O; 6.62, t, *J* 6.9 Hz, 1H, Ar; 6.68, br d, *J* 8.5 Hz, 1H, Ar; 7.19, brt, *J* 7.9 Hz, 1H, Ar; 7.32 - 7.46, m, 3H, Ar; 7.89, m, 2H, Ar. ^{13}C NMR ($CDCl_3$) δ 14.4, 31.7, 41.7, 51.5, 61.2, 110.4, 110.9, 115.0, 124.4, 126.4, 129.2, 131.0, 131.7, 132.0, 134.5, 139.7, 150.3, 166.4, 168.8.

Synthesis of the SN diol **151**

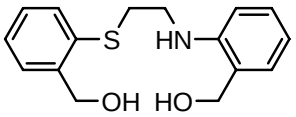

A suspension of the diester **150** (33.5 g, 0.09 mol) was slowly added to a stirred suspension of $LiAlH_4$ (7.8 g, 0.2 mol) in dry freshly distilled THF (500 ml) under a nitrogen atmosphere at 0 ˚C. The mixture was stirred overnight and placed again on ice after which the excess $LiAlH_4$ was hydrolysed by dropwise addition of water (7.8 ml), 10% NaOH (12.3 ml) and water (12.3 ml). The mixture was stirred at room temperature for 1h during which fine white precipitate formed. The solution was filtered through a small 'plug' of celite and the precipitate was washed several times with DCM. Evaporation of the solvent yielded a pale yellow oil which required chromatography through a short silica gel column using DCM with up to 5% acetone as solvent. Removal of the solvent yielded the diol **151** as an off white solid which was then recrystallised from a mixture of DCM/cyclohexane (yield 24.2 g, 90%). (Found (ES): $[M + Na]^+$, 312.1025. $C_{16}H_{19}NO_2S$ requires $[M + Na]^+$, 312.1029). ^{1}H NMR ($CDCl_3$) δ 3.12, br t, *J* 6.0 Hz, 2H, SC**H**$_2$; 3.26, br t, *J* 6.0 Hz, 2H, NHC**H**$_2$; 4.46, s, 2H, C**H**$_2$OH; 4.65, s, 2H, C**H**$_2$OH; 6.53, br d, *J* 8.1 Hz, 1H, Ar; 6.62, dt, *J* 7.2, 0.9Hz, 1H, Ar; 6.95, dd, *J* 7.2, 1.5 Hz, 1H, Ar; 7.10-7.22, m, 3H, Ar; 7.30, dd, *J* 6.6, 2.7 Hz, 1H, Ar; 7.38, dd, *J* 6.9, 1.5 Hz, 1H, Ar. ^{13}C NMR ($CDCl_3$) δ 34.3, 42.1, 63.5, 64.5, 110.6, 116.9, 124.7, 127.1, 128.3, 128.8, 129.2, 129.5, 131.1, 133.5, 141.5, 146.7.

Synthesis of the SN dialdehyde **152**

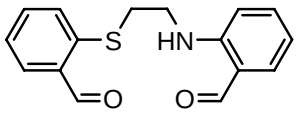

Barium manganate (66.0 g, 0.26 mol) was added to a stirred solution of **151** (4.4 g, 0.015 mol) in dry, freshly distilled DCM (150 ml). The mixture was stirred overnight, then filtered through a small amount of silica gel and the black residue was washed several times with DCM. Evaporation of the combined filtrates yielded **152** as an orange solid, which was recrystallised from a mixture of EtOH/$CHCl_3$ (2.7 g, 62%). (Found: C, 66.9; H, 5.4; N, 5.0%. $C_{16}H_{15}NO_2S$ requires C, 67.3; H, 5.3; N, 4.9%). ^{1}H NMR ($CDCl_3$) δ 3.23, m, 2H, SC**H**$_2$; 3.55, m, 2H, NHC**H**$_2$; 6.64, brd, *J* 9.0 Hz, 1H, Ar; 6.73, t, *J* 7.2 Hz, 1H, Ar; 7.33-7.56, m, 5H, Ar; 7.86, dd, *J* 7.8, 1.2 Hz, 1H, Ar; 8.54 brs,

1H, N**H**; 9.81, s, 1H, C**H**O; 10.42, s, 1H, C**H**O. ^{13}C NMR ($CDCl_3$) δ 32.8, 41.2, 110.3, 115.4, 118.6, 126.1, 129.3, 131.4, 133.8, 134.6, 135.7, 136.6, 139.8, 149.7, 191.0, 193.7.

Synthesis of the intermediate **154**

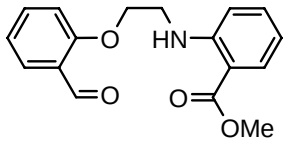

The mesylate **147** (20.0 g, 0.073 mol) and salicylaldehyde **153** (10.7 g, 0.088 mol) were heated with K_2CO_3 (20 g, 0.15 mol) in dry, freshly distilled DMF (100 ml) for 4 h. The resulting mixture was poured into water (500 ml) and the mixture extracted with diethyl ether (3 x 200 ml). The combined organic extracts were washed with water (3 x 100 ml), dried over anhydrous Na_2SO_4, and then evaporated to yield the ester **154** as a viscous oil, (17.8 g, 81%). (Found: (ES): $[M + Na]^+$, 322.1048. $C_{17}H_{17}NO_4$ requires $[M + Na]^+$ 322.1050). ^{1}H NMR ($CDCl_3$) δ 3.73, br t, *J* 5.7 Hz, 2H, NC**H**$_2$; 3.86, s, 3H, OC**H**$_3$; 4.33, t, *J* 5.7 Hz, 2H, OC**H**$_2$; 6.64, dt, *J* 1, 7 Hz, 1H, Ar; 6.78, d, *J* 7.9 Hz, 1H, Ar; 6.99, d, *J* 8.1 Hz, 1H, Ar; 7.05, br t, *J* 7.5 Hz, 1H, Ar; 7.39, dt, *J* 1.6, 8.5Hz, 1H, Ar; 7.53, dt, *J* 1.8, 8.8 Hz, 1H, Ar; 7.85, dd, *J* 1.8, 7.7 Hz, 1H, Ar; 7.92, dd, *J* 1.7, 8.1 Hz, 1H, Ar; 8.11, 1H, brs, N**H**; 10.52, s, C**H**O. ^{13}C NMR ($CDCl_3$) δ 42.0, 51.6, 67.1, 110.7, 111.0, 112.5, 115.2, 121.0, 125.1, 128.3, 131.8, 134.5, 135.6, 150.6, 160.8, 168.9, 189.4.

Synthesis of the ON diol **155**

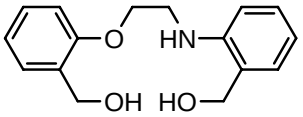

Method 1: The ester **154** (10.09 g, 0.034 mol) in dry THF (50 ml) was slowly added to a stirred suspension of $LiAlH_4$ (1.8 g, 0.047 mol) in THF under a nitrogen atmosphere. The reaction mixture was stirred for 1 h, then cooled in an ice bath, and the excess $LiAlH_4$ quenched by dropwise addition of water (1.8 ml), 10% NaOH (2.9 ml), and again water (2.9 ml). The mixture was stirred overnight, then filtered through a small 'plug' of celite and the precipitate washed several times with DCM. Evaporation of the filtrate yielded the product as an oil. Rapid column chromatography on silica gel, using DCM with up to 10% acetone as eluant, afforded the pure diol **155** as a white crystalline solid (5.0 g, 54%). (Found: C, 70.4; H, 7.0; N, 5.0%. $C_{16}H_{19}NO_3$ requires C, 70.3; H, 7.0; N, 5.1%). ^{1}H NMR ($CDCl_3$) δ 3.56, br t, *J* 5.1 Hz, 2H, NC**H**$_2$; 4.26, t, *J* 5.1 Hz, 2H, OC**H**$_2$; 4.59, s, 4H, C**H**$_2$OH; 6.67 - 6.73, m, 2H, Ar; 6.88, d, *J* 8.1 Hz, 1H, Ar; 6.94, dt, *J*

0.8, 7.6 Hz, 1H, Ar; 7.02, dd, *J* 1.5, 7.3 Hz, 1H, Ar; 7.21 – 7.28, m, 3H, Ar. ^{13}C NMR ($CDCl_3$) δ 42.8, 61.1, 64.3, 66.3, 110.8, 111.3, 117.1, 121.0, 125.1, 129.1, 129.2, 129.3, 129.4, 129.7, 147.3, 156.5.

Method 2: The ester **154** (8.05 g, 0.027 mol) was dissolved in dry THF (200 ml) and $LiAlH_4$ (3.06 g, 0.087 mol, 1:3 molar ratio) added in very small portions at 0 ˚C with vigorous stirring under nitrogen. The mixture was stirred for 1 h after which a further 0.824 g of $LiAlH_4$ was added. The reaction mixture was allowed to stir overnight, then placed in ice and the excess $LiAlH_4$ quenched by successive dropwise additions of water (4.104 g), 10% NaOH (6.47 ml) and again water (12.31 ml). The mixture was again stirred overnight, filtered through celite and the precipitate washed several times with DCM. Rapid column chromatography of the crude oil afforded the pure diol **155** as a white crystalline solid which was recrystallised from DCM (containing 10% hexane) in a much improved yield (6.36 g, 86%). The NMR data obtained for this product was identical to that shown above for **155**.

Synthesis of the ON dialdehyde **156**

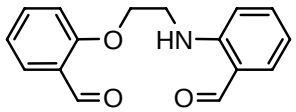

Barium manganate (45.0 g, 0.18 mol) was added to a stirred solution of the diol **155** (3.0 g, 0.01 mol) in dry DCM (120 ml). After 4 h a further 10 g of $BaMnO_4$ was added and the reaction was stirred overnight, then filtered through silica gel. The residue was washed well with DCM. Evaporation of the yellow filtrate yielded the product **156** as a pale yellow solid (2.2 g, 74%). When chromatography was required prior to recrystallisation it was carried out on silica gel with hexane/DCM (1:1). (Found: C, 71.0; H, 5.9; N, 5.3%. $C_{16}H_{15}NO_3$ requires C, 71.4; H, 5.6; N, 5.2%). ^{1}H NMR ($CDCl_3$) δ 3.76, dd, *J* 11.3, 5.6 Hz, 2H, NC**H**$_2$; 4.31, br t, *J* 5.6 Hz, 2H, OC**H**$_2$; 6.75, t, *J* 7.4 Hz, 1H, Ar; 6.78, d, *J* 8.5 Hz, 1H, Ar; 6.98, d, *J* 8.4 Hz, 1H, Ar; 7.05, t, *J* 7.5 Hz, 1H, Ar; 7.41-7.56, m, 3H, Ar; 7.85, dd, *J* 1.8, 7.7 Hz, 1H, Ar; 8.65, br s, 1H, NH; 9.82, s, 1H, C**H**O; 10.50, s, 1H, C**H**O. ^{13}C NMR ($CDCl_3$) δ 41.4, **C**H_2N; 66.9, **C**H_2O; 110.6, 112.4, 115.6, 118.8, 121.2, 125.1, 128.4, 135.8, 135.9, 136.8, 150.3, 160.7, 189.6, 194.1.

Synthesis of Di(2-aminoethyl)sulfide

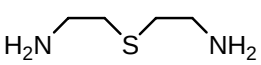

Sodium (7.8 g, 0.34 mol) was added in small portions with stirring to dry MeOH (100 ml). To this mixture was added a solution of aminoethanethiol hydrochloride (11.87 g, 0.1 mol) in MeOH (50 ml). To this was added in small portions, with vigorous stirring, a solution of 2-bromoethylamine hydrobromide (20.50 g, 0.1mol) in MeOH (50 ml). The reaction mixture was stirred overnight under a dry nitrogen atmosphere and then filtered. The filtrate was concentrated and the resulting oil was distilled under reduced pressure to yield the product as a clear colourless oil. ^{1}H NMR ($CDCl_3$) δ 2.61, dt, *J* 2.1, 6.3 Hz, 4H, SC**H**$_2$; 2.87, dt, *J* 2.4, 6.6 Hz, 4H, NC**H**$_2$. ^{13}C NMR ($CDCl_3$) δ 40.4, 42.2.

2.5.3 Synthesis of macrocycles

Synthesis of **132**

(a) Initial preparation

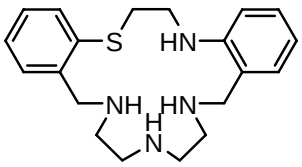

Di(2-aminoethyl)amine (0.93 g, 0.009 mol) in MeOH (20 ml) was added very slowly to a stirred solution of dialdehyde **152** (2.56 g, 0.009 mol) in MeOH (140 ml) with heating (65 ºC). The mixture was heated with stirring for a further 1 h and then allowed to cool. Excess $NaBH_4$ (2.0 g, 0.053 mol) was added rapidly, followed by slow addition of ice, resulting in a total volume of 500 ml. The mixture was left stirring overnight, during which time an off-white gum separated out. The mixture was extracted with DCM (3 x 100 ml) followed by a water wash (100 ml) of the combined extracts. The DCM extract was then dried with anhydrous Na_2SO_4. Removal of the solvent on the rotary evaporator yielded the crude macrocycle which was chromatographed on silica with 7% NH_3 in EtOH. Recrystallisation from acetonitrile afforded **132** as an off-white crystalline solid (2.1 g, 65%). (Found: C, 66.7; H, 7.5; N, 15.3%. $C_{20}H_{28}N_4S$ requires: C, 67.4; H, 7.9; N, 15.7%). (Found (ES): $[M + H]^+$, 357.2124. $C_{20}H_{28}N_4S$ requires $[M + H]^+$, 357.2107).

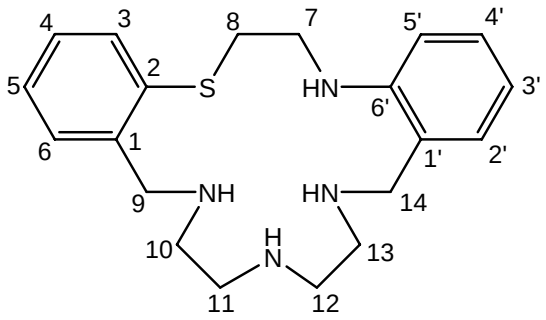

^{1}H NMR ($CDCl_3$) δ 1.75, br s, 4H, NH; 2.71, m, 4H, H11 & H12; 2.82, m 2H, H10; 2.87, m, 2H, H13; 3.37, m, 2H, H8; 3.52, m, 2H, H7; 3.79, s, 2H, H14; 3.87, s, 2H, H9; 6.63, m, 2H, Ar; 7.02, dd, *J* 7.8, 1.8 Hz, 1H, Ar; 7.10-7.25, m, 4H, Ar; 7.33, dd, *J* 8.1, 0.1 Hz, 1H Ar. ^{13}C NMR ($CDCl_3$) δ 32.0, 41.9, 48.4, 49.5, 49.6, 49.8, 53.4, 54.3, 109.9, 116.4, 124.2, 125.2, 126.9, 127.9, 128.5, 129.7, 130.1, 137.3, 138.5, 147.7.

(b)Alternative synthesis for **132**

Di(2-aminoethyl)amine (0.310 g, 0.003 mol) in HPLC grade MeOH (150 ml) was added dropwise to SN-dialdehyde **152** (0.689 g, 0.0024 mol) in HPLC grade MeOH (450 ml) and the mixture heated at reflux overnight under an atmosphere of dry N_2. Addition of excess $NaBH_4$ (1.70 g, 0.046 mol) and further heating (2.5 h), was followed by removal of the solvent under vacuum and partitioning the crude product between DCM (100 ml) and aqueous 1M NaOH (100 ml). The layers were separated and the aqueous phase was extracted twice more with DCM (100 ml and 50 ml). The combined organic fractions were back-washed with water and then washed with saturated NaCl solution (200 ml). The organic fraction was separated, filtered and the DCM removed under vacuum. No chromatography was required in this case and pure **132** was obtained by recrystallisation from acetonitrile (0.68 g, 80%). The NMR data obtained for this product was identical to that shown above for **132**.

Synthesis of **133** *and* **134**

N-(2-aminoethyl)-1,3-propanediamine (1.08 g, 0.009 mol) in MeOH (10 ml) was added

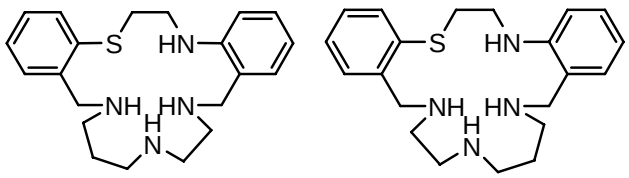

slowly dropwise to a stirred solution of dialdehyde **152** (2.19 g, 0.008 mol) in MeOH (500 ml). The mixture was refluxed for 45 min then allowed to cool slightly and excess $NaBH_4$ (2.5 g, 0.07 mol) was added rapidly. The volume was reduced to 75 ml and ice water was added to a total volume of 500 ml. A yellow gum separated; this was extracted into DCM (3 x 100 ml), followed by a water back-wash of the combined organic extracts. After drying the solution with anhydrous Na_2SO_4 the DCM was removed. The residue was shown (by ^{1}H NMR) to consist of a 60:40 mixture of the two macrocycles (2.59 g) shown above. These were separated by repeated column chromatography on silica gel using a mixture of $CHCl_3$ and Et_3N (gradual increase of Et_3N from 0 to 20%) as eluent.

Macrocycle **133** containing the propyl portion of the triamine adjacent to the thioether group was the less polar of the two products and eluted first from the column. (Found (ES): $[M + H]^+$, 371.2255. $C_{21}H_{30}N_4S$ requires $[M + H]^+$, 371.2264).
^{1}H NMR ($CDCl_3$) δ 1.62, m, 2H; 2.12, brs, 4H, N**H**; 2.65, m, 8H; 3.25, m, 2H; 3.40, m, 2H; 3.71, s, 2H; 3.80, s, 2H; 6.56, brd, *J* 7.9 Hz, 1H, Ar; 6.60, t, *J* 7.4 Hz, 1H, Ar; 6.98, dd, *J* 7.3, 1.3 Hz, 1H, Ar; 7.10 – 7.23, m, 4H, Ar; 7.44, dd, *J* 7.8, 1.0 Hz, 1H, Ar. ^{13}C NMR ($CDCl_3$) δ 27.5, 34.2, 42.1, 46.5, 46.9, 48.5, 48.8, 52.5, 53.5, 109.5, 115.8, 123.6, 125.5, 127.3, 127.9, 129.2, 129.3, 129.5, 136.2, 139.6, 147.2.

NMR assignments for **134** were made by analogy with those employed for its isomer **133**. ^{1}H NMR ($CDCl_3$) δ 1.68, m, 2H, $NCH_2C\mathbf{H}_2CH_2NHCH_2CH_2Ar$; 2.52, br s, 4H, NH; 2.78-2.67, m, 8H, $NC\mathbf{H}_2CH_2CH_2NHCH_2Ar$, $NCH_2CH_2C\mathbf{H}_2NHCH_2Ar$ and $NCH_2C\mathbf{H}_2NHCH_2Ar$, $NC\mathbf{H}_2CH_2NHC\mathbf{H}_2Ar$; 3.27, m, 2H, $SC\mathbf{H}_2$; 3.52, m, 2H, $ArNHC\mathbf{H}_2$; 3.75, s, $NCH_2CH_2CH_2NHC\mathbf{H}_2Ar$; 3.84, s, 2H, $NCH_2CH_2NHC\mathbf{H}_2Ar$; 6.64, m, 2H, Ar; 7.02, br d, *J* 6.0 Hz, 1H, Ar; 7.15-7.27, m, 2H, Ar; 7.41, brd, *J* 6.60 Hz, 1H, Ar. ^{13}C NMR ($CDCl_3$) δ 28.6, 34.8, 46.7, 47.0, 47.1, 47.6, 52.1, 53.0, 53.1, 110.1, 116.4, 126.2, 128.1, 128.4, 128.6, 129.9, 130.2, 130.3, 136.6, 139.6, 147.3.

Synthesis of **135**

Di(3-aminopropyl)amine (0.660 g, 0.005 mol) in MeOH (10 ml) was added very slowly to a stirred solution of

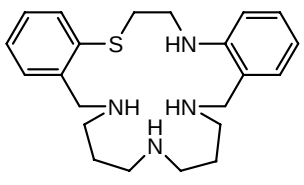

dialdehyde **152** (1.50 g, 0.005 mol) in MeOH (150 ml) with heating. The mixture was refluxed for 1 h and then allowed to cool. Excess $NaBH_4$ (1.0 g, 0.027 mol) was added rapidly. The reaction volume was reduced to 50 ml and ice water added slowly to a total volume of 400 ml. The mixture was allowed to stir overnight, during which time a yellow gum separated out. Reaction workup was carried out as outlined for **132**. The ^{1}H NMR spectrum of the crude reaction mixture (and TLC analysis) revealed the presence of mainly polymeric material. No chromatography was attempted in this case.

Synthesis of **136**

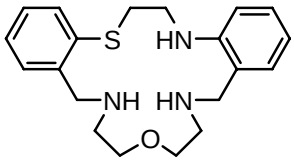

Di(2-aminoethyl)ether dihydrochloride (0.363 g, 0.002 mol) was dissolved in absolute EtOH (200 ml) containing NaOH (0.2 g, 0.005 mol). This solution was added slowly (10 h) under dry N_2 to a solution of SN-dialdehyde **152** (0.570 g, 0.002 mol) in absolute EtOH (500 ml). The mixture was refluxed for a further 2 h after which traces of dialdehyde could still be observed by TLC. A further 0.05 g of di(2-aminoethyl)ether dihydrochloride was added and the reaction mixture was allowed to reflux for 1 h. No remaining dialdehyde could be detected in the resulting reaction mixture; excess $NaBH_4$ (3.0 g, 0.081 mol) was added and the reaction mixture was refluxed for another 3 h. The ethanol was removed under vacuum and the resulting crude mixture was partitioned between DCM (100 ml) and 1M NaOH (100 ml). The layers were separated and the aqueous phase was extracted twice more with DCM (100 ml and 50 ml). The combined organic layers were back-washed with water (100 ml) and then washed with saturated NaCl (200 ml). The solution was filtered and the DCM removed to yield a pale brown oil. Rapid column chromatography on silica gel with 20% MeOH in DCM as eluent followed by recrystallisation from CH_3CN afforded **136** as a white crystalline solid (0.380 g, 53%). (Found: C, 66.99; H, 7.66; N, 11.79; S, 8.71%. $C_{20}H_{27}N_3OS$ requires C, 67.19; H, 7.61; N, 11.75; S, 8.96%). ^{1}H NMR ($CDCl_3$) δ 2.79, brt, *J* 4.8 Hz, 2H; 2.84, brt, *J* 4.5 Hz, 2H; 3.39, m, 2H; 3.55, m, 2H; 3.57, m, 2H; 3.68, m, 2H; 3.85, s, 2H; 3.88, s, 2H; 6.63, d, *J* 7.8 Hz, 1H, Ar; 6.66, m, 1H, Ar; 7.03, brd, *J* 7.5 Hz, 1H, Ar; 7.11, m, 1H, Ar; 7.18, dt, *J* 1.5, 7.8 Hz, 1H, Ar; 7.24, m, 1H, Ar; 7.25, m, 1H, Ar; 7.26, m, 1H, Ar. ^{13}C NMR

($CDCl_3$) δ 31.2, 40.9, 47.7, 48.7, 52.6, 53.7, 69.40, 69.45, 110.0, 116.5, 123.9, 124.86, 124.94, 128.1, 128.5, 129.9, 130.9, 136.1, 136.7, 147.6.

Synthesis of **137**

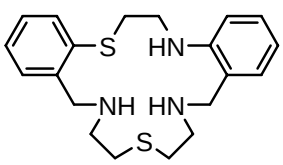

Di(2-aminoethyl)sulfide (0.270 g, 0.0023 mol) in absolute EtOH (250 ml) was added to SN-dialdehyde **152** (0.573 g, 0.002 mol) in absolute EtOH (600 ml) over 6 h at reflux under dry N_2. The reaction mixture was heated at the reflux for another 3 h, after which it was reduced with excess $NaBH_4$ (1.2 g, 0.032 mol) and allowed to reflux overnight. Prior to work-up, ^{1}H NMR analysis of a small aliquot of the reaction mixture revealed incomplete reduction of the imine functions; consequently further $NaBH_4$ (2.0 g, 0.054 mol) was added followed by a 12 h reflux. The persistence of imine protons in the resultant ^{1}H NMR spectrum led to the removal of the ethanol under vacuum and the product mixture was extracted in DCM (100 ml) and washed with 1M NaOH (100 ml). The organic phase was removed and the aqueous layer was once more extracted with DCM (100 ml). The combined DCM extracts were then washed with water (50 ml) followed by saturated NaCl (150 ml). Filtration and removal of the solvent afforded the crude product as an orange-brown glass, which was shown by ^{1}H NMR to be a complex mixture. Chromatography on silica gel with diethyl ether resulted in the recovery of a small amount of the SN-diol **151** (0.122 g) as well as some of the required macrocycle **137** macrocycle (0.240 g, 32%); a third fraction was identified as the mono-imine **144**. ^{1}H and ^{13}C NMR ($CDCl_3$) data for **137** are given below.

Alternative preparation for **137**

Di(2-aminoethyl)sulfide (0.275 g, 0.0023 mol) in absolute EtOH (250 ml) was added dropwise to a solution of SN-dialdehyde **152** (0.566 g, 0.0019 mol) in absolute EtOH (500 ml) over 3 h. Prior to use, the absolute EtOH was passed over a small plug of K_2CO_3. The reaction mixture was refluxed overnight under a positive atmosphere of dry N_2, reduced with excess $NaBH_4$ (2.0 g, 0.054 mol), then heated at reflux for a further 12 h. The solvent was removed under vacuum and the residue was partitioned between aqueous 1M NaOH (100 ml) and DCM (100 ml). The organic phase was removed and the

aqueous layer was once more extracted with DCM (100 ml). The combined DCM extracts were then washed with water (50 ml) followed by saturated NaCl (100 ml). Filtration and removal of the solvent afforded the crude product as an orange-brown glass. Chromatography on silica gel with 2% MeOH in DCM as eluent, followed by recrystallisation from a mixture of DCM/hexane/Et_2O yielded the pure **137** as off-white crystals (0.415 g, 56%) (Found: C, 64.08; H, 7.23; N, 11.25; S, 17.29%. $C_{20}H_{27}N_3S_2$ requires C, 64.30; H, 7.28; N, 11.25; S, 17.17%). ^{1}H NMR ($CDCl_3$) δ 2.77, m, 2H; 2.79, m, 2H; 2.82, m, 2H; 2.86, m, 2H; 3.38, m, 2H; 3.56, m, 2H; 3.78, s, 2H; 3.92, s, 2H; 6.64, dt, *J* 1.1, 7.4 Hz, 1H, Ar; 6.65, dd, *J* 1.1, 8.0 Hz, 1H, Ar; 7.02, dd, *J* 1.7, 7.5 Hz, 1H, Ar; 7.13, dt, *J* 1.2, 7.4 Hz, 1H, Ar; 7.19, dt, *J* 1.6, 7.7 Hz, 1H, Ar; 7.23, dt, *J* 1.6, 7.9 Hz, 1H, Ar; 7.28, brd, *J* 7.4 Hz, 1H, Ar; 7.31, brd, *J* 7.9 Hz, 1H, Ar. ^{13}C NMR ($CDCl_3$) δ 32.4, 32.4, 32.7, 41.8, 46.8, 47.6, 52.4, 53.4, 110.0, 116.5, 123.8, 125.3, 126.5, 128.2, 128.6, 129.8, 130.7, 136.4, 137.3, 147.6.

Preparation of **137** *using HPLC grade MeOH*

To a solution of the SN-dialdehyde **152** (0.335 g, 0.0012 mol) in MeOH (250 ml) was added di(2-aminoethyl)sulfide (0.165 g, 0.0016 mol) in 150 ml MeOH over 3 h. Subsequent detection of dialdehyde in the reaction mixture prompted the addition of further diamine (0.060 g, 0.0006 mol). The reaction was heated at reflux for a further 1 h. Reduction with $NaBH_4$ (1.0 g, 0.027 mol) followed by reaction workup, chromatography and recrystallisation as described above afforded **137** (0.370 g, 82 %). The NMR data obtained in this case was identical to that shown above for **137** and was used to confirm the purity of the product.

Synthesis of **138**

(a) Initial preparation

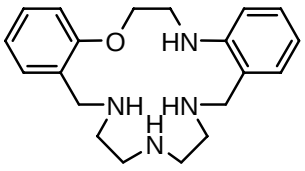

Di(2-aminoethyl)amine (0.38 g, 0.004 mol) in MeOH (5 ml) was added dropwise to ON-dialdehyde **156** (1.0 g, 0.004 mol) in MeOH (100 ml). The reaction mixture was refluxed for 10 min and $NaBH_4$ (0.45 g, 0.012 mol) was added slowly. Ice water (400 ml) was then added slowly and the product separated out as

a pale cream gum. The gum was extracted into DCM (3 x 100 ml) followed by a water (50 ml) back-wash of the DCM solution; the latter was dried over anhydrous Na_2SO_4. Removal of the DCM under reduced pressure yielded **138** which was recrystallised as a white solid from acetonitrile (0.7 g, 56%). (Found: C, 70.4; H, 8.4; N, 16.0%. $C_{20}H_{28}N_4O$ requires C, 70.6; H, 8.3; N, 16.5%). ^{1}H NMR ($CDCl_3$) δ 2.59-2.62, m, 4H; 2.72-2.75, m, 4H; 3.58, br m, 2H, NC**H**$_2$; 3.79, s, 2H; 3.80, s, 2H; 4.28, br t, *J* 4.3Hz, 2H, OC**H**$_2$; 6.47, br s, 1H, N**H**; 6.63-6.67, m, 2H, Ar; 6.68-6.93, m, 2H, Ar; 7.03, dd, *J* 7.2, 1.5 Hz, 1H, Ar; 7.16 – 7.25, m, 3H, Ar. ^{13}C NMR ($CDCl_3$) δ 43.2, 47.4, 48.4, 48.5, 48.5, 50.2, 53.7, 67.5, 109.9, 111.5, 116.5, 120.6, 124.2, 128.3, 128.5, 128.5, 129.9, 130.9, 147.7, 157.5.

(b)Alternative synthesis for **138**

Di(2-aminoethyl)amine (0.30 g, 0.003 mol) was dissolved in HPLC grade MeOH (150 ml) and added dropwise over 4 h to a solution of ON-dialdehyde **156** (0.665 g, 0.0025 mol) in HPLC grade MeOH (400 ml) at reflux and under an atmosphere of dry N_2. The reaction mixture was heated at reflux for a further hour, after which $NaBH_4$ (0.7 g, 0.019 mol) was added. Addition of excess reducing agent (1.0 g) and further heating for 1 h was followed by removal of the solvent and partitioning of the crude product between DCM and 1M NaOH as previously described. The combined organic extracts were in this instance dried with anhydrous Na_2SO_4. An attempt to crystallise the macrocycle from CH_3CN without prior chromatography was in this case successful and **138** was obtained in 80% yield (0.760 g). The NMR data obtained in this case was identical to that shown above for **138** and was used to confirm the purity of the product.

Synthesis of **139** *and* **140**

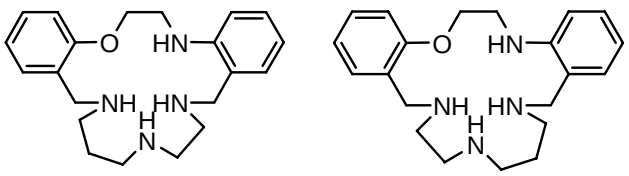

N-(2-aminoethyl)-1,3-propanediamine (0.49 g, 0.0041 mol) in MeOH (10 ml) was added dropwise (and slowly) to a stirred refluxing solution of ON-dialdehyde **156** (1.0 g, 0.0035 mol) in MeOH (100 ml). The mixture was heated at reflux for a further 45 min then allowed to cool slightly and excess $NaBH_4$ (1.25 g, 0.035 mol) was added rapidly. The volume was reduced to 75 ml and ice

water was added to produce a total volume of 500 ml. A yellow gum separated; this was extracted into DCM (3 x 100 ml), followed by a water back-wash of the combined DCM extracts. Following drying with anhydrous Na_2SO_4, the DCM was removed under vacuum. The ^1H NMR spectrum of the crude reaction mixture revealed the presence of what appeared to be mainly a mixture of polymeric material. In view of this no chromatography was attempted. No further effort was made to synthesise these isomers.

Synthesis of **141**

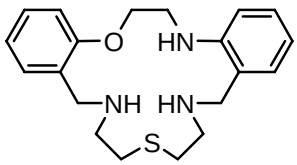

Di(2-aminoethyl)sulfide (0.320 g, 0.0026 mol) in absolute EtOH (250 ml) was added slowly (12 h) to a stirred solution of ON-dialdehyde **156** (0.545 g, 0.009 mol) in absolute EtOH (500 ml) with heating. The mixture was refluxed overnight under nitrogen and then reduced rapidly with excess $NaBH_4$ (2.50 g, 0.068 mol). The mixture was stirred overnight after which ^1H NMR indicated that some imine was still present. A further addition of $NaBH_4$ (1.0 g, 0.027 mol) followed by refluxing for another 4 h failed to completely reduce the imine groups. The reaction was stopped and the ethanol removed under vacuum. The crude mixture was partitioned between DCM (100 ml) and aqueous 1M NaOH (100 ml). The layers were separated and the aqueous phase was extracted twice more with DCM (100 ml and 50 ml). The combined organic extracts were back-washed with water (100 ml) and then washed with saturated NaCl solution (200 ml). The solution was filtered and the DCM removed to yield a light-brown glass. Repeated chromatography with MeOH (5 – 50%) in DCM as eluent resulted in **141** (0.321 g, 45%) as an off-white solid which was recrystallised from CH_3CN. (Found: C, 66.87; 66.73; H, 7.63; 7.65; N, 11.85; 11.85; S, 8.03; 8.31%. $C_{20}H_{27}N_3OS$ requires C, 67.19; H, 7.61; N, 11.75; S, 8.96%). ^1H NMR ($CDCl_3$) δ 2.68 – 2.75, m, 4H; 2.88 – 2.95, m, 4H; 3.65, brt, *J* 4.5 Hz, 2H; 3.74, s, 2H; 3.86, s, 2H; 4.26, brt, *J* 4.5 Hz, 2H; 6.64, m, 1H, Ar; 6.66, brd, *J* 8.1 Hz, 1H, Ar; 6.88, brd, *J* 8.1 Hz, 1H, Ar; 6.90, brt, *J* 6.9 Hz, 1H, Ar; 7.04, brd, *J* 7.2 Hz, 1H, Ar; 7.22, m, 3H, Ar. ^{13}C NMR ($CDCl_3$) δ 31.9, 32.3, 43.0, 47.0, 47.5, 49.5, 52.6, 66.6, 109.6, 111.1, 116.2, 120.6, 123.8, 126.6, 128.6, 128.9, 129.9, 130.6, 147.5, 157.3.

Synthesis of **142**

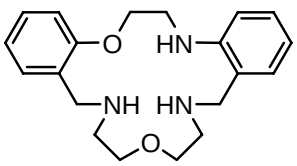

Di(2-aminoethyl)ether dihydrochloride (0.514 g, 0.0029 mol) was dissolved in absolute EtOH (200 ml) containing NaOH (0.31 g, 0.0078 mol). This solution was added very slowly (24 h) under dry N_2 to a solution of the ON-dialdehyde **156** (0.749 g, 0.0029 mol) in absolute EtOH (600 ml). The mixture was refluxed for a further 0.5 h after which excess $NaBH_4$ (3.0 g) was added and the reaction mixture was again refluxed for another 3 h. The ethanol was removed under vacuum and the crude mixture was partitioned between DCM (100 ml) and 1M NaOH aqueous solution (100 ml). The layers were separated and the aqueous phase was twice more extracted with DCM (100 ml and 50 ml). The combined organic layers were back-washed with water (100 ml) and then washed with saturated NaCl (200 ml). The solution was filtered, and the DCM removed under vacuum to yield an off-white glass. Repeated chromatography of this product on silica gel with MeOH (5 – 20%) in DCM afforded **142** which was recrystallised from CH_3CN and MeOH as a white crystalline solid (630 mg, 66%) (Found: C, 70.42; H, 8.25; N, 12.26%. $C_{20}H_{27}N_3O_2$ requires C, 70.35; H, 7.97; N, 12.31%). ^{1}H NMR ($CDCl_3$) δ 2.72, brt, *J* 4.8 Hz, 2H; 2.77, brt, *J* 4.8 Hz, 2H; 3.41, brt, *J* 4.8 Hz, 2H; 3.57, brt, *J* 4.5 Hz, 2H; 3.61, brt, *J* 4.9 Hz, 2H; 3.81, s, 2H; 3.84, s, 2H; 4.29, brt, *J* 4.5 Hz, 2H; 6.66, brd, *J* 7.8 Hz, 1H, Ar; 6.67, m, 1H, Ar; 6.92, dt, *J* 1.2, 6.9 Hz, 1H, Ar; 6.93, brd, *J* 7.8 Hz, 1H, Ar; 7.05, dd, *J* 1.4, 7.8 Hz, 1H, Ar; 7.21, m, 1H, Ar; 7.22, m, 1H, Ar; 7.23, m, 1H, Ar. ^{13}C NMR ($CDCl_3$) δ 43.2, 47.1, 48.6, 50.5, 53.8, 67.3, 68.9, 69.9, 109.8, 111.2, 116.4, 120.4, 124.3, 128.2, 128.38, 128.44, 129.7, 130.8, 147.9, 157.4.

(b) Second preparation of **142**

Di(2-aminoethyl)ether dihydrochloride (0.366 g, 0.002 mol) was added to the dialdehyde **159** (0.536, 0.002 mol) over 18 h, followed by heating of the reaction mixture at reflux overnight. $NaBH_4$ (2.0 g) was rapidly added and this was followed by heating at reflux for 6 h, further addition of reducing reagent (1.0 g) and finally again heating at reflux overnight. Work-up of the product so obtained was as described above. The yield for **142** was much improved (0.610 g, 88%) compared to that mentioned above (66%). The NMR

data obtained was identical to that shown above for **142** and was used to confirm the purity of the product.

Mono-imine **143**

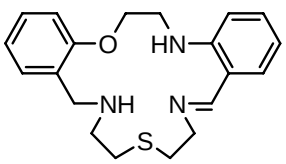

^{1}H NMR ($CDCl_3$) δ 2.71, m, 2H; 2.76, m, 2H; 2.90, m, 2H; 3.74, m, 2H; 3.83, m, 2H; 3.87, s, 2H; 4.27, brt, *J* 4.2 Hz, 2H; 6.71, m, 2H, Ar; 6.88, m, 2H, Ar; 7.28 – 7.19, m, 4H, Ar; 8.34, s, 1H, imine proton; 9.49, brt, *J* 4.9 Hz, 1H, anilino N**H**. ^{13}C NMR ($CDCl_3$) δ 31.5, 32.5, 42.5, 47.3, 50.0, 61.7, 66.0, 109.5, 110.8, 114.7, 117.1, 120.5, 127.7, 128.4, 130.7, 131.4, 134.2, 148.7, 157.2, 164.9.

Mono-imine **144**

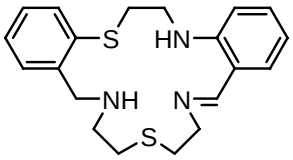

^{1}H NMR ($CDCl_3$) δ 2.84, brs, 4H; 2.94, m, 2H; 3.38, m, 2H; 3.64, m, 2H; 3.83, m, 2H; 3.94, s, 2H; 6.67, brt, *J* 7.2 Hz, 1H; 6.68, d, *J* 7.8 Hz, 1H, Ar; 7.12, dt, *J* 2.1, 7.2 Hz, 1H, Ar; 7.21, brd, *J* 6.6 Hz, 1H, Ar; ~7.26, m, 3H, Ar; 7.29, m, 1H, Ar; 8.34, s, 1H, imine proton; 9.39, brt, *J* 4.8 Hz, 1H, anilino N**H**. ^{13}C NMR ($CDCl_3$) δ 32.0, 32.3, 33.7, 40.8, 46.9, 51.9, 60.7, 109.7, 115.0, 117.3, 125.4, 126.3, 128.4, 131.5, 131.9, 134.2, 136.0, 136.2, 148.6, 164.9.

Bicyclic product **157**

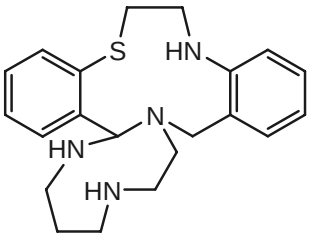

^{1}H NMR ($CDCl_3$, 600MHz) δ 1.61, quint, *J* 6.9 Hz, 2H; 2.64, m, 2H; 2.72, m, 2H; 2.75, m, 2H; 2.87, m, 2H; 3.00, m, 1H; 3.09, m, 1H; 3.54, m, 1H; 3.66, brd, *J* 16.0 Hz, 1H; 4.11, brs, 1H; 4.15, d, *J* 16.1 Hz, 1H; 5.38, s, 1H; 6.60, dt, *J* 0.8, 7.3 Hz, 1H, Ar; 6.62, d, *J* 8.3 Hz, 1H, Ar; 6.87, dd, *J* 1.0, 7.3 Hz, 1H, Ar; 7.04, brt, *J* 7.5 Hz, 1H, Ar; 7.06, brt, *J* 7.7 Hz, 1H, Ar; 7.18, brt, *J* 7.1 Hz, 1H, Ar; 7.36, dd, *J* 1.3, 7.7 Hz, 1H, Ar; 7.68, brd, *J* 7.9 Hz, 1H, Ar. ^{13}C NMR ($CDCl_3$) δ 32.4, 33.3, 40.3, 47.5, 47.7, 49.1, 49.2, 53.1, 77.7, 110.0, 116.6, 119.5, 126.8, 127.19, 127.21, 127.3, 128.8, 132.7, 134.0, 143.2, 143.3. (Found (ES): $[M + Na]^+$, 391.1904. $C_{21}H_{28}N_4S$ requires $[M + Na]^+$, 391.1912).

Benzylic alcohol **158**

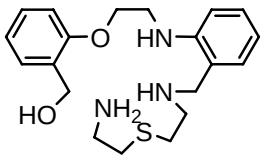

The NMR experiments for this compound were carried out on a Bruker 600 MHz spectrometer. ^{1}H NMR ($CDCl_3$) δ 2.51, brt, *J* 5.9 Hz, 2H; 2.60, brt, *J* 6.1 Hz, 2H; 2.77, m, 4H; 3.56, brt, *J* 4.7 Hz, 2H; 3.79, s, 2H; 4.28, brt, *J* 4.6 Hz, 2H; 4.68, s, 2H; 6.67, t, *J* 7.4 Hz, 1H, Ar; 6.69, d, *J* 8.7 Hz, 1H, Ar; 6.89, d, *J* 8.2 Hz, 1H, Ar; 6.96, brt, *J* 7.4 Hz, 1H, Ar; 7.03, d, *J* 7.2 Hz, 1H, Ar; 7.20, t, *J* 7.8 Hz, 1H, Ar; 7.26, brt, *J* 7.7 Hz, 1H, Ar; 7.34, d, *J* 7.3 Hz, 1H, Ar. ^{13}C NMR ($CDCl_3$) δ 31.9, 35.5, 40.8, 42.8, 47.6, 52.5, 60.9, 66.8, 110.1, 111.1, 116.7, 120.8, 123.8, 128.4, 128.5, 128.6, 129.9, 130.0, 147.9, 156.4.

[2 + 1] *condensation product* **159**

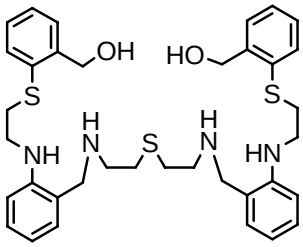

An attempt to synthesise macrocycle **137** by the procedure mentioned earlier but using $NaBH_3CN$ *in situ* did not improve the yield. On the contrary only some SN-diol **151** was recovered together with a small amount of the [2 + 1] condensation product **159.** The latter was isolated by chromatography using 2% MeOH in DCM as eluent. ^{1}H NMR ($CDCl_3$) δ 2.67, brt, *J* 6.4 Hz, 4H; 2.80, brt, *J* 6.2 Hz, 4H; 3.19, brt, *J* 6.1 Hz, 4H; 3.32, brt, *J* 6.2 Hz, 4H; 3.79, s, 4H; 4.73, s, 4H; 6.55, brd, *J* 7.5 Hz, 2H, Ar; 6.64, dt, *J* 0.9, 7.4 Hz, 2H, Ar; 7.01, dd, *J* 7.5, 1.2 Hz, 2H, Ar; 7.15, dt, *J* 1.5, 8.1 Hz, 2H, Ar; 7.18, m, 2H; 7.20, m, 2H, Ar; 7.36, m, 2H; 7.42, m, 2H, Ar. ^{13}C NMR ($CDCl_3$) δ 31.3, 34.1, 42.1, 47.1, 51.6, 63.3, 110.7, 116.9, 122.0, 127.0, 128.3, 128.8, 129.2, 130.4, 130.9, 133.8, 141.6, 147.1.

2.6 References

1. R. Pasche, D. Balkow and E. Sinn, *Inorg. Chem.*, 2002, **41**, 1949.
2. B. Shi, M. Scobie and R. W. Boyle, *Tetrahedron Lett.*, 2003, **44**, 5083.
3. A. Kuik, Z. Szarka, R. Skoda-Foldes and L. Kollar, *Letters Org. Chem.*, 2004, **1**, 151.
4. K.-H. Park, *J. Org. Chem.*, 2005, **70**, 2075.
5. C. Lodeiro, R. Bastida, E. Bertolo, A. Macias and A. Rodriguez, *Transition Metal Chemistry*, 2003, **28**, 388.
6. M. K. Taylor, K. D. Trotter, J. Reglinski, L. E. A. Berlouis, A. R. Kennedy, C. M. Spickett and R. J. Sowden, *Inorg. Chim. Acta*, 2008, **361**, 2851.
7. N. Kuhnert and B. Tang, *Tetrahedron Lett.*, 2006, **47**, 2985.
8. C. Godoy-Alcantar, A. K. Yatsimirsky and J.-M. Lehn, *J. Phys. Org. Chem.*, 2005, **18**, 979.
9. J.-M. Lehn, *Chem. Eur. J.*, 2006, **12**, 5910.
10. P. Guerriero, P. A. Vigatto, D. E. Fenton and P. C. Hellier, *Acta Chem. Scand.*, 1992, **46**, 1025.
11. P. Guerriero, S. Tamburini and P. A. Vigatto, *Coord. Chem. Rev.*, 1995, **139**, 17.
12. P. A. Vigatto and S. Tamburini, *Coord. Chem. Rev.*, 2004, **248**, 1717.
13. P. A. Vigatto, S. Tamburini and L. Bertollo, *Coord. Chem. Rev.*, 2007, **251**, 1311.
14. W. B. Callaway, J. M. Veauthier and J. L. Sessler, *J. Porphyrins Phthalocyanins*, 2004, **8**, 1.
15. N. E. Borisova, M. D. Reshetova and Y. A. Ustynyuk, *Chem. Rev.*, 2007, **107**, 46.
16. L. F. Lindoy, *The Chemistry of Macrocyclic Ligand Complexes*, Cambridge University Press, Cambridge, 1989.
17. M. C. Thompson and D. H. Busch, *J. Am. Chem. Soc.*, 1962, **84**, 1762.
18. M. C. Thompson and D. H. Busch, *J. Am. Chem. Soc.*, 1964, **86**, 3651.
19. T. J. Hubin and D. H. Busch, *Coord. Chem. Rev.*, 2000, **200-202**, 5.
20. M. C. Thompson and D. H. Busch, *J. Am. Chem. Soc.*, 1964, **86**, 213.
21. L. F. Lindoy, *Quart. Rev.*, 1971, **25**, 379.
22. S. M. Nelson, *Pure & Appl. Chem.*, 1980, **52**, 2461.

23. S. C. Tang, S. Koch, G. N. Weinstein, R. W. Lane and R. H. Holm, *Inorg. Chem.*, 1973, **12**, 2589.
24. P. G. Owston, R. Peters, E. Ramsammy, P. A. Tasker and J. Trotter, *J. Chem. Soc., Chem. Comm.*, 1980, 1218.
25. E. C. Constable, *Coordination Chemistry of Macrocyclic Compounds*, Oxford University Press, 1999.
26. J. Gao and A. E. Martell, *Org. Biomol. Chem.*, 2003, **1**, 2795.
27. T. A. Khan, S. Naseem, S. N. Khan, A. U. Khan and M. Shakir, *Spectrochim. Acta, Part A*, 2009, **73**, 622.
28. J. L. Everett, J. J. Roberts and W. C. J. Ross, *J. C. S.*, 1953, 2386.
29. A. I. Vogel, *Practical Organic chemistry*, 3rd edn., Longmans, London, 1967.
30. H. Firouzabadi and E. Ghaderi, *Tetrahedron Lett.*, 1978, **9**, 839.
31. H. Firouzabadi and Z. Mostafavipoor, *Bull. Chem. Soc. Jpn.*, 1983, **56**, 914.
32. R. M. Silverstein, F. X. Webster and D. J. Kiemle, *Spectrometric Identification of Organic Compounds*, 7th edn., John Wiley and Sons Inc., New York, 2005.
33. M. J. Bjerrum, T. Lailer and E. Larsen, *Inorg. Chem.*, 1986, **25**, 816.
34. S. M. Nelson, C. V. Knox, M. McCann and M. G. B. Drew, *J. C. S., Dalton*, 1981, 1669.
35. M. G. B. Drew, J. Nelson and S. M. Nelson, *J. C. S., Dalton*, 1981, 1679.
36. H. Adams, N. A. Bailey, D. E. Fenton, P. D. Hempstead and G. P. Westwood, *J. Inclusion Phenom. Mol. Recognit. Chem.*, 1991, **11**, 63.
37. H. Adams, N. A. Bailey, P. Bertrand, S. R. Collinson, D. E. Fenton and S. J. Kitchen, *J. Chem. Soc., Dalton Trans.*, 1996, 1181.
38. D. A. Rockcliffe, D. A. Martell and J. H. Reibenspies, *J. Chem. Soc., Dalton Trans.*, 1996, 167.
39. G. M. Sheldrick, Institut fur Anorganische Chemie der Universitat, Gottingen, Germany, 1997.
40. L. J. Farrugia, *J. Appl. Cryst.*, 1997, **30**, 365.
41. L. J. Farrugia, *J. Appl. Cryst.*, 1999, **32**, 837.

42. A. Altomare, M. C. Burla, M. Camalli, G. L. Cascarano, C. Giocavazzo, A. Guagliardi, A. G. C. Moliterni, G. Polidori and S. Spagna, *J. Appl. Cryst.*, 1999, **32**, 115.

43. G. M. Sheldrick, in *Empirical Absorption and Correction Software*, University of Goettingen, Germany, 1999-2007.

44. G. M. Sheldrick, in *Programs for Crystal Structure Analysis*, University of Goettingen, Germany, 1997.

Chapter 3 – Interaction of the new potentially pentadentate macrocyclic ligands with selected transition and post-transition metal ions

3.1 Background

As discussed in Chapter 1, a series of 16- to 19-membered dibenzo-substituted macrocycles incorporating oxygen, nitrogen and/or sulfur heteroatoms had previously been synthesised in the author's laboratory[1] as part of studies aimed at investigating discrimination behaviour involving Co(II), Ni(II), Cu(II), Zn(II), Cd(II), Ag(I) and Pb(II). Several examples of such discrimination within this metal-ion sequence were documented.[2-4]

This chapter presents an extension of the above studies describing the results of an investigation of the metal ion specificity of the new unsymmetrical systems of general structure **162** already described in Chapter 2.

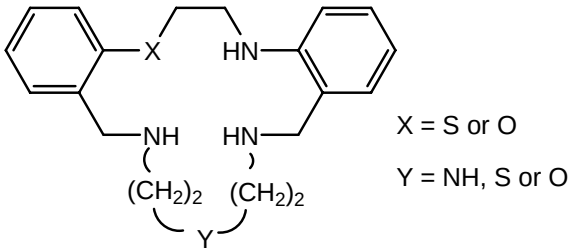

162

3.2 Results and Discussion

3.2.1 Metal complex synthesis

During the course of the present investigation, attempts were made to synthesise and isolate selected crystalline metal complexes of the new 17-membered mixed donor macrocycles **132**, **136** – **138**, **141** and **142** which would be suitable for X-ray diffraction analysis. It was anticipated that the solid state structures might provide a useful background for the stability constant studies which are the main focus of this chapter,

although it is recognised that solid state geometries are not necessarily a reliable indicator of solution structure since solution complexation is a dynamic process (in the present case carried out in the presence of a low-coordinating perchlorate medium). Under such circumstances, it seems likely that all potential macrocyclic ring donor atoms will make some contribution to the overall stability of individual complexes.

The following complexes [Ni**L**Cl]Cl·3H_2O (**L** = **138**), [Ni**L**Cl]Cl·0.125CH_3CN·3.75H_2O (**L** = **142**), [Cu**L**Cl_2]·CH_3CN (**L** = **138**), [Cu**L**Cl_2]·CH_3CN (**L** = **142**), [Cu**L**Cl]Cl·2.375H_2O (**L** = **141**), [Cd**L**$(NO_3)_2$]·CH_3OH (**L** = **138**), [Cd**L**(NO_3)] (NO_3)·CH_3CH_2OH (**L** = **132**), [Ag**L**]PF_6 (**L** = **132**) and [Ag**L**]PF_6 (**L** = **141**) were isolated (see below) as part of the study. In addition, the metal free diprotonated nitrate salt (**L**H_2)$(NO_3)_2$ (**L** = **137**) was also obtained. In general, the complexes were prepared by the addition of a hot solution of the metal salt to a boiling solution of the required macrocyclic ligand; the choice of solvent (or solvent mixture) employed was largely determined by the solubilities of individual ligands. In each case the reaction mixture was stirred with heating, filtered and, generally, divided into two parts: one of which was set aside for slow evaporation of the solvent while the other was subjected to slow diffusion of diethyl ether vapour into the solution.

3.2.2 X-ray structures of Co(II), Ni(II) and Cu(II) complexes

X-ray quality crystals were obtained for the Ni(II) and Cu(II) complexes of several of the macrocyclic ligands of type **162**, while attempts to obtain suitable crystals for the Co(II) complexes were unsuccessful; it is noted that other workers have reported a similar difficulty with respect to this latter metal ion and related ligand systems.[2]

In previous studies on the Ni(II) complexes of related O_2N_3-,[5] S_2N_3-,[6] S_3N_2-,[7] and S_2N_2O-donor[8] macrocycles[#] (namely **100, 112, 113** and **114** respectively) each macrocycle acts as a pentadentate ligand, with the –NYN– fragment (Y = N, O, S) of the ring binding to the metal ion in a facial manner. There are also literature reports of Ni(II) complexes

[#]A plate with the structures of the compounds referred to in the following discussion is available as an insert in the back cover.

formed with the O_2N_3-donor ring **100** where the 1,4,7-triazaheptane macrocyclic fragment again coordinates facially (as expected), but in these structures the remaining three coordination sites around the nickel are occupied by two oxygen atoms of a bidentate nitrate and one oxygen atom from a monodentate nitrate ion[9] or, in the case of an N-bridged thiocyanato (dimeric) structure[10] each Ni(II) achieves a pseudo-octahedral geometry via coordination of the three macrocyclic nitrogens, one nitrogen from a terminal isothiocyanato group and two N-bridging isothiocyanato groups (with a Ni – Ni distance of 3.03 Å). The non-coordination of ether oxygen donors in these structures is not unexpected since the affinity of such atoms for Ni(II) is known to be relatively low;[11] non-coordination of ether groups in a number of other Ni(II) macrocyclic complexes has been confirmed by X-ray diffraction studies.[12, 13] Furthermore there are some more recent reports on the effect of anion variation on the mode of coordination of **100**.[14]

The X-ray structures of the Ni(II) complexes of **138** and **142** show near octahedral coordination geometries, with the metal ion coordinating to all 5 donor atoms of the macrocycle together with a chloro ligand in each complex.

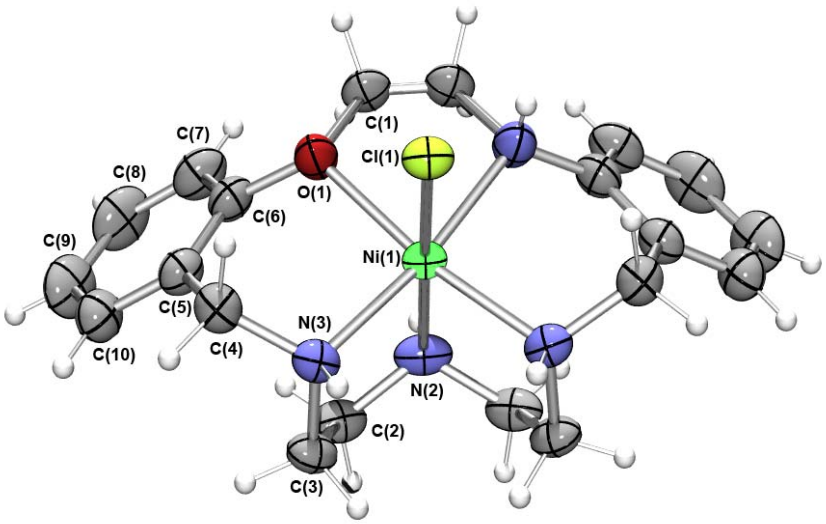

Figure 3.1 ORTEP plot of $[Ni\mathbf{L}Cl]^+$ (**L** = **138**); symmetry code used for generating equivalent atoms: x, -y, z. Selected bond lengths (Å) and angles (˚): N(3)-Ni(1) 2.0675(17), N(2)-Ni(1) 2.113(2), Cl(1)-Ni(1) 2.4481(7), Ni(1)-O(1) 2.1214(17); N(3)-Ni(1)-N(3) 99.15(10), N(3)-Ni(1)-N(2) 84.38(6), N(3)-Ni(1)-O(1) 89.78(7), N(2)-Ni(1)-O(1) 96.71(7), N(3)-Ni(1)-N(1) 171.07(7), O(1)-Ni(1)-N(1) 81.30(9), N(3)-Ni(1)-Cl(1) 91.85(5), N(2)-Ni(1)-Cl(1) 174.15(7), O(1)-Ni(1)-Cl(1) 87.71(6).

In the complex cation of [Ni**L**Cl]Cl·3H_2O (**L** = **138**) (**Figure 3.1**) all donor atoms of the macrocycle coordinate, with the –NNN– fragment again coordinating facially while a chloro ligand occupies the sixth coordination site. The distortion from regular octahedral geometry undoubtedly reflects the steric requirements of the macrocyclic ligand. The 'bite' angles for the 5-membered chelate rings have values of 81.30(9) and 84.38(6)º while the corresponding angles for the two 6-membered rings are each 89.78(7)º. The two halves of the [Ni**L**Cl]$^+$ (**L** = **138**) cation are crystallographically equivalent. The Ni-O bond of 2.1214(17) Å slightly exceeds the sum of the covalent radii[15] of octahedral Ni(II) (1.39 Å) and O (0.66 Å) however, it is comparable to the mean literature value of 2.15 Å for this bond type.[16] The Ni-N distances 2.0675(17) – 2.1214(17) Å for the present complex fall within the range (2.03 – 2.16 Å) observed for such bonds involving neutral sp^3-hybridised nitrogen atoms in macrocyclic high-spin Ni(II) complexes.[17] Crystal data and a summary of data collection for [Ni**L**Cl]Cl·3H_2O (**L** = **138**) as well as non-hydrogen bond lengths and bond angles are given in **Appendix B**, **Tables B.13** – **B.15**.

The [Ni**L**Cl]$^+$ (**L** = **142**) cation (**Figure 3.2**) is characterised by the presence of two chemically identical but crystallographically distinct molecules per unit cell. As for the Ni(II) complex of **138**, the sixth coordination position is occupied by a chloro group. The distortion from regular octahedral geometry results again from the small 'bite' of the 5-membered chelate rings with angles ranging between 79.61(13) – 82.74(15)º, while the 6-membered chelate rings range between 88.17(15) – 90.93(15)º. The Ni-N distances 2.056(4) – 2.122(4) Å and Ni-O bond lengths 2.105(4) – 2.166(4) Å are both unexceptional. Crystal data and a summary of data collection for [Ni**L**Cl]Cl·0.125CH_3CN·3.75H_2O (**L** = **142**) as well as non-hydrogen bond lengths and bond angles are given in **Appendix B**, **Tables B.16** – **B.18**.

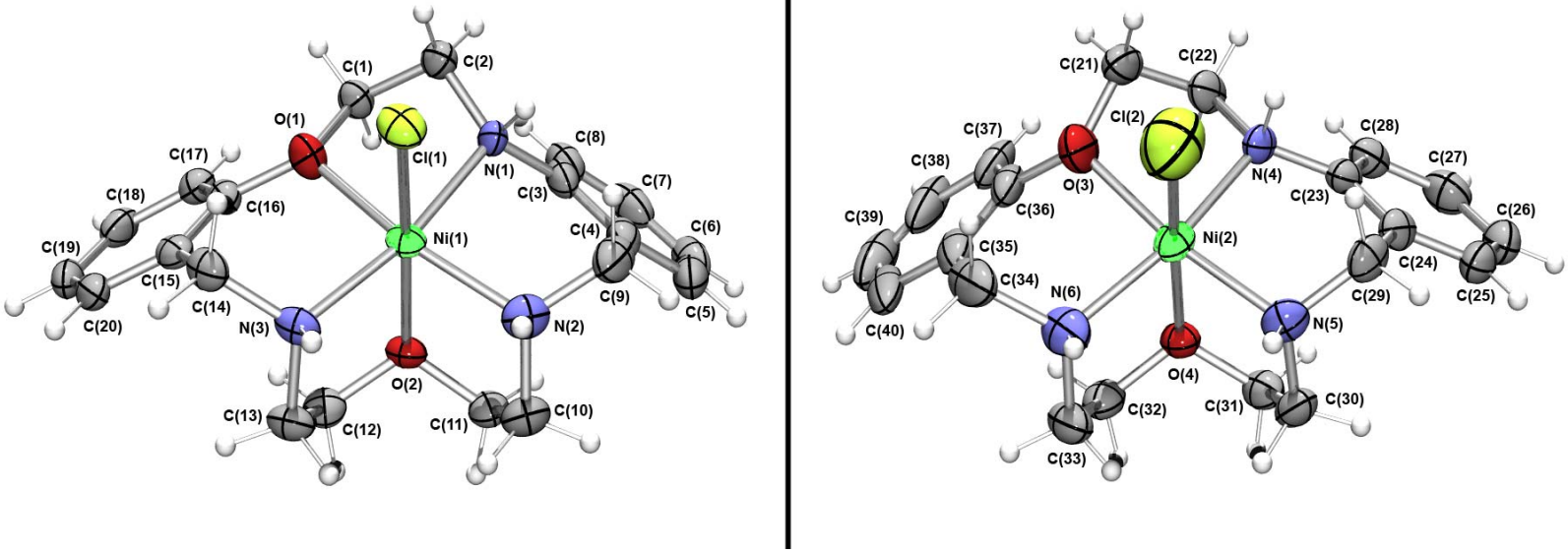

Figure 3.2 ORTEP plots of the two independent cations of type [Ni**L**Cl]$^{+}$ (**L** = **142**) present in the unit cell. Selected bond lengths (Å) and angles (˚): N(1)-Ni(1) 2.118(3), N(2)-Ni(1) 2.082(4), N(3)-Ni(1) 2.056(4), N(4)-Ni(2) 2.122(4), N(5)-Ni(2) 2.060(4), N(6)-Ni(2) 2.089(5), O(1)-Ni(1) 2.166(4), O(2)-Ni(1) 2.164(3), O(3)-Ni(2) 2.105(4), O(4)-Ni(2) 2.148(3), Cl(1)-Ni(1) 2.4030(11), Cl(3)-Ni(2) 2.383(2) ; N(3)-Ni(1)-N(2) 103.32(16), N(3)-Ni(1)-N(1) 168.50(15), N(2)-Ni(1)-N(1) 88.17(15), N(3)-Ni(1)-O(2) 81.80(12), N(2)-Ni(1)-O(2) 82.07(13), N(1)-Ni(1)-O(2) 99.84(12), N(3)-Ni(1)-O(1) 88.98(14), N(2)-Ni(1)-O(1) 165.31(14), N(1)-Ni(1)-O(1) 79.61(13), O(2)-Ni(1)-O(1) 91.94(12), N(3)-Ni(1)-Cl(1) 91.96(10), N(2)-Ni(1)-Cl(1) 94.59(11), N(1)-Ni(1)-Cl(1) 87.27(10), O(2)-Ni(1)-Cl(1) 172.00(9), O(1)-Ni(1)-Cl(1) 92.96(9), N(5)-Ni(2)-N(6) 101.06(19), N(5)-Ni(2)-O(3) 171.39(17), N(6)-Ni(2)-O(3) 87.56(18), N(5)-Ni(2)-N(4) 90.93(15), N(6)-Ni(2)-N(4) 166.39(18), O(3)-Ni(2)-N(4) 80.51(15), N(5)-Ni(2)-O(4) 82.74(14), N(6)-Ni(2)-O(4) 82.24(15), O(3)-Ni(2)-O(4) 98.64(14), N(4)-Ni(2)-O(4) 93.04(13), N(5)-Ni(2)-Cl(3) 90.81(12), N(6)-Ni(2)-Cl(3) 93.95(13), O(3)-Ni(2)-Cl(3) 88.51(12), N(4)-Ni(2)-Cl(3) 92.27(12), O(4)-Ni(2)-Cl(3) 171.71(11).

Suitable crystals for X-ray diffraction were obtained for the Cu(II) complexes [Cu**L**Cl_2]·CH_3CN (**L** = **138**), [Cu**L**Cl_2]·CH_3CN (**L** = **142**) and [Cu**L**Cl]Cl·2.375H_2O (**L** = **141**). In both complexes of type [Cu**L**Cl_2] (**L** = **138** and **L** = **142**), the Cu(II) centres are five-coordinate (with the position of the metal ion relative to the macrocyclic cavity differing considerably between the two complexes), while in the complex of **141** the metal ion is six-coordinate. The Cu(II) is coordinated to the –NYN– (Y = N, O, S) fragment in all three cases while the aryl ether oxygens and anilino nitrogens remain uncoordinated in the complexes of **138** and **142**, but coordinated in $[Cu\mathbf{L}Cl]^+$ (**L** = **141**).

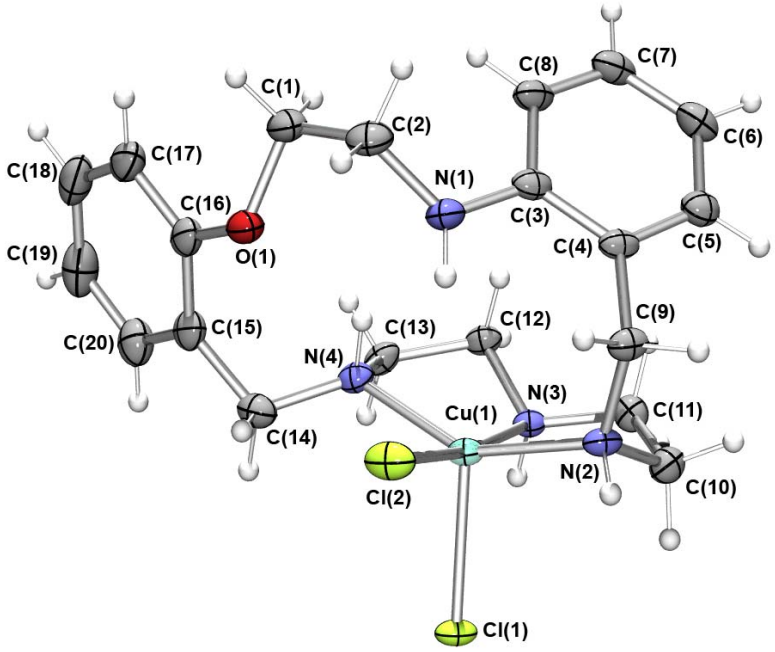

Figure 3.3 ORTEP plot of [Cu**L**Cl_2] (**L** = **138**). Selected bond lengths (Å) and angles (˚): N(2)-Cu(1) 2.0361(15), N(3)-Cu(1) 2.0281(14), N(4)-Cu(1) 2.0540(15), Cl(1)-Cu(1) 2.4705(4), Cl(2)-Cu(1) 2.3003(5); N(3)-Cu(1)-N(2) 84.40(6), N(3)-Cu(1)-N(4) 83.01(6), N(2)-Cu(1)-N(4) 146.91(6), N(3)-Cu(1)-Cl(2) 171.52(4), N(2)-Cu(1)-Cl(2) 93.15(4), N(4)-Cu(1)-Cl(2) 94.84(4), N(3)-Cu(1)-Cl(1) 89.44(4), N(2)-Cu(1)-Cl(1) 101.91(4), N(4)-Cu(1)-Cl(1) 108.43(4), Cl(2)-Cu(1)-Cl(1) 99.015(16).

The coordination sphere of [Cu**L**Cl_2] (**L** = **138**) (**Figure 3.3**) is comprised of the 1,4,7-triazaheptane macrocyclic fragment and a chloro ligand in an equatorial fashion, while the second chloro ligand occupies an axial position in a distorted square pyramidal coordination geometry. The macrocyclic ring is ‘folded’ and coordinates in an *exo*

manner such that the copper is not contained in the macrocyclic cavity. The Cu-N bond distances are unexceptional (mean value 2.0394 Å). Similarly, the Cu-Cl lengths of 2.3003(5) and 2.4705(4) Å fall well within the range (2.11 – 2.64 Å) of values observed for related five-coordinated complexes.[18] The aryl ether oxygen O(1) does not coordinate. This is not unexpected since ether oxygen donors have been documented to be generally poor to 'borderline' donors towards Cu(II). For example, classical crown ethers show little affinity for Cu(II)[19] and X-ray studies have confirmed the non-coordination of ether functions in copper compounds of mixed oxygen-nitrogen donor macrocycles related to those under discussion.[18, 20, 21]

Addison's τ parameter[22] is defined as $\tau = (\beta - \alpha)/60^{\circ}$, where α and β are the largest angles in the coordination sphere. This geometric parameter is applicable to five-coordinate structures as a measure of the degree of trigonality. For a perfectly square pyramidal geometry $\tau = 0$, while for a perfectly trigonal-bipyramidal geometry $\tau = 1$. The choice of axial donor is made using the criterion that it should not be any of the four donors which define the two largest angles. A value $\tau = 0.41$ ($171.52^{\circ} - 146.91^{\circ})/60^{\circ} = 0.41$) was obtained for [Cu**L**Cl_2] (**L** = **138**) which places Cl(1) in the axial coordination site and confirms the distorted square pyramidal assignment for the structure of [Cu**L**Cl_2] (**L** = **138**). Crystal data and a summary of data collection for [Cu**L**Cl_2]·CH_3CN (**L** = **138**) as well as non-hydrogen bond lengths and bond angles are given in **Appendix B**, **Tables B.19** – **B.21**.

In contrast to the above structure, in the case of [Cu**L**Cl_2]·CH_3CN (**L** = **142**) the copper centre is contained inside the macrocyclic cavity (**Figure 3.4**) with the overall coordination geometry being close to square pyramidal ($\tau = 0.04$, $\alpha = 158.72^{\circ}$, $\beta = 161.10^{\circ}$). The equatorial positions are occupied by two chloro ligands and the nitrogen donors of the –NON– fragment, while the ether oxygen O(2) coordinates in the axial position.

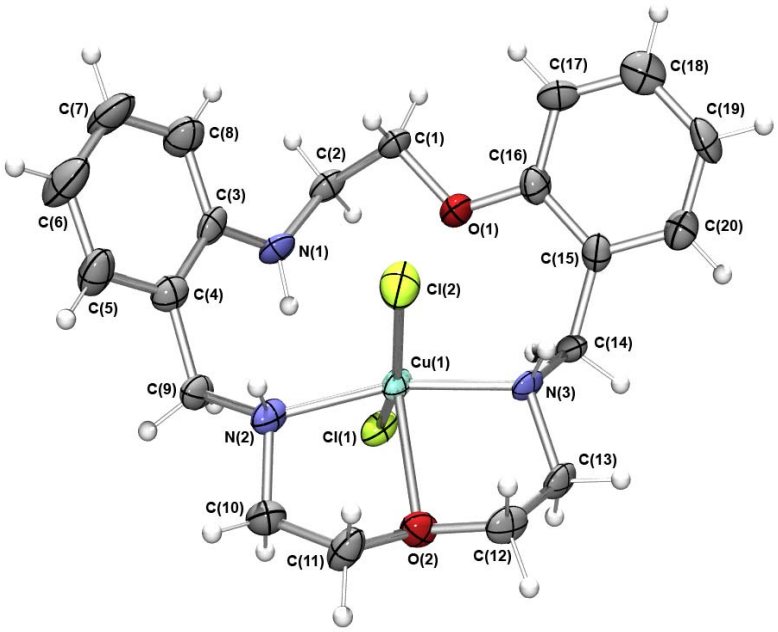

Figure 3.4 ORTEP plot of [Cu**L**Cl_2] (**L** = **142**). Selected bond lengths (Å) and angles (˚): N(3)-Cu(1) 2.035(4), Cl(1)-Cu(1) 2.3029(14), N(2)-Cu(1) 2.079(5), O(2)-Cu(1) 2.252(4), Cl(2)-Cu(1) 2.2920(15); N(3)-Cu(1)-N(2) 161.10(18), N(3)-Cu(1)-O(2) 81.29(16), N(2)-Cu(1)-O(2) 81.48(17), N(3)-Cu(1)-Cl(2) 90.02(13), N(2)-Cu(1)-Cl(2) 87.79(13), O(2)-Cu(1)-Cl(2) 107.54(12), N(3)-Cu(1)-Cl(1) 95.94(13), N(2)-Cu(1)-Cl(1) 92.84(13), O(2)-Cu(1)-Cl(1) 93.57(11), Cl(2)-Cu(1)-Cl(1) 158.72(6).

The Cu-N distances (2.079(5) and 2.035(4) Å) in [Cu**L**Cl_2] (**L** = **142**) fall within the range of values (1.88 – 2.24 Å) reported for other related five-coordinate Cu(II) complexes. The Cu-O bond (at 2.252(4) Å) falls towards the lower end of the range (2.11 – 2.75 Å) found in other Cu(II)-ether complexes.[18] The small angles (81.29(16) and 81.48(17) Å) resulting from the formation of the two 5-membered chelate rings cause the two nitrogen donors to be slightly bent out of plane towards the axial oxygen. Once again, the aryl ether oxygen O(1) and nitrogen N(1) do not coordinate to the copper centre. Crystal data and a summary of data collection for [Cu**L**Cl_2]·CH_3CN (**L** = **142**) as well as non-hydrogen bond lengths and bond angles are given in **Appendix B**, **Tables B.22** – **B.24**.

The X-ray structure of [Cu**L**Cl]Cl·2.375H_2O (**L** = **141**) reveals the presence of two molecules per unit cell; the macrocycle coordinates via all its five donor atoms to the central metal. The geometry around Cu(II) is distorted octahedral with a chloro ligand in the sixth position (**Figure 3.5**). The distortion from regular octahedral geometry can be seen in the range of angles, the smallest being the 5-membered chelate rings incorporating the –ON– donor fragment at 76.3(2) and 76.8(2)º. The Cu(2)-O(2) distance is somewhat long (2.511(5) Å), but lies within the overall range reported for such Cu-O distances (2.11 – 2.75 Å);[23] however, its length may reflect the presence of a Jahn-Teller distortion. The Cu(1)-S(1) distance of 2.3662(19) Å is shorter than the equivalent bond in the Cu(II) complex of the N_4S-donor analogue ring **95**.[24] Crystal data and a summary of data collection for [Cu**L**Cl]Cl·2.375H_2O (**L** = **141**) as well as non-hydrogen bond lengths and bond angles are given in **Appendix B**, **Tables B.25** – **B.27**.

In summary, it is seen that **138**, **141** and **142** interact with Cu(II) to yield both five and six coordinate complexes in which the respective macrocycles act as both tridentate and pentadentate ligands; this undoubtedly largely reflects the different affinities of the O, N and S donors for this ‘borderline’ metal ion.

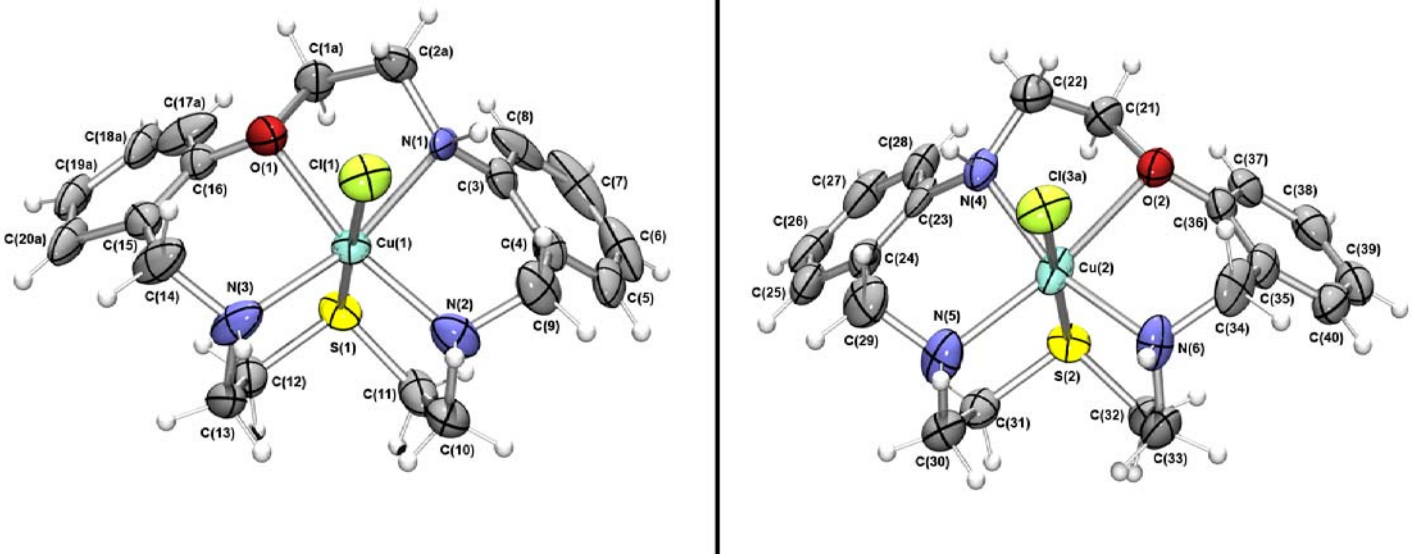

Figure 3.5 ORTEP plots of the two independent cations of type $[Cu\mathbf{L}Cl]^{+}$ (**L** = **141**). Selected bond lengths (Å) and angles (˚): N(1A)-Cu(1) 2.332(6), N(2)-Cu(1) 2.092(7), N(3)-Cu(1) 2.134(7), N(4)-Cu(2) 2.090(6), N(5)-Cu(2) 2.225(7), N(6)-Cu(2) 2.008(6), O(1)-Cu(1) 2.238(6), O(2)-Cu(2) 2.511(5), S(1)-Cu(1) 2.3662(19), S(2)-Cu(2) 2.3757(19), Cl(1)-Cu(1) 2.3303(19), Cl(3A)-Cu(2) 2.312(3), Cl(3B)-Cu(2) 2.437(10); N(2)-Cu(1)-N(3) 107.1(2), N(2)-Cu(1)-O(1) 163.9(2), N(3)-Cu(1)-O(1) 87.5(2), N(2)-Cu(1)-Cl(1) 94.29(19), N(3)-Cu(1)-Cl(1) 95.26(19), O(1)-Cu(1)-Cl(1) 91.15(18), N(2)-Cu(1)-N(1A) 88.3(2), N(3)-Cu(1)-N(1A) 162.3(2), O(1)-Cu(1)-N(1A) 76.3(2), Cl(1)-Cu(1)-N(1A) 91.97(17), N(2)-Cu(1)-S(1) 85.11(19), N(3)-Cu(1)-S(1) 85.22(19), O(1)-Cu(1)-S(1) 89.35(18), Cl(1)-Cu(1)-S(1) 179.32(8), N(1A)-Cu(1)-S(1) 87.70(17), N(6)-Cu(2)-N(4) 162.4(3), N(6)-Cu(2)-N(5) 107.8(3), N(4)-Cu(2)- N(5) 89.8(2), N(6)-Cu(2)-Cl(3A) 88.9(2), N(4)-Cu(2)-Cl(3A) 89.55(18), N(5)-Cu(2)-Cl(3A) 93.8(2), N(6)-Cu(2)-S(2) 86.09(19), N(4)-Cu(2)-S(2) 96.39(17), N(5)-Cu(2)-S(2) 83.99(18), Cl(3A)-Cu(2)-S(2) 173.64(10), N(6)-Cu(2)-Cl(3B) 94.3(3), N(4)-Cu(2)-Cl(3B) 79.4(3), N(5)-Cu(2)-Cl(3B) 108.2(3), Cl(3A)-Cu(2)-Cl(3B) 17.9(2), S(2)-Cu(2)-Cl(3B) 166.9(3), N(6)-Cu(2)-O(2) 86.2(2), N(4)-Cu(2)-O(2) 76.8(2), N(5)-Cu(2)-O(2) 160.4(2), Cl(3A)-Cu(2)-O(2) 100.26(15), S(2)-Cu(2)-O(2) 83.38(13), Cl(3B)-Cu(2)-O(2) 83.6(3).

3.2.3 X-ray structures of Zn(II) and Cd(II) complexes

Previous efforts in the author's laboratory to synthesise Zn(II) and Cd(II) [as well as Ni(II)] complexes of a number of the dibenzo-substituted macrocycles incorporating other than an aliphatic N_3-donor fragment in their backbone resulted in the isolation of salts of the corresponding protonated ligands.[8] There are also examples of protonated salts being obtained even with ligands which incorporate an N_3-donor fragment – for example, the 18-membered O_2N_3-donor macrocycle **103** (see page 53) yields such a salt.[25]

Attempts to synthesise solid Zn(II) complexes suitable for structural studies were also unsuccessful in the current studies. One such preparation yielded the metal free diprotonated nitrate salt of **137** (**Figure 3.6**) in which the macrocycle adopts a different conformation from its non-protonated form (**Figure 2.12**). Protonation of **137** occurred at the two secondary nitrogen donor atoms; non-protonation of the anilino nitrogen is consistent with it having reduced basicity relative to the secondary amine nitrogens. The flexibility inherent in the aliphatic fragment of the macrocyclic ring allows for rotation of the protonated ligand backbone in such manner that all the NH hydrogen atoms are directed away from the cavity of the macrocycle in an '*exo*' fashion; the lone pairs of the aromatic sulfur donor are now in a near '*endo*' orientation. Crystal data and a summary of data collection for (**L**H_2)$(NO_3)_2$ (**L** = **137**) as well as non-hydrogen bond lengths and bond angles are given in **Appendix B**, **Tables B.43** – **B.45**.

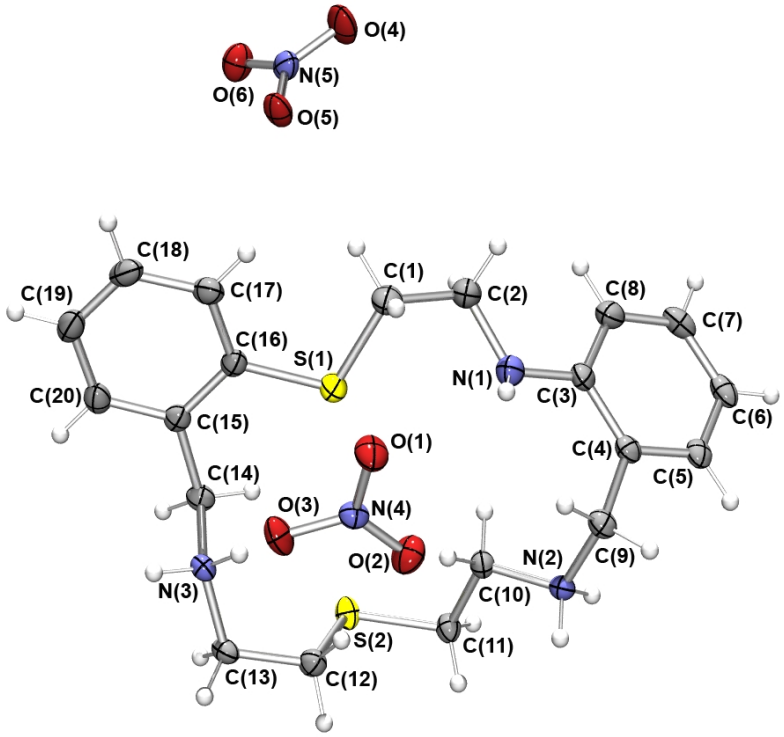

Figure 3.6 X-ray structure of (**L**H_2)(NO_3)$_2$ (**L** = **137**).

The ease of isolation of such derivatives is very likely influenced by the moderately strong basic nature of these ligands; other factors such as low solubilities of the ligand salts in alcohol compared to the corresponding metal complexes together with moderate stabilities of the latter may also contribute. For the present study it appears that, under the conditions employed, the effective affinity of **137** for protons is greater than for Zn(II).

X-ray quality crystals were obtained for [Cd**L**(NO_3)$_2$]·CH_3OH (**L** = **138**) and [Cd**L**(NO_3)](NO_3)·CH_3CH_2OH (**L** = **132**) and the structures are shown in **Figures 3.7** and **3.8** respectively. Crystal data and a summary of data collection as well as non-hydrogen bond lengths and bond angles for [Cd**L**(NO_3)$_2$]·CH_3OH (**L** = **138**) and [Cd**L**(NO_3)](NO_3)·CH_3CH_2OH (**L** = **132**) are given in **Appendix B**, **Tables B.28 – B.30** and **B.31 – B.33** respectively.

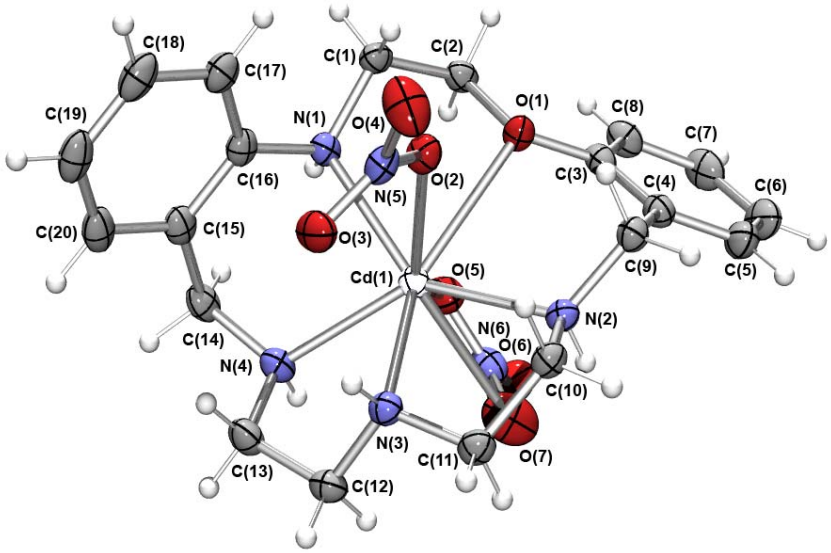

Figure 3.7 ORTEP plot of [Cd**L**$(NO_3)_2$] (**L** = **138**). Selected bond lengths (Å) and angles (˚): N(1)-Cd(1) 2.3885(14), N(2)-Cd(1) 2.3498(14), N(3)-Cd(1) 2.3511(14), N(4)-Cd(1) 2.4331(15), O(2)-Cd(1) 2.5819(13), O(5)-Cd(1) 2.4255(17); N(2)-Cd(1)-N(3) 75.47(5), N(2)-Cd(1)-N(1) 140.04(5), N(3)-Cd(1)-N(1) 131.71(5), N(2)-Cd(1)-O(5) 102.42(5), N(3)-Cd(1)-O(5) 130.10(5), N(1)-Cd(1)-O(5) 81.67(5), N(2)-Cd(1)-N(4) 140.66(5), N(3)-Cd(1)-N(4) 73.82(5), N(1)-Cd(1)-N(4) 79.30(5), O(5)-Cd(1)-N(4) 79.79(5), N(2)-Cd(1)-O(2) 77.16(4), N(3)-Cd(1)-O(2) 87.50(4), N(1)-Cd(1)-O(2) 76.00(4), O(5)-Cd(1)-O(2) 141.62(4), N(4)-Cd(1)-O(2) 124.91(5).

As found for the previously reported structure of [Cd**L**$(NO_3)_2$] (L = **100**), the X-ray structure of [Cd**L**$(NO_3)_2$] (**L** = **138**) shows that this complex has a distorted pentagonal bipyramidal coordination geometry, with the Cd(II) ion lying in the cavity of five 'equatorial' donor atoms arising from the macrocyclic ring; the two 'axial' sites are occupied by monodentate nitrate groups. The Cd-O(1) bond is somewhat long, at 2.695(1) Å, but still comparable to the Cd(II) to ether oxygen distances of 2.614(3) and 2.732(3) Å previously reported for [Cd**L**$(NO_3)_2$] (L = **100**).[26] All of these fall in the reported range of 2.36 – 2.84 Å found for similar bonds in other Cd(II) complexes.[27] The Cd-N bond lengths are also comparable to the values reported for the cadmium complexes of **100** and **94** (O_2N_3- and N_4O-donors respectively).[26, 28] The 5-membered chelate rings subtend angles of 68.14(4), 73.82(5) and 75.47(5) Å at the metal ion, while

the values for the 6-membered rings are 75.45(4) and 79.30(5) Å. The conformation of the macrocycle is slightly twisted such that the orientation of the benzene rings with respect to each other is close to 90º; the two rings are bent towards opposite sides of plane of the macrocyclic cavity.

The X-ray structure of $[Cd\mathbf{L}(NO_3)]^+$ (**L** = **132**) (**Figure 3.8**), which crystallises with two molecules per unit cell, shows that the metal is again seven-coordinate and binds to all the macrocyclic ligand donors but, in this case, only to one nitrate group which coordinates in a bidentate fashion. The macrocycle adopts a different conformation to that occurring in the previous example, with both benzene rings bent towards the same side of the macrocyclic ring plane. Bond lengths to the bidentate nitrate oxygen atoms fall within the range 2.29 – 2.83 Å reported previously for related complexes.[28, 29] Unsymmetrical binding of the bidentate nitrate groups [O(7)-Cd(2) and O(8)-Cd(2)] is evident with the Cd-O bond lengths being 2.618(7) and 2.400(7) Å respectively. A similar situation has been observed to occur in related systems; for example, in the Cd(II) complex of **83** (where X = NH)[30] (see page 43). The Cd-S distances are rather long (2.806(3) and 2.891(2) Å) compared to the usually observed range (2.6 – 2.7 Å) for seven-coordinated cadmium.[30]

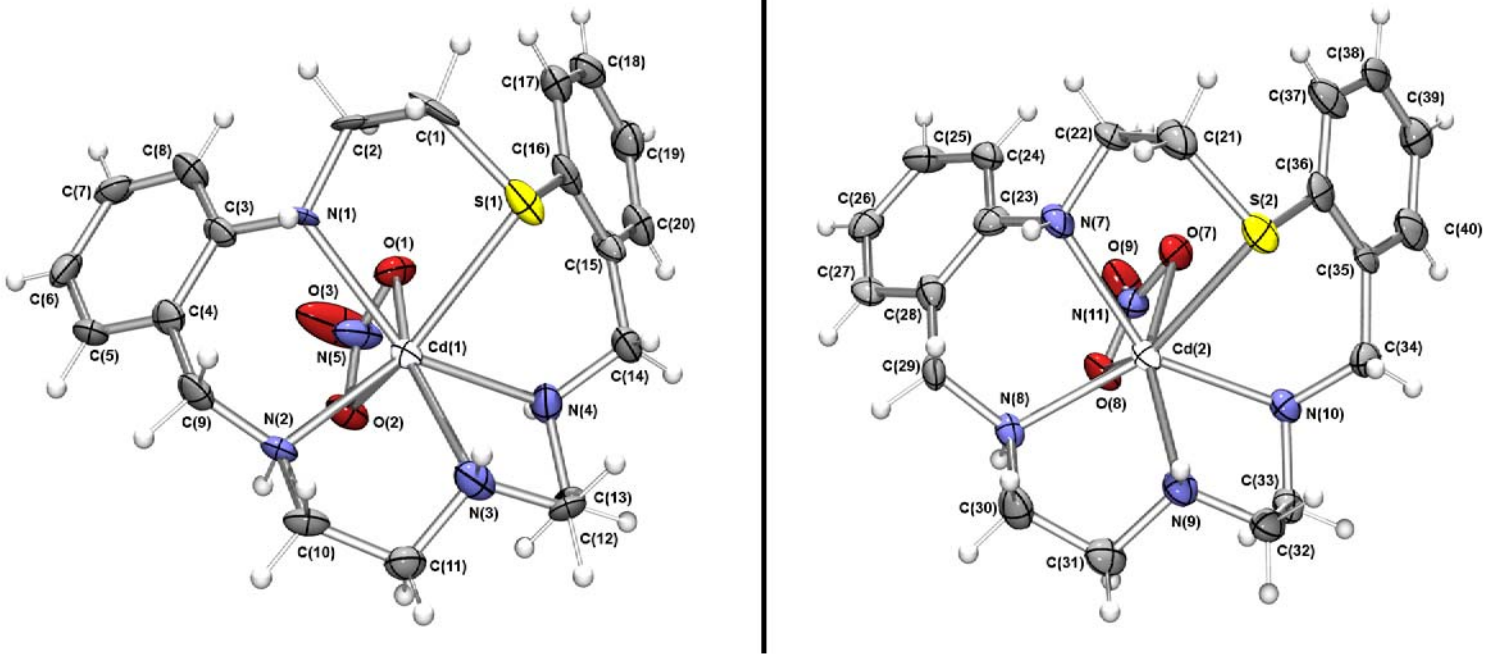

Figure 3.8 ORTEP plots of the two independent cations of type $[Cd\mathbf{L}(NO_3)]^+$ (**L** = **132**). Selected bond lengths (Å) and angles (˚): N(1)-Cd(1) 2.468(8), N(2)-Cd(1) 2.358(7), N(3)-Cd(1) 2.421(8), N(4)-Cd(1)-2.449(8), N(7)-Cd(2) 2.425(8), N(8)-Cd(2) 2.389(7), N(9)-Cd(2) 2.395(8), N(10)-Cd(2) 2.404(8), O(1)-Cd(1) 2.441(6), O(2)-Cd(1) 2.526(7), O(7)-Cd(2) 2.618(7), O(8)-Cd(2) 2.400(7), S(1)-Cd(1) 2.806(3), S(2)-Cd(2) 2.891(2); N(2)-Cd(1)-N(3) 75.3(3), N(2)-Cd(1)-O(1) 118.7(3), N(3)-Cd(1)-O(1) 152.9(3), N(2)-Cd(1)-N(4) 130.2(3), N(3)-d(1)-N(4) 73.5(3), O(1)-Cd(1)-N(4) 80.4(3), N(2)-Cd(1)-N(1) 82.5(2), N(3)-Cd(1)-N(1) 129.0(3), O(1)-Cd(1)-N(1) 77.6(3), N(4)-d(1)-N(1) 146.8(2), N(2)-Cd(1)-O(2) 78.9(2), N(3)-Cd(1)-O(2) 116.0(3), O(1)-Cd(1)-O(2) 51.6(2), N(4)-Cd(1)-O(2) 81.1(3), N(1)-Cd(1)-O(2) 103.5(3), N(2)-Cd(1)-S(1) 141.0(2), N(3)-Cd(1)-S(1) 94.7(2), O(1)-Cd(1)-S(1) 87.30(17), N(4)-Cd(1)-S(1) 79.6(2), N(1)-Cd(1)-S(1) 74.97(18), O(2)-Cd(1)-S(1) 136.93(15), N(8)-Cd(2)-N(9) 75.6(3), N(8)-Cd(2)-O(8) 79.4(2), N(9)-d(2)-O(8) 123.3(2), N(8)-Cd(2)-N(10) 133.8(2), N(9)-Cd(2)-N(10) 75.6(3), O(8)-Cd(2)-N(10) 87.2(3), N(8)-Cd(2)-N(7) 80.9(3), N(9)-Cd(2)-N(7) 126.5(3), O(8)-Cd(2)-N(7) 97.9(3), N(10)-Cd(2)-N(7) 145.0(3), N(8)-Cd(2)-O(7) 122.1(2), N(9)-Cd(2)-O(7) 153.2(3), O(8)-Cd(2)-O(7) 51.0(2), N(10)-Cd(2)-O(7) 77.9(2), N(7)-Cd(2)-O(7) 78.8(3), N(8)-Cd(2)-S(2) 135.97(19), N(9)-Cd(2)-S(2) 90.74(19), O(8)-Cd(2)-S(2) 138.94(16), N(10)-Cd(2)-S(2) 79.44(19), N(7)-Cd(2)-S(2) 74.14(19), O(7)-Cd(2)-S(2) 88.10(15).

3.2.4 X-ray structures of Ag(I) and Pb(II) complexes

Crystals suitable for structural studies were obtained for two Ag(I) complexes: [Ag**L**]PF_6 (**L** = **132**) and [Ag**L**]PF_6 (**L** = **141**). However, no crystalline metal complexes were isolated for Pb(II).

The X-ray structure of $[Ag\mathbf{L}]^+$ (**L** = **132**) (**Figure 3.9**) shows that this complex crystallises with two molecules per unit cell. The coordination requirements of the central silver ion are met solely by the binding to all five donor atoms of the macrocycle. The coordination geometry around silver can be best described as close to square pyramidal, according to the Addison τ value.[22] An average value τ = 0.033 was obtained for $[Ag\mathbf{L}]^+$ (**L** = **132**) which places the N(4) and N(8) donors in the respective axial coordination sites of the two independent molecules present in the unit cell. The Ag-S and Ag-N bond lengths are comparable to the equivalent ones in the complexes of **112** (SS/NNN) and **113** (SS/NSN) in which the ligands also use all their donor atoms for complexation.[6, 7] The bite angle values for the 5-membered chelate rings formed by the N_3-donor fragment of **132** are also comparable to those in the complex of **112** (SS/NNN), while the bite size of the third 5-membered chelate ring (N-Ag-S) is, as expected, smaller [average 74.36(4) Å] than the S-Ag-S equivalents (82.3(1) and 81.5(1) Å in the complexes of **112** (SS/NNN) and **113** (SS/NSN) respectively [for which the Ag(I) coordination was described as distorted pentagonal bipyramid in each case].[6, 7] Crystal data and a summary of data collection for [Ag**L**]PF_6 (**L** = **132**) as well as non-hydrogen bond lengths and bond angles are given in **Appendix B**, **Tables B.34** – **B.36**.

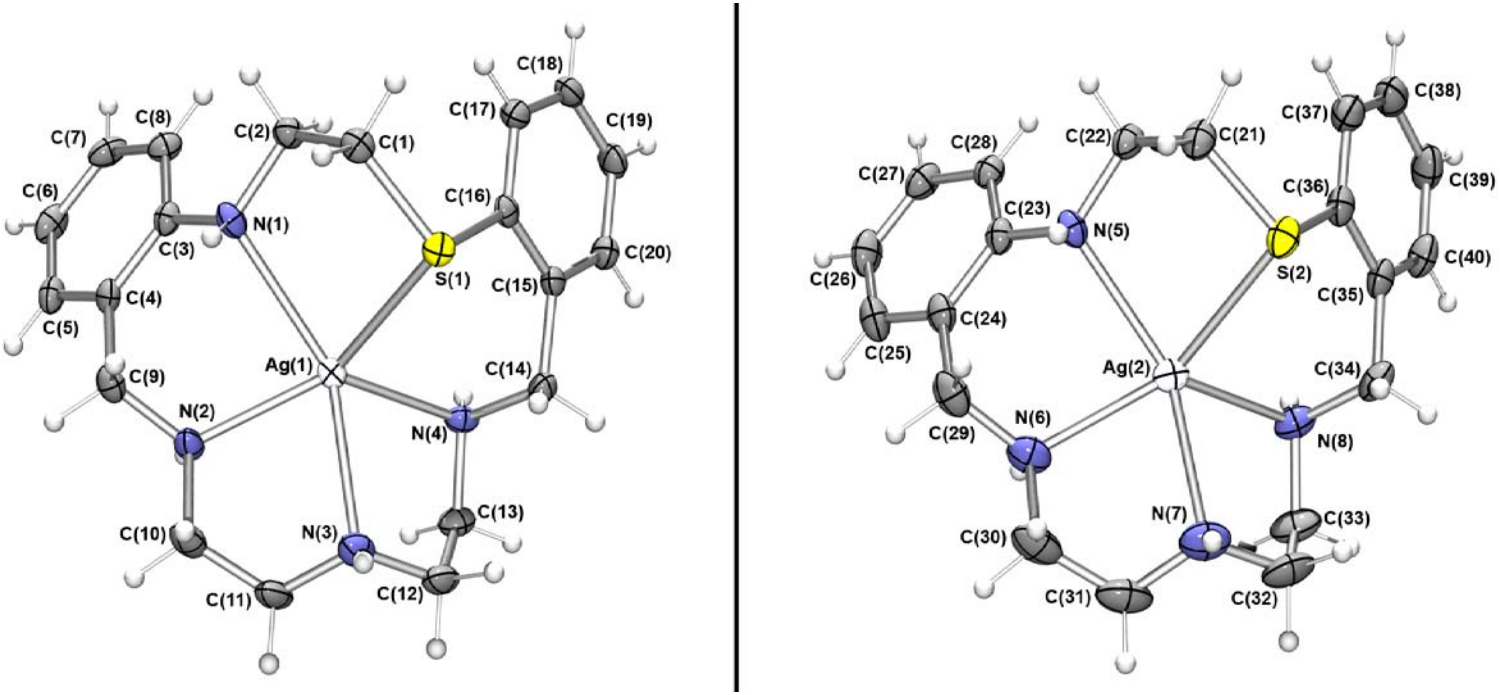

Figure 3.9 ORTEP plots of the two independent cations of $[Ag\mathbf{L}]^+$ (**L** = **132**). The coordination requirements of the central silver ion are met solely by the binding to all five donor atoms of the macrocycle. Selected bond lengths (Å) and angles (˚): N(1)-Ag(1) 2.6096(19), N(2)-Ag(1) 2.3625(18), N(3)-Ag(1) 2.5162(19), N(4)-Ag(1) 2.3722(18), N(5)-Ag(2) 2.5328(19), N(6)-Ag(2) 2.391(2), N(7)-Ag(2) 2.478(2), N(8)-Ag(2) 2.357(2), S(1)-Ag(1) 2.7044(6), S(2)-Ag(2) 2.7717(6); N(2)-Ag(1)-N(4) 125.53(6), N(2)-Ag(1)-N(3) 75.52(6), N(4)-Ag(1)-N(3) 74.39(6), N(2)-Ag(1)-N(1) 81.30(6), N(4)-Ag(1)-N(1) 141.27(6), N(3)-Ag(1)-N(1) 144.11(6), N(2)-Ag(1)-S(1) 145.65(5), N(4)-Ag(1)-S(1) 88.07(5), N(3)-Ag(1)-S(1) 112.07(5), N(1)-Ag(1)-S(1) 74.08(4), N(8)-Ag(2)-N(6) 126.54(7), N(8)-Ag(2)-N(7) 75.80(8), N(6)-Ag(2)-N(7) 75.34(8), N(8)-Ag(2)-N(5) 140.28(7), N(6)-Ag(2)-N(5) 81.85(7), N(7)-Ag(2)-N(5) 143.44(7), N(8)-Ag(2)-S(2) 86.64(5), N(6)-Ag(2)-S(2) 145.80(6), N(7)-Ag(2)-S(2) 110.23(6), N(5)-Ag(2)-S(2) 74.64(4).

The crystal structure of $[Ag\mathbf{L}]^+$ (**L** = **141**) shows that each silver ion coordinates to both benzylic amine nitrogens of one macrocycle and to the thioether sulfur donor from a second bound macrocycle (**Figure 3.10**, bond to second macrocycle not shown). The result is a one-dimensional coordination polymer of the type illustrated in **Figure 3.11**. In addition, two long bonds from Ag(1) to N(1a) (2.848(3)Å) and to O(1a) (2.851(3)Å) complete the coordination sphere (not shown in **Figure 3.11**).

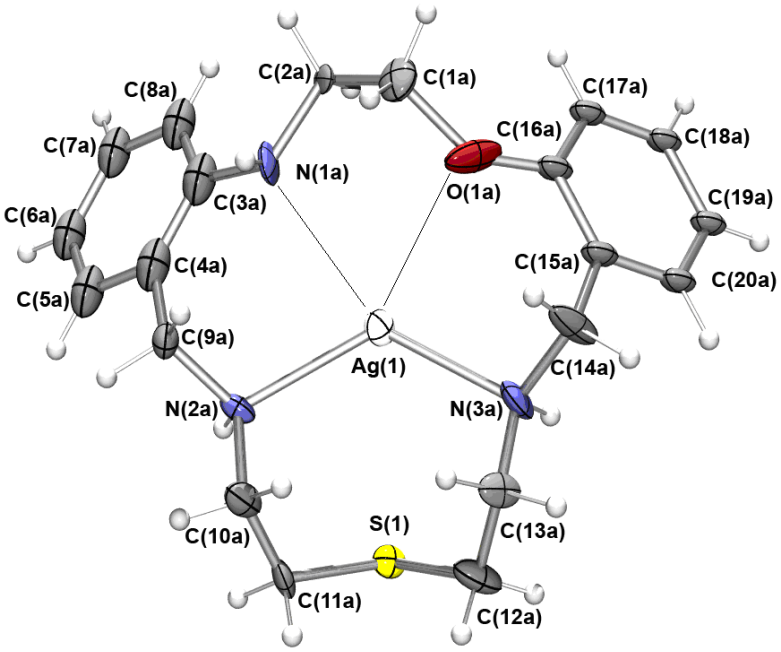

Figure 3.10 ORTEP plot of $[Ag\mathbf{L}]^+$ (**L** = **141**). Selected bond lengths (Å) and angles (˚): N(1A)-Ag(1) 2.848(3), N(1B)-Ag(1) 2.726(2), N(2A)-Ag(1) 2.391(4), N(2B)-Ag(1) 2.331(3), N(3A)-Ag(1) 2.340(4), N(3B)-Ag(1) 2.308(4), O(1A)-Ag(1) 2.851(3), O(1B)-Ag(1) 2.739(2), S(1)-Ag(1) 2 2.6294(7), Ag(1)-S(1) 2 2.6294(7); N(3B)-Ag(1)-N(2B) 97.49(8), N(3B)-Ag(1)-N(3A) 20.6, N(2B)-Ag(1)-N(3A) 111.93(9), N(3B)-Ag(1)-N(2A)-111.32(8), N(2B)-Ag(1)-N(2A) 19.4, N(3A)-Ag(1)-N(2A) 120.92(8), N(3B)-Ag(1)-S(1) 2 130.10(12), N(2B)-Ag(1)-S(1) 2 130.24(14), N(3A)-Ag(1)-S(1) 2 111.45(11), N(2A)-Ag(1)-S(1) 2 112.56(14), N(3B)-Ag(1)-N(1B) 113.66(9), N(2B)-Ag(1)-N(1B) 74.27(9), N(3A)-Ag(1)-N(1B) 130.42(11), N(2A)-Ag(1)-N(1B) 81.79(10), S(1) 2 Ag(1)-N(1B) 95.07(8), N(3B)-Ag(1)-O(1B) 74.24(9), N(2B)-Ag(1)-O(1B) 114.81(8), N(3A)-Ag(1)-O(1B) 82.08(11), N(2A)-Ag(1)-O(1B) 130.49(10), S(1) 2 Ag(1)-O(1B) 94.15(7), N(1B)-Ag(1)-O(1B) 53.9, N(3B)-Ag(1)-O(1A) 76.53(10), N(2B)-Ag(1)-O(1A) 124.81(8), N(3A)-Ag(1)-O(1A) 80.80(11), N(2A)-Ag(1)-O(1A) 139.51(10), S(1) 2 Ag(1)-O(1A) 85.16(8), N(1B)-Ag(1)-O(1A) 59.9, O(1B)-Ag(1)-O(1A) 10.3, N(3B)-Ag(1)-N(1A) 122.85(8), N(2B)-Ag(1)-N(1A) 76.58(9), N(3A)-Ag(1)-N(1A) 138.59(11), N(2A)-Ag(1)-N(1A) 80.99(11), S(1) 2 Ag(1)-N(1A) 86.64(8), N(1B)-Ag(1)-N(1A) 9.5, O(1B)-Ag(1)-N(1A) 59.0, O(1A)-Ag(1)-N(1A) 63.3.

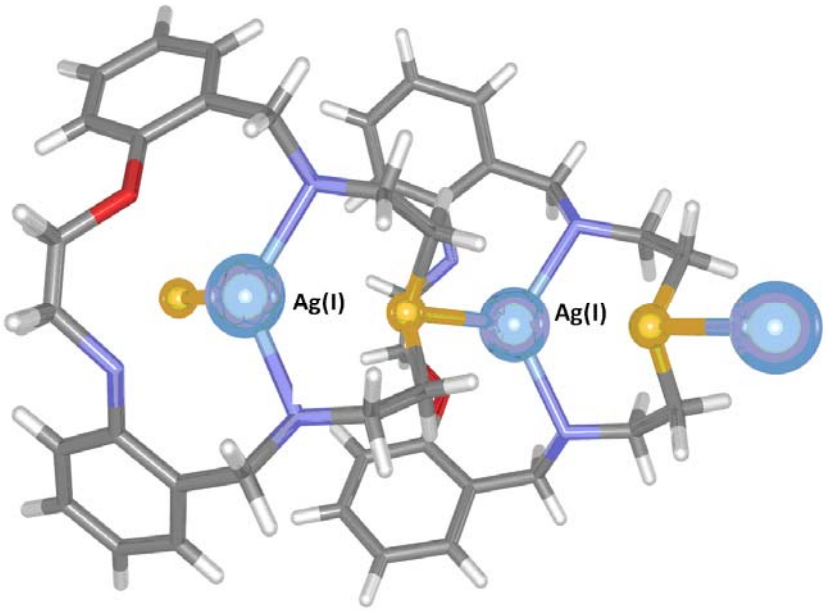

Figure 3.11 One-dimensional polymeric structure of $([Ag\mathbf{L}]^+$ (**L** = **141**))$_n$.

Crystal data and a summary of data collection for $[Ag\mathbf{L}]PF_6$ (**L** = **141**) as well as non-hydrogen bond lengths and bond angles are given in **Appendix B**, **Tables B.37** – **B.39**.

As already mentioned, it has commonly been observed in other studies that variation of the donor atoms in related 17-membered, mixed-donor, dibenzo-substituted macrocycles results in marked changes in the solid state geometries of the ensuing Ag(I) complexes.[14, 31] In particular, the solid state structures of both $[Ag\mathbf{L}]^+$ (**L** = **132**, NS/NNN) and $[Ag\mathbf{L}]^+$ (**L** = **141,** NO/NSN) are in agreement with these observations. Finally, the current study provides further evidence for the previous observation that the d^{10} silver ion does not show a strong preference for a particular coordination polyhedron.[7]

3.2.5 Stability constant determinations

3.2.5.1 Protonation constants

The initial phase of the solution studies involved the determination of protonation constants for the new macrocycles listed in **Table 3.1**. The overall protonation constants β_1, β_2, and β_3 for a given macrocycle L are defined as:

$$L + H^+ \rightleftharpoons LH^+ \quad ; \quad \beta_1 = \frac{[LH^+]}{[L]\,[H^+]}$$

$$L + 2H^+ \rightleftharpoons LH_2^{2+} \; ; \quad \beta_2 = \frac{[LH_2^{2+}]}{[L]\,[H^+]^2}$$

$$L + 3H^+ \rightleftharpoons LH_3^{3+} \; ; \quad \beta_3 = \frac{[LH_3^{3+}]}{[L]\,[H^+]^3}$$

The β values for a given system may be influenced by a number of factors such as conformational changes, electronic interactions and/or solvation effects;[32] however, an in-depth analysis of the relative significance of these factors is beyond the scope of this discussion. The values of the constants were obtained by potentiometric (pH) titrations of the protonated macrocycles with tetraethylammonium hydroxide in 95% methanol at 25 ˚C. A local version of MINIQUAD[33] was used to process the data and a summary of the respective constants is given in **Table 3.1**.

Table 3.1 Protonation constants of the new macrocyclic ligands (I = 0.1; NEt_4ClO_4) (95% methanol, 25 ˚C)

Ligand	log β_1	log β_2	log β_3
132	9.44	16.16	18.60
136	8.84	16.24	18.84
137	8.37	15.34	18.18
138	9.54	17.49	-
142	9.08	16.74	19.52
141	8.76	15.48	17.46

The observed values confirm that each of these ligands is a moderately strong base.

3.2.5.2 Macrocyclic ligand complex stabilities

The metal complex stability constants were also determined by means of potentiometric titrations. The log *K* values represent the mean of between two and four determinations at varying metal:macrocycle ratios. The measurements were performed under the same conditions as described previously[34] and as employed for determination of the ligand protonation constants (see above). The choice of these conditions allowed comparison of the data with values obtained for previously reported 17-membered macrocyclic analogues. The stability constants obtained in the present study are summarised in **Table 3.2**.

Table 3.2 Metal stability constants (ML^{n+}) for the macrocycles listed (95% methanol, 25 ˚C).

Ligand	Co(II)	Ni(II)	Cu(II)	Zn(II)	Cd(II)	Ag(I)	Pb(II)
132	-[a]	-[a]	15.1	8.8	9.6	11.5	8.5
136	3.6	6.1	9.7	4.2	7.1	10.5	5.2
137	5.4	7.8	12.4	4.2	6.5	12.2	4.7
138	9.2	-[a]	15.6	9.8	10.9	9.8	8.8
142	4.1	5.5	9.3	4.8	8.4	9.1	5.7
141	6.2	7.2	11.2	6.6	6.4	9.9	4.6

[a]Precipitation, hydrolysis or slow approach to equilibrium prevented determination of this log *K* value.

While precipitation, hydrolysis or slow approach to equilibrium prevented the collection of a full set of data in two cases, it is clear from the stability data obtained that variation of the donor atom set, and especially the central aliphatic donor in the –NYN– fragment

(Y = N, O, S), as expected, markedly affects the stabilities of the resultant metal complexes (**Figures 3.12** and **3.13**).

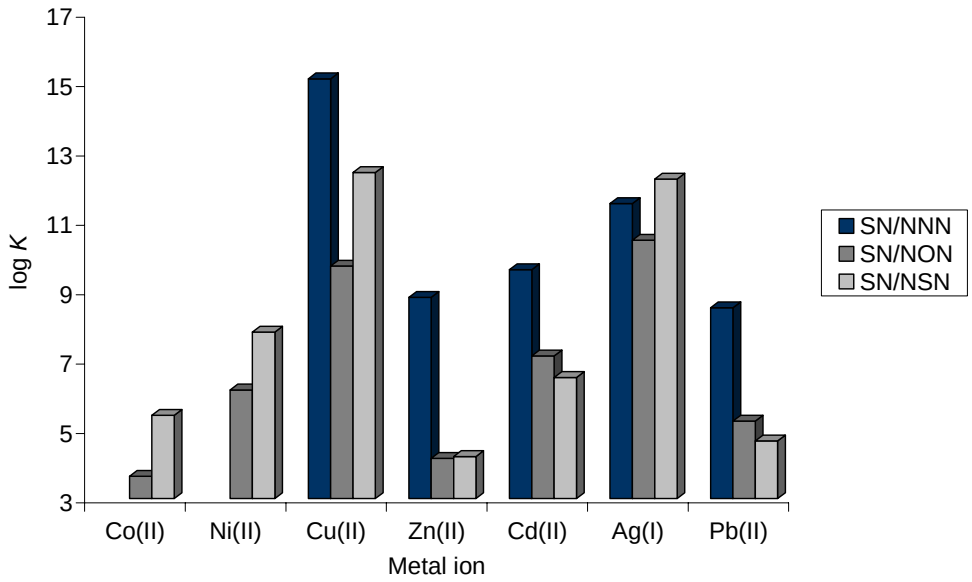

Figure 3.12 Comparison of the log *K* values for 1:1 (metal:ligand) complexation by the SN-dialdehyde-derived macrocycles **132**(SN/NNN), **136**(SN/NON) and **137**(SN/NSN)

Where full data are available, the stabilities for these systems follow the Irving-Williams order Co(II) < Ni(II) < Cu(II) > Zn(II).[35] This parallels the stability constant behaviour previously reported for the related symmetrical macrocyclic ligand complexes discussed in Chapter 1 (see **Table 1.6**).

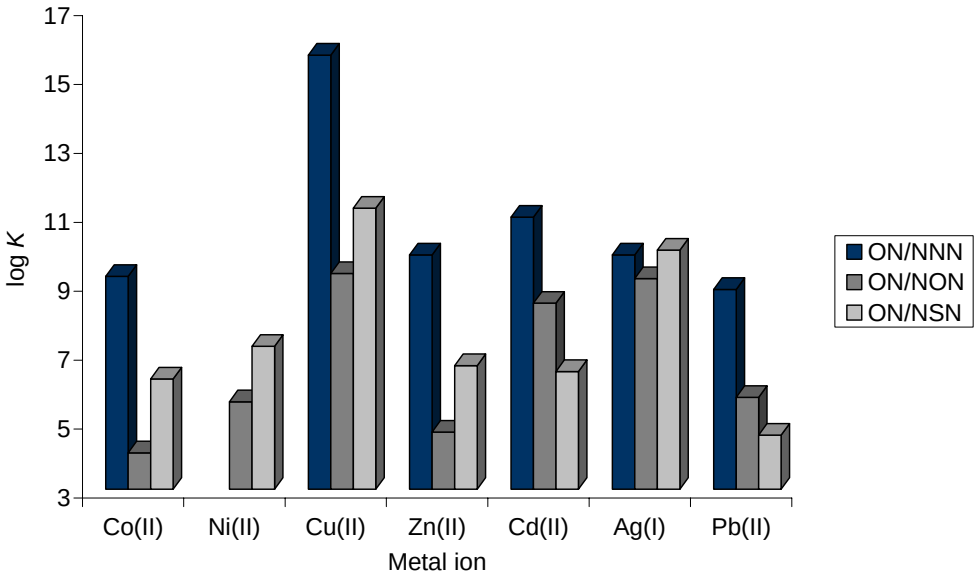

Figure 3.13 Comparison of the log *K* values for 1:1 (metal:ligand) complexation by the ON-dialdehyde-derived macrocycles **138**(ON/NNN), **142**(ON/NON) and **141**(ON/NSN)

3.2.6 Co(II), Ni(II) and Cu(II) complex stabilities

(i) Co(II) complexes

In the prior studies, the Co(II) complexes were generally found to be of lower stability than their nickel and copper analogues (**Table 1.6**) and hence are in accordance with the Irving-Williams order. However, because of the greater uncertainties associated with these relatively low log *K* values, it appeared inappropriate to attempt to rationalise the observed order of stability for these Co(II) species. By comparison, the data for the new unsymmetrical systems **132**, **136** – **138**, **141** and **142** determined in the present study (**Table 3.2**, **Figure 3.14**) clearly show a dependence of the log *K* value on the nature of the Y donor in the –NYN– fragment. In particular, for the Co(II) complexes of the ON-dialdehyde-derived macrocycles, there is a clear increase in stability when Y = S compared with Y = O, while the highest stability is achieved for Y = N (to yield an aliphatic N_3-backbone). That is, the Co(II) complex of **138** (ON/NNN) is at least 10^5 more stable than that of **142** (ON/NON) and 10^3 more stable than that of **141** (ON/NSN). These results are in keeping with the expected low affinity of ether oxygen donors for the

latter first-row transition metal ions Co(II), Ni(II) and Cu(II) and also the lower affinity of thioether sulfur (relative to amine nitrogen) for these metals.[11, 36-39] A comparison of stability constants for the Co(II) complexes of **132**, **136** – **138**, **141** and **142** with those obtained previously for related mixed donor 17-membered dibenzo-substituted systems is shown in **Figure 3.14**[#]. These data also document the manner by which variation of the

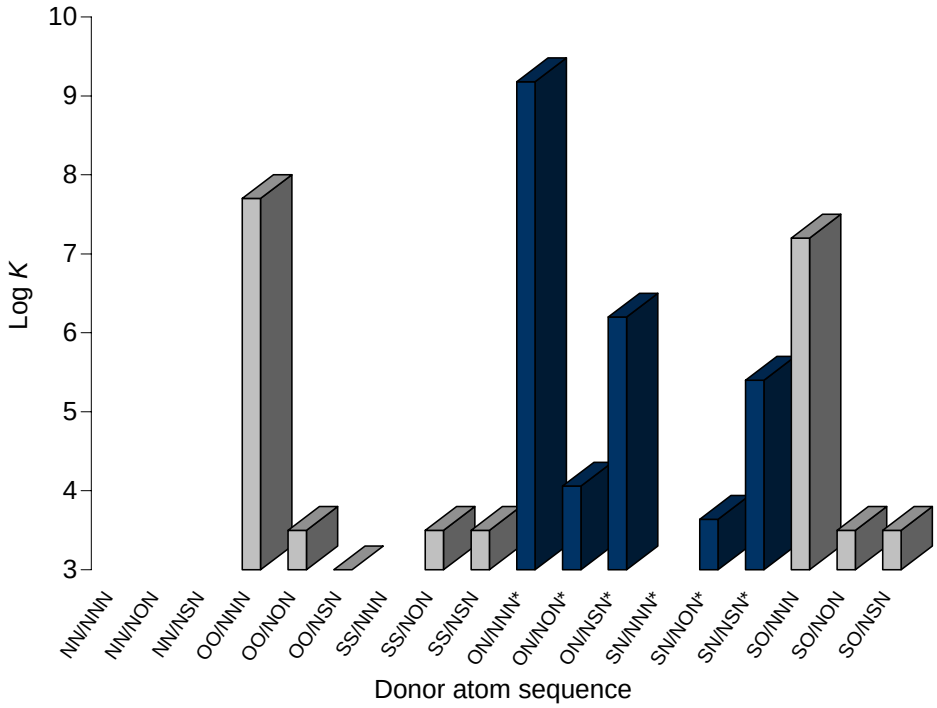

Figure 3.14 Log *K* values for the Co(II) complexes of related 5-donor 17-membered macrocycles shown (*this study)

X donor in the –NX– donor fragment affects the stability of the Co(II) complexes. Thus, replacing the thioether donor in the SO/NNN donor sequence with nitrogen, to achieve a NO/NNN sequence, results in an increase in stability of ~10^2. As already mentioned, this is in accordance with the documented contribution of the individual donor atoms to the complex stabilities falling in the order NH(aliphatic) > NH(anilino) > S > O with respect to Co(II) (and also the remaining latter row first transition metal ions).[11]

[#]In this and subsequent comparative bar graphs no bars are shown where no experimental data is available. However, the full complement of ligands is included each time for completeness.

In accord with this, the stability of the respective Co(II) complexes increases on moving from the OO/NNN donor sequence (log K = 7.7) to the NO/NNN sequence (log K = 9.2).

(ii) Ni(II) complexes

Stability constants for the Ni(II) complexes of **136**, **137**, **141** and **142** are given in **Table 3.2**. In part due to long equilibration times, corresponding values for **132** and **138** were not determined. The comparative bar graph (**Figure 3.15**) shows that, for nickel there is also a direct relationship between the nature of the Y donor and the stability of the resulting complexes, with the log K values being invariably higher when Y = NH. It is also evident that, in accordance with the previously mentioned weak donor capacity of ether and thioether groups for most divalent first row transition metal ions,[36, 40] the stabilities are less dependent on whether Y = O or S. Thus, the complexes of **137** (NS/NSN) and **141** (NO/NSN) are less than 10^2 more stable than **136** (NS/NON) and **142** (NO/NON) respectively.

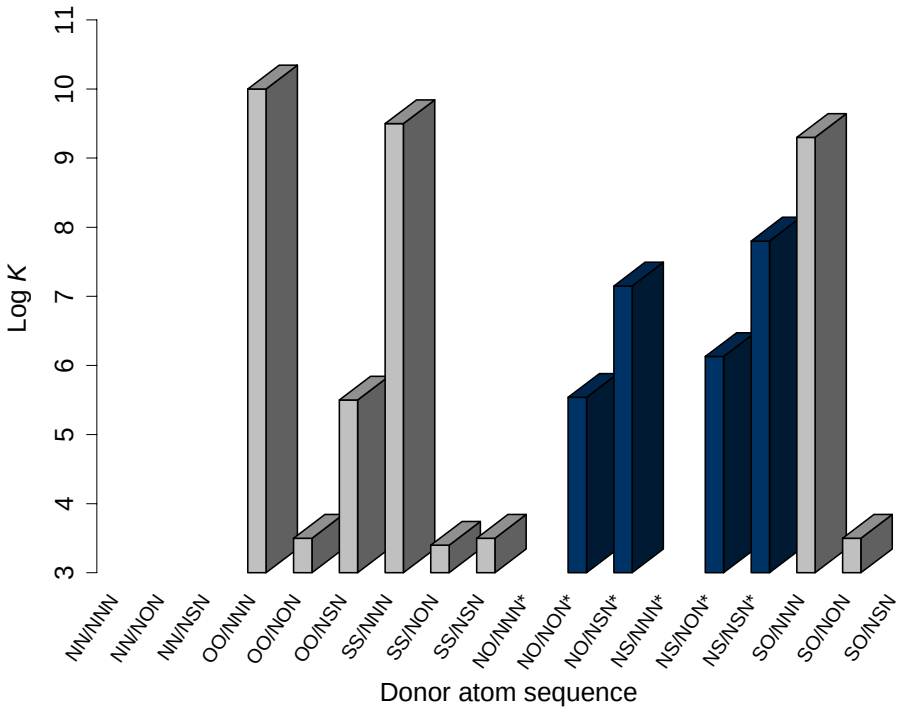

Figure 3.15 Log K values for the Ni(II) complexes of related 5-donor, 17-membered macrocycles (*this study)

In this context it is noted that thermodynamic studies involving Ni(II) complexes of linear polyamines of the type $NH_2(CH_2)_2Y(CH_2)_2NH_2$ (where Y = NH, O or S) indicate that the enhanced stability of the triamine complex, relative to the complexes in which S or O donors are present, derives primarily from an enhanced enthalpic contribution to binding by the NH group.[41-44] Further, it was claimed that, in the formation of complexes of this type, the coordination of ether oxygen or thioether donors is an endothermic process.[44]

Finally, the data presented in **Figure 3.15** also confirm that altering the donor atom sequence in the macrocyclic backbone has a marked effect on the stability of the corresponding Ni(II) complexes. For example, for the ligands containing an O_2N_3-donor set, varying the sequence from OO/NNN (**100**) to NO/NON (**142**) results in a drop in the log *K* value from 10.0 to 5.5 (however, this of course may in part reflect the substitution of a secondary alkyl amine with an anilino amine in the case of **142**). Similar observations on the effect of variation of donor atom sequence and the impact this has on the thermodynamic stability of the resulting complexes of other macrocyclic systems has been documented previously.[12, 45]

(iii) Cu(II) complexes

In accord with the Irving-Williams series, the Cu(II) stability constants for the present ligand series (**132**, **136 – 138**, **141** and **142**) are invariably higher (**Table 3.2**) relative to the corresponding values for Co(II) or Ni(II). For example, the stability of the Cu(II) complex of **137** is more than 10^4 higher than that of Ni(II) and 10^7 higher than that of Co(II). Further, once again, the comparative data given in **Figure 3.16** shows a clear dependence of the stability of the copper complexes on the nature of the donor atom in the Y position of the macrocycle. From this data, it is once again evident that, the contribution to overall stability of the donor atoms falls in the order NH(aliphatic) > NH(anilino) > S > O. The small preference of Cu(II) for thioether sulfur over ether oxygen donors evident in **Figure 3.16** has also been reported previously.[11, 46, 47]

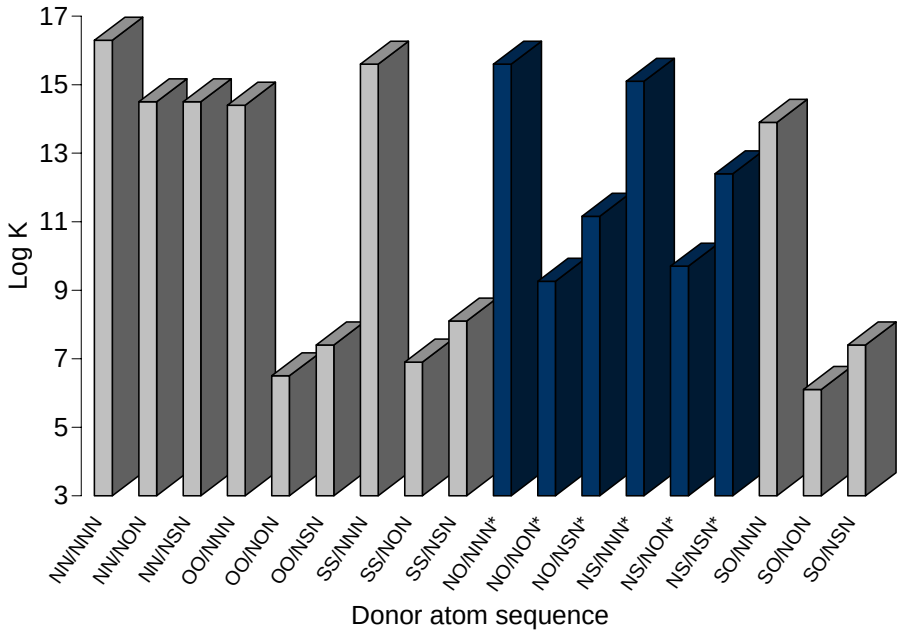

Figure 3.16 Log *K* values for the Cu(II) complexes of related 5-donor, 17-membered macrocycles (*this study)

Thus, replacement of oxygen donors by sulfur results in a moderate increase in the stability of the complexes of **137** (NS/NSN) and **141** (NO/NSN) compared to those of **136** (NS/NON) and **142** (NO/NON) respectively. With respect to the stabilities of Cu(II) complexes of the ON-dialdehyde-derived macrocycles, as already mentioned, both **138** (NO/NNN) and **142** (NO/NON) coordinate in the solid state structure facially via their –NYN– fragments. If a similar mode of coordination predominates in solution then it would be reasonable to assume that the different binding strengths of these donors (Y = NH or O) for Cu(II) are largely responsible for the observed difference in stability of the complexes of **138** and **142** (log *K* = 15.6 and 9.3 respectively).

(iv) Effect of increasing the number of nitrogen donors

As observed previously,[24] for a series of macrocycles with similar backbone structure, the magnitude of a particular log *K* value is strongly influenced by the number of nitrogen donor atoms present. This is also evident from the current study which shows that

replacing the aryl oxygen in the backbone of **129** (SO/NSN) with a nitrogen in **137** (NS/NSN), while maintaining the –NSN– donor fragment unchanged, results in the latter Cu(II) complex being 10^5 more stable. Notwithstanding the lower basicity of the anilino NH group (relative to the secondary alkyl amine group), it nevertheless makes a significant contribution to the stability of the Cu(II) complexes as is clearly evident on inspection of the log *K* values shown in **Figure 3.16**. A similar trend was obtained for the corresponding complexes of Co(II) and Ni(II). For example, comparing the stabilities for the Co(II) complexes of **127** (SO/NNN) and **138** (NO/NNN) (**Figure 3.14**), on replacing the thioether sulfur with an anilino NH group results in an increase of the log *K* value from 7.2 to 9.2. This is also evident for nickel (**Figure 3.15**), when the stability constant of log $K < 3.5$ obtained for the complex of **128** (SO/NON) is compared with that obtained for **136** (NS/NON) where log $K = 6.1$.

3.2.7 Zn(II) and Cd(II) complex stabilities

(i) Zn(II) complexes

Solution studies (**Table 3.2**) confirm that the 'natural' complex stability order[35] Cu(II) > Zn(II) holds for each of the complexes of **132**, **136** – **138**, **141** and **142**. Concerning the relative stabilities of Zn(II) and Cd(II), the 'natural' stability order for these metals with respect to simple polyamine ligands such as ethylenediamine or diethylenetriamine is Zn(II) > Cd(II).[48] Similar results were obtained in the author's laboratory with tetraaza-ligands – both linear and macrocyclic – containing fused dibenzosubstituents.[49] However, in the present study it was found that overall, the order is reversed for the above mixed donor macrocycles, with a small additional stability for the Cd(II) complexes being evident compared to those for Zn(II). A similar order was observed for the related 17-membered, dibenzo-substituted mixed-donor ligands reviewed in Chapter 1 (**Table 1.6**).

The magnitude of the log *K* values for the zinc complexes is again strongly influenced by the number of nitrogen donors. For example, for Zn(II) there is a 10^5 drop in stability in moving from the complex of **138** (ON/NNN) to the one of **142** (ON/NON) (**Table 3.2**) and a difference of 4.6 log *K* units between the stabilities of the complexes of **132**

(NS/NNN) and **136** (NS/NON). This is consistent with ether oxygen donors being hard Lewis bases[50] while in terms of the HSAB principle Zn(II) is borderline.[51] Further, in accordance with the documented low affinity of Zn(II) for soft thioether sulfur donors,[52, 53] the stability constants of the complexes of **137** (NS/NSN) and **141** (NO/NSN) where Y = S parallel those with Y = O in also being relatively low. For comparison, stability data obtained during previous investigations in the author's laboratory for ligands with an identical structural backbone are included in **Figure 3.17**. The contribution of the macrocyclic –NX– (X = S or O) donor fragment to the overall stability of the Zn(II) complexes can be assessed from a comparison of the stability constants for complexes of the previously reported ligands **100** (OO/NNN, log *K* = 7.5) and **112** (SS/NNN, log *K* = 6.3) with the values obtained for the complexes of **138** (NO/NNN) and **132** (NS/NNN) (log *K* = 9.8 and 8.8 respectively).

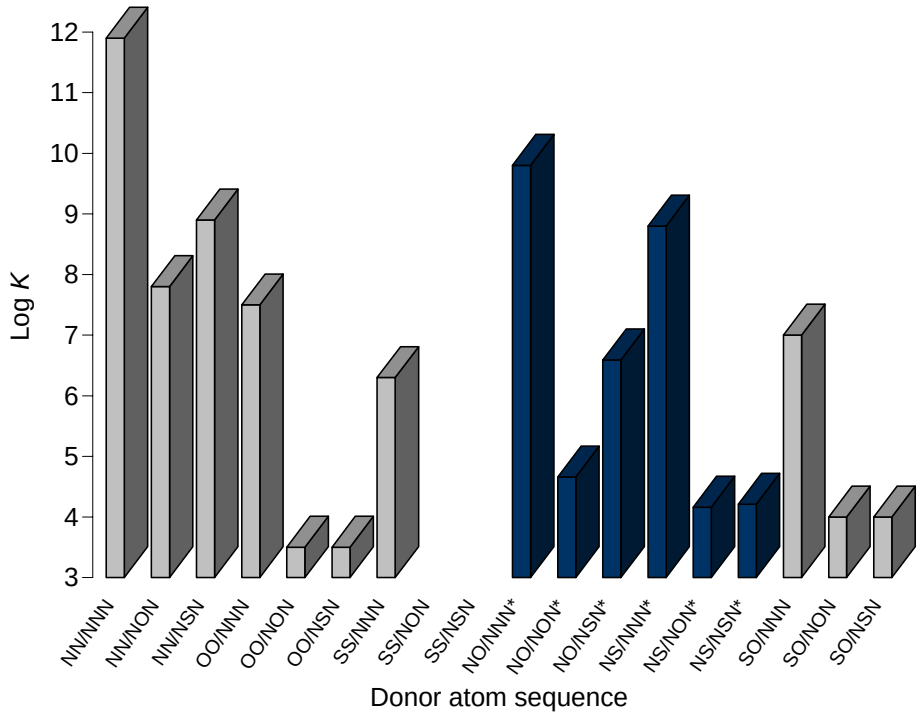

Figure 3.17 Log *K* values for the Zn(II) complexes of related 5-donor 17-membered macrocycles (*this study)

An X-ray diffraction study of the Zn(II) complex of **100** shows that the ether oxygen donors do not coordinate in the solid state, with the zinc ion lying outside of the

macrocycle cavity.[27] This result suggests that the coordination of the –NS– and –NO– donor fragments in solution is likely to contribute only in a minor way to the overall complex stability.

(ii) Cd(II) complexes

The relatively high stabilities for the Cd(II) complexes of **138** (NO/NNN) and **132** (NS/NNN) are reflected in the corresponding solid structures by all macrocyclic donors being bound to the respective Cd(II) centres. As for the previous metal systems, the number of nitrogen donors has a marked effect on the stability of the Cd(II) complexes, with overall stability highest for **93** (NN/NNN) (**Figure 3.18**). In the case of **132**, **136** – **138**, **141** and **142**, the highest relative stability is for the complexes of **132** (NS/NNN) and **138** (NO/NNN) which contain an aliphatic N_3-donor fragment. As illustrated in **Figure 3.18**, the Cd(II) complexes of **132** (NS/NNN) and **138** (NO/NNN), which contain the same N_3-donor fragment, yield lower stabilities when X = S (**132**) than when X = O (**138**) which in this case is contrary to expectation based on HSAB considerations.[51]

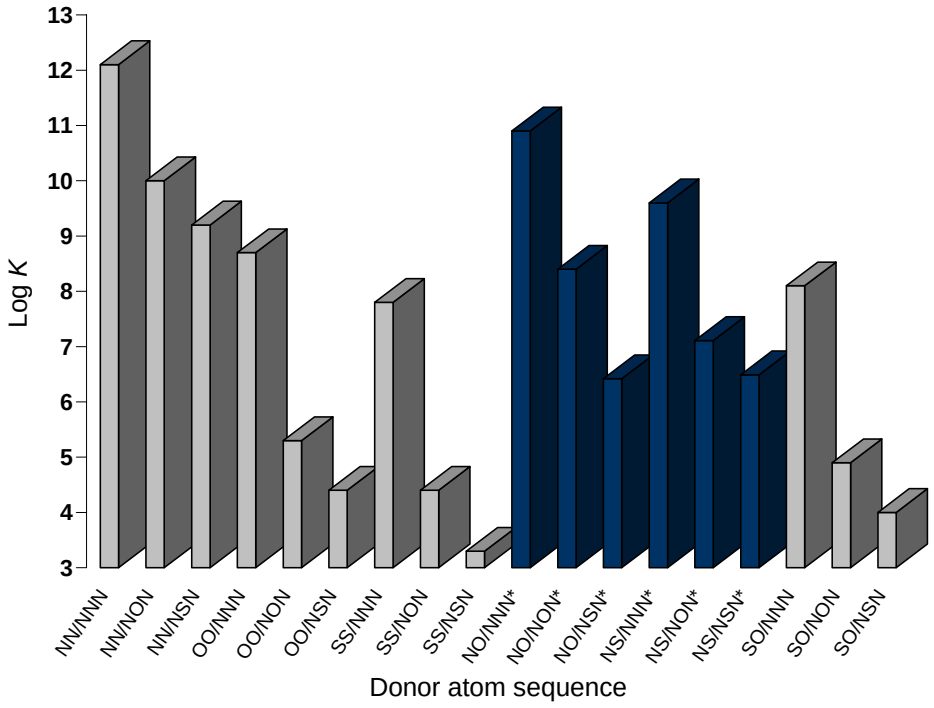

Figure 3.18 Log *K* values for the Cd(II) complexes of related 5-donor 17-membered macrocycles (*this study)

However, a possible contribution to this could be the well documented tendency of thioether donors to adopt orientations with their lone pairs pointing out (*exo*) with respect to the macrocyclic cavity (see Chapter 1). In this situation the conformational rearrangement of the –NS– fragment required by coordination to the cadmium ion will cost energy which in turn is expected to translate into a lowering of the corresponding stability constants.

3.2.8 Ag(I) and Pb(II) complex stabilities

(i) Ag(I) complexes

As mentioned already, there are many examples in the literature of the solution interaction of Ag(I) and Pb(II) with macrocyclic ligands.[11, 36] Much attention has been given in the author's laboratory to investigating the factors which influence the discrimination between these ions.[54] As discussed in Chapter 1, systematic variation of the macrocyclic structural parameters has resulted in the synthesis of **113** (SS/NSN) which was shown to yield a stability constant that is approximately 10^9 in favour of silver.[3] A further aspect of the current solution results (**Table 3.2**) is that they serve to demonstrate the quite significant effect of varying the relative positions of a given donor atom set in an otherwise unchanged macrocyclic backbone on the respective stabilities of the resulting complexes.

The comparative bar graph for the Ag(I) complexes (**Figure 3.19**) clearly illustrates the above-mentioned strong affinity of thioether donors for silver in systems of the present type. For example, the stability of the Ag(I) complex of the N_5-donor ring **93** (NN/NNN, log K = 10.3) is lower than that of **132** (NS/NNN, log K = 11.5) and **137** (NS/NSN, log K = 12.2). This contrasts with the results obtained for the complexes of each of the other

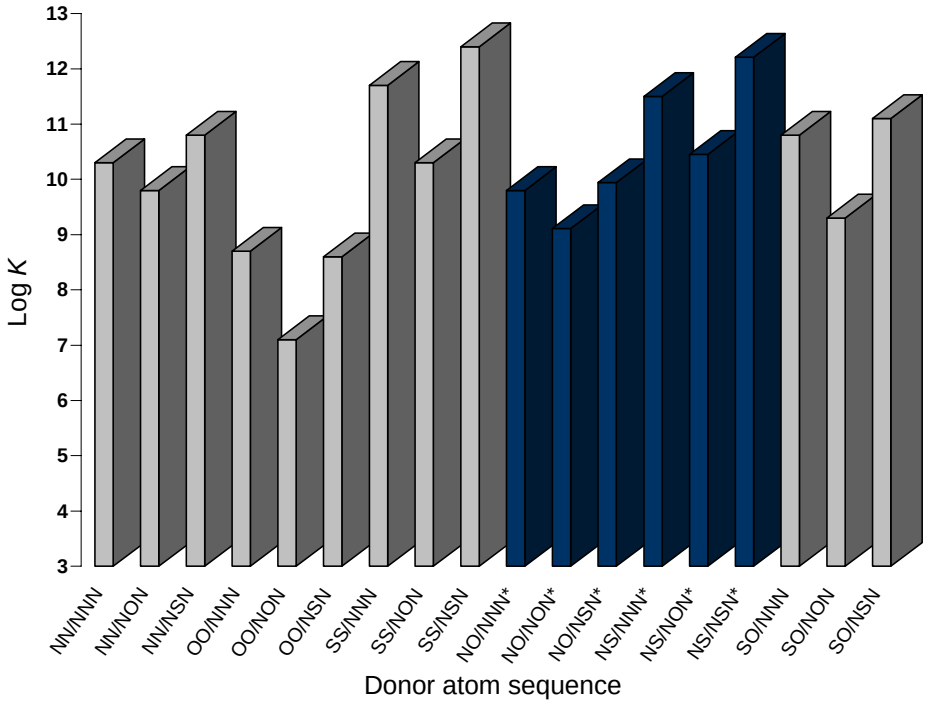

Figure 3.19 Log *K* values for the Ag(I) complexes of 5-donor 17-membered macrocycles (*this study)

metal ions investigated in this study [including Pb(II), see **Figure 3.20**] where the complexes with the highest relative stabilities were obtained with **93**, the all-nitrogen donor macrocycle. It is also noted that the log *K* values for the Ag(I) complexes of **132** (NS/NNN) and **137** (NS/NSN) are relatively close and therefore in agreement with conclusions from an earlier study which indicated that for such systems, the affinities for Ag(I) of a thioether or a secondary amine donor, when at the Y position, are broadly similar.[55]

On comparing the relative contributions to Ag(I) complex stabilities of anilino nitrogen and aryl thioether donors, it is found that replacement of one anilino nitrogen in **95** (NN/NSN) with a thioether sulfur in **137** (SN/NSN) results in a stability increase ($\Delta\log K$ = 1.4) for the complex of the latter. Conversely, an increase in complex stability ($\Delta\log K$ = 1.2) was obtained on replacing one of the anilino nitrogens in the N_5-donor **93** system with a sulfur donor in **132** (NS/NNN).

In keeping with the documented poor affinity of ether oxygen donors for the ‘soft’ Ag(I) ion, the lowest stability constant values in the comparative bar graph were obtained for the complexes which contain two or more ether oxygens in the macrocyclic backbone.

(ii) Pb(II) complexes

In contrast to the Ag(I) ion complexes, the stabilities of the Pb(II) complexes with the series of mixed donor macrocycles shown in **Figure 3.20** display a much greater dependence on the nature of the Y donor. Thus, in agreement with the ‘borderline’ nature of Pb(II),[51] stabilities observed with respect to the Y donor follow the order NH > O > S. The considerable influence of the donor at the Y position is clearly demonstrated by comparing the log *K* values for the Pb(II) complexes of **138** (NO/NNN), **142** (NONON) and **141** (NO/NSN) where the log *K* values are 8.8, 5.7 and 4.6 respectively. These results are paralleled by the Pb(II) complexes of **132** (NS/NNN), **136** (NS/NON) and **137** (NS/NSN) with log *K* values of 8.5, 5.2 and 4.7 respectively.

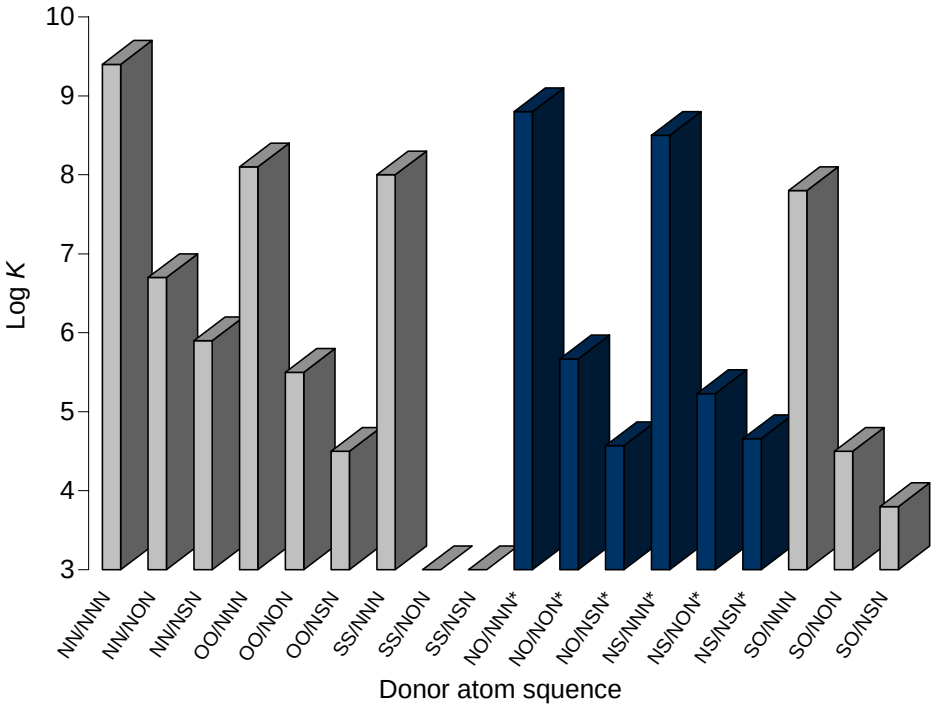

Figure 3.20 Log *K* values for the Pb(II) complexes of related 5-donor 17-membered macrocycles (*this study)

With respect to the above, it is clear that silver shows greater tolerance than lead for an ether oxygen donor at the Y position. For example the stability constant values for the Ag(I) complexes of **138** (NO/NNN) and **142** (NO/NON) are 9.8 and 8.8 respectively (**Table 3.2**) while the Pb(II) complexes of these ligands have log *K* values of 8.8 and 5.7 respectively.

(iii) Effect of donor atom sequence on Ag(I)/Pb(II) discrimination

The relative stabilities for the Ag(I) complexes of **132** (NS/NNN, log *K* = 11.5) and **112** (SS/NNN, log *K* =11.7) as well as the complexes of **132** (NS/NNN, log *K* = 11.5) and **137** (NS/NSN, log *K* = 12.2), clearly indicate that changing the relative position in the macrocyclic backbone of the second sulfur donor has only a minor effect on Ag(I) complex stability.

As already mentioned, the highest stability for the Pb(II) complexes in this series is achieved for the N_5-donor macrocycle **93** (log *K* = 9.4). The effect of introducing a thioether sulfur donor and the influence the relative position of this sulfur has on complex stability is seen on comparing the log *K* values for the Pb(II) complexes of **93** (NN/NNN, log *K* = 9.4) and **132** (NS/NNN log *K* = 8.5) resulting in $\Delta\log K$ = 0.9; a comparison of the stability of Pb(II) complexes of **93** (NN/NNN, log *K* = 9.4) and **95** (NN/NSN log *K* = 5.9) reveals a much greater difference ($\Delta\log K$ = 3.5). The consequence of replacing a second nitrogen in the macrocyclic backbone with a sulfur donor is seen on comparing stability constants for the Pb(II) complexes of **132** (NS/NNN, log *K* = 8.5) with **112** (SS/NNN, log *K* = 8.0), resulting in $\Delta\log K$ = 0.5 as well as **132** (NS/NNN, log *K* = 8.5) with **137** (NS/NSN, log *K* = 4.7) a difference of 3.8 log *K* units.

The data in **Table 3.3** summarises the effect of changing the donor atom sequence on the stability constants of Ag(I) and Pb(II) complexes and, in turn, on the discrimination between these two metal ions. The latter is particularly evident for the S_2N_3-donor systems, especially for the complexes of **137**(NS/NSN). This macrocycle shows very good discrimination for Ag(I) over Pb(II), with a difference between the log *K* values of

the respective complexes of 7.5 log *K* units, the *second highest* difference (*cf.* **113** with 9 log *K* units difference) in the current 5-donor, 17-membered macrocycle series.

Table 3.3 Comparison of the log *K* values for Ag(I) and Pb(II) complexes with macrocycles containing different donor atom sequences (95% methanol, 25 ˚C).

Donor atom sequence	Ag(I)	Pb(II)	Δlog *K*
NN/NSN (**95**)	10.8	5.9	4.9
NS/NNN (**132**)	11.5	8.5	3.0
SS/NNN (**112**)	11.7	8.5	3.2
NS/NSN (**137**)	12.2	4.7	7.5

The above results indicate that within the present dibenzo-macrocycle framework, it is largely the difference in affinities of the thioether sulfur donors for these two metal ions that dominates the observed discrimination under the conditions employed. Further, the discrimination in favour of Ag(I) is also dependent on the relative position of these donors. Extending the matrix of related mixed-donor macrocycles in the present study has thus provided the opportunity to investigate further the factors which influence discrimination for Ag(I) over Pb(II).

3.2.9 Conclusions

Previous studies on thiacrown ether reagents with high-specificity for Ag(I) over Pb(II) and Hg(II) have found that an optimum combination of ‘soft’, ‘hard’ and ‘borderline’ donor atoms together with their placement in the ligand is required to reach maximum selectivity for Ag(I) over other transition and post-transition metal ions.[56] This was also found to be the case in the current investigation which again emphasises the important role which mixed donor macrocyclic ligands may play in achieving recognition and/or discrimination within the group of metals discussed above.

The results presented in this chapter confirm that significant metal ion recognition can be achieved by changing both the available donor set and the sequential arrangement of the respective donors for a given donor set in the macrocyclic backbone of 17-membered dibenzo-substituted systems of the present type. Moreover, the results of such variation appear to a certain degree somewhat predictable – an observation that formed the motivation for the investigation presented in the following chapter of this thesis.

3.3 Experimental

3.3.1 Synthesis of metal complexes

General procedure for the preparation of the metal complexes

Unless otherwise stated, warm solutions of the metal salts were added with stirring to warm solutions of the respective macrocycles. The mixture was allowed to stir with gentle heating for up to 1 h, then filtered and divided into two or three parts, one of which was allowed to undergo slow evaporation of the solvent while the other (or others), were set up for slow diffusion (at different rates) of diethyl ether vapour into the solution. The preparation of the metal complexes was carried out for the purpose of obtaining X-ray quality crystals for structural studies. As a result, the yields for the preparations were not optimised. In general, approximate yields of between 10 – 40% were obtained.

Mass Spectrometry

High resolution mass spectra were recorded by Dr David Bourne at DSTO Melbourne. Samples were dissolved in acetonitrile and analysed directly by flow infusion at a rate of 2.5 μL per minute. The analysis was performed on a Bruker Apex Ultra Qe mass spectrometer with a 9.4T magnet and a Bruker Electrospray Ion source. Spectra were recorded in positive mode with a scan range 200-1000 daltons. Data set size was 512k. Accurate mass determination was carried out after external calibration using Agilent ESI-L tuning mix.

Preparation of [Ni**L**Cl]Cl·3H_2O (**L** = **138**)

$NiCl_2$·6H_2O (0.0179 g, 7.53x10^{-5} mol) was dissolved in warm EtOH (10 ml) and added to a warm solution of **138** (0.025 g, 7.34 x10^{-5} mol) in EtOH (20 ml) with stirring. The

reaction mixture was heated with stirring for 1 h. Several small green prisms of [Ni**L**Cl]$^{-}$ Cl·3H_2O were obtained following diethyl ether diffusion into the EtOH solution. Positive ion ESI-HRMS m/z detected as M^+ 433.13001 ($C_{20}H_{28}N_4OClNi$ requires 433.1296, error 0.1 ppm).

Preparation of [Ni**L**Cl]Cl·0.125CH_3CN·3.75H_2O (**L** = **142**)
$NiCl_2$·6H_2O (0.0191 g, 8.05x10^{-5} mol) was dissolved in warm EtOH (20 ml) and added to a warm solution of **142** (0.025 g, 7.32 x10^{-5} mol) in EtOH (20 ml) with stirring. The reaction mixture was heated with stirring for 1 h. A green, multi-faceted crystal of [Ni**L**Cl]Cl·0.125CH_3CN·3.75H_2O suitable for X-ray analysis was obtained following slow evaporation of the EtOH solution. Positive ion ESI-HRMS m/z detected as M^+ 434.11402. ($C_{20}H_{27}N_3O_2ClNi$ requires 434.11398, error 0.1 ppm).

Preparation of [Cu**L**Cl_2]·CH_3CN (**L** = **138**)
$CuCl_2$·2H_2O (0.015 g, 8.79x10^{-5} mol) in warm CH_3CN (10 ml) was added to a warm solution of **138** (0.0199 g, 5.84x10^{-5} mol) in warm CH_3CN (15 ml) and the reaction mixture was stirred with low heat for 1 h. A single green block-like crystal of [Cu**L**Cl_2]·CH_3CN (**L** = **138**) was obtained following slow diethyl ether vapour diffusion into the reaction solution. Positive ion ESI-HRMS m/z detected as [M – Cl^{-}]$^{+}$ 438.12385. ($C_{20}H_{28}N_4OClCu$ requires 438.12422, error 0.8 ppm).

Preparation of [Cu**L**Cl_2]·CH_3CN (**L** = **142**)
$CuCl_2$·2H_2O (0.0138 g, 8.09x10^{-5} mol) in warm CH_3CN (5 ml) was added dropwise to a warm CH_3CN solution (20 ml) of **142** (0.0257, 7.53 x10^{-5} mol). A single, green, block-like crystal of [Cu**L**Cl_2]·CH_3CN suitable for X-ray crystallography study was obtained following slow diethyl ether diffusion into the CH_3CN reaction solution. Positive ion ESI-HRMS m/z detected as [M – H_2, – Cl^{-}]$^{+}$ 437.09258. ($C_{20}H_{25}N_3O_2CuCl$ requires 437.09258, error 0.005 ppm).

Preparation of [Cu**L**Cl]Cl·2.375H_2O (**L** = **141**)

$CuCl_2$·2H_2O (0.0138 g, 8.09x10^{-5} mol) in warm EtOH (5 ml) was added with stirring to an ethanol solution of **141** (0.0257 g, 7.32x10^{-5} mol) (20 ml). Several small blue block-like crystals of [Cu**L**Cl]Cl·2.375H_2O were obtained following slow evaporation of the ethanol solution. Positive ion ESI-HRMS m/z detected as $[(M - H_2)]^+$ 453.07017 ($C_{20}H_{25}N_3OSCuCl$ requires 453.07047, error 0.9 ppm).

Preparation of (**L**H_2)(NO_3)$_2$ (**L** = **137**)

$Zn(NO_3)_2$·6H_2O (0.0220 g, 7.40x10^{-5} mol) in warm EtOH (10 ml) was added to a solution of **137** (0.0195 g , 5.40x10^{-5} mol) in warm CH_3CN (10 ml). Several yellow shard-like crystals of (**L**H_2)(NO_3)$_2$ (**L** = **137**) were obtained following slow evaporation of this reaction solution. Positive ion ESI-HRMS m/z detected as $[(M - H_2) + H^+]$ 374.17210. ($C_{20}H_{28}N_3S_2$ requires 374.17246, error 0.5 ppm).

Preparation of [Cd**L**(NO_3)$_2$]·CH_3OH (**L** = **138**)

$Cd(NO_3)_2$·4H_2O (0.0312 g, 1.04x10^{-4} mol) in warm CH_3OH (10 ml) was added to a solution of **138** (0.296 g, 8.69x10^{-5} mol) in warm MeOH (15 ml). A single colourless block-like crystal of [Cd**L**(NO_3)$_2$]·CH_3OH was obtained by slow diffusion of diethyl ether vapour into the reaction solution. Positive ion ESI-HRMS m/z detected as $[M - NO_3^-]^+$ 508.12029. ($C_{20}H_{27}N_5O_4Cd$ requires 508.12004, error 0.5 ppm).

Preparation of [Cd**L**(NO_3)] (NO_3)·CH_3CH_2OH (**L** = **132**)

$Cd(NO_3)_2$·4H_2O (0.0207 g, 6.73x10^{-5} mol) in warm ethanol (5 ml) was added to a solution of **132** (0.0197 g, 5.53x10^{-5} mol) in warm EtOH (10 ml). A colourless shard-like crystal of [Cd**L**(NO_3)] (NO_3)·CH_3CH_2OH (**L** = **132**) was obtained following slow diffusion of diethyl ether vapour into the reaction solution. Positive ion ESI-HRMS m/z detected as $[M - NO_3^-]^+$ 524.09741. ($C_{20}H_{28}N_5O_3SCd$ requires 524.09719, error 0.4 ppm).

Preparation of [Ag**L**]PF_6 (**L** = **132**)

AgPF6 (0.0158 g, 6.22x10^{-5} mol) in warm CH_3CN (5 ml) was added to a solution of **132** (0.020 g, 5.61x10^{-5} mol) in 10 ml warm CH_3CN without stirring. Slow evaporation of the reaction solution yielded a yellow shard-like crystal of [Ag**L**]PF_6 (**L** = **132**) suitable for X-ray studies. Positive ion ESI-HRMS m/z detected as M^+ 463.10817. ($C_{20}H_{28}N_4SAg$ requires m/z 463.10801, error 0.3 ppm).

Preparation of [Ag**L**]PF_6 (**L** = **141**)

AgPF6 (0.0194 g, 7.69x10^{-5} mol) was dissolved in warm CH_3CN (5 ml) and added to a solution of **141** (0.0255 g, 6.99x10^{-5} mol) in warm CH_3CN (20 ml) without stirring. Colourless plate-like crystals (0.0127g, 39.7%) of [Ag**L**]PF_6 (**L** = **141**) were obtained by slow evaporation of the reaction solution. Elemental analysis (%) calcd. for $C_{20}H_{27}AgF_6N_3OPS$: C 39.36, H 4.46, N 6.88; Found: C 39.55, H4.56, N 6.92.

3.3.2 X-ray crystallographic studies – data collection

Data for [Cd**L**$(NO_3)_2$]·CH_3OH (**L** = **138**), [Ni**L**Cl]Cl·$3H_2O$ (**L** = **138**), (**L**H_2)$(NO_3)_2$ (**L** = **137**) and [Cd**L**(NO_3)] (NO_3)·CH_3CH_2OH (**L** = **132**) were collected with ω scans to approximately 56° 2θ using a Bruker SMART 1000 diffractometer employing graphite-monochromated Mo-Kα radiation generated from a sealed tube (0.71073 Å) at 150(2) K [Bruker (1995), SMART, SAINT and XPREP. Bruker Analytical X-ray Instruments Inc., Madison, Wisconsin, USA]. Data for [Ag**L**]PF_6 (**L** = **141**), [Cu**L**Cl]Cl·$2.375H_2O$ (**L** = **141**), [Ni**L**Cl]Cl·$0.125CH_3CN$·$3.75H_2O$ (**L** = **142**), [Cu**L**Cl_2]·CH_3CN (**L** = **138**), [Ag**L**]PF_6 (**L** = **132**) and [Cu**L**Cl_2]·CH_3CN (**L** = **142**) were collected on a Bruker-Nonius APEX2-X8-FR591 diffractometer employing graphite-monochromated Mo-Kα radiation generated from a rotating anode (0.71073 Å) with ω and ψ scans to approximately 56° 2θ at 150(2) K [Bruker-Nonius (2003). APEX v2.1, SAINT v.7 and XPREP v.6.14. Bruker AXS Inc. Madison, Wisconsin, USA.]. Data integration and reduction were undertaken with SAINT and XPREP [Bruker (1995), SMART, SAINT and XPREP. Bruker Analytical X-ray Instruments Inc., Madison, Wisconsin, USA]**.** Subsequent computations were carried out using the WinGX-32 graphical user interface, WinGX-32: System of programs for solving, refining and analysing single crystal X-ray diffraction data for

small molecules.[57] Structures were solved by direct methods using SIR97[58] Multi-scan empirical absorption corrections, when applied, were applied to the data sets using the programs TWINABS or SADABS[59] Data were refined and extended with SHELXL-97[60] In general, non-hydrogen atoms with occupancies greater than 0.5 were refined anisotropically. Carbon-bound hydrogen atoms were included in idealised positions and refined using a riding model. Oxygen and nitrogen bound hydrogen atoms were first located in the difference Fourier map before refinement. Where these hydrogen atoms could not be located, they were not modelled. Disorder was modelled, and twinning where present accounted for, using standard crystallographic methods including constraints, restraints and rigid bodies where necessary. All structures were determined by Dr Jack K. Clegg at the School of Chemistry, The University of Sydney. Crystal data and a summary of data collection as well as tables of non-hydrogen bond lengths and non-hydrogen bond angles are given in **Appendix B**. Crystallographic information files are presented on the accompanying compact disc.

3.3.3 Potentiometric titration studies

The protonation constants and metal stability constants were determined by the potentiometric (pH titration) technique. All metal complex log *K* values are the mean of between two and four individual determinations at varying metal:macrocycle ratios. All measurements were performed in 95% methanol at 25 ± 0.1 ˚C (I = 0.1; NEt_4ClO_4). AR grade MeOH was fractionated and distilled over magnesium before use. The methanol-water (95:5) solvent mixture was employed in order that the current results might be directly comparable with those obtained for related metal-ligand systems reported previously.[4, 61] The potentiometric titration apparatus consisted of a water-jacketed titration vessel and a water-jacketed calomel reference electrode, connected by a salt bridge. A Philips glass electrode (GA-110) was used for all pH measurements. Tetraethylammonium perchlorate (0.1 M), used as the background electrolyte, was also employed in the salt bridge, while the calomel reference contained tetraethylammonium perchlorate (0.09 M) and tetraethylammonium chloride (0.01 M) in 95% methanol. Methanol-saturated nitrogen was bubbled through the solution of the measuring cell; tetraethylammonium hydroxide solution was introduced into the cell using a Metrohm

Dosimat 665 automatic titration apparatus under PC control. A Corning model 130 Research pH meter was employed for the pH determinations. The apparatus was calibrated daily by titration with solution of standard base. In virtually all cases it was not possible to obtain complete titration curves because of precipitation during the course of the titration. The titration data was recorded as milivolts versus mililitres of base added. The titration data corresponding to the lower portions of respective titration curves for the complexes of **132, 136 – 138, 141** and **142** refined satisfactorily assuming 1:1 metal to macrocycle complexation. Data were processed using a local version of MINIQUAD.[33]

3.4 References

1. D. S. Baldwin, P. A. Duckworth, G. R. Erickson, L. F. Lindoy, M. McPartlin, G. M. Mockler, W. E. Moody and P. A. Tasker, *Aust. J. Chem.*, 1987, **40**, 1861.
2. K. R. Adam, M. Antolovich, D. S. Baldwin, L. G. Brigden, P. A. Duckworth, L. F. Lindoy, A. Bashall, M. McPartlin and P. A. Tasker, *J. Chem. Soc., Dalton Trans.*, 1992, 1869.
3. K. R. Adam, D. S. Baldwin, P. A. Duckworth, L. F. Lindoy, M. McPartlin, A. Bashall, H. R. Powell and P. A. Tasker, *J. Chem. Soc., Dalton Trans.*, 1995, 1127.
4. K. R. Adam, D. S. Baldwin, L. F. Lindoy, G. V. Meehan, I. M. Vasilescu and G. Wei, *Inorg. Chim. Acta*, 2003, **352**, 46.
5. K. R. Adam, L. G. Brigden, K. Henrick, L. F. Lindoy, M. McPartlin, B. Mimnagh and P. A. Tasker, *J. Chem. Soc., Chem. Commun.*, 1985, 710.
6. U. Kallert and R. Mattes, *Inorg. Chim. Acta*, 1991, **180**, 263.
7. U. Kallert and R. Mattes, *Polyhedron*, 1992, **11**, 617.
8. D. S. Baldwin, PhD Thesis, James Cook University, 1987.
9. S. Bilge, Z. Kılıç, T. Hökelekb and B. Erdoğan, *J. Molec. Struct.*, 2004, **691**, 85.
10. K. R. Adam, A. J. Leong, L. F. Lindoy, B. J. McCool, A. Ekstrom, I. Liepa, P. A. Harding, K. Henrick, M. McPartlin and P. A. Tasker, *J.Chem. Soc., Dalton Trans.*, 1987, 2537.
11. R. M. Izatt, J. S. Bradshaw, S. A. Nielsen, J. D. Lamb, J. J. Christensen and D. Sen, *Chem. Rev.*, 1985, **85**, 271.
12. D. E. Fenton, B. P. Murphy, A. J. Leong, L. F. Lindoy, A. Bashall and M. McPartlin, 1987, 2543.
13. K. R. Adam, G. Anderegg, K. Henrick, A. J. Leong, L. F. Lindoy, H. C. Lip, M. McPartlin, R. J. Smith and P. A. Tasker, *Inorg. Chem.*, 1981, **20**, 4048.
14. J.-E. Lee, J. Y. Lee, J. Seo, S. Y. Lee, H. J. Kim, Park, K.-M. Park, L. F. Lindoy and S. S. Lee, *Polyhedron*, 2008, **27**, 3004.
15. L. Pauling, *The Nature of the Chemical Bond*, 3rd edn., Cornell University Press, Ithaca, NY, 1960.
16. H. J. Goodwin, K. Henrick, L. F. Lindoy, M. McPartlin and P. A. Tasker, *Inorg. Chem.*, 1982, 3261 and references therein.

17. A. Ekstrom, L. F. Lindoy, H. C. Lip, R. J. Smith, H. J. Goodwin, M. McPartlin and P. A. Tasker, *J. C. S. Dalton*, 1979, 1027 and references therein.
18. K. R. Adam, G. Anderegg, L. F. Lindoy, H. C. Lip, M. McPartlin, J. H. Rea, R. J. Smith and P. A. Tasker, *Inorg. Chem.*, 1980, **19**, 2959 and references therein.
19. L. F. Lindoy, *The Chemistry of Macrocyclic Ligand Complexes*, Cambridge University Press, Cambridge, 1989.
20. K. R. Adam, L. F. Lindoy, H. C. Lip, J. H. Rea, B. W. Skelton and A. H. White, *J. C. S. Dalton*, 1981, 74.
21. J. Seo, S. Park, S. S. Lee, M. Feinerman-Melnikova and L. F. Lindoy, *Inorg. Chem.*, 2009, **48**, 2770.
22. A. W. Addison, T. N. Rao, J. Reedijck, J. v. Rijn and G. C. Verschoor, *J. Chem. Soc., Dalton Trans.*, 1984, 1349.
23. N. A. Bailey, D. E. Fenton, S. J. Kitchen, T. H. Lilley, M. G. Williams, P. A. Tasker, A. J. Leong and L. F. Lindoy, *J. Chem. Soc., Dalton Trans.*, 1991, 627 and references therein.
24. K. R. Adam, D. S. Baldwin, P. A. Duckworth, A. J. Leong, L. F. Lindoy, M. McPartlin and P. A. Tasker, *J. Chem. Soc., Chem. Commun.*, 1987, 1124.
25. L. Babosa, L. F. Lindoy, B. W. Skelton and A. H. White, *Polyhedron*, 2007, **26**, 653.
26. K. R. Adam, K. P. Dancey, B. A. Harrison, A. J. Leong, L. F. Lindoy, M. McPartlin and P. A. Tasker, *J. Chem. Soc., Chem. Commun.*, 1983, 1351.
27. K. R. Adam, K. P. Dancey, A. J. Leong, L. F. Lindoy, B. J. McCool, M. McPartlin and P. A. Tasker, *J. Am. Chem. Soc.*, 1988, **110**, 8471 and references therein.
28. K. R. Adam, S. P. H. Arshad, D. S. Baldwin, P. A. Duckworth, A. J. Leong, L. F. Lindoy, B. J. McCool, M. McPartlin, B. A. Tailor and P. A. Tasker, *Inorg. Chem.*, 1994, **33**, 1194.
29. K. R. Adam, B. J. McCool, A. J. Leong, L. F. Lindoy, C. W. G. Ansell, P. J. Bailie, K. P. Dancey, L. A. Drummond, K. Henrick, M. McPartlin, D. K. Uppal and P. A. Tasker, *J. Chem. Soc., Dalton Trans.*, 1990, 3435 and references therein.

30. Y. Jin, I. Yoon, J. Seo, J.-E. Lee, S.-T. Moon, J. Kim, S. W. Han, K.-M. Park, L. F. Lindoy and S. S. Lee, *Dalton Trans.*, 2005, 788.
31. I. Yoon, J. Seo, J.-E. Lee, M. R. Song, S. Y. Lee, K. S. Choi, O.-S. Jung, K.-M. Park and S. S. Lee, *Dalton Trans.*, 2005, 2352.
32. D. D. Perrin, B. Dempsey and E. P. Serjeant, *pKa Prediction for Organic Acids and Bases*, Chapman and Hall, London, 1981.
33. P. Gans, A. Sabatini and A. Vacca, *Inorg. Chim. Acta*, 1976, **18**, 237.
34. H. J. Kim, A. J. Leong, L. F. Lindoy, J. Kim, J. Nachbaur, A. Nezhadali, G. Rounaghi and G. Wei, *J. Chem. Soc., Dalton Trans.*, 2000, 3453 and references therein.
35. H. Irving and R. J. P. Williams, *J. Chem. Soc.*, 1953, 3192.
36. R. M. Izatt, K. Pawlak, J. S. Bradshaw and R. L. Bruening, *Chem. Rev.*, 1991, **91**, 1721.
37. R. M. Izatt, K. Pawlak and J. S. Bradshaw, *Chem. Rev.*, 1995, **95**, 2529.
38. G. Reid and M. Schroder, *Chem. Soc. Rev.*, 1990, **19**, 239.
39. A. J. Blake and M. Schroder, 1990, **35**, 1.
40. E. C. Constable, *Coordination Chemistry of Macrocyclic Compounds*, Oxford University Press, 1999.
41. J. R. Lotz, B. P. Block and W. C. Fernelius, *J. Phys. Chem.*, 1959, **63**, 541.
42. M. Ciampolini, M. Paoletti and L. Sacconi, *J. Chem. Soc.*, 1961, 2994.
43. G. G. Herman, A. M. Goeminne and H. F. DeBrabander, *Thermochim. Acta*, 1979, **32**, 27.
44. R. Barbucci and A. Vacca, *J. Chem. Soc., Dalton Trans.*, 1974, 2363.
45. F. Arnaud-Neu, M. J. Schwing-Weill, R. Louis and R. Weiss, *Inorg. Chem.*, 1979, **18**, 2956.
46. J.-H. Kim, M.-H. Cho, D.-H. Hyeoun, H. B. Park, S. J. Kim and I.-C. Lee, *J. Korean Chem. Soc.*, 1990, **34**, 418.
47. K. R. Adam, M. Antolovich, D. S. Baldwin, P. A. Duckworth, A. J. Leong, L. F. Lindoy, M. McPartlin and P. A. Tasker, *J. Chem. Soc., Dalton Trans.*, 1993, 1013.

48. R. M. Smith and A. E. Martell, in *Critical Stability Constants, Amines*, Plenum, New York, 1975, vol. 2.
49. K. R. Adam, B. J. McCool, A. J. Leong, L. F. Lindoy, C. W. G. Ansell, P. J. Bailey, K. P. Dancey, L. A. Drummond, K. Henrick, M. McPartlin, D. K. Uppal and P. A. Tasker, *J. Chem. Soc., Dalton Trans.*, 1990, 3435.
50. B. G. Cox and H. Schneider, *Coordination and Transport Properties of Macrocyclic Compounds in Solution*, Elsevier, 1992.
51. R. G. Pearson, *J. Am. Chem. Soc.*, 1963, **85**, 3533.
52. M. G. B. Drew, D. A. Rice and C. W. Timewell, *J. Chem. Soc., Dalton Trans.*, 1975, 144.
53. M. G. B. Drew and S. Hollis, *J. Chem. Soc., Dalton Trans.*, 1978, 511.
54. L. F. Lindoy, *Pure and Appl. Chem.*, 1997, **69**, 2179 and references therein.
55. D. S. Baldwin, L. F. Lindoy and D. P. Graddon, *Aust. J. Chem.*, 1988, **41**, 1347.
56. G. Wu, W. Jiang, J. D. Lamb, J. S. Bradshaw and R. M. Izatt, *J. Am. Chem. Soc.*, 1991, **113**, 6538 and references therein.
57. L. J. Farrugia, *J. Appl. Cryst.*, 1999, **32**, 837.
58. A. Altomare, M. C. Burla, M. Camalli, G. L. Cascarano, C. Giocavazzo, A. Guagliardi, A. G. C. Moliterni, G. Polidori and S. Spagna, *J. Appl. Cryst.*, 1999, **32**, 115.
59. G. M. Sheldrick, University of Goettingen, Germany, 1999-2007.
60. G. M. Sheldrick, University of Goetingen, Germany, 1997.
61. J. R. Price, M. Feinerman-Melnikova, D. E. Fenton, K. Gloe, L. F. Lindoy, T. Rambusch, B. W. Skelton, P. Turner, A. H. White and K. Wichmann, *Dalton Trans.*, 2004, 3715.

Chapter 4 – Modeling the stability constants of related 17-membered mixed-donor macrocyclic metal ion complexes

4.1 Background

As discussed already in this thesis, there has been very considerable effort focussed on the rational design of metal ion selective ligands.[1] Studies aimed at understanding the factors underlying complex stability such as electronic and steric effects, enthalpic and entropic terms as well as solvent dependencies are often very far from straight forward and early research in this area of macrocyclic chemistry has been for the most part experimentally based.[2] However, more recently, the evolution of computational chemistry has made it possible, through the use of computer modeling, to simulate metal complex structures and energies with the potential of such results to be employed in metal ion discrimination studies.[3] Nevertheless, such procedures, while often very effective, tend to be computationally expensive and normally need the input of an experienced computational chemist. In contrast, this chapter describes a simple procedure for modeling metal complex stability constants for the complexes of a series of closely related ligands – namely, mixed-donor dibenzo-substituted 17-membered macrocycles of the type presented so far in this thesis, with the discussion focussing on the complexes of Co(II), Ni(II), Cu(II), Zn(II), Cd(II), Ag(I) and Pb(II).

4.2 Modeling of log *K* values

The prospect of relating the magnitude of individual stability constants to the respective donor sets presented to a given central metal ion is partly based on previous studies which demonstrated that for many supramolecular complexes the free energy of complexation can be partitioned into single contributions by linear correlations between ΔG and the sum of single interactions[4] and that the log K_{M-L} value can be estimated from the sum of fixed contributions for each type of donor atom.[5] Thus, for interaction of a metal ion M^{n+} with a number of binding sites A, B, C, … representing different donor atoms in a ligand, the total binding free energy can be approximated as follows:

$$\Delta G = \Delta G_{M-A} + \Delta G_{M-B} + \Delta G_{M-C} + \ldots\ldots$$

where ΔG_{M-A} represents the contributions from the interactions of the metal ion with the respective donor atoms. In the proposed model, each of these terms is considered to be independent of the others and also transferable between closely related complexes of the same metal. Since $\Delta G^0 = -2.303RT \log K$, the logarithms of the binding constants can also be partitioned in similar fashion to give:

$$\log K = \log K_{M-A} + \log K_{M-B} + \log K_{M-C} + \ldots\ldots$$

Clearly, such partitioning is only valid if the nature of the complexes is restricted to types in which the metal-donor atom interactions occur in generally similar environments as is the case with the 17-membered mixed-donor ligands of type **163**.

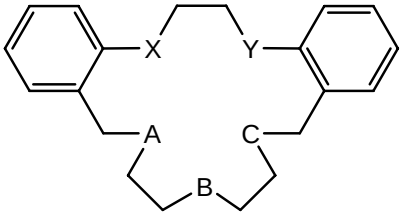

163

These ligands represent an array of related macrocyclic structures in which the type and position of the donor atoms vary in a systematic manner. In the discussion that follows, individual complexes are represented by the shorthand notation M/XY/ABC, and the log *K* of such a metal complex may be expressed as:

$$\log K = \log K_{M-X} + \log K_{M-Y} + \log K_{M-A} + \log K_{M-B} + \log K_{M-C} \ldots\ldots\ldots\ldots\ldots (1)$$

The experimental log *K* data used to obtain values for each of the contributing terms in equation (1) are from that already presented in Chapters 1 and 3 and are shown in **Table 4.1**. Inspection of the stability data in **Table 4.1** shows that, as the donor set is varied in a step-wise manner, the log *K* values for the corresponding complexes vary in a somewhat predictable pattern. In addition, density functional theory (DFT) calculations carried out on a number of individual complexes of the above type by Dr. K. R. Adam of the School of Pharmacy and Molecular Sciences, James Cook University, indicated that, provided

the same central metal ion is maintained, relatively little variation in the nature of a given metal–donor bond type occurs from one complex to the next.[6] Both these observations lend further support to the possibility of quantifying the individual log *K* values in terms of the donor set presented by the respective macrocycles to a given metal ion.

Table 4.1 Log *K* values for the 1:1 complexes of 17-membered macrocyclic ligand complexes of type **163** (95% methanol, I = 0.1, Et_4NClO_4, 25.0 °C).

L	Donor set	Co(II)	Ni(II)	Cu(II)	Zn(II)	Cd(II)	Ag(I)	Pb(II)
100	OO/NNN	7.7(1)	10.0(1)	14.2(1)	7.5(1)	8.7(1)	8.7(1)	8.1(1)
101	OO/NON	<3.5	<3.5	6.5(1)	<3.5	5.3(1)	7.1(1)	5.5 (2)
102	OO/NSN	~3.3	5.5(1)	7.4(1)	<3.5	4.4(2)	8.6(1)	4.5(1)
112	SS/NNN	-[a]	9.5(1)	~15.6	6.3(1)	7.8(1)	~11.7	8.0(1)
114	SS/NON	<3.5	~3.4	6.9(2)	-[a]	4.4(1)	10.3(2)	~3.0
113	SS/NSN	<3.5	-[a]	8.1(1)	~3.3	-[a]	12.4(1)	~3.0
128	OS/NON	<3.5	<3.5	6.1(1)	< 4.0	4.9(1)	9.3(1)	4.5(1)
129	OS/NSN	<3.5	-[a]	7.4(1)	< 4.0	~4.0	11.1(1)	~3.8
93	NN/NNN	-[a]	-[a]	16.3(3)	11.9(1)	12.1(1)	10.3(1)	9.4(1)
94	NN/NON	7.0(1)	-[a]	14.5(3)	7.8(1)	10.0(1)	9.8(1)	6.7(1)
95	NN/NSN	-[a]	-[a]	14.5(2)	8.9 (1)	9.2(1)	10.8(1)	5.9(1)
138	ON/NNN	9.2(1)	-[a]	15.6(3)	9.8(1)	10.9(1)	9.8(1)	8.8(1)
127	OS/NNN	7.2(1)	~9.5	13.9(3)	7.0(1)	8.1(1)	10.8(1)	7.8(1)
132	SN/NNN	-[a]	-[a]	15.1(1)	8.0(1)	9.6(1)	11.5(1)	8.5(1)
137	SN/NSN	5.4(1)	7.8(1)	12.4(1)	4.8(1)	6.5(1)	12.2(1)	4.7(1)
136	SN/NON	3.6(1)	6.1(1)	9.7(1)	4.2(1)	7.1(1)	10.5(1)	5.2(1)
141	ON/NSN	6.2(1)	7.2(1)	11.2(1)	6.6(1)	6.4(1)	9.9(1)	4.6(1)
142	ON/NON	4.1(1)	5.5(1)	9.3(1)	4.8(1)	8.4(1)	9.1(1)	5.7(1)

[a]As mentioned in Chapters 1 and 3 these values were unable to be determined due to precipitation, hydrolysis or slow approach to equilibrium. Values preceded by ~ or < are of lower reliability and were not used in the present computations; log *K* values > 15 were also discarded.

4.2.1 Internal consistency check

Prior to computing individual log *K* values, a check was made of the consistency of the model, based on the experimental log *K* data listed in **Table 4.1**. Considering, for example, the complexes of the same metal M with two ligands X_1Y_1/ABC and X_1Y_2/ABC (where a change of subscript represents a change of donor atom type), expressing the log *K* for each complex using equation (1) and then subtracting the two expressions gives:

$\log K$ (M/ X_1Y_1/ABC) – $\log K$ (M/ X_1Y_2/ABC) = $\log K_{M–Y1} – \log K_{M–Y2}$

due to cancellation of like terms. A similar calculation for another pair of complexes such as M/X_2Y_1/ABC and M/X_2Y_2/ABC produces another value for $\log K_{M–Y1} – \log K_{M–Y2}$. The equality or otherwise of the two values provides a test of the validity of the model. For the experimental data in **Table 4.1**, when the values of high uncertainty are discarded (values < 3.5 or > 15 are outside the optimum range for log *K* measurements under the conditions employed and for the ligands of the present type) there are a total of 199 such subtractions which are shown in **Tables 4.2 – 4.13** (see **Appendix C.1**); in these tables less precise experimental data are denoted with '*', while '-' indicates no experimental values were obtained for at least one of the metal complex pairs. **Table 4.14** shows the distribution of the deviations of the values in each row in **Tables 4.2 – 4.13** from the average for that row.

Table 4.14 Deviation distribution for **Tables 4.2 – 4.13** (**Appendix C.1**).

Band (log *K*)	0.0 - 0.3	0.3 - 0.6	0.6 - 1.0	1.0 - 2.0	> 2.0	Total
No of points	119	43	32	5	-	199

It was found that of these 199 values, 119 lie within 0.3 log *K* units of being constant and therefore well within experimental error and a further 43 lie between 0.3 – 0.6 log *K* units which may also be considered acceptable, considering that differences of log *K* values are involved. There are only 5 clearly unacceptable values that fall in the 1.0 – 2.0 log *K* units band, while the presence of 32 values in the 0.6 – 1.0 log *K* units band is perhaps not unexpected given the simple nature of the model proposed.

4.2.2 Determination of log *K* parameters

As discussed above, in theory, the log *K* data for the complexes formed by the macrocyclic ligands listed in **Table 4.1** can be used to obtain values for each of the contributing terms in equation (1), which can subsequently be used to compute log *K* values for complexes formed by any ligands of type **163** with the previously mentioned metal ions. However, this is to some extent complicated by the limited range of data available since all ligands listed in **Table 4.1** have an NBN-donor pattern in the lower

bridge. This in turn gives rise to linear dependencies in the equations and as a result it is not possible to obtain values for all of the parameters. Consequently, separate values for the parameters corresponding to the donor atoms in the bottom bridge can not be obtained; instead only the sum of these values can be derived and, in effect, equation (1) is re-written as:

$$\log K = \log K_{M-X} + \log K_{M-Y} + \log K_{M-ABC} \quad \text{..... (2)}$$

For each metal ion it is possible to obtain six parameters:

$\log K_{M-S}$……a metal S donor interaction in the upper bridge
$\log K_{M-N}$……a metal N donor interaction in the upper bridge
$\log K_{M-O}$……a metal O donor interaction in the upper bridge
$\log K_{M-NNN}$……a metal NNN donor combination interaction in the lower bridge
$\log K_{M-NON}$……a metal NON donor combination interaction in the lower bridge
$\log K_{M-NSN}$……a metal NSN donor combination interaction in the lower bridge

It should be noted that the proposed model assumes the coordination of all donor atoms in solution. In addition, since all experimental log *K* data for the ligands in **Table 4.1** were obtained under identical conditions, it was considered unnecessary to include in equation (2) a term to account for contributions from any coordinated solvent molecules. All experimental data labeled as being of low reliability in **Table 4.1** were excluded when constructing the equations for this fitted set. Solutions were sought to minimise the sum of the squares of the deviations between measured and the computed log *K* values for the complexes in the fitted set. This was achieved by a direct minimisation technique. The solution however is complicated by many local minima and a simulated annealing algorithm starting from a set of initial ‘guessed’ values was at first used to obtain an approximate solution which was further refined by a local Newton type minimiser. Once a set of parameters was determined, the values were then substituted back into equation (2) in order to obtain calculated log *K* values for the various metal complexes. A

summary of the observed and the calculated stability data obtained using the proposed model is shown in **Table 4.15**.

Table 4.15 Log *K* values (observed *vs* calculated) for the 17-membered mixed donor dibenzo-substituted macrocycles of type **163**.

L	Donor set	Co(II)	Ni(II)	Cu(II)	Zn(II)	Cd(II)	Ag(I)	Pb(II)
100	OO/NNN obs.	7.7	10.0	14.2	7.5	8.7	8.7	8.1
	calc.	7.5	9.7	13.9	7.6	8.5	8.7	8.2
101	OO/NON obs.	<3.5	<3.5	6.5	<3.5	5.3	7.1	5.5
	calc.	-[b]	-[b]	6.0	-[b]	5.6	7.5	5.1
102	OO/NSN obs.	~3.3	5.5	7.4	<3.5	4.4	8.6	4.5
	calc.	-[b]	5.5	7.4	-[b]	4.6	9.0	4.3
112	SS/NNN obs.	-[a]	9.5	~15.6	6.3	7.8	~11.7	8.0
	calc.	-[a]	9.8	-[b]	5.9	7.4	-[b]	7.6
114	SS/NON obs.	<3.5	~3.4	6.9	-[a]	4.4	10.3	~3.0
	calc.	-[b]	-[b]	6.7	-[a]	4.6	11.0	-[b]
113	SS/NSN obs.	<3.5	-[a]	8.1	~3.3	-[a]	12.4	~3.0
	calc.	-[b]	-[a]	8.0	-[b]	-[a]	12.5	-[b]
128	OS/NON obs.	<3.5	<3.5	6.1	< 4.0	4.9	9.3	4.5
	calc.	-[b]	-[b]	6.4	-[b]	5.1	9.2	4.8
129	OS/NSN obs.	<3.5	-[a]	7.4	< 4.0	~4.0	11.1	~3.8
	calc	-[b]	-[a]	7.7	-[b]	-[b]	10.7	-[b]
93	NN/NNN obs.	-[a]	-[a]	16.3	11.9	12.1	10.3	9.4
	calc.	-[a]	-[a]	-[b]	12.2	12.7	10.8	9.5
94	NN/NON obs.	7.0	-[a]	14.5	7.8	10.0	9.8	6.7
	calc.	6.5	-[a]	13.7	7.3	9.9	9.6	6.4
95	NN/NSN obs.	-[a]	-[a]	14.5	8.9	9.2	10.8	5.9
	calc.	-[a]	-[a]	15.1	8.6	8.9	11.1	5.6
138	ON/NNN obs.	9.2	-[a]	15.6	9.8	10.9	9.8	8.8
	calc.	9.7	-[a]	-[b]	9.7	10.6	9.7	8.8
127	OS/NNN obs.	7.2	~9.5	13.9	7.0	8.1	10.8	7.8
	calc.	6.9	-[b]	14.2	6.8	8.0	10.4	7.9
132	SN/NNN obs.	-[a]	-[a]	15.1	8.0	9.6	11.5	8.5
	calc.	-[a]	-[a]	-[b]	9.0	10.1	11.5	8.6
137	SN/NSN obs.	5.4	7.8	12.4	4.8	6.5	12.2	4.7
	calc.	5.5	7.5	11.6	5.5	6.2	11.8	4.7
136	SN/NON obs.	3.6	6.1	9.7	4.2	7.1	10.5	5.2
	calc.	3.8	5.9	10.2	4.2	7.2	10.3	5.5
141	ON/NSN obs.	6.2	7.2	11.2	6.6	6.4	9.9	4.6
	calc.	6.1	7.5	11.2	6.3	6.8	10.0	5.0
142	ON/NON obs.	4.1	5.5	9.3	4.7	8.4	9.1	5.7
	calc.	4.4	5.8	9.9	5.1	7.7	8.5	5.8

[a]No experimental log *K* data available; [b]data deemed imprecise (see text).

The values for the individual parameters obtained for each metal ion–donor atom interaction, as well as the differences between the calculated and the observed log *K* values are listed in **Appendix C.2**.

4.3 Discussion

In general, good agreement with the experimentally determined log *K* values was obtained across the present ligand series. This is especially true for the d^{10} metal ion systems Zn(II), Cd(II), Ag(I) and Pb(II) which are all free of crystal field effects and electronic interactions of the type underlying the Irving-Williams stability order. For most of these complexes the difference between the observed and calculated values does not exceed 0.3 log *K* units (see **Appendix C.2**). Nevertheless, the calculations were extended to include the remaining ions, Co(II), Ni(II) and Cu(II). In spite of likely complications due to electronic interactions and the limited amount of reliable experimental data available for these metal ions from which a set of interaction parameters could be derived (see **Table 4.1**), for both Co(II) and Ni(II) the difference between most observed and calculated log *K* values does not exceed 0.3 and there is no difference greater that 0.5 log *K* units (see **Appendix C.2**). Given the coordination sphere for Cu(II) is more 'flexible' than that of Co(II) and Ni(II) and in addition the Jahn-Teller effect may also come into play and affect a given geometry, the results for this metal ion are still reasonably good (although not as good as for the other metals), with nine out of the fourteen log *K* values calculated for Cu(II) situated inside 0.3 log *K* units difference relative to the observed data (see **Appendix C.2**).

Closer inspection of the data in **Appendix C.2** reveals that some of the fitted donor group contribution parameters have negative values which correspond to a destabilisation effect. No attempt has been made in the current study to attach any physical significance to these other that the solutions obtained should simply be regarded only as useful fitting parameters which, in most cases, give rise to good matches between the experimental and computed log *K* values.

The model's application for discrimination behaviour studies is illustrated, for example, in the predicted increase in Ag(I)/Pb(II) discrimination for the NS/NSN macrocycle (**137**) relative to the original symmetrical ligand SS/NNN (**112**). Thus, prior to the synthesis of the unsymmetrical ligand, model parameters derived for related complexes for which log *K* data were available[7] were used by the author to calculate log *K* values for complexes for which experimental data were missing at the time. For NS/NSN the predicted log *K* values were 11.6 for Ag(I) and 5.1 with Pb(II)[8] The subsequent determination of additional experimental data, as the present project progressed, allowed for further refinement of the model and, as expected, the current calculated values of 11.8 and 4.7 are very close to those observed of 12.2 and 4.7 for Ag(I) and Pb(II) respectively. Thus, in this case, the model was successful in predicting that variation of donor atom positions in the macrocyclic backbone will result in an increase in Ag(I)/Pb(II) discrimination. Overall, the present results also indicate the likely suitability of the model for predicting log *K* values for complexes of other systems of type **163** for which experimental data is not yet available.

4.4 References

1. P. Comba, *Coord. Chem. Rev.*, 1999, **185-186**, 81 and references therein.
2. R. M. Izatt, J. S. Bradshaw, S. A. Nielsen, J. D. Lamb, J. J. Christensen and D. Sen, *Chem. Rev.*, 1985, **85**, 271.
3. K. R. Adam and L. F. Lindoy, in *Crown Compounds: Towards Future Applications*, ed. S. R. Cooper, Weinheim, Germany, 1992, pp. 69-79 and references therein.
4. H. J. Schneider, V. Rudiger and O. A. Raevsky, *J. Org. Chem.*, 1993, **58**, 3648 and references therein.
5. W. R. Harris, *J. Coord. Chem.*, 1983, **13**, 17.
6. K. R. Adam, unpublished work, 2002.
7. K. R. Adam, D. S. Baldwin, L. F. Lindoy, G. V. Meehan, I. M. Vasilescu and G. Wei, *Inorg. Chim. Acta.*, 2003, **352**, 46.
8. K. R. Adam, D. S. Baldwin, L. F. Lindoy, G. V. Meehan, I. M. Vasilescu and G. Wei, unpublished work.

Chapter 5 – Rational ligand design for metal ion recognition. Synthesis of an N-benzylated S_3N_2-donor macrocycle for enhanced Ag(I) discrimination

5.1 Background

As discussed already in Chapter 1, much of the research in the author's laboratory has been concerned with the factors influencing metal-ion recognition and discrimination by mixed-donor macrocycles. In particular, these investigations were focused on the coordination behaviour of such macrocycles towards the following transition and post-transition ions Co(II), Ni(II), Cu(II), Zn(II), Cd(II), Ag(I) and Pb(II) and significant metal-ion recognition has been achieved in a number of instances.[1-3] For example, step-wise 'tuning' of the donor set present within 17-membered rings of type **82** (X = NH, S, O; Y = NH, S, O; see Chapter 1, **Table 1.2**, p 42) resulted in the S_3N_2-donor macrocycle **113** showing $>10^9$ discrimination for Ag(I) over Pb(II).[4] For the same macrocycle, discrimination for Ag(I) over Cu(II), while less spectacular, was still $\sim10^4$.[5] As expected from a consideration of HSAB theory,[6, 7] the above study confirmed that progressive substitution of thioether sulfur atoms for oxygen in an O_3N_2-donor ring of type **82** leads to increased Ag(I) discrimination. In addition to the effect of the macrocyclic donor set present (as illustrated above), as outlined in previous chapters of this thesis, three other design elements that influence the discrimination for Ag(I) over the above transition and post-transition ions have been documented: (i) the macrocyclic ring size, (ii) the macrocyclic donor atom sequence and (iii) the nature of any donor atom substituents present.

To take each of the above in turn, studies involving ligands of type **82** led to the general observation that both the strength of binding as well as the observed silver ion discrimination tended to peak for the 17-membered ring system (which forms three five-membered and two six-membered chelate rings when all donors bind to the central metal ion). In this context, it is noted that the X-ray structures of the 1:1 (Ag^+:**L**) complexes, where **L** = **82**, with X = S, Y = O,[4] X = S, Y = NH,[8] and X = S, Y = S[9] (all 17-membered

rings) confirm coordination of all five macrocyclic ring donors to silver in each case, with no other ligands present in the coordination sphere.

Secondly, the presence of a $NHCH_2CH_2YCH_2CH_2NH$ (Y = O or S) donor atom sequence rather than the corresponding sequence with Y = NH, was also demonstrated to promote enhanced silver discrimination,[4] even though the absolute log *K* values across the series tend to be smaller when Y = O (see **Table 1.6**, p 55).

Finally, as discussed in Chapter 1, in a number of studies, it has been documented that N-benzylation of a secondary amine donor in a variety of aza-macrocyclic systems leads to enhanced discrimination for silver over a range of transition and post-transition metal ions,[10] so called 'selective detuning'.[11] In particular, it has been recognised that N-benzylation of the nitrogen donors in a number of mixed nitrogen-oxygen donor macrocycles leads to enhanced metal ion discrimination for Ag(I) within the transition and post-transition metal ions mentioned above.[12, 13]

Analogous behaviour to the above has been reported for the tetra-N-benzylated derivative of cyclam (tbc), which shows both substantial affinity and selectivity for Ag(I).[14] Thus, in bulk liquid (water-dichloromethane-water) membrane transport experiments[15, 16] it was found that silver (as its perchlorate) was the only cation transported by tbc relative to the perchlorates of lithium, sodium, potassium, ammonium, caesium, barium, lead, calcium, magnesium, cobalt, nickel, copper and zinc under the conditions employed.

5.2 The present study

The synthesis of the new dibenzyl-N-substituted 17-membered macrocyclic ring **163,** which contains an S_3N_2-donor set as well as the desired N–S–N donor atom sequence, was carried out based on all four design elements mentioned above. As such, it was expected to exhibit excellent discrimination for silver over the other transition and post-transition ions mentioned earlier.

5.2.1 Ligand synthesis

Macrocycle **164** was prepared by direct N-benzylation of its unsubstituted precursor **113** using benzylbromide in acetonitrile in the presence of sodium hydrogen carbonate as a base (**Scheme 5.1**).

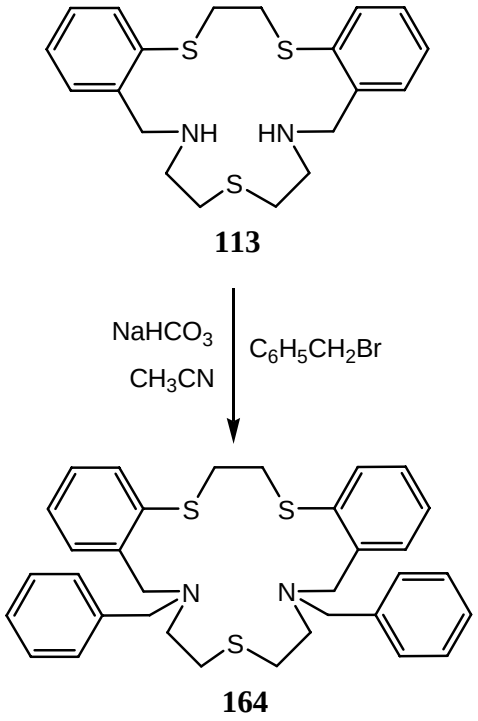

113

164

Scheme 5.1 Synthesis of the dibenzylated S_3N_2-donor macrocycle **164**.

Macrocycle **113** was prepared in the usual manner from the corresponding dialdehyde as outlined in **Scheme 5.2** which is based on previously described methods.[17-19] Interestingly, the procedure employed in the present study resulted in a significantly enhanced yield for the macrocycle over that reported for the original preparation (63% yield compared with the original 40%).[17]

The ^{1}H and ^{13}C NMR data for the macrocycle precursors shown in **Scheme 5.2** were analogous to those previously reported for these species and hence no further structural characterisation was undertaken. Similarly, the NMR spectral data for **113** were identical to those previously reported for this ring.[17]

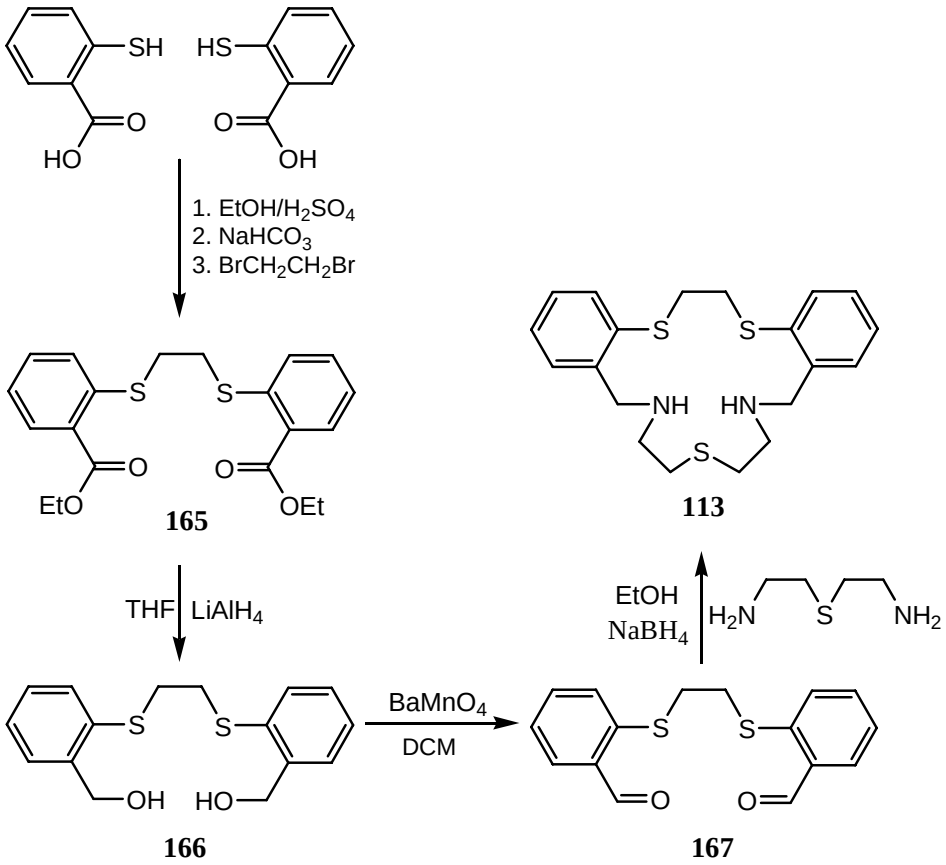

Scheme 5.2 Synthesis of the S_3N_2-donor macrocycle **113**.

5.2.2 Stability constants

Stability constants for the 1:1 complexes of **164** with Co(II), Ni(II), Cu(II), Zn(II), Cd(II), Ag(I) and Pb(II) were determined potentiometrically by the pH titration method in 95% MeOH (I = 0.1, Et_4NClO_4; 25.0 ˚C) under identical conditions to those described previously[10] (and as used for the solution studies reported in Chapter 3). Use of this solvent system for the stability constant measurement once again allowed comparison with the log *K* values determined previously.[4, 20, 21] The results are summarised in **Table 5.1**. It is evident from this data that, as in the case of the non-dibenzylated derivative **113**, the new ligand shows clear discrimination for Ag(I) over the remaining six metals, with the silver complex being at least 10^5 more stable than any of the remaining complexes investigated.

Table 5.1 Log *K* values for the 1:1 complexes of **113** and **164** (95% methanol, I = 0.1, Et_4NClO_4, 25.0 °C).

Ligand	Co(II)	Ni(II)	Cu(II)	Zn(II)	Cd(II)	Ag(I)	Pb(II)
113 [a]	<3.5	-[b]	8.1	~3.3	-[b]	12.4	~3
164	<3	<3	3.6	<3	<3	8.7	~3

[a]Values from previous studies.[4, 20]

[b]Precipitation, hydrolysis or slow approach to equilibrium prevented log *K* determination.

In particular, Ag(I)/Cu(II) discrimination is an order of magnitude higher for **164** than obtained for **113**, even though (as expected) steric[22] and possible electronic influences on N-benzylation of **113** result in a general reduction of the respective log *K* values for the complexes of **164**. However since these effects are much greater for Cu(II) than for Ag(I) (**Figure 5.1**), these results provide yet another example of 'selective detuning' of the type mentioned previously.[11, 12]

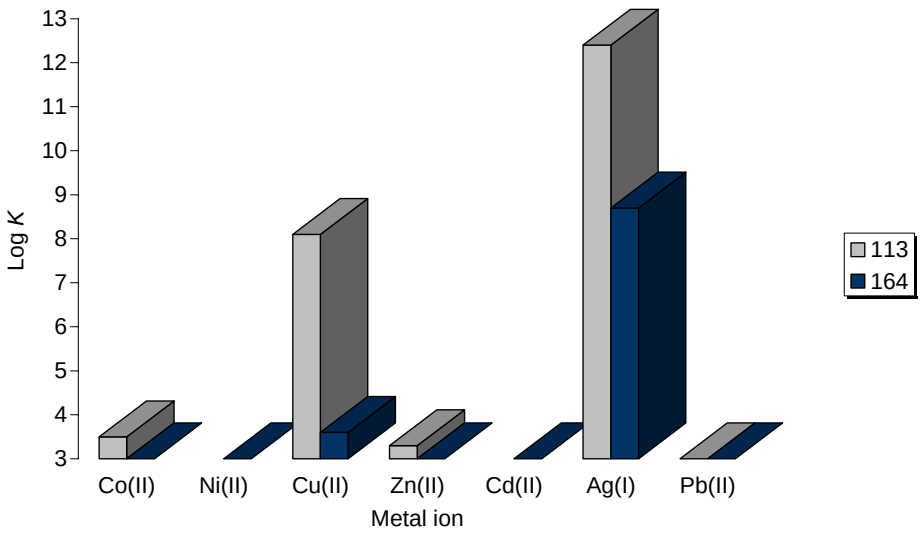

Figure 5.1 Bar graph of the stability constants for the parent **113** and its dibenzylated derivative **164**.

As mentioned in Chapter 1, Meyerstein and coworkers[23, 24] have presented a rationale for N-alkylation in related macrocyclic systems favouring monovalent over divalent metal-ion binding. In their studies, N-alkylation was shown to cause several contradictory effects such as, on the one hand, an increase in the σ-donation properties of the nitrogen donors and, on the other, steric effects and a decrease in the solvation energy. It has been postulated by the above authors that solvational effects dominate, leading to lower valent transition metal complexes being stabilised by N-alkylation.

5.2.3 Silver complex characterisation

The ESI mass spectrum of a mixture of **164** and Ag(I) nitrate in a methanol-acetonitrile mixture yielded (as expected) a peak corresponding to the formation of the 1:1 complex AgL^+ (L = **164**) and a solid complex of this stoichiometry was isolated as its hexafluorophosphate salt on reaction of silver hexafluorophosphate with **164** in acetonitrile-dichloromethane. Crystals suitable for X-ray diffraction were obtained by slow evaporation of an acetonitrile solution of the complex.

The X-ray structure of [Ag**L**]$PF_6 \cdot CH_3CN$ (**L** = **164**) (**Figure 5.2**) shows that the Ag(I) ion is bound to all five donor atoms of **164** in the complex cation and adopts a close to square pyramidal geometry (**Figure 5.3**). This is consistent with the strong ligand to silver coordination inferred from the solution studies (**Table 5.1**). There is an acetonitrile molecule present in the lattice but it is not coordinated [despite the known affinity of this solvent for Ag(I)]. Crystal data and a summary of data collection for [Ag**164**]$PF_6 \cdot CH_3CN$ as well as non-hydrogen bond lengths and bond angles are shown in **Appendix B**, **Tables B.40 – B.42**.

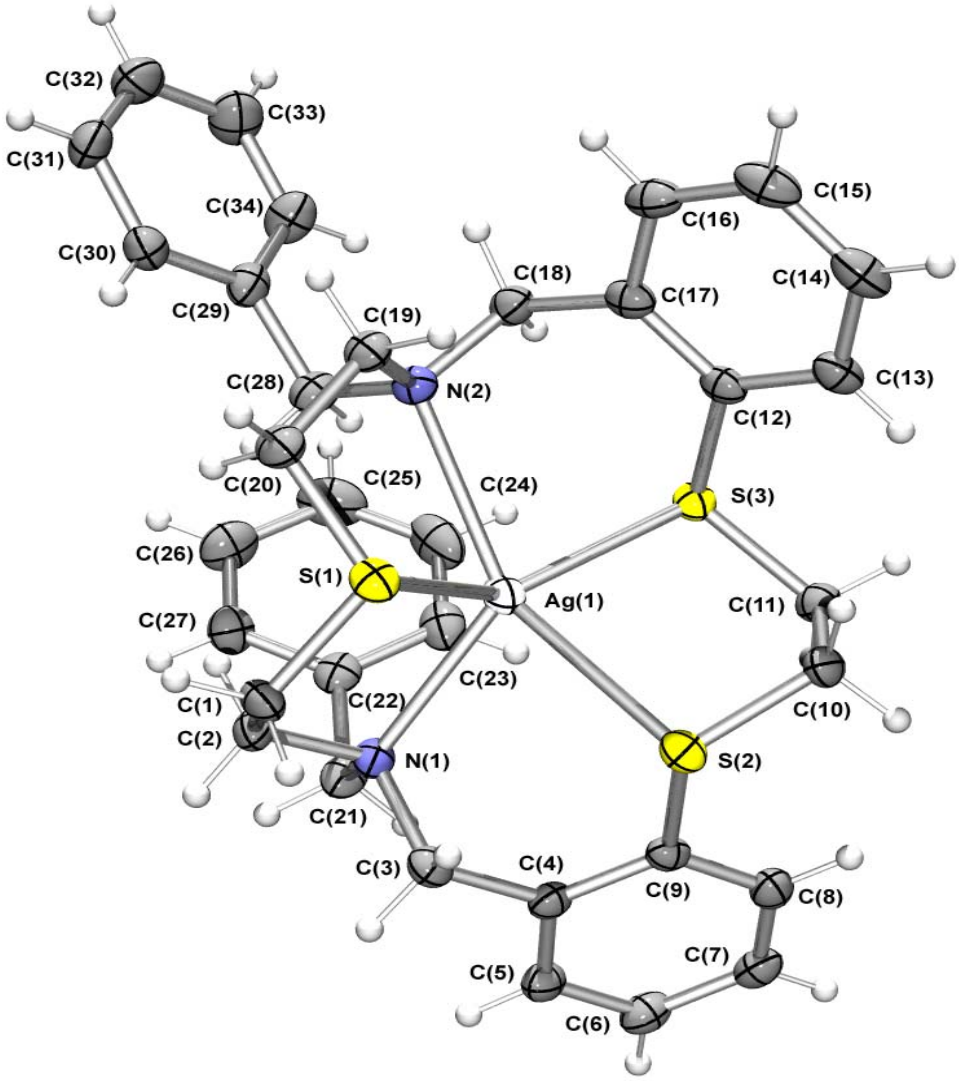

Figure 5.2 ORTEP plot of the $[Ag\mathbf{L}]^+$ cation in $[Ag\mathbf{L}]PF_6 \cdot MeCN$ (**L** = **164**) shown with 50 % probability ellipsoids. (Solvent and counter-ion omitted for clarity) Selected bond lengths (Å) and angles (˚): N(2)-Ag(1) 2.617(2), S(2)-Ag(1) 2.8307(9), N(1)-Ag(1) 2.387(2), S(1)-Ag(1) 2.5938(8), S(3)-Ag(1) 2.5097(8); N(1)-Ag(1)-S(3) 141.78(5), N(1)-Ag(1)-S(1) 82.22(6), S(3)-Ag(1)-S(1) 134.39(2), N(1)-Ag(1)-N(2) 122.22(7), S(3)-Ag(1)-N(2) 83.23(5), S(1)-Ag(1)-N(2) 77.20(5), N(1)-Ag(1)-S(2) 86.15(5), S(3)-Ag(1)-S(2) 83.17(2), S(1)-Ag(1)-S(2) 91.02(2), N(2)-Ag(1)-S(2) 146.53(5).

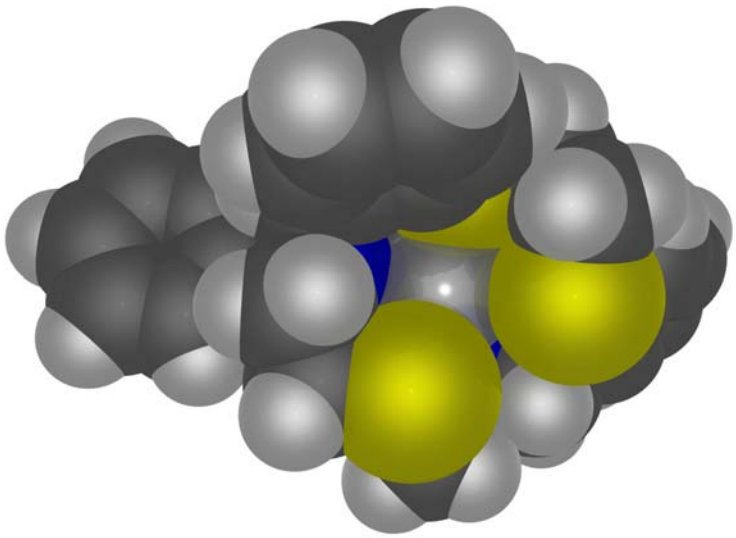

Figure 5.3 A space-filling representation of the X-ray structure of the complex cation in [Ag**L**]PF_6·MeCN (L = **164**) (view rotated 180° with respect to **Figure 5.2**); yellow atoms are sulfur, the blue atom is nitrogen.

5.2.4 Bulk membrane transport

Bulk membrane (water-chloroform-water) transport studies across a pH gradient were performed using a transport cell of the type shown schematically in **Figure 5.4**. The dibenzylated macrocycle **164** was employed as the ionophore; full details of the concentric cell apparatus have been published previously.[25] The aqueous source phase was buffered at pH 4.9 ± 0.1 and contained an equimolar solution of the nitrate salts of Co(II), Ni(II), Cu(II), Zn(II), Cd(II), Ag(I) and Pb(II), each at concentration of 1×10^{-2} M. The chloroform phase contained **164** at 1×10^{-3} M. The aqueous receiving phase was buffered at pH 3.0 ± 0.1 and the transport runs were terminated after 24 h; these conditions are identical to those employed previously in the author's laboratory for a previous study.[26]

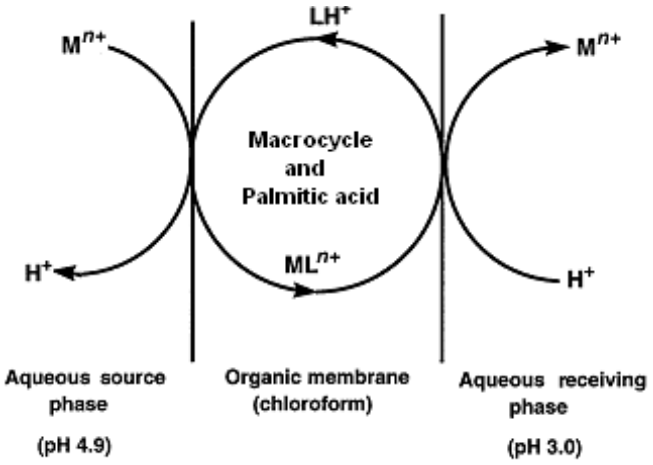

Figure 5.4 Schematic representation of the arrangement used for the transport of a metal ion across a chloroform membrane phase.[27]

Sole transport selectivity for Ag(I) into the aqueous receiving phase was observed under the conditions employed. That is, silver was transported with a flux corresponding to 137×10^{-7} moles per 24 hour while no transport of the other six metals present in the source phase was observed. Although theory dictates that stability and transport behaviour need not necessarily parallel each other, [26, 28, 29] this was nevertheless found to occur for the present system.

5.2.5 Final remarks

The design and synthesis of the macrocyclic ligand **164** was successfully carried out in the present investigation based on results from prior studies in the author's laboratory aimed at elucidating individual factors underlying Ag(I) discrimination. As anticipated, the new system **164** showed substantial discrimination for silver over the other six transition and post-transition metal ions investigated, both in its thermodynamic stability and transport behaviour. Apart from the possibility of employing **164** for the sensing or separation of silver, the study also serves to exemplify the use of a stepwise strategy for

rational ligand design leading, in this case, to significantly enhanced discrimination for silver.

5.3 Experimental

5.3.1 Synthesis of macrocycle precursors

Di(2-aminoethyl)sulfide was prepared as described in section **2.5.2**.

Synthesis of **165**

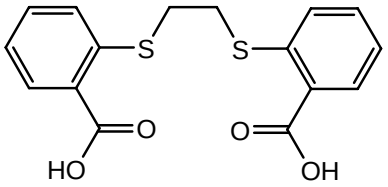

The diester **165** was prepared by the literature procedure.[17] Thiosalicylic acid (100 g, 0.65 mol) was dissolved in absolute EtOH (1000 ml) and concentrated H_2SO_4 (32 ml) added slowly with stirring. The mixture was refluxed overnight, then cooled to room temperature and following addition of $NaHCO_3$ (96 g, 1.2 mol) the mixture was re-heated and refluxed for a further 1 h. Dibromoethane (71.0 g, 0.38 mol) was added slowly dropwise with stirring and the reaction mixture was heated at reflux for a further 3 h. The mixture was cooled, poured into water (2 l) and extracted with chloroform (2 x 500 ml). Following filtration and evaporation of the chloroform, the crude solid was recrystallised from acetonitrile (yield 54.24 g, 50%). ^{1}H NMR ($CDCl_3$) δ 1.41, t, *J* 7.1 Hz, 6H, C**H**$_3$CH$_2$O; 3.22, s, 4H, SC**H**$_2$; 4.39, q, *J* 7.1 Hz, 4H, CH$_3$C**H**$_2$O; 7.20, brt, *J* 7.2 Hz, 2H, Ar; 7.29, brd, *J* 7.2 Hz, 2H, Ar; 7.44, brt, *J* 7.4 Hz, 2H, Ar; 7.98, dd, *J* 7.7, 1.7 Hz, 2H, Ar. ^{13}C NMR ($CDCl_3$) δ 14.3, 30.5, 61.2, 124.4, 125.7, 128.8, 131.3, 132.4, 139.8, 166.4.

Synthesis of **166**

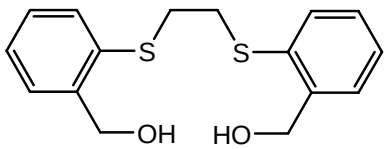

The diol **166** was prepared by a modification of the literature procedure.[17] The diester **165** (3.10 g, 0.008 mol) was dissolved in dry THF (100 ml) and $LiAlH_4$ (6.40 g, 0.016 mol) added in very small portions at 0 ˚C with vigorous stirring under nitrogen. The reaction mixture was allowed to stir overnight, then cooled in ice and the excess $LiAlH_4$ was quenched by successive

dropwise additions of water (3.10 ml), 10% NaOH (4.89 ml) and again water (4.89 ml). The mixture was stirred again overnight, filtered through celite and the precipitate washed several times with warm distilled acetone. Recrystallisation from $CHCl_3$ afforded the pure diol as a white crystalline solid (2.19 g, 90%) ^{1}H NMR ($CDCl_3$) δ 2.36, t, *J* 6.1 Hz, 2H, O**H**; 3.10, s, 4H, SC**H**$_2$; 4.77, d, *J* 6.0 Hz, 4H, C**H**$_2$OH; 7.23 – 7.43, m, 8H, Ar. ^{13}C NMR ($CDCl_3$) δ 33.7, 63.7, 127.4, 128.5, 128.8, 131.0, 133.1, 141.6.

Synthesis of **167**

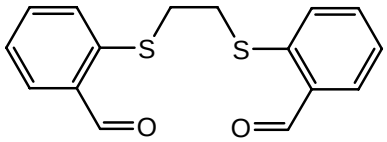

The dialdehyde **167** was prepared by the literature procedure.[17] Barium manganate (25.0 g, 0.10 mol) was added to a stirred solution of the diol **166** (2.0 g, 0.0065 mol) in dry DCM (50 ml). The reaction mixture was allowed to stir overnight, then filtered through a small amount of silica gel and the $BaMnO_4$ residue washed repeatedly with DCM. Evaporation of the combined filtrates yielded the product **167**, which was recrystallised from EtOH as a white crystalline solid (1.56 g, 80%). ^{1}H NMR ($CDCl_3$) δ 3.21, s, 4H, SC**H**$_2$; 7.35 – 7.39, m, 4H, Ar; 7.52, m, 2H, Ar; 7.87, dd, *J* 8.3, 2.2 Hz, 2H, Ar; 10.38, s, 2H, C**H**O. ^{13}C NMR ($CDCl_3$) δ 32.1, 126.2, 128.6, 132.4, 134.1, 134.5, 139.8, 191.4.

5.3.2 Synthesis of macrocycles

Synthesis of **113**

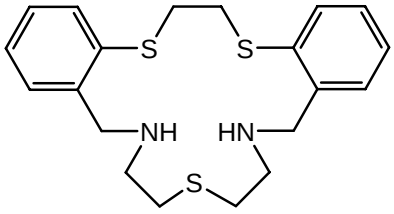

The S_3N_2 macrocycle **113** was prepared via a modification of the literature procedure.[17] Di(2-aminoethyl)sulfide (0.258 g, 0.002 mol) was dissolved in absolute ethanol (250 ml) and added dropwise over a period of 3 h to a solution dialdehyde **167** (0.610 g, 0.002 mol) in absolute ethanol (600 ml). The reaction mixture was refluxed for 3 h. Sodium borohydride (1.0 g, 0.025 mol) was added with minimum delay and refluxing continued for 12 h. The solvent was removed on a rotary evaporator and the resulting solid was dissolved in dichloromethane (50 ml) and 1M NaOH (15 ml) was added. The mixture was shaken, the organic layer was removed and the NaOH

solution was again extracted with dichloromethane (50 ml). The combined organic extracts were washed with saturated sodium chloride (20 ml), then taken to dryness on a rotary evaporator. The resulting white solid was recrystallised from acetonitrile (0.493 g, 63%). ^{1}H NMR ($CDCl_3$) δ 2.13, br s, 2H, N**H**; 2.73-2.77, m, 4H, SC**H**$_2$CH_2N; 2.84-2.88, m, 4H, SCH_2C**H**$_2$N; 3.23, s, 4H, SC**H**$_2$C**H**$_2$S; 3.87, s, 4H, ArC**H**$_2$; 7.18-7.34, m, 8H, Ar. ^{13}C NMR ($CDCl_3$) δ 32.9, 33.9, 48.2, 52.3, 126.9, 127.9, 130.6, 130.8, 134.2, 140.7. These data correspond to those reported previously for this compound.[17]

Synthesis of **164**

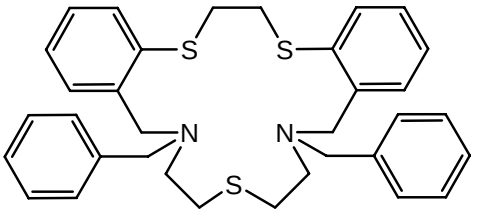

Sodium hydrogen carbonate (1.32 g, 0.016 mol) was added with stirring to a solution of **113** (0.350 g, 0.0008 mol) in acetonitrile (50 ml) and the mixture was heated to reflux. Benzyl bromide (0.306 g, 0.0018 mmol) in acetonitrile (75 ml) was added dropwise over 1.5 h. The reaction mixture was filtered and the filtrate was taken to dryness on a rotary evaporator. The solid that remained was partitioned between water (50 ml) and DCM (100 ml). The organic layer was separated and the water layer was washed with a further 2 x 50 ml of DCM. The combined organic fractions were backwashed with water (50 ml), dried over anhydrous sodium sulfate, filtered, and the solvent removed on a rotary evaporator. The resulting mixture was chromatographed using petroleum ether containing 10% diethyl ether, on petroleum ether pre-washed silica gel. The desired product **164** was recrystallised from acetone/methanol (1:1) containing small amounts of acetonitrile and dichloromethane (Yield, 0.326 g, 63.8%). (Found: C, 69.87; H, 6.18; N, 4.85%. $C_{34}H_{38}N_2S_3$ requires C, 69.48; H, 6.55; N, 4.73%). ^{1}H NMR ($CDCl_3$) δ 2.58-2.63, m, 4H, SCH_2C**H**$_2$N; 2.71-2.76, m, 4H, SC**H**$_2$CH_2N; 3.16, s, 4H, SC**H**$_2$C**H**$_2$S; 3.56, s, 4H, C_6H_5C**H**$_2$; 3.73, s, 4H, ArC**H**$_2$; 7.14-7.43, m, 18H, Ar. ^{13}C NMR ($CDCl_3$) δ 28.7, 33.9, 54.4, 57.0, 57.7, 126.1, 126.8, 127.4, 128.1, 128.6, 129.8, 130.0, 135.1, 139.3, 140.5. MS ESI (methanol): m/z = 571.2 $(M + H)^+$; when Ag(I) nitrate was added to the ligand sample the ESI (methanol/acetonitrile) spectrum also yielded a peak at m/z = 679.3 corresponding to $(M + Ag)^+$.

Synthesis of [Ag(**L**)]PF_6·0.5CH_3CN (**L** = **164**)

$AgPF_6$ (0.053 g, 0.00021 mol) in acetonitrile (4 ml) was added to **164** (0.118 g, 0.00021 mol) in dichloromethane (2 ml). Diethylether vapour was slowly diffused into this solution to yield needle-like crystals which were filtered off and washed with diethylether. These crystals were crushed and dried under vacuum before microanalysis (yield 0.143 g, 84%). M.p. 126-128 °C. MS (ESI): m/z = 679.3 $(M + Ag)^+$ (Found: C, 49.84; H, 4.98; N, 4.03%. $C_{34}H_{38}AgF_6N_2PS_3$·0.5CH_3CN requires C, 49.80; H, 4.72; N, 4.15%). ^{1}H NMR (CD_3CN) δ 2.63-2.69, m, 4H, SCH_2CH_2N**,** 2.95-3.00, m, 4H, SCH_2CH_2N, 3.36, s, 4H, SCH_2CH_2S; 3.66, s, 4H, $C_6H_5CH_2$; 3.70, s, 4H, $C_6H_4CH_2$; 7.19-7.50, m, 18H, Ar. ^{13}C NMR (CD_3CN) δ 27.16, 30.04, 51.24, 56.49, 57.76, 124.98, 125.92, 127.86, 128.40, 129.21, 130.24, 131.94, 133.42, 134.27, 135.77. Crystals of X-ray quality were obtained on slow evaporation of an acetonitrile solution of the above product.

X-ray structural data

Data for [Ag(**164**)]PF_6·0.5CH_3CN was collected with ω scans to approximately 56° 2θ using a Bruker SMART 1000 diffractometer employing graphite-monochromated Mo-K*a* radiation generated from a sealed tube (0.71073 Å) at 150(2) K [Bruker (1995), SMART, SAINT and XPREP. Bruker Analytical X-ray Instruments Inc., Madison, Wisconsin, USA]. Crystal data and a summary of data collection as well as non-hydrogen bond lengths and bond angles are given in **Appendix B**, **Tables B.40 – B.42**.

Potentiometric titration studies

These were undertaken as described in Chapter 3. The titration data corresponding to the lower portions of respective titration curves for the complexes of **164** refined satisfactorily assuming 1:1 metal to macrocycle complexation. Data were processed using a local version of MINIQUAD.[30]

Membrane transport

All aqueous solutions were prepared using deionised water. The chloroform used for the membrane phase was presaturated with water by shaking a two-phase water–chloroform

mixture then removing the aqueous phase. The transport experiments employed a ‘concentric cell’ in which the aqueous source phase (10 ml) and receiving phase (30 ml) were separated by a chloroform phase (50 ml). For each experiment both aqueous phases and the chloroform phase were stirred separately at 10 rpm by means of a coupled single (geared) synchronous motor; the cell was enclosed by a water jacket and thermostatted at 25 ˚C. The aqueous source phase consisted of a buffer (sodium acetate–acetic acid) solution at pH 4.9 ± 0.1 containing an equimolar mixture of nitrate salts of the seven metal ions, each at a concentration of 10^{-2} M. The chloroform phase contained the ionophore **164** at 10^{-3} M. The aqueous receiving phase consisted of a buffer (sodium formate–formic acid) solution at pH 3.0 ± 0.1. All transport runs were terminated after 24 hours and atomic absorption spectroscopy was used to determine the amount of each metal ion transported over this period; the respective receiving phases were analysed (using a Varian Spectra AA-800 spectrometer) at the completion of each transport run. The transport result is quoted as the average value obtained from duplicate runs; transport flux (*J* values) is in mol/24 h and represents mean values measured over 24 h. *J* values equal to or less than 20×10^{-7} mol/24 h are within experimental error of zero and were ignored in the analysis of the results. Silver was transported with a flux corresponding to 137×10^{-7} moles per 24 hour. No transport of the other six metals present in the source phase was observed.

5.4 References

1. I. M. Atkinson, J. D. Chartres, G. W. Everett, X.-K. Ji, L. F. Lindoy, O. A. Matthews, G. V. Meehan, B. W. Skelton, G. Wei and A. H. White, *J. Chem. Soc., Dalton Trans.*, 2000, 1191 and references therein.
2. R. R. Fenton, R. Gauci, P. C. Junk, L. F. Lindoy, R. C. Luckay, G. V. Meehan, J. R. Price, P. Turner and G. Wei, *J. Chem. Soc., Dalton Trans.*, 2002, 2185.
3. J. D. Chartres, M. S. Davies, L. F. Lindoy, G. V. Meehan and G. Wei, *Inorg. Chem. Commun.*, 2006, **9**, 751, and references therein.
4. K. R. Adam, D. S. Baldwin, P. A. Duckworth, L. F. Lindoy, M. McPartlin, A. Bashall, H. R. Powell and P. A. Tasker, *J. Chem. Soc., Dalton Trans.*, 1995, 1127.
5. K. R. Adam, D. S. Baldwin, P. A. Duckworth, A. J. Leong, L. F. Lindoy, M. McPartlin and P. A. Tasker, *J. Chem. Soc., Chem. Commun.*, 1987, 1124.
6. R. G. Pearson, *J. Am. Chem. Soc.*, 1963, **85**, 3533.
7. R. G. Pearson, *Coord. Chem. Rev.*, 1990, **100**, 403.
8. U. Kallert and R. Mattes, *Inorg. Chim. Acta*, 1991, **180**, 263.
9. U. Kallert and R. Mattes, *Polyhedron*, 1992, **11**, 617.
10. J. R. Price, M. Fainerman-Melnikova, R. R. Fenton, K. Gloe, L. F. Lindoy, T. Rambusch, B. W. Skelton, P. Turner, A. H. White and K. Wichmann, *Dalton Trans.*, 2004, 3715 and references therein.
11. L. F. Lindoy, *Pure Appl. Chem.*, 1997, **69**, 2179.
12. T. W. Hambley, L. F. Lindoy, J. R. Reimers, P. Turner, G. Wei and N. Widmer-Cooper, *J. Chem. Soc., Dalton Trans.*, 2001, 614.
13. J. Kim, T.-H. Ahn, M. Lee, A. J. Leong, L. F. Lindoy, B. R. Rumbel, B. W. Skelton, T. Strixner, G. Wei and A. H. White, *J. Chem. Soc., Dalton Trans.*, 2002, 3993.
14. Y. Dong, S. Farquhar, K. Gloe, L. F. Lindoy, B. R. Rumbel, P. Turner and K. Wichmann, *Dalton Trans.*, 2003, 1558.
15. H. Tsukube, K. Tagaki, T. Higashiyama, T. Iwachido and N. Hayama, *J. Chem. Soc., Perkin Trans. 1*, 1986, 1033.
16. H. Tsukube, K. Yamashita, T. Iwachido and M. Zenki, *J. Chem. Soc., Perkin Trans. 1*, 1991, 1661.

17. D. S. Baldwin, P. A. Duckworth, G. R. Erickson, L. F. Lindoy, M. McPartlin, G. M. Mockler, W. E. Moody and P. A. Tasker, *Aust. J. Chem.*, 1987, **40**, 1861.
18. L. F. Lindoy and D. H. Busch, *J. Am. Chem. Soc.*, 1969, **91**, 4690.
19. L. F. Lindoy and R. J. Smith, *Inorg. Chem.*, 1981, **20**, 1314.
20. K. R. Adam, M. Antolovich, D. S. Baldwin, L. G. Brigden, P. A. Duckworth, L. F. Lindoy, A. Bashall, M. McPartlin and P. A. Tasker, *J. Chem. Soc., Dalton Trans.*, 1992, 1869.
21. K. R. Adam, D. S. Baldwin, L. F. Lindoy, G. V. Meehan, I. M. Vasilescu and G. Wei, *Inorg. Chim. Acta*, 2003, **352**, 46.
22. M. Feinerman-Melnikova, A. Nezhadali, G. Rounaghi, J. C. McMurtrie, J. Kim, K. Gloe, M. Langer, S. S. Lee, L. F. Lindoy, T. Nishimura, K.-M. Park and J. Seo, *Dalton Trans.*, 2004, 122.
23. N. Navon, G. Golub, H. Cohen, P. Paoletti, B. Valtancoli, A. Bencini and D. Meyerstein, *Inorg. Chem.*, 1999, **38**, 3484.
24. T. Clark, M. Hennemann, R. van Eldick and D. Meyerstein, *Inorg. Chem.*, 2002, **41**, 2927, and references therein.
25. P. S. K. Chia, L. F. Lindoy, G. W. Walker and G. W. Everett, *Pure Appl. Chem.*, 1993, **65**, 521.
26. S. S. Lee, I. Yoon, K.-M. Park, J. H. Jung, L. F. Lindoy, A. Nezhadali and G. Rounaghi, *J. Chem. Soc., Dalton Trans.*, 2002, 2180.
27. J. Kim, A. J. Leong, L. F. Lindoy, J. Kim, J. Nachbaur, A. Nezhadali, G. Rounaghi and G. Wei, *J. Chem. Soc., Dalton Trans.*, 2000, 3453.
28. J. S. Bradshaw, G. E. Maas, J. D. Lamb, R. M. Izatt and J. J. Christensen, *J. Am. Chem. Soc.*, 1980, **102**, 467.
29. J. D. Goddard, *J. Phys. Chem.*, 1985, **89**, 1825.
30. P. Gans, A. Sabatini and A. Vacca, *Inorg. Chim. Acta*, 1976, **18**, 237.

Appendix A

Example NMR Spectra

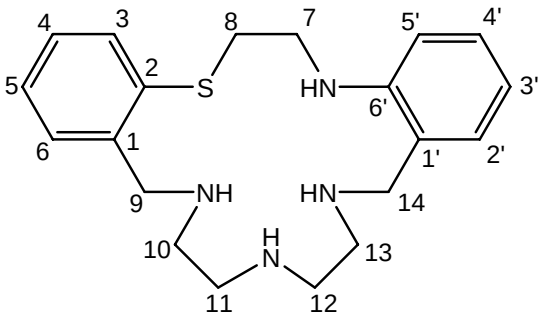

132

Figure A.1 Non-systematic numbering scheme for macrocycle **132**.

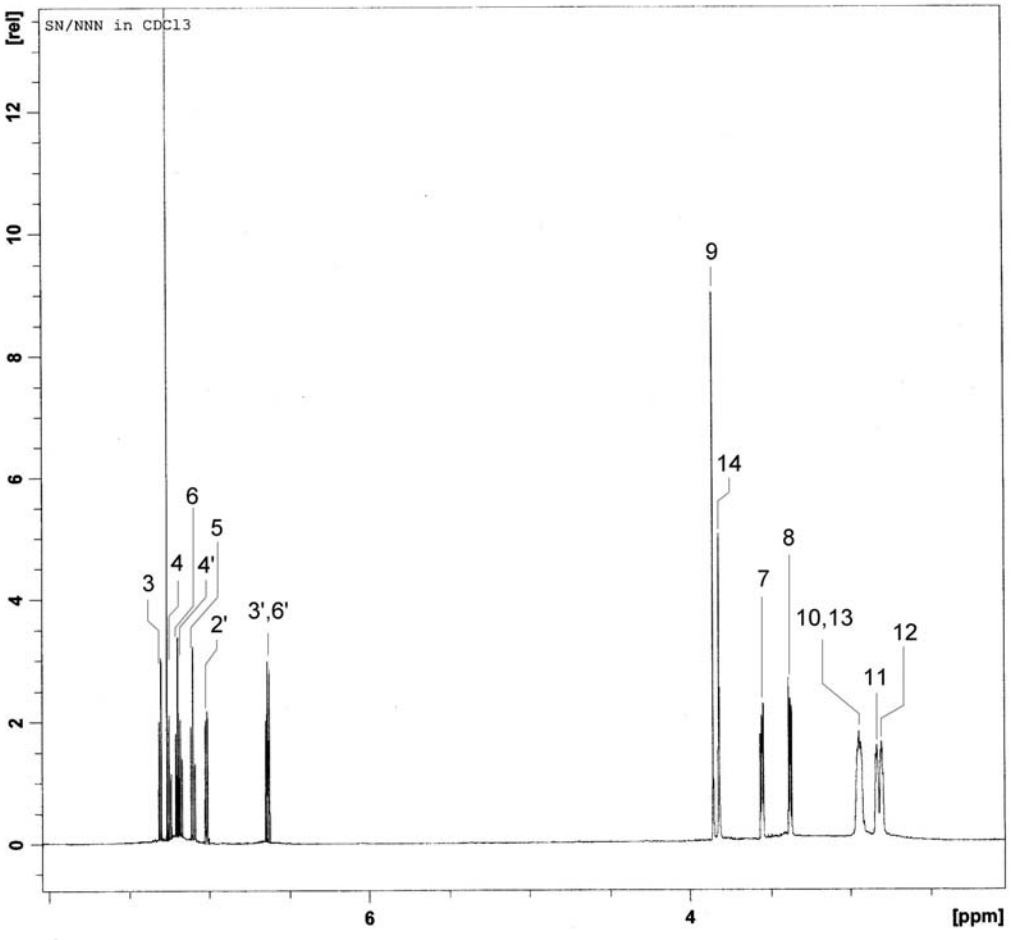

Figure A.2 The ^{1}H NMR spectrum assignments of **132** (SN/NNN) in $CDCl_3$.

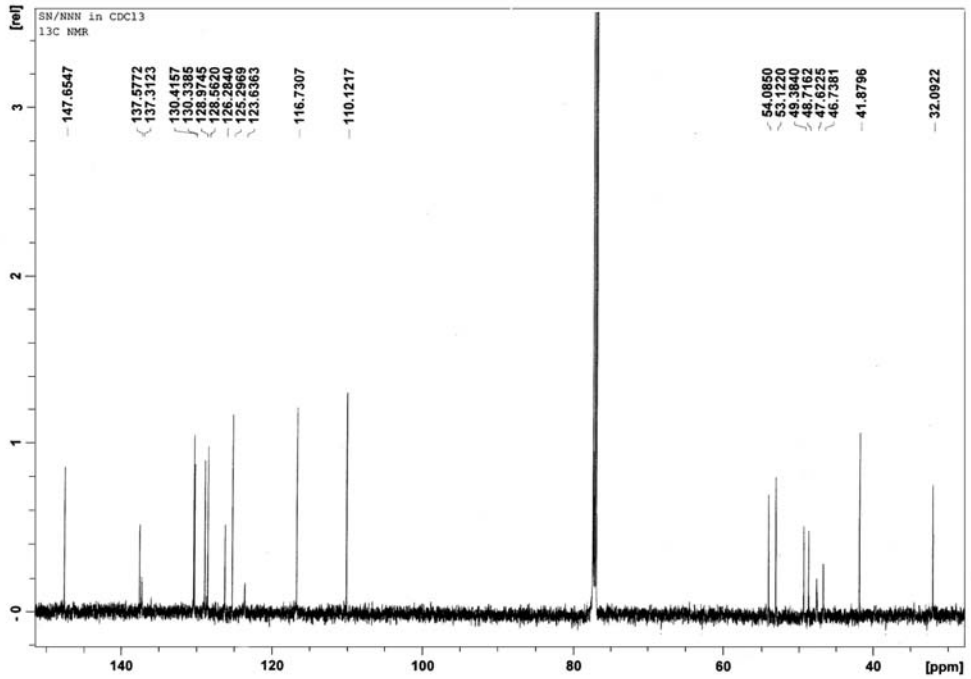

Figure A.3 The ^{13}C NMR spectrum of **132** (SN/NNN) in $CDCl_3$.

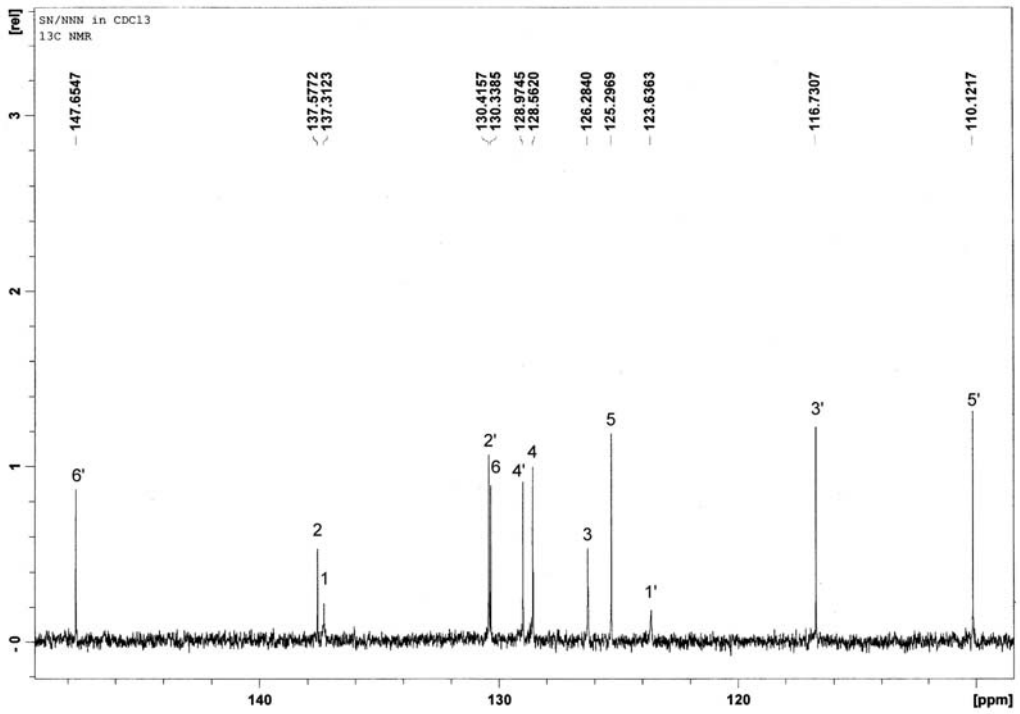

Figure A.4 The ^{13}C NMR spectrum assignments of the aromatic region of **132** (SN/NNN) in $CDCl_3$.

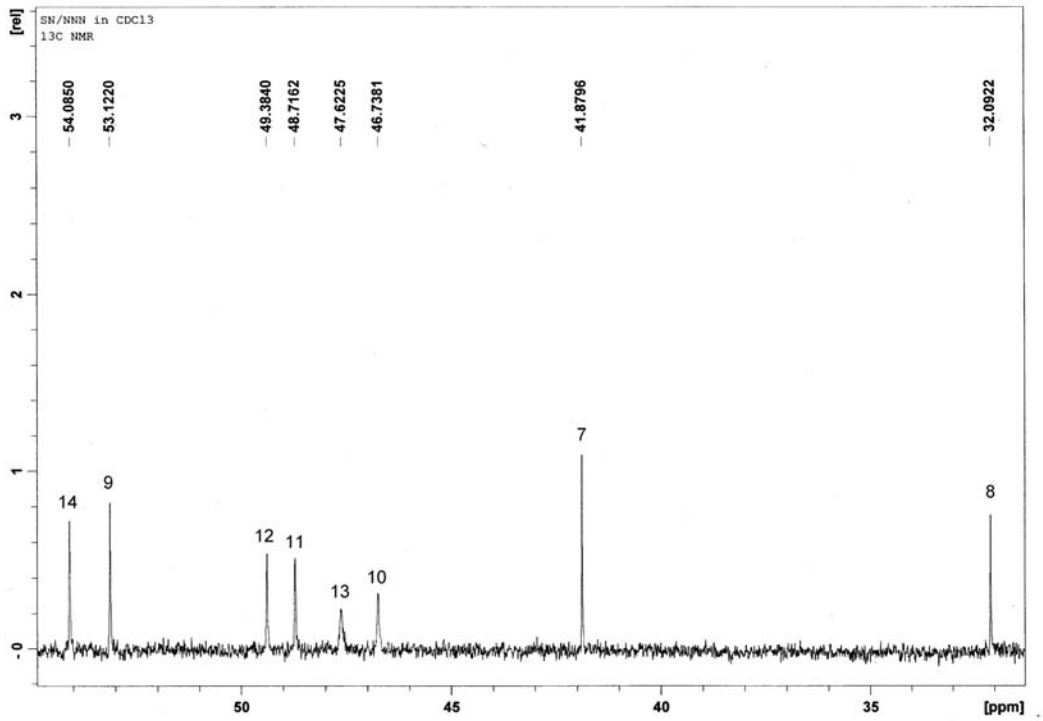

Figure A.5 The ^{13}C NMR spectrum assignments of the aliphatic region of **132** (SN/NNN) in $CDCl_3$.

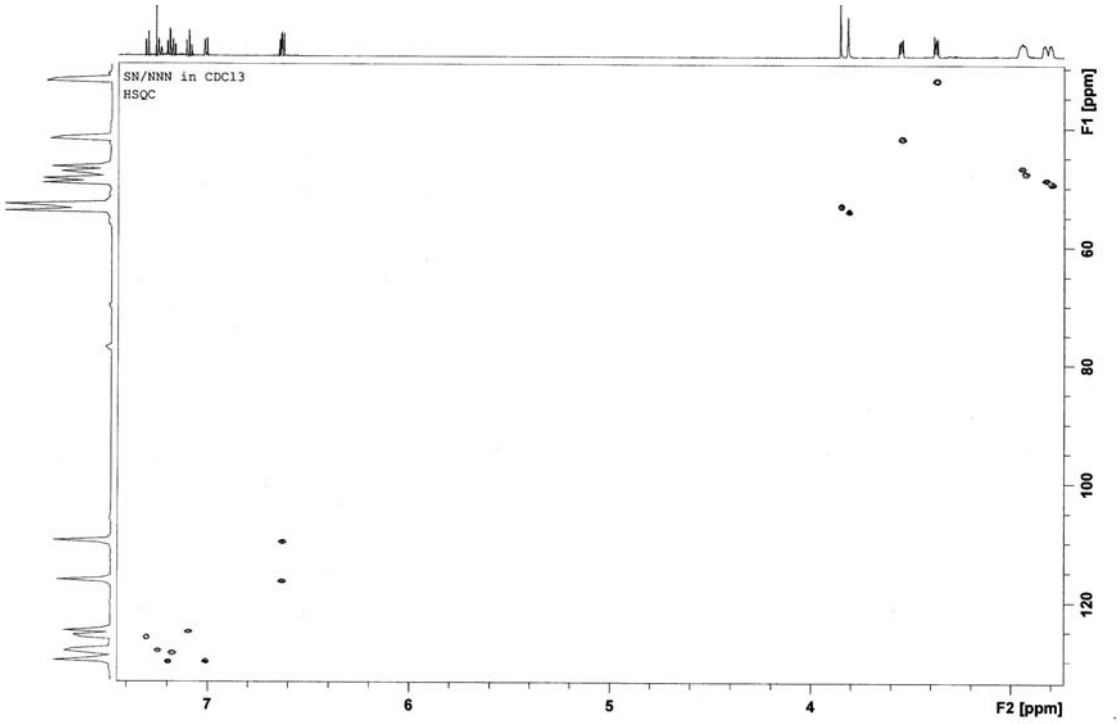

Figure A.6 The HSQC (J = 140 Hz) spectrum of **132** (SN/NNN) in $CDCl_3$.

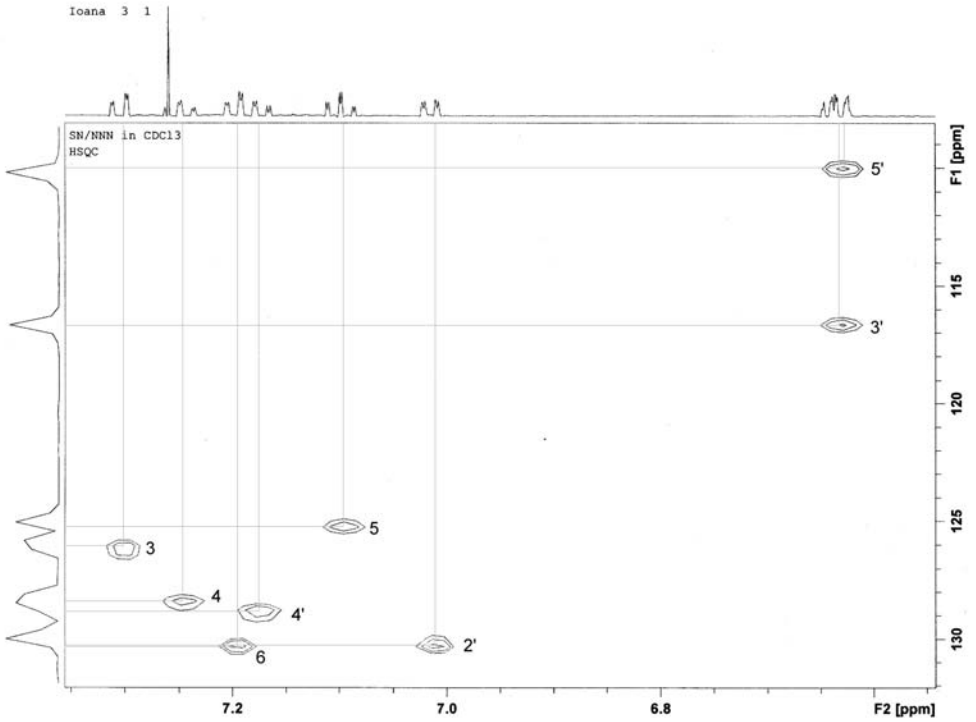

Figure A.7 The aromatic region of the HSQC (J = 140 Hz) spectrum of **132** (SN/NNN) in $CDCl_3$ highlighting ^{1}H – ^{13}C correlations.

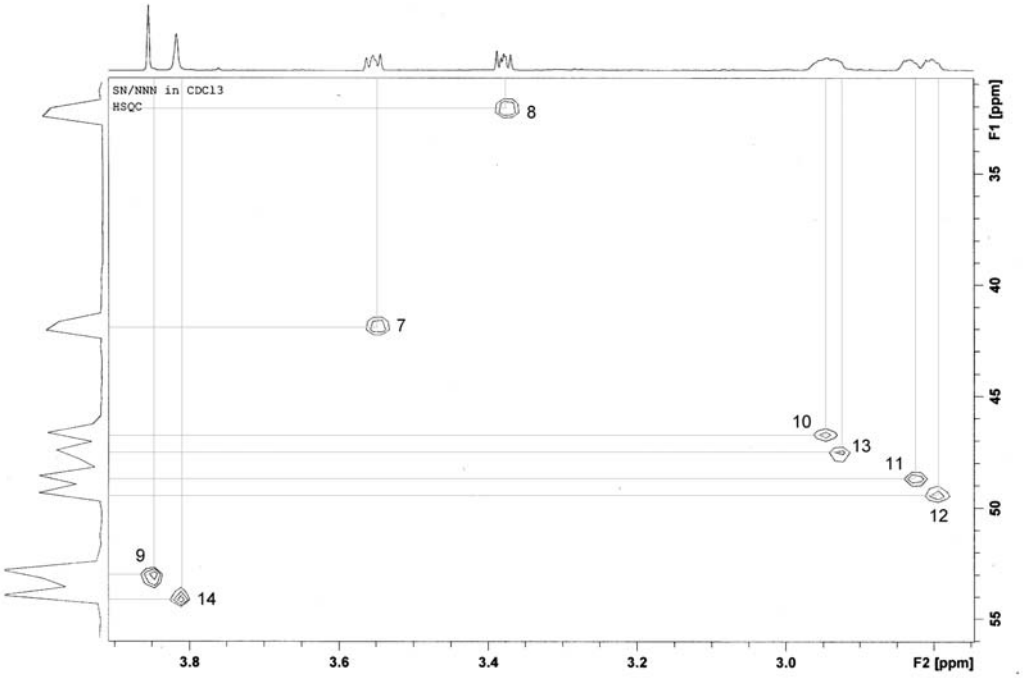

Figure A.8 The aliphatic region of the HSQC (J = 140 Hz) spectrum of **132** (SN/NNN) in $CDCl_3$ highlighting ^{1}H – ^{13}C correlations.

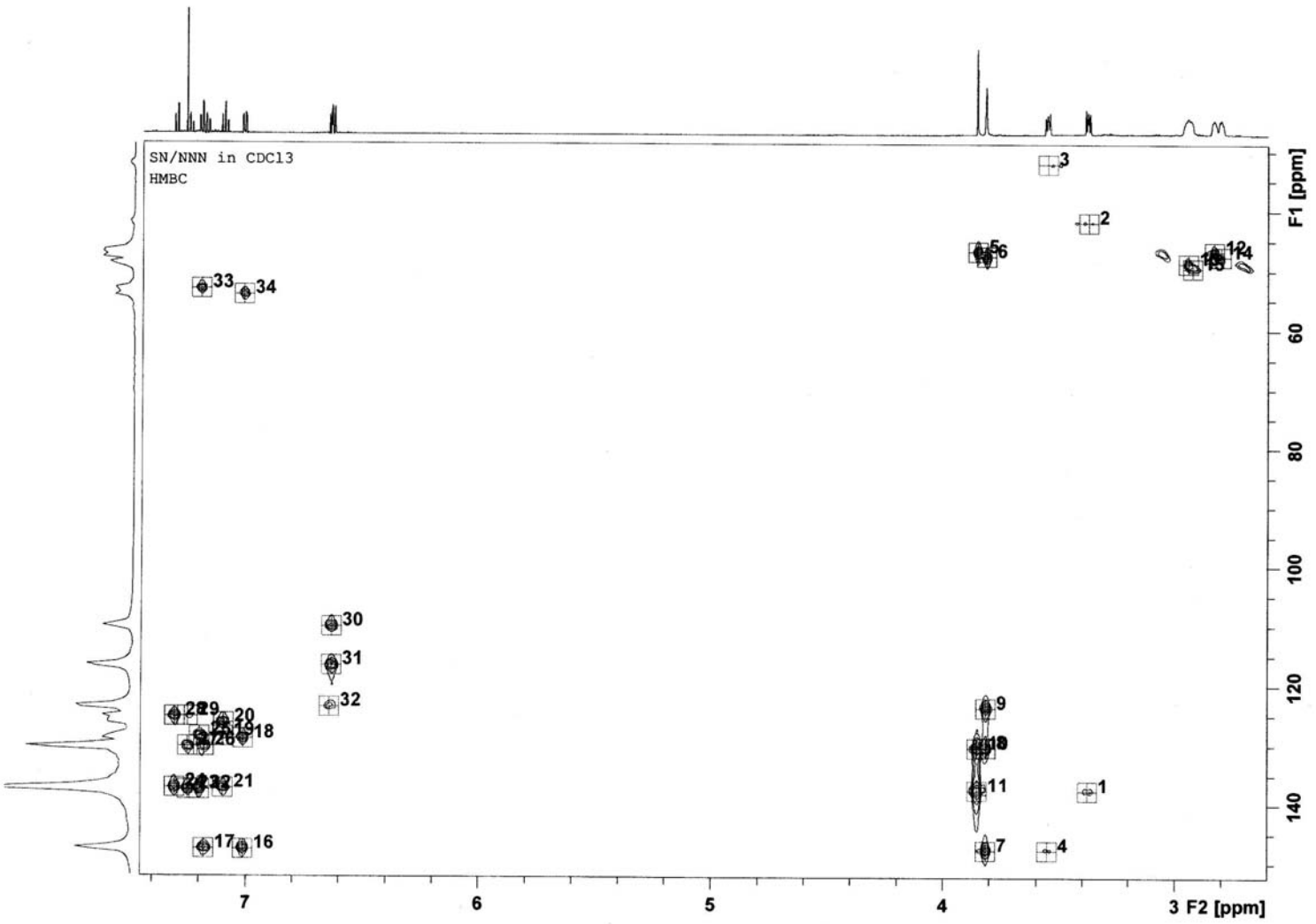

Figure A.9 The HMBC (J = 8 Hz) spectrum of **132** (SN/NNN) in $CDCl_3$ highlighting long range $^{1}H - ^{13}C$ correlations; to be used in conjunction with **Figure A.10**

Figure A.10 HMBC (J = 8 Hz) correlations for **132** (SN/NNN) relating to the HMBC contour map shown in **Figure A.9**

Peak	ν(F2) [ppm]	ν(F1) [ppm]	Intensity [abs]	Annotation
24	7.3045	137.2538	95020354.00	
28	7.3045	125.2043	82375548.00	
29	7.2487	125.2232	14046240.00	
27	7.2484	130.2919	61065978.00	
23	7.2475	137.5507	75372503.00	
22	7.1990	137.5507	103582776.00	
25	7.1990	128.5455	66641268.00	
33	7.1986	53.0827	52897930.00	
26	7.1791	130.2919	66108031.00	
17	7.1790	147.5453	79111644.00	
19	7.0986	128.5455	20977072.00	
21	7.0986	137.3033	67954712.00	
20	7.0980	126.2695	66976352.00	
34	7.0157	54.0875	53300558.00	
16	7.0142	147.6443	96770913.00	
18	7.0142	128.9908	82223347.00	
32	6.6416	123.5310	24689399.00	
30	6.6334	110.0575	83125287.00	
31	6.6331	116.6142	122005298.00	
5	3.8550	46.7218	46435349.50	
10	3.8548	130.3691	139186824.50	
11	3.8548	137.4310	355919881.00	
8	3.8176	130.2463	77278934.00	
7	3.8175	147.6248	72449132.00	
9	3.8175	123.6142	75818104.50	
6	3.8174	47.5341	43095512.00	
3	3.5530	32.0691	1342477.50	
4	3.5527	147.6502	4991680.50	
1	3.3787	137.5449	6276774.50	
2	3.3781	41.8501	1713864.00	
13	2.9453	48.6895	67303452.00	
15	2.9266	49.4562	24910544.00	
12	2.8334	46.7078	57196617.00	
14	2.8053	47.5323	29108402.00	

Appendix B

X-ray Crystallography

Part 1. X-ray data for the free macrocycles

Table B.1 Crystal data and a summary of data collection for **132** and **138**.

Compound	**132** (SN/NNN)	**138** (ON/NNN)
Mol. Formula	$C_{20}H_{28}N_4S$	$C_{20}H_{28}N_4O$
Mol. Wt.	356.52	340.46
T , K	296	296
Space group	$P\bar{1}$	$P\bar{1}$
a, Å	9.0948(9)	8.8072(13)
b, Å	11.124(2)	11.3487(11)
c, Å	11.884(3)	11.8399(15)
α, deg	117.427(11)	118.405(13)
β, deg	110.050(2)	109.825(10)
γ, deg	93.620(3)	90.588(10)
V, Å^3	966.6(3)	957.9(2)
Z	2	2
D_c, g cm^{-3}	1.225	1.180
μ, mm^{-1}	0.178	0.075
$T_{max,min}$	0.9645, 0.9570	0.9926, 0.9635
Dimensions, mm	0.25 x 0.20 x 0.20	0.5 x 0.2 x 0.1
F(000)	348	368
radiation	Mo Kα	Mo Kα
θ range, deg	2.09-24.96	2.09-24.96
N_{coll}	3630	3607
N_{obs}	3395	3364
N_{var}	242	242
Sigma cutoff	I>2σ(I)	I>2σ(I)
R	0.064	0.056
R_w	0.181	0.129

Table B.2 Selected bond lengths (Å) for **132** and **138**.

132(SN/NNN)		**138**(ON/NNN)	
S(1)-C(2a)	1.760(4)	O(1)-C(2a)	1.376(4)
S(1)-C(1a)	1.802(3)	O(1)-C(1a)	1.437(4)
N(1)-C(8a)	1.457(5)	N(1)-C(8a)	1.451(5)
N(1)-C(9a)	1.449(5)	N(1)-C(9a)	1.456(5)
N(2)-C(8b)	1.464(5)	N(2)-C(8b)	1.454(5)
N(2)-C(9b)	1.443(5)	N(2)-C(9b)	1.450(5)
N(3)-C(10a)	1.462(5)	N(3)-C(10a)	1.455(5)
N(3)-C(10b)	1.450(5)	N(3)-C(10b)	1.443(5)

N(4)-C(1b)	1.445(5)	N(4)-C(1b)	1.443(5)
N(4)-C(2b)	1.384(4)	N(4)-C(2b)	1.380(4)
C(1a)-C(1b)	1.515(5)	C(1a)-C(1b)	1.493(5)
C(7a)-C(8a)	1.493(5)	C(7a)-C(8a)	1.487(5)
C(9a)-C(10a)	1.502(6)	C(9a)-C(10a)	1.501(6)
C(7b)-C(8b)	1.506(5)	C(7b)-C(8b)	1.495(5)
C(9b)-C(10b)	1.513(6)	C(9b)-C(10b)	1.495(5)

Table B.3 Selected bond angles (º) for **132** and **138**.

132(SN/NNN)		**138**(ON/NNN)	
C(2a)-S(1)-C(1a)	103.31(17)	C(2a)-O(1)-C(1a)	117.1(3)
C(1b)-C(1a)-S(1)	109.7(2)	O(1)-C(1a)-C(1b)	109.3(3)
C(3a)-C(2a)-S(1)	122.8(3)	O(1)-C(2a)-C(3a)	123.0(4)
C(7a)-C(2a)-S(1)	117.7(3)	O(1)-C(2a)-C(7a)	115.6(3)
C(9a)-N(1)-C(8a)	111.6(3)	C(8a)-N(1)-C(9a)	111.6(3)
C(9b)-N(2)-C(8b)	113.7(3)	C(9b)-N(2)-C(8b)	113.1(3)
C(10b)-N(3)-C(10a)	115.0(3)	C(10a)-N(3)-C(10b)	115.4(4)
C(2b)-N(4)-C(1b)	120.5(3)	C(2b)-N(4)-C(1b)	120.4(3)
N(1)-C(8a)-C(7a)	112.3(3)	N(1)-C(8a)-C(7a)	112.0(3)
N(1)-C(9a)-C(10a)	112.3(3)	N(1)-C(9a)-C(10a)	111.9(4)
N(3)-C(10a)-C(9a)	112.1(3)	N(3)-C(10a)-C(9a)	111.5(4)
N(3)-C(10b)-C(9b)	110.6(3)	N(3)-C(10b)-C(9b)	111.5(3)
N(2)-C(8b)-C(7b)	112.7(3)	N(2)-C(8b)-C(7b)	112.4(3)
N(2)-C(9b)-C(10b)	111.0(3)	N(2)-C(9b)-C(10b)	111.3(3)
N(4)-C(1b)-C(1a)	110.6(3)	N(4)-C(1b)-C(1a)	111.6(3)
N(4)-C(2b)-C(3b)	123.6(3)	N(4)-C(2b)-C(3b)	123.3(3)
N(4)-C(2b)-C(7b)	117.8(3)	N(4)-C(2b)-C(7b)	118.3(3)
C(6a)-C(7a)-C(8a)	120.3(4)	C(6a)-C(7a)-C(8a)	119.5(4)
C(2a)-C(7a)-C(8a)	121.7(3)	C(2a)-C(7a)-C(8a)	122.5(3)
C(6b)-C(7b)-C(8b)	120.7(3)	C(6b)-C(7b)-C(8b)	121.8(3)
C(2b)-C(7b)-C(8b)	120.5(3)	C(2b)-C(7b)-C(8b)	119.3(3)

Table B.4 Crystal data and a summary of data collection for **136** (SN/NON).

Formula of the Refinement Model	$C_{20}H_{27}N_3OS$
Model Molecular Weight	357.51
Crystal System	triclinic
Space Group	$P\ \bar{1}$(#2)
a	8.9772(8) Å
b	11.2223(8) Å
c	11.6609(15) Å
α	116.367(8)º
β	110.079(9)º
γ	94.316(6)º
V	951.70(20) $Å^3$
D_c	1.248 g cm^{-3}
Z	2
Crystal Size	0.280x0.120x0.110 mm
Crystal Colour	colourless
Crystal Habit	shard
Temperature	150(2) Kelvin
λ(MoKα)	0.71073 Å
μ(MoKα)	0.183 mm^{-1}
T(SADABS)$_{min,max}$	0.826, 0.980
$2\theta_{max}$	66.32º
hkl range	-13 13, -17 17, -17 17
N	45310
N_{ind}	7186(R_{merge} 0.0720)
N_{obs}	5719(I > 2σ(I))
N_{var}	235
Residuals* *R*1(*F*), *wR*2(F^2)	0.0539, 0.1234
GoF(all)	1.054
Residual Extrema	-0.375, 0.489 e^- $Å^{-3}$

*$R1 = \Sigma||F_o| - |F_c||/\Sigma|F_o|$ for $F_o > 2\sigma(F_o)$; $wR2 = (\Sigma w(F_o^2 - F_c^2)^2/\Sigma(wF_c^2)^2)^{1/2}$ all reflections

$w=1/[\sigma^2(F_o^2)+(0.0466P)^2+0.3262P]$ where $P=(F_o^2+2F_c^2)/3$

Table B.5 Non-hydrogen bond lengths (Å) for **136** (SN/NON).

C(1)-N(3)	1.3863(15)	C(1)-C(6)	1.4077(17)
C(1)-C(2)	1.4233(17)	C(2)-C(3)	1.3905(17)
C(2)-C(7)	1.5170(17)	C(3)-C(4)	1.3960(19)
C(4)-C(5)	1.3897(19)	C(5)-C(6)	1.3955(17)
C(7)-N(1)	1.4662(15)	C(8)-N(1)	1.4602(16)
C(8)-C(9)	1.5134(19)	C(9)-O(1)	1.4255(16)
C(10)-O(1)	1.4265(15)	C(10)-C(11)	1.519(2)
C(11)-N(2)	1.4648(16)	C(12-N(2)	1.4696(17)
C(12)-C(13)	1.5072(19)	C(13)-C(18)	1.3956(18)
C(13)-C(14)	1.4136(17)	C(14)-C(15)	1.4009(17)
C(14)-S(1)	1.7739(12)	C(15)-C(16)	1.3925(18)
C(16)-C(17)	1.382(2)	C(17)-C(18)	1.393(2)
C(19)-C(20)	1.5233(16)	C(19)-S(1)	1.8174(11)
C(20)-N(3)	1.4529(15)		

Symmetry Operators
(1) x, y, z (2) -x, -y, -z

Table B.6 Non-hydrogen bond angles (º) for **136** (SN/NON).

N(3)	C(1)	C(6)	122.79(11)
N(3)	C(1)	C(2)	118.46(11)
C(6)	C(1)	C(2)	118.71(11)
C(3)	C(2)	C(1)	119.10(11)
C(3)	C(2)	C(7)	120.79(11)
C(1)	C(2)	C(7)	120.08(10)
C(2)	C(3)	C(4)	122.04(12)
C(5)	C(4)	C(3)	118.74(11)
C(4)	C(5)	C(6)	120.81(11)
C(5)	C(6)	C(1)	120.59(11)
N(1)	C(7)	C(2)	113.02(10)
N(1)	C(8)	C(9)	109.76(11)
O(1)	C(9)	C(8)	107.61(10)
O(1)	C(10)	C(11)	113.66(10)
N(2)	C(11)	C(10)	111.16(10)
N(2)	C(12)	C(13)	111.74(10)
C(18)	C(13)	C(14)	118.38(12)
C(18)	C(13)	C(12)	120.16(12)
C(14)	C(13)	C(12)	121.45(11)
C(15)	C(14)	C(13)	119.82(11)

C(15)	C(14)	S(1)	122.63(9)
C(13)	C(14)	S(1)	117.55(10)
C(16)	C(15)	C(14)	120.21(13)
C(17)	C(16)	C(15)	120.51(14)
C(16)	C(17)	C(18)	119.42(13)
C(17)	C(18)	C(13)	121.66(13)
C(20)	C(19)	S(1)	109.67(8)
N(3)	C(20)	C(19)	110.79(10)
C(8)	N(1)	C(7)	113.52(10)
C(11)	N(2)	C(12)	111.54(10)
C(1)	N(3)	C(20)	120.67(10)
C(9)	O(1)	C(10)	114.26(10)
C(14)	S(1)	C(19)	102.86(6)

Symmetry Operators

(1) x, y, z (2) -x, -y, -z

Table B.7 Crystal data and summary of data collection for **137** (SN/NSN).

Formula of the Refinement Model	$C_{20}H_{27}N_3S_2$
Model Molecular Weight	373.57
Crystal System	triclinic
Space Group	$P\ \bar{1}$(#2)
a	9.4397(12) Å
b	10.8410(14) Å
c	11.552(2) Å
α	104.996(13)º
β	104.979(13)º
γ	111.385(9)º
V	978.1(3) $Å^3$
D_c	1.268 g cm^{-3}
Z	2
Crystal Size	0.170x0.090x0.07 mm
Crystal Colour	colourless
Crystal Habit	shard
Temperature	150(2) Kelvin
λ(MoKα)	0.71073 Å
μ(MoKα)	0.280 mm^{-1}
T(SADABS)$_{min,max}$	0.799, 0.981
$2\theta_{max}$	56.66º

hkl range	-12 12, -14 14, -15 15
N	45395
N_{ind}	4854(R_{merge} 0.0872)
N_{obs}	4082(I > 2σ(I))
N_{var}	235
Residuals* *R*1(*F*), *wR*2(F^2)	0.0644, 0.1274
GoF(all)	1.178
Residual Extrema	-0.289, 0.458 e^- $Å^{-3}$

*$R1 = \Sigma||F_o| - |F_c||/\Sigma|F_o|$ for $F_o > 2\sigma(F_o)$; $wR2 = (\Sigma w(F_o^2 - F_c^2)^2/\Sigma(wF_c^2)^2)^{1/2}$ all reflections

$w=1/[\sigma^2(F_o^2)+(0.0353P)^2+0.7706P]$ where $P=(F_o^2+2F_c^2)/3$

Table B.8 Non-hydrogen bond lengths (Å) for **137** (SN/NSN).

atom	atom	Distance	atom	atom	Distance
C(1)	C(6)	1.406(3)	C(1)	C(2)	1.407(3)
C(1)	S(2)	1.776(2)	C(2)	C(3)	1.397(3)
C(2)	C(7)	1.511(3)	C(3)	C(4)	1.392(3)
C(4)	C(5)	1.385(4)	C(5)	C(6)	1.391(3)
C(7)	N(1)	1.466(3)	C(8)	N(1)	1.459(3)
C(8)	C(9)	1.516(3)	C(9)	S(1)	1.830(2)
C(10)	C(11)	1.519(4)	C(10)	S(1)	1.821(2)
C(11)	N(2)	1.471(3)	C(12)	N(2)	1.475(3)
C(12)	C(13)	1.513(3)	C(13)	C(18)	1.394(3)
C(13)	C(14)	1.418(3)	C(14)	N(3)	1.385(3)
C(14)	C(15)	1.412(3)	C(15)	C(16)	1.395(3)
C(16)	C(17)	1.380(3)	C(17)	C(18)	1.396(3)
C(19)	N(3)	1.453(3)	C(19)	C(20)	1.523(3)
C(20)	S(2)	1.817(2)			

Symmetry Operators

(1) x, y, z (2) -x, -y, -z

Table B.9 Non-hydrogen bond angles (º) for **137** (SN/NSN).

atom	atom	atom	angle
C(6)	C(1)	C(2)	119.7(2)
C(6)	C(1)	S(2)	122.76(18)
C(2)	C(1)	S(2)	117.57(16)
C(3)	C(2)	C(1)	118.9(2)
C(3)	C(2)	C(7)	120.1(2)
C(1)	C(2)	C(7)	121.0(2)
C(4)	C(3)	C(2)	121.4(2)
C(5)	C(4)	C(3)	119.4(2)
C(4)	C(5)	C(6)	120.6(2)
C(5)	C(6)	C(1)	120.1(2)
N(1)	C(7)	C(2)	111.00(18)
N(1)	C(8)	C(9)	110.18(19)
C(8)	C(9)	S(1)	113.57(17)
C(11)	C(10)	S(1)	110.27(16)
N(2)	C(11)	C(10)	111.3(2)
N(2)	C(12)	C(13)	111.94(18)
C(18)	C(13)	C(14)	119.2(2)
C(18)	C(13)	C(12)	120.7(2)
C(14)	C(13)	C(12)	120.1(2)
N(3)	C(14)	C(15)	122.3(2)
N(3)	C(14)	C(13)	119.0(2)
C(15)	C(14)	C(13)	118.6(2)
C(16)	C(15)	C(14)	120.3(2)
C(17)	C(16)	C(15)	121.3(2)
C(16)	C(17)	C(18)	118.6(2)
C(13)	C(18)	C(17)	121.9(2)
N(3)	C(19)	C(20)	110.58(18)
C(19)	C(20)	S(2)	108.66(15)
C(8)	N(1)	C(7)	112.88(18)
C(11)	N(2)	C(12)	112.55(19)
C(14)	N(3)	C(19)	121.41(19)
C(10)	S(1)	C(9)	99.74(12)
C(1)	S(2)	C(20)	104.43(11)

Symmetry Operators

(1) x, y, z (2) -x, -y, -z

Table B.10 Crystal data and a summary of data collection for **142** (ON/NON).

Formula of the Refinement Model	$C_{20}H_{27}N_3O_2$
Model Molecular Weight	341.45
Crystal System	triclinic
Space Group	$P\ \bar{1}$(#2)
a	9.1852(10) Å
b	10.0015(9) Å
c	10.9234(8) Å
α	71.742(6)º
β	86.090(7)º
γ	73.961(8)º
V	915.69(15) $Å^3$
D_c	1.238 g cm^{-3}
Z	2
Crystal Size	0.300x0.100x0.080 mm
Crystal Colour	colourless
Crystal Habit	shard
Temperature	150(2) Kelvin
λ(MoKα)	0.71073 Å
μ(MoKα)	0.081 mm^{-1}
$T(\text{SADABS})_{\text{min,max}}$	0.801, 0.990
$2\theta_{\text{max}}$	66.14º
hkl range	-14 14, -15 14, -16 16
N	36808
N_{ind}	6910(R_{merge} 0.0554)
N_{obs}	5032(I > 2σ(I))
N_{var}	232
Residuals* *R*1(*F*), *wR*2(F^2)	0.0604, 0.1730
GoF(all)	1.053
Residual Extrema	-0.456, 0.579 e^- $Å^{-3}$

*$R1 = \Sigma||F_o| - |F_c||/\Sigma|F_o|$ for $F_o > 2\sigma(F_o)$; $wR2 = (\Sigma w(F_o^2 - F_c^2)^2/\Sigma(wF_c^2)^2)^{1/2}$ all reflections

$w=1/[\sigma^2(F_o^2)+(0.0734P)^2+0.4525P]$ where $P=(F_o^2+2F_c^2)/3$

Table B.11 Non-hydrogen bond lengths (Å) for **142** (ON/NON).

atom	atom	Distance	atom	atom	Distance
C(1)	O(2)	1.3833(16)	C(1)	C(6)	1.399(2)
C(1)	C(2)	1.4126(18)	C(2)	C(3)	1.3993(19)
C(2)	C(7)	1.506(2)	C(3)	C(4)	1.398(2)
C(4)	C(5)	1.387(2)	C(5)	C(6)	1.400(2)
C(7)	N(1)	1.4619(19)	C(8)	N(1)	1.4602(18)
C(8)	C(9)	1.513(2)	C(9)	O(1)	1.4147(18)
C(10)	O(1)	1.4228(19)	C(10)	C(11)	1.511(2)
C(11)	N(2)	1.4625(18)	C(12)	N(2)	1.4601(18)
C(12)	C(13)	1.5129(19)	C(13)	C(18)	1.3944(19)
C(13)	C(14)	1.4131(18)	C(14)	N(3)	1.3888(16)
C(14)	C(15)	1.4016(18)	C(15)	C(16)	1.3943(19)
C(16)	C(17)	1.388(2)	C(17)	C(18)	1.398(2)
C(19)	N(3)	1.4445(16)	C(19)	C(20)	1.5113(19)
C(20)	O(2)	1.4432(15)			

Symmetry Operators

(1) x, y, z (2) -x, -y, -z

Table B.12 Non-hydrogen bond angles (º) for **142** (ON/NON).

atom	atom	atom	angle
O(2)	C(1)	C(6)	123.12(12)
O(2)	C(1)	C(2)	116.85(12)
C(6)	C(1)	C(2)	120.03(12)
C(3)	C(2)	C(1)	118.42(13)
C(3)	C(2)	C(7)	120.84(12)
C(1)	C(2)	C(7)	120.74(12)
C(4)	C(3)	C(2)	121.96(13)
C(5)	C(4)	C(3)	118.68(13)
C(4)	C(5)	C(6)	120.97(14)
C(1)	C(6)	C(5)	119.93(13)
N(1)	C(7)	C(2)	112.02(11)
N(1)	C(8)	C(9)	109.75(12)
O(1)	C(9)	C(8)	108.06(11)

O(1)	C(10)	C(11)	107.92(11)
N(2)	C(11)	C(10)	110.98(12)
N(2)	C(12)	C(13)	115.19(11)
C(18)	C(13)	C(14)	118.55(12)
C(18)	C(13)	C(12)	121.53(12)
C(14)	C(13)	C(12)	119.89(12)
N(3)	C(14)	C(15)	123.02(11)
N(3)	C(14)	C(13)	117.42(11)
C(15)	C(14)	C(13)	119.53(12)
C(16)	C(15)	C(14)	120.64(12)
C(17)	C(16)	C(15)	120.29(12)
C(16)	C(17)	C(18)	119.07(13)
C(13)	C(18)	C(17)	121.90(13)
N(3)	C(19)	C(20)	110.74(11)
O(2)	C(20)	C(19)	110.38(11)
C(8)	N(1)	C(7)	113.09(11)
C(12)	N(2)	C(11)	112.41(12)
C(14)	N(3)	C(19)	118.74(10)
C(9)	O(1)	C(10)	113.36(11)
C(1)	O(2)	C(20)	117.96(11)

Symmetry Operators

(1) x, y, z (2) -x, -y, -z

Part 2. X-ray data for the metal complexes

(i) Ni(II)

Table B.13 Crystal data and a summary of data collection for [Ni**L**Cl]Cl·3H_2O (L = **138**).

Formula of the Refinement Model	$C_{20}H_{34}Cl_2N_4NiO_4$
Model Molecular Weight	524.12
Crystal System	monoclinic
Space Group	*C*2/m(#12)
a	16.696(2) Å
b	15.556(2) Å
c	8.8940(12) Å
β	90.522(2)º
V	2309.9(5) $Å^3$
D_c	1.507 g cm^{-3}
Z	4
Crystal Size	0.400x0.350x0.300 mm
Crystal Colour	green
Crystal Habit	prism
Temperature	150(2) Kelvin
λ(MoKα)	0.71073 Å
μ(MoKα)	1.106 mm^{-1}
$T(SADABS)_{min,max}$	0.6146, 0.7457
$2\theta_{max}$	56.58º
hkl range	-21 21, -20 19, -11 11
N	11490
N_{ind}	2854(R_{merge} 0.0223)
N_{obs}	2677(I > 2σ(I))
N_{var}	170
Residuals* *R*1(*F*), *wR*2(F^2)	0.0320, 0.0876
GoF(all)	1.091
Residual Extrema	-0.500, 0.548 e^- $Å^{-3}$

*$R1 = \Sigma||F_o| - |F_c||/\Sigma|F_o|$ for $F_o > 2\sigma(F_o)$; $wR2 = (\Sigma w(F_o^2 - F_c^2)^2/\Sigma(wF_c^2)^2)^{1/2}$ all reflections

$w=1/[\sigma^2(F_o^2)+(0.0459P)^2+3.0824P]$ where $P=(F_o^2+2F_c^2)/3$

Table B.14 Non-hydrogen bond lengths (Å) for [Ni**L**Cl]Cl·3H_2O (**L** = **138**).

atom	atom	Distance	atom	atom	Distance
C(1)	C(1) 6	1.093(8)	C(1)	N(1)	1.547(4)
C(1A)	C(1A) 6	1.377(9)	C(2)	N(2)	1.482(3)
C(2)	C(3)	1.531(3)	C(3)	N(3)	1.484(2)
C(4)	N(3)	1.484(3)	C(4)	C(5)	1.499(3)
C(5)	C(10)	1.390(3)	C(5)	C(6)	1.398(3)
C(6)	C(7)	1.398(3)	C(6)	N(1)	1.420(3)
C(7)	C(8)	1.373(4)	C(8)	C(9)	1.376(4)
C(9)	C(10)	1.393(3)	N(1)	Ni(1)	2.1214(17)
N(2)	C(2) 6	1.482(3)	N(2)	Ni(1)	2.113(2)
N(3)	Ni(1)	2.0675(17)	Cl(1)	Ni(1)	2.4481(7)
Ni(1)	N(3) 6	2.0675(17)	Ni(1)	O(1) 6	2.1214(17)
Ni(1)	N(1) 6	2.1214(17)			

Symmetry Operators

(1) x, y, z	(2) -x, y, -z	(3) x+1/2, y+1/2, z
(4) -x+1/2, y+1/2, -z	(5) -x, -y, -z	(6) x, -y, z
(7) -x+1/2, -y+1/2, -z	(8) x+1/2, -y+1/2, z	

Table B.15 Non-hydrogen bond angles (º) for [Ni**L**Cl]Cl·3H_2O (**L** = **138**).

atom		atom	atom	angle
C(1)	6	C(1)	N(1)	122.71(16)
N(2)		C(2)	C(3)	111.76(17)
N(3)		C(3)	C(2)	110.82(16)
N(3)		C(4)	C(5)	111.48(17)
C(10)		C(5)	C(6)	118.69(19)
C(10)		C(5)	C(4)	120.18(19)
C(6)		C(5)	C(4)	121.07(19)
C(5)		C(6)	C(7)	120.2(2)
C(5)		C(6)	N(1)	116.37(18)
C(7)		C(6)	N(1)	123.4(2)
C(8)		C(7)	C(6)	119.8(2)
C(7)		C(8)	C(9)	120.9(2)
C(8)		C(9)	C(10)	119.6(2)

C(5)		C(10)	C(9)		120.8(2)
C(6)		N(1)	C(1)		112.7(2)
C(6)		N(1)	Ni(1)		118.68(13)
C(1)		N(1)	Ni(1)		104.28(18)
C(2)		N(2)	C(2)	6	113.9(2)
C(2)		N(2)	Ni(1)		108.05(13)
C(2)	6	N(2)	Ni(1)		108.05(13)
C(3)		N(3)	C(4)		113.43(16)
C(3)		N(3)	Ni(1)		110.01(13)
C(4)		N(3)	Ni(1)		112.89(12)
N(3)		Ni(1)	N(3)	6	99.15(10)
N(3)		Ni(1)	N(2)		84.38(6)
N(3)	6	Ni(1)	N(2)		84.38(6)
N(3)		Ni(1)	O(1)	6	171.07(7)
N(3)	6	Ni(1)	O(1)	6	89.78(7)
N(2)		Ni(1)	O(1)	6	96.71(7)
N(3)		Ni(1)	N(1)	6	171.07(7)
N(3)	6	Ni(1)	N(1)	6	89.78(7)
N(2)		Ni(1)	N(1)	6	96.71(7)
O(1)	6	Ni(1)	N(1)	6	0.00(14)
N(3)		Ni(1)	N(1)		89.78(7)
N(3)	6	Ni(1)	N(1)		171.07(7)
N(2)		Ni(1)	N(1)		96.71(7)
O(1)	6	Ni(1)	N(1)		81.30(9)
N(1)	6	Ni(1)	N(1)		81.30(9)
N(3)		Ni(1)	Cl(1)		91.85(5)
N(3)	6	Ni(1)	Cl(1)		91.85(5)
N(2)		Ni(1)	Cl(1)		174.15(7)
O(1)	6	Ni(1)	Cl(1)		87.71(6)
N(1)	6	Ni(1)	Cl(1)		87.71(6)
N(1)		Ni(1)	Cl(1)		87.71(6)

Symmetry Operators

(1) x, y, z	(2) -x, y, -z	(3) x+1/2, y+1/2, z
(4) -x+1/2, y+1/2, -z	(5) -x, -y, -z	(6) x, -y, z
(7) -x+1/2, -y+1/2, -z	(8) x+1/2, -y+1/2, z	

Table B.16 Crystal data and a summary of data collection for [Ni**L**Cl]Cl·0.125CH_3CN·3.75H_2O (**L** = **142**).

Formula of the Refinement Model	$C_{40.50}H_{69.75}Cl_4N_{6.25}Ni_2O_{11.50}$
Model Molecular Weight	1087.50
Crystal System	monoclinic
Space Group	$P2_1/n$(#14)
a	12.0787(8) Å
b	18.0874(13) Å
c	24.7617(18) Å
β	100.238(2)º
V	5323.6(6) $Å^3$
D_C	1.357 g cm^{-3}
Z	4
Crystal Size	0.300x0.250x0.200 mm
Crystal Colour	green
Crystal Habit	multi-face
Temperature	150(2) Kelvin
λ(MoKα)	0.71073 Å
μ(MoKα)	0.966 mm^{-1}
$T(\text{SADABS})_{min,max}$	0.693, 0.824
$2\theta_{max}$	55.28º
hkl range	-15 13, -22 23, -32 27
N	42041
N_{ind}	12336(R_{merge} 0.0757)
N_{obs}	7686(I > 2σ(I))
N_{var}	651
Residuals* *R*1(*F*), *wR*2(F^2)	0.0776, 0.2642
GoF(all)	1.021
Residual Extrema	-1.239, 1.314 e^- $Å^{-3}$

*$R1 = \Sigma||F_o| - |F_c||/\Sigma|F_o|$ for $F_o > 2\sigma(F_o)$; $wR2 = (\Sigma w(F_o^2 - F_c^2)^2/\Sigma(wF_c^2)^2)^{1/2}$ all reflections

$w=1/[\sigma^2(F_o^2)+(0.1775P)^2+0.0000P]$ where $P=(F_o^2+2F_c^2)/3$

Table B.17 Non-hydrogen bond lengths (Å) for [Ni**L**Cl]Cl·0.125CH_3CN·3.75H_2O (**L** = **142**).

atom	atom	Distance	atom	atom	Distance
C(1)	O(1)	1.472(5)	C(1)	C(2)	1.504(6)
C(2)	N(1)	1.452(6)	C(3)	C(4)	1.381(7)
C(3)	C(8)	1.400(7)	C(3)	N(1)	1.421(5)
C(4)	C(5)	1.402(7)	C(4)	C(9)	1.503(7)
C(5)	C(6)	1.389(8)	C(6)	C(7)	1.347(9)
C(7)	C(8)	1.397(7)	C(9)	N(2)	1.492(7)
C(10)	N(2)	1.488(6)	C(10)	C(11)	1.497(7)
C(11)	O(2)	1.464(6)	C(12)	O(2)	1.445(6)
C(12)	C(13)	1.525(6)	C(13)	N(3)	1.491(5)
C(14)	N(3)	1.478(6)	C(14)	C(15)	1.505(6)
C(15)	C(20)	1.396(6)	C(15)	C(16)	1.398(6)
C(16)	C(17)	1.391(6)	C(16)	O(1)	1.425(5)
C(17)	C(18)	1.393(6)	C(18)	C(19)	1.376(7)
C(19)	C(20)	1.359(7)	C(21)	O(3)	1.445(7)
C(21)	C(22)	1.500(8)	C(22)	N(4)	1.459(6)
C(23)	C(24)	1.387(6)	C(23)	C(28)	1.391(7)
C(23)	N(4)	1.444(6)	C(24)	C(25)	1.399(7)
C(24)	C(29)	1.492(7)	C(25)	C(26)	1.387(8)
C(26)	C(27)	1.370(8)	C(27)	C(28)	1.404(7)
C(29)	N(5)	1.475(7)	C(30)	N(5)	1.479(6)
C(30)	C(31)	1.511(7)	C(31)	O(4)	1.454(6)
C(32)	O(4)	1.446(6)	C(32)	C(33)	1.519(7)
C(33)	N(6)	1.498(7)	C(34)	C(35)	1.435(10)
C(34)	N(6)	1.525(8)	C(35)	C(36)	1.401(9)
C(35)	C(40)	1.404(9)	C(36)	C(37)	1.378(9)
C(36)	O(3)	1.416(6)	C(37)	C(38)	1.372(9)
C(38)	C(39)	1.253(13)	C(39)	C(40)	1.458(13)
N(1)	Ni(1)	2.118(3)	N(2)	Ni(1)	2.082(4)
N(3)	Ni(1)	2.056(4)	N(4)	Ni(2)	2.122(4)
N(5)	Ni(2)	2.060(4)	N(6)	Ni(2)	2.089(5)
O(1)	Ni(1)	2.166(4)	O(2)	Ni(1)	2.164(3)
O(3)	Ni(2)	2.105(4)	O(4)	Ni(2)	2.148(3)
N(1A)	C(2A)	0.75(2)	C(1A)	C(2A)	1.34(3)
Cl(1)	Ni(1)	2.4030(11)	Cl(3)	Ni(2)	2.383(2)

Symmetry Operators

(1) x, y, z (2) -x+1/2, y+1/2, -z+1/2 (3) -x, -y, -z
(4) x-1/2, -y-1/2, z-1/2

Table B.18 Non-hydrogen bond angles (º) for [Ni**L**Cl]Cl·0.125CH_3CN·3.75H_2O (**L** = **142**).

atom	atom	atom	angle
O(1)	C(1)	C(2)	107.2(4)
N(1)	C(2)	C(1)	109.5(4)
C(4)	C(3)	C(8)	122.5(4)
C(4)	C(3)	N(1)	115.2(4)
C(8)	C(3)	N(1)	122.2(5)
C(3)	C(4)	C(5)	117.0(5)
C(3)	C(4)	C(9)	119.8(4)
C(5)	C(4)	C(9)	123.2(5)
C(6)	C(5)	C(4)	121.0(6)
C(7)	C(6)	C(5)	120.7(5)
C(6)	C(7)	C(8)	120.7(5)
C(7)	C(8)	C(3)	118.1(5)
N(2)	C(9)	C(4)	112.1(4)
N(2)	C(10)	C(11)	111.2(4)
O(2)	C(11)	C(10)	111.7(4)
O(2)	C(12)	C(13)	111.8(4)
N(3)	C(13)	C(12)	109.8(4)
N(3)	C(14)	C(15)	112.0(3)
C(20)	C(15)	C(16)	117.9(4)
C(20)	C(15)	C(14)	121.0(4)
C(16)	C(15)	C(14)	121.1(4)
C(17)	C(16)	C(15)	121.1(4)
C(17)	C(16)	O(1)	122.5(4)
C(15)	C(16)	O(1)	116.3(4)
C(16)	C(17)	C(18)	118.6(4)
C(19)	C(18)	C(17)	120.7(5)
C(20)	C(19)	C(18)	120.2(5)
C(19)	C(20)	C(15)	121.4(5)
O(3)	C(21)	C(22)	109.2(4)
N(4)	C(22)	C(21)	107.3(4)
C(24)	C(23)	C(28)	121.0(5)
C(24)	C(23)	N(4)	117.3(4)
C(28)	C(23)	N(4)	121.7(4)
C(23)	C(24)	C(25)	118.1(5)
C(23)	C(24)	C(29)	121.7(4)
C(25)	C(24)	C(29)	120.2(4)
C(26)	C(25)	C(24)	121.8(5)
C(27)	C(26)	C(25)	119.3(5)
C(26)	C(27)	C(28)	120.5(5)
C(23)	C(28)	C(27)	119.4(5)
N(5)	C(29)	C(24)	111.8(4)

N(5)	C(30)	C(31)	112.0(4)
O(4)	C(31)	C(30)	111.2(4)
O(4)	C(32)	C(33)	111.8(4)
N(6)	C(33)	C(32)	109.7(4)
C(35)	C(34)	N(6)	114.0(5)
C(36)	C(35)	C(40)	116.5(8)
C(36)	C(35)	C(34)	122.0(5)
C(40)	C(35)	C(34)	121.5(8)
C(37)	C(36)	C(35)	122.3(5)
C(37)	C(36)	O(3)	124.0(6)
C(35)	C(36)	O(3)	113.6(5)
C(38)	C(37)	C(36)	117.8(8)
C(39)	C(38)	C(37)	124.4(9)
C(38)	C(39)	C(40)	120.1(7)
C(35)	C(40)	C(39)	118.7(8)
C(3)	N(1)	C(2)	119.8(4)
C(3)	N(1)	Ni(1)	116.0(3)
C(2)	N(1)	Ni(1)	110.0(3)
C(10)	N(2)	C(9)	113.3(4)
C(10)	N(2)	Ni(1)	109.5(3)
C(9)	N(2)	Ni(1)	113.5(3)
C(14)	N(3)	C(13)	113.4(4)
C(14)	N(3)	Ni(1)	112.0(3)
C(13)	N(3)	Ni(1)	112.5(3)
C(23)	N(4)	C(22)	116.2(4)
C(23)	N(4)	Ni(2)	119.3(3)
C(22)	N(4)	Ni(2)	108.8(3)
C(29)	N(5)	C(30)	114.5(4)
C(29)	N(5)	Ni(2)	111.2(3)
C(30)	N(5)	Ni(2)	110.7(3)
C(33)	N(6)	C(34)	111.6(5)
C(33)	N(6)	Ni(2)	109.9(3)
C(34)	N(6)	Ni(2)	113.7(4)
C(16)	O(1)	C(1)	115.8(3)
C(16)	O(1)	Ni(1)	121.6(3)
C(1)	O(1)	Ni(1)	109.4(3)
C(12)	O(2)	C(11)	113.8(3)
C(12)	O(2)	Ni(1)	109.0(2)
C(11)	O(2)	Ni(1)	109.3(2)
C(36)	O(3)	C(21)	119.2(5)
C(36)	O(3)	Ni(2)	120.3(3)
C(21)	O(3)	Ni(2)	109.4(3)
C(32)	O(4)	C(31)	114.5(4)
C(32)	O(4)	Ni(2)	109.4(2)
C(31)	O(4)	Ni(2)	108.8(3)
N(1A)	C(2A)	C(1A)	173(3)

N(3)	Ni(1)	N(2)	103.32(16)
N(3)	Ni(1)	N(1)	168.50(15)
N(2)	Ni(1)	N(1)	88.17(15)
N(3)	Ni(1)	O(2)	81.80(12)
N(2)	Ni(1)	O(2)	82.07(13)
N(1)	Ni(1)	O(2)	99.84(12)
N(3)	Ni(1)	O(1)	88.98(14)
N(2)	Ni(1)	O(1)	165.31(14)
N(1)	Ni(1)	O(1)	79.61(13)
O(2)	Ni(1)	O(1)	91.94(12)
N(3)	Ni(1)	Cl(1)	91.96(10)
N(2)	Ni(1)	Cl(1)	94.59(11)
N(1)	Ni(1)	Cl(1)	87.27(10)
O(2)	Ni(1)	Cl(1)	172.00(9)
O(1)	Ni(1)	Cl(1)	92.96(9)
N(5)	Ni(2)	N(6)	101.06(19)
N(5)	Ni(2)	O(3)	171.39(17)
N(6)	Ni(2)	O(3)	87.56(18)
N(5)	Ni(2)	N(4)	90.93(15)
N(6)	Ni(2)	N(4)	166.39(18)
O(3)	Ni(2)	N(4)	80.51(15)
N(5)	Ni(2)	O(4)	82.74(14)
N(6)	Ni(2)	O(4)	82.24(15)
O(3)	Ni(2)	O(4)	98.64(14)
N(4)	Ni(2)	O(4)	93.04(13)
N(5)	Ni(2)	Cl(3)	90.81(12)
N(6)	Ni(2)	Cl(3)	93.95(13)
O(3)	Ni(2)	Cl(3)	88.51(12)
N(4)	Ni(2)	Cl(3)	92.27(12)
O(4)	Ni(2)	Cl(3)	171.71(11)

Symmetry Operators

(1) x, y, z (2) -x+1/2, y+1/2, -z+1/2 (3) -x, -y, -z
(4) x-1/2, -y-1/2, z-1/2

(ii) Cu(II)

Table B.19 Crystal data and a summary of data collection for $[Cu\mathbf{L}Cl_2]\cdot CH_3CN$ (**L** = **138**).

Formula of the Refinement Model	$C_{22}H_{31}Cl_2CuN_5O$
Model Molecular Weight	515.96
Crystal System	monoclinic
Space Group	*C*2/c(#15)
a	21.9824(12) Å
b	8.3281(4) Å
c	26.8453(15) Å
β	97.319(3)º
V	4874.6(4) Å^3
D_C	1.406 g cm^{-3}
Z	8
Crystal Size	0.280x0.250x0.180 mm
Crystal Colour	green
Crystal Habit	block
Temperature	150(2) Kelvin
λ(MoKα)	0.71073 Å
μ(MoKα)	1.139 mm^{-1}
T(SADABS)$_{min,max}$	0.738, 0.815
$2\theta_{max}$	60.06º
hkl range	-30 30, -11 11, -37 37
N	51326
N_{ind}	7111(R_{merge} 0.0428)
N_{obs}	5492(I > 2σ(I))
N_{var}	293
Residuals* *R*1(*F*), *wR*2(F^2)	0.0338, 0.0842
GoF(all)	1.026
Residual Extrema	-0.323, 1.000 e$^-$ Å^{-3}

*$R1 = \Sigma||F_o| - |F_c||/\Sigma|F_o|$ for $F_o > 2\sigma(F_o)$; $wR2 = (\Sigma w(F_o^2 - F_c^2)^2/\Sigma(wF_c^2)^2)^{1/2}$ all reflections

$w=1/[\sigma^2(F_o^2)+(0.0355P)^2+5.1593P]$ where $P=(F_o^2+2F_c^2)/3$

Table B.20 Non-hydrogen bond lengths (Å) for [Cu**L**Cl_2]·CH_3CN (**L** = **138**).

atom	atom	Distance	atom	atom	Distance
C(1)	O(1)	1.444(2)	C(1)	C(2)	1.507(3)
C(2)	N(1)	1.469(2)	C(3)	N(1)	1.384(2)
C(3)	C(4)	1.409(2)	C(3)	C(8)	1.422(3)
C(4)	C(5)	1.372(3)	C(5)	C(6)	1.385(3)
C(6)	C(7)	1.397(3)	C(7)	C(8)	1.390(3)
C(8)	C(9)	1.516(2)	C(9)	N(2)	1.500(2)
C(10)	N(2)	1.487(2)	C(10)	C(11)	1.529(3)
C(11)	N(3)	1.474(2)	C(12)	N(3)	1.480(2)
C(12)	C(13)	1.513(3)	C(13)	N(4)	1.488(2)
C(14)	N(4)	1.470(2)	C(14)	C(15)	1.519(3)
C(15)	C(20)	1.398(3)	C(15)	C(16)	1.400(3)
C(16)	O(1)	1.374(2)	C(16)	C(17)	1.393(3)
C(17)	C(18)	1.392(3)	C(18)	C(19)	1.375(4)
C(19)	C(20)	1.393(3)	C(21)	N(5)	1.138(3)
C(21)	C(22)	1.457(3)	N(2)	Cu(1)	2.0361(15)
N(3)	Cu(1)	2.0281(14)	N(4)	Cu(1)	2.0540(15)
Cl(1)	Cu(1)	2.4705(4)	Cl(2)	Cu(1)	2.3003(5)

Symmetry Operators

(1) x, y, z
(2) -x, y, -z+1/2
(3) x+1/2, y+1/2, z
(4) -x+1/2, y+1/2, -z+1/2
(5) -x, -y, -z
(6) x, -y, z-1/2
(7) -x+1/2, -y+1/2, -z
(8) x+1/2, -y+1/2, z-1/2

Table B.21 Non-hydrogen bond angles (º) for [Cu**L**Cl_2]·CH_3CN (**L** = **138**).

atom	atom	atom	angle
O(1)	C(1)	C(2)	107.42(15)
N(1)	C(2)	C(1)	114.39(16)
N(1)	C(3)	C(4)	119.91(17)
N(1)	C(3)	C(8)	121.84(15)
C(4)	C(3)	C(8)	118.24(17)
C(5)	C(4)	C(3)	121.26(18)
C(4)	C(5)	C(6)	121.16(17)
C(5)	C(6)	C(7)	118.32(19)
C(8)	C(7)	C(6)	122.17(18)
C(7)	C(8)	C(3)	118.78(16)

C(7)	C(8)	C(9)	118.41(16)
C(3)	C(8)	C(9)	122.67(16)
N(2)	C(9)	C(8)	115.59(14)
N(2)	C(10)	C(11)	110.51(14)
N(3)	C(11)	C(10)	109.41(14)
N(3)	C(12)	C(13)	106.43(13)
N(4)	C(13)	C(12)	108.33(14)
N(4)	C(14)	C(15)	112.08(15)
C(20)	C(15)	C(16)	118.39(19)
C(20)	C(15)	C(14)	122.20(18)
C(16)	C(15)	C(14)	119.30(18)
O(1)	C(16)	C(17)	123.87(18)
O(1)	C(16)	C(15)	115.40(16)
C(17)	C(16)	C(15)	120.72(19)
C(18)	C(17)	C(16)	119.6(2)
C(19)	C(18)	C(17)	120.6(2)
C(18)	C(19)	C(20)	119.8(2)
C(19)	C(20)	C(15)	120.9(2)
N(5)	C(21)	C(22)	179.6(3)
C(3)	N(1)	C(2)	123.18(15)
C(10)	N(2)	C(9)	115.20(14)
C(10)	N(2)	Cu(1)	106.96(10)
C(9)	N(2)	Cu(1)	116.61(11)
C(11)	N(3)	C(12)	114.88(13)
C(11)	N(3)	Cu(1)	112.27(10)
C(12)	N(3)	Cu(1)	108.76(10)
C(14)	N(4)	C(13)	112.26(14)
C(14)	N(4)	Cu(1)	121.70(11)
C(13)	N(4)	Cu(1)	109.78(11)
C(16)	O(1)	C(1)	118.16(15)
N(3)	Cu(1)	N(2)	84.40(6)
N(3)	Cu(1)	N(4)	83.01(6)
N(2)	Cu(1)	N(4)	146.91(6)
N(3)	Cu(1)	Cl(2)	171.52(4)
N(2)	Cu(1)	Cl(2)	93.15(4)
N(4)	Cu(1)	Cl(2)	94.84(4)
N(3)	Cu(1)	Cl(1)	89.44(4)
N(2)	Cu(1)	Cl(1)	101.91(4)
N(4)	Cu(1)	Cl(1)	108.43(4)
Cl(2)	Cu(1)	Cl(1)	99.015(16)

Symmetry Operators

(1) x, y, z (2) -x, y, -z+1/2 (3) x+1/2, y+1/2, z

(4) -x+1/2, y+1/2, -z+1/2 (5) -x, -y, -z (6) x, -y, z-1/2

(7) -x+1/2, -y+1/2, -z (8) x+1/2, -y+1/2, z-1/2

Table B.22 Crystal data and a summary of data collection for $[CuLCl_2]\cdot CH_3CN$ (**L** = **142**).

Formula of the Refinement Model	$C_{22}H_{30}Cl_2CuN_4O_2$
Model Molecular Weight	516.94
Crystal System	monoclinic
Space Group	$P2_1/c$(#14)
a	10.629(1) Å
b	9.932(1) Å
c	22.721(10) Å
β	90.271(5)º
V	2398.6(11) Å^3
D_c	1.432 g cm^{-3}
Z	4
Crystal Size	0.280x0.250x0.200 mm
Crystal Colour	green
Crystal Habit	block
Temperature	150(2) Kelvin
λ(MoKα)	0.71073 Å
μ(MoKα)	1.159 mm^{-1}
T(SADABS)$_{min,max}$	0.712, 0.793
$2\theta_{max}$	59.86º
hkl range	-14 14, 0 13, 0 31
N	6408
N_{obs}	4371(I > 2σ(I))
N_{var}	284
Residuals* $R1(F)$, $wR2(F^2)$	0.0846, 0.2087
GoF(all)	1.016
Residual Extrema	-0.860, 1.138 e$^-$ Å^{-3}

*$R1 = \Sigma||F_o| - |F_c||/\Sigma|F_o|$ for $F_o > 2\sigma(F_o)$; $wR2 = (\Sigma w(F_o^2 - F_c^2)^2/\Sigma(wF_c^2)^2)^{1/2}$ all reflections

$w=1/[\sigma^2(F_o^2)+(0.0500P)^2+35.4000P]$ where $P=(F_o^2+2F_c^2)/3$

Table B.23 Non-hydrogen bond lengths (Å) for [Cu**L**Cl_2]·CH_3CN (**L** = **142**).

atom	atom	Distance	atom	atom	Distance
C(1)	O(1)	1.437(7)	C(1)	C(2)	1.509(8)
C(2)	N(1)	1.446(8)	C(3)	N(1)	1.381(7)
C(3)	C(4)	1.397(8)	C(3)	C(8)	1.407(8)
C(4)	C(5)	1.397(8)	C(4)	C(9)	1.516(8)
C(5)	C(6)	1.370(9)	C(6)	C(7)	1.385(10)
C(7)	C(8)	1.381(9)	C(9)	N(2)	1.496(7)
C(10)	C(11)	1.508(8)	C(10)	N(2)	1.510(8)
C(11)	O(2)	1.420(7)	C(12)	O(2)	1.446(7)
C(12)	C(13)	1.500(8)	C(13)	N(3)	1.502(7)
C(14)	N(3)	1.496(7)	C(14)	C(15)	1.513(8)
C(15)	C(20)	1.389(8)	C(15)	C(16)	1.401(8)
C(16)	O(1)	1.377(7)	C(16)	C(17)	1.418(8)
C(17)	C(18)	1.370(9)	C(18)	C(19)	1.390(9)
C(19)	C(20)	1.403(8)	C(21)	N(4)	1.131(10)
C(21)	C(22)	1.455(12)	N(2)	Cu(1)	2.079(5)
N(3)	Cu(1)	2.035(4)	O(2)	Cu(1)	2.252(4)
Cl(1)	Cu(1)	2.3029(14)	Cl(2)	Cu(1)	2.2920(15)

Symmetry Operators

(1) x, y, z (2) -x, y+1/2, -z+1/2 (3) -x, -y, -z
(4) x, -y-1/2, z-1/2

Table B.24 Non-hydrogen bond angles (º) for [Cu**L**Cl_2]·CH_3CN (**L** = **142**).

atom	atom	atom	angle
O(1)	C(1)	C(2)	107.4(5)
N(1)	C(2)	C(1)	114.8(5)
N(1)	C(3)	C(4)	119.8(5)
N(1)	C(3)	C(8)	121.7(5)
C(4)	C(3)	C(8)	118.5(5)
C(5)	C(4)	C(3)	119.7(5)
C(5)	C(4)	C(9)	117.8(5)
C(3)	C(4)	C(9)	122.5(5)
C(6)	C(5)	C(4)	121.2(6)
C(5)	C(6)	C(7)	119.6(6)
C(8)	C(7)	C(6)	120.4(6)

C(7)	C(8)	C(3)	120.6(6)
N(2)	C(9)	C(4)	112.5(5)
C(11)	C(10)	N(2)	110.9(5)
O(2)	C(11)	C(10)	105.1(5)
O(2)	C(12)	C(13)	104.4(4)
C(12)	C(13)	N(3)	110.5(5)
N(3)	C(14)	C(15)	111.2(5)
C(20)	C(15)	C(16)	118.6(5)
C(20)	C(15)	C(14)	120.6(5)
C(16)	C(15)	C(14)	120.6(5)
O(1)	C(16)	C(15)	116.7(5)
O(1)	C(16)	C(17)	123.1(5)
C(15)	C(16)	C(17)	120.2(5)
C(18)	C(17)	C(16)	119.1(6)
C(17)	C(18)	C(19)	121.9(6)
C(18)	C(19)	C(20)	118.3(5)
C(15)	C(20)	C(19)	121.6(6)
N(4)	C(21)	C(22)	178.9(8)
C(3)	N(1)	C(2)	123.8(5)
C(9)	N(2)	C(10)	110.1(4)
C(9)	N(2)	Cu(1)	122.9(4)
C(10)	N(2)	Cu(1)	106.5(3)
C(14)	N(3)	C(13)	110.5(4)
C(14)	N(3)	Cu(1)	120.8(3)
C(13)	N(3)	Cu(1)	108.8(3)
C(16)	O(1)	C(1)	119.0(4)
C(11)	O(2)	C(12)	116.7(4)
C(11)	O(2)	Cu(1)	104.1(3)
C(12)	O(2)	Cu(1)	102.9(3)
N(3)	Cu(1)	N(2)	161.10(18)
N(3)	Cu(1)	O(2)	81.29(16)
N(2)	Cu(1)	O(2)	81.48(17)
N(3)	Cu(1)	Cl(2)	90.02(13)
N(2)	Cu(1)	Cl(2)	87.79(13)
O(2)	Cu(1)	Cl(2)	107.54(12)
N(3)	Cu(1)	Cl(1)	95.94(13)
N(2)	Cu(1)	Cl(1)	92.84(13)
O(2)	Cu(1)	Cl(1)	93.57(11)
Cl(2)	Cu(1)	Cl(1)	158.72(6)

Symmetry Operators

(1) x, y, z (2) -x, y+1/2, -z+1/2 (3) -x, -y, -z
(4) x, -y-1/2, z-1/2

Table B.25 Crystal data and a summary of data collection for [Cu**L**Cl]Cl·2.375H_2O (**L** = **141**).

Formula of the Refinement Model	$C_{80}H_{127.00}Cl_8Cu_4N_{12}O_{13.50}S_4$
Model Molecular Weight	2138.94
Crystal System	monoclinic
Space Group	*C*2/c(#??)
a	16.9284(17) Å
b	16.2096(17) Å
c	38.129(4) Å
β	95.261(4)º
V	10418.5(18) $Å^3$
D_c	1.354 g cm^{-3}
Z	4
Crystal Size	0.100x0.0750x0.050 mm
Crystal Colour	blue
Crystal Habit	block
Temperature	150(2) Kelvin
λ(MoKα)	0.71073 Å
μ(MoKα)	1.149 mm^{-1}
$T(SADABS)_{min,max}$	0.806, 0.944
$2\theta_{max}$	44.10º
hkl range	-17 17, -13 17, -31 40
N	23228
N_{ind}	6334(R_{merge} 0.0316)
N_{obs}	5150(I > 2σ(I))
N_{var}	586
Residuals* *R*1(*F*), *wR*2(F^2)	0.0774, 0.2396
GoF(all)	0.956
Residual Extrema	-0.486, 1.259 e^- $Å^{-3}$

*$R1 = \Sigma||F_o| - |F_c||/\Sigma|F_o|$ for $F_o > 2\sigma(F_o)$; $wR2 = (\Sigma w(F_o^2 - F_c^2)^2/\Sigma(wF_c^2)^2)^{1/2}$ all reflections

$w=1/[\sigma^2(F_o^2)+(0.1824P)^2+77.2105P]$ where $P=(F_o^2+2F_c^2)/3$

Table B.26 Non-hydrogen bond lengths (Å) for [Cu**L**Cl]Cl·2.375H_2O (**L** = **141**).

atom	atom	Distance	atom	atom	Distance
C(1B)	O(1)	1.57(2)	C(1B)	C(2B)	1.57(3)
C(2B)	N(1A)	1.43(2)	C(1A)	C(2A)	1.46(2)
C(2A)	O(1)	1.470(13)	C(3)	N(1A)	1.349(10)
C(3)	C(4)	1.398(10)	C(3)	C(8)	1.430(12)
C(4)	C(5)	1.396(11)	C(4)	C(9)	1.498(11)
C(5)	C(6)	1.351(14)	C(6)	C(7)	1.331(16)
C(7)	C(8)	1.394(16)	C(9)	N(2)	1.470(10)
C(10)	N(2)	1.486(11)	C(10)	C(11)	1.520(13)
C(11)	S(1)	1.793(9)	C(12)	C(13)	1.510(12)
C(12)	S(1)	1.798(8)	C(13)	N(3)	1.491(11)
C(14)	C(15)	1.465(12)	C(14)	N(3)	1.511(10)
C(15)	C(20A)	1.303(19)	C(15)	C(16)	1.381(10)
C(15)	C(18B)	1.63(3)	C(16)	O(1)	1.379(9)
C(16)	C(17)	1.381(12)	C(17)	C(20B)	1.00(3)
C(17)	C(18A)	1.490(18)	C(18A)	C(19A)	1.42(3)
C(19A)	C(20A)	1.42(3)	C(18B)	C(19B)	1.48(5)
C(19B)	C(20B)	1.38(4)	C(21)	O(2)	1.447(9)
C(21)	C(22)	1.489(12)	C(22)	N(4)	1.471(10)
C(23)	C(24)	1.377(11)	C(23)	C(28)	1.411(12)
C(23)	N(4)	1.454(9)	C(24)	C(25)	1.399(12)
C(24)	C(29)	1.500(13)	C(25)	C(26)	1.402(15)
C(26)	C(27)	1.347(14)	C(27)	C(28)	1.375(12)
C(29)	N(5)	1.481(11)	C(30)	N(5)	1.456(11)
C(30)	C(31)	1.501(12)	C(31)	S(2)	1.823(8)
C(32)	C(33)	1.510(12)	C(32)	S(2)	1.801(8)
C(33)	N(6)	1.488(11)	C(34)	C(35)	1.486(12)
C(34)	N(6)	1.500(11)	C(35)	C(40)	1.380(11)
C(35)	C(36)	1.390(11)	C(36)	O(2)	1.368(9)
C(36)	C(37)	1.384(11)	C(37)	C(38)	1.397(12)
C(38)	C(39)	1.372(13)	C(39)	C(40)	1.360(12)
N(1A)	Cu(1)	2.332(6)	N(2)	Cu(1)	2.092(7)
N(3)	Cu(1)	2.134(7)	N(4)	Cu(2)	2.090(6)
N(5)	Cu(2)	2.225(7)	N(6)	Cu(2)	2.008(6)
O(1)	Cu(1)	2.238(6)	O(2)	Cu(2)	2.511(5)
S(1)	Cu(1)	2.3662(19)	S(2)	Cu(2)	2.3757(19)
Cl(1)	Cu(1)	2.3303(19)	Cl(3A)	Cu(2)	2.312(3)
Cl(3B)	Cu(2)	2.437(10)			

Symmetry Operators

(1) x, y, z
(2) -x, y, -z+1/2
(3) x+1/2, y+1/2, z
(4) -x+1/2, y+1/2, -z+1/2
(5) -x, -y, -z
(6) x, -y, z-1/2

Table B.27 Non-hydrogen bond angles (º) for [Cu**L**Cl]Cl·2.375H_2O (**L** = **141**).

atom	atom	atom	angle
O(1)	C(1B)	C(2B)	94.2(14)
N(1A)	C(2B)	C(1B)	107.1(15)
C(1A)	C(2A)	O(1)	112.3(11)
N(1A)	C(3)	C(4)	117.4(7)
N(1A)	C(3)	C(8)	124.3(8)
C(4)	C(3)	C(8)	118.3(8)
C(5)	C(4)	C(3)	118.6(7)
C(5)	C(4)	C(9)	120.5(8)
C(3)	C(4)	C(9)	120.8(7)
C(6)	C(5)	C(4)	121.5(9)
C(7)	C(6)	C(5)	121.7(10)
C(6)	C(7)	C(8)	120.3(9)
C(7)	C(8)	C(3)	119.6(9)
N(2)	C(9)	C(4)	115.4(6)
N(2)	C(10)	C(11)	112.7(7)
C(10)	C(11)	S(1)	114.2(6)
C(13)	C(12)	S(1)	114.1(6)
N(3)	C(13)	C(12)	113.8(6)
C(15)	C(14)	N(3)	111.7(6)
C(20A)	C(15)	C(16)	122.1(13)
C(20A)	C(15)	C(14)	115.8(13)
C(16)	C(15)	C(14)	122.1(7)
C(16)	C(15)	C(18B)	110.1(16)
C(14)	C(15)	C(18B)	127.7(16)
O(1)	C(16)	C(15)	116.3(7)
O(1)	C(16)	C(17)	122.1(8)
C(15)	C(16)	C(17)	121.6(8)
C(20B)	C(17)	C(16)	133(2)
C(16)	C(17)	C(18A)	116.9(12)
C(19A)	C(18A)	C(17)	118.8(15)
C(20A)	C(19A)	C(18A)	117.9(18)
C(15)	C(20A)	C(19A)	122(2)
C(19B)	C(18B)	C(15)	112(3)
C(20B)	C(19B)	C(18B)	121(3)
C(17)	C(20B)	C(19B)	121(3)
O(2)	C(21)	C(22)	105.6(7)
N(4)	C(22)	C(21)	114.0(6)
C(24)	C(23)	C(28)	121.5(7)
C(24)	C(23)	N(4)	117.4(7)
C(28)	C(23)	N(4)	121.1(7)
C(23)	C(24)	C(25)	118.3(8)
C(23)	C(24)	C(29)	122.1(7)

C(25)	C(24)	C(29)	119.6(8)
C(24)	C(25)	C(26)	119.4(9)
C(27)	C(26)	C(25)	121.3(8)
C(26)	C(27)	C(28)	120.8(9)
C(27)	C(28)	C(23)	118.6(9)
N(5)	C(29)	C(24)	111.6(7)
N(5)	C(30)	C(31)	113.8(7)
C(30)	C(31)	S(2)	115.5(6)
C(33)	C(32)	S(2)	114.0(5)
N(6)	C(33)	C(32)	112.4(6)
C(35)	C(34)	N(6)	115.8(6)
C(40)	C(35)	C(36)	117.2(8)
C(40)	C(35)	C(34)	122.2(8)
C(36)	C(35)	C(34)	120.6(7)
O(2)	C(36)	C(37)	122.8(7)
O(2)	C(36)	C(35)	115.1(7)
C(37)	C(36)	C(35)	122.1(7)
C(36)	C(37)	C(38)	117.9(8)
C(39)	C(38)	C(37)	121.0(9)
C(40)	C(39)	C(38)	119.3(8)
C(39)	C(40)	C(35)	122.6(8)
C(3)	N(1A)	C(2B)	138.0(11)
C(3)	N(1A)	Cu(1)	116.6(4)
C(2B)	N(1A)	Cu(1)	100.3(9)
C(9)	N(2)	C(10)	113.4(7)
C(9)	N(2)	Cu(1)	111.8(5)
C(10)	N(2)	Cu(1)	113.1(5)
C(13)	N(3)	C(14)	113.1(7)
C(13)	N(3)	Cu(1)	112.7(5)
C(14)	N(3)	Cu(1)	111.5(5)
C(23)	N(4)	C(22)	118.1(7)
C(23)	N(4)	Cu(2)	115.2(4)
C(22)	N(4)	Cu(2)	110.5(4)
C(30)	N(5)	C(29)	112.5(7)
C(30)	N(5)	Cu(2)	113.8(5)
C(29)	N(5)	Cu(2)	110.2(5)
C(33)	N(6)	C(34)	114.0(6)
C(33)	N(6)	Cu(2)	113.5(5)
C(34)	N(6)	Cu(2)	112.3(5)
C(16)	O(1)	C(2A)	130.2(8)
C(16)	O(1)	C(1B)	101.7(10)
C(16)	O(1)	Cu(1)	116.4(4)
C(2A)	O(1)	Cu(1)	105.4(6)
C(1B)	O(1)	Cu(1)	109.3(8)
C(36)	O(2)	C(21)	118.7(6)

C(36)	O(2)	Cu(2)	115.2(4)
C(21)	O(2)	Cu(2)	102.4(4)
C(11)	S(1)	C(12)	101.3(4)
C(11)	S(1)	Cu(1)	99.3(3)
C(12)	S(1)	Cu(1)	99.6(3)
C(32)	S(2)	C(31)	103.6(4)
C(32)	S(2)	Cu(2)	97.5(3)
C(31)	S(2)	Cu(2)	99.4(2)
N(2)	Cu(1)	N(3)	107.1(2)
N(2)	Cu(1)	O(1)	163.9(2)
N(3)	Cu(1)	O(1)	87.5(2)
N(2)	Cu(1)	Cl(1)	94.29(19)
N(3)	Cu(1)	Cl(1)	95.26(19)
O(1)	Cu(1)	Cl(1)	91.15(18)
N(2)	Cu(1)	N(1A)	88.3(2)
N(3)	Cu(1)	N(1A)	162.3(2)
O(1)	Cu(1)	N(1A)	76.3(2)
Cl(1)	Cu(1)	N(1A)	91.97(17)
N(2)	Cu(1)	S(1)	85.11(19)
N(3)	Cu(1)	S(1)	85.22(19)
O(1)	Cu(1)	S(1)	89.35(18)
Cl(1)	Cu(1)	S(1)	179.32(8)
N(1A)	Cu(1)	S(1)	87.70(17)
N(6)	Cu(2)	N(4)	162.4(3)
N(6)	Cu(2)	N(5)	107.8(3)
N(4)	Cu(2)	N(5)	89.8(2)
N(6)	Cu(2)	Cl(3A)	88.9(2)
N(4)	Cu(2)	Cl(3A)	89.55(18)
N(5)	Cu(2)	Cl(3A)	93.8(2)
N(6)	Cu(2)	S(2)	86.09(19)
N(4)	Cu(2)	S(2)	96.39(17)
N(5)	Cu(2)	S(2)	83.99(18)
Cl(3A)	Cu(2)	S(2)	173.64(10)
N(6)	Cu(2)	Cl(3B)	94.3(3)
N(4)	Cu(2)	Cl(3B)	79.4(3)
N(5)	Cu(2)	Cl(3B)	108.2(3)
Cl(3A)	Cu(2)	Cl(3B)	17.9(2)
S(2)	Cu(2)	Cl(3B)	166.9(3)
N(6)	Cu(2)	O(2)	86.2(2)
N(4)	Cu(2)	O(2)	76.8(2)
N(5)	Cu(2)	O(2)	160.4(2)
Cl(3A)	Cu(2)	O(2)	100.26(15)
S(2)	Cu(2)	O(2)	83.38(13)
Cl(3B)	Cu(2)	O(2)	83.6(3)

Symmetry Operators
(1) x, y, z (2) -x, y, -z+1/2 (3) x+1/2, y+1/2, z
(4) -x+1/2, y+1/2, -z+1/2 (5) -x, -y, -z (6) x, -y, z-1/2
(7) -x+1/2, -y+1/2, -z (8) x+1/2, -y+1/2, z-1/2

(iii) Cd(II)

Table B.28 Crystal data and a summary of data collection for $[Cd\mathbf{L}(NO_3)_2]\cdot CH_3OH$ (**L** = **138**).

Formula of the Refinement Model	$C_{21}H_{32}CdN_6O_8$
Model Molecular Weight	608.93
Crystal System	monoclinic
Space Group	$P2_1/c$(#14)
a	10.2458(9) Å
b	20.2082(17) Å
c	12.7539(11) Å
β	108.5180(10)º
V	2504.0(4) Å^3
D_c	1.615 g cm^{-3}
Z	4
Crystal Size	0.450x0.400x0.350 mm
Crystal Colour	colourless
Crystal Habit	block
Temperature	150(2) Kelvin
λ(MoKα)	0.71073 Å
μ(MoKα)	0.930 mm^{-1}
T(SADABS)$_{min,max}$	0.6505, 0.7457
$2\theta_{max}$	56.60º
hkl range	-13 13, -26 25, -16 16
N	24471
N_{ind}	6025(R_{merge} 0.0212)
N_{obs}	5449(I > 2σ(I))
N_{var}	339
Residuals* $R1(F)$, $wR2(F^2)$	0.0230, 0.0605
GoF(all)	1.025
Residual Extrema	-0.519, 1.233 e$^-$ Å^{-3}

*$R1 = \Sigma||F_o| - |F_c||/\Sigma|F_o|$ for $F_o > 2\sigma(F_o)$; $wR2 = (\Sigma w(F_o^2 - F_c^2)^2/\Sigma(wF_c^2)^2)^{1/2}$ all reflections

$w=1/[\sigma^2(F_o^2)+(0.0303P)^2+1.6677P]$ where $P=(F_o^2+2F_c^2)/3$

Table B.29 Non-hydrogen bond lengths (Å) for [Cd**L**$(NO_3)_2$]·CH_3OH (**L** = **138**).

---

atom	atom	Distance	atom	atom	Distance
C(1)	N(1)	1.475(2)	C(1)	C(2)	1.509(2)
C(2)	O(1)	1.4430(19)	C(3)	O(1)	1.3756(19)
C(3)	C(8)	1.391(2)	C(3)	C(4)	1.399(2)
C(4)	C(5)	1.387(2)	C(4)	C(9)	1.506(2)
C(5)	C(6)	1.390(3)	C(6)	C(7)	1.380(3)
C(7)	C(8)	1.392(3)	C(9)	N(2)	1.477(2)
C(10)	N(2)	1.475(2)	C(10)	C(11)	1.523(2)
C(11)	N(3)	1.471(2)	C(12)	N(3)	1.469(2)
C(12)	C(13)	1.510(3)	C(13)	N(4)	1.475(2)
C(14)	N(4)	1.479(2)	C(14)	C(15)	1.506(3)
C(15)	C(20)	1.396(2)	C(15)	C(16)	1.404(2)
C(16)	C(17)	1.390(2)	C(16)	N(1)	1.440(2)
C(17)	C(18)	1.394(3)	C(18)	C(19)	1.375(3)
C(19)	C(20)	1.385(3)	C(21)	O(8)	1.397(3)
N(1)	Cd(1)	2.3885(14)	N(2)	Cd(1)	2.3498(14)
N(3)	Cd(1)	2.3511(14)	N(4)	Cd(1)	2.4331(15)
N(5)	O(3)	1.2405(19)	N(5)	O(4)	1.253(2)
N(5)	O(2)	1.2609(18)	N(6)	O(6)	1.223(2)
N(6)	O(5)	1.248(2)	N(6)	O(7)	1.262(2)
O(2)	Cd(1)	2.5819(13)	O(5)	Cd(1)	2.4255(17)

Symmetry Operators

(1) x, y, z (2) -x, y+1/2, -z+1/2 (3) -x, -y, -z
(4) x, -y-1/2, z-1/2

Table B.30 Non-hydrogen bond angles (º) for [Cd**L**$(NO_3)_2$]·CH_3OH (**L** = **138**).

atom	atom	atom	angle
N(1)	C(1)	C(2)	109.63(13)
O(1)	C(2)	C(1)	105.96(13)
O(1)	C(3)	C(8)	123.54(16)
O(1)	C(3)	C(4)	115.38(14)
C(8)	C(3)	C(4)	121.07(15)
C(5)	C(4)	C(3)	118.47(16)
C(5)	C(4)	C(9)	120.82(16)
C(3)	C(4)	C(9)	120.70(14)
C(4)	C(5)	C(6)	121.20(18)
C(7)	C(6)	C(5)	119.42(17)
C(6)	C(7)	C(8)	120.89(17)
C(3)	C(8)	C(7)	118.92(17)
N(2)	C(9)	C(4)	110.78(13)
N(2)	C(10)	C(11)	109.44(13)
N(3)	C(11)	C(10)	110.34(13)
N(3)	C(12)	C(13)	108.95(14)
N(4)	C(13)	C(12)	111.21(14)
N(4)	C(14)	C(15)	111.02(14)
C(20)	C(15)	C(16)	118.60(17)
C(20)	C(15)	C(14)	121.05(16)
C(16)	C(15)	C(14)	120.30(15)
C(17)	C(16)	C(15)	120.03(16)
C(17)	C(16)	N(1)	122.28(15)
C(15)	C(16)	N(1)	117.62(15)
C(16)	C(17)	C(18)	119.85(18)
C(19)	C(18)	C(17)	120.74(18)
C(18)	C(19)	C(20)	119.41(17)
C(19)	C(20)	C(15)	121.35(18)
C(16)	N(1)	C(1)	116.92(13)
C(16)	N(1)	Cd(1)	106.40(10)
C(1)	N(1)	Cd(1)	113.70(10)
C(10)	N(2)	C(9)	111.73(13)
C(10)	N(2)	Cd(1)	106.61(9)
C(9)	N(2)	Cd(1)	118.65(10)
C(12)	N(3)	C(11)	113.66(13)
C(12)	N(3)	Cd(1)	109.19(10)
C(11)	N(3)	Cd(1)	110.21(10)
C(13)	N(4)	C(14)	111.63(14)
C(13)	N(4)	Cd(1)	108.88(10)
C(14)	N(4)	Cd(1)	115.97(10)
O(3)	N(5)	O(4)	120.19(14)
O(3)	N(5)	O(2)	120.85(14)

O(4)	N(5)	O(2)	118.96(15)
O(6)	N(6)	O(5)	121.94(18)
O(6)	N(6)	O(7)	120.75(17)
O(5)	N(6)	O(7)	117.30(17)
C(3)	O(1)	C(2)	117.58(12)
N(5)	O(2)	Cd(1)	123.35(10)
N(6)	O(5)	Cd(1)	109.83(13)
N(2)	Cd(1)	N(3)	75.47(5)
N(2)	Cd(1)	N(1)	140.04(5)
N(3)	Cd(1)	N(1)	131.71(5)
N(2)	Cd(1)	O(5)	102.42(5)
N(3)	Cd(1)	O(5)	130.10(5)
N(1)	Cd(1)	O(5)	81.67(5)
N(2)	Cd(1)	N(4)	140.66(5)
N(3)	Cd(1)	N(4)	73.82(5)
N(1)	Cd(1)	N(4)	79.30(5)
O(5)	Cd(1)	N(4)	79.79(5)
N(2)	Cd(1)	O(2)	77.16(4)
N(3)	Cd(1)	O(2)	87.50(4)
N(1)	Cd(1)	O(2)	76.00(4)
O(5)	Cd(1)	O(2)	141.62(4)
N(4)	Cd(1)	O(2)	124.91(5)

Symmetry Operators

(1) x, y, z (2) -x, y+1/2, -z+1/2 (3) -x, -y, -z
(4) x, -y-1/2, z-1/2

Table B.31 Crystal data and a summary of data collection for $[Cd\mathbf{L}(NO_3)](NO_3)\cdot CH_3CH_2OH$ (**L** = **132**).

Formula of the Refinement Model	$C_{42}H_{62}Cd_2N_{12}O_{13}S_2$
Model Molecular Weight	1232.00
Crystal System	triclinic
Space Group	$P\ \bar{1}$(#2)
a	10.1473(9) Å
b	16.4522(15) Å
c	16.789(1) Å
α	64.685(7)º
β	85.967(4)º
γ	88.050(6)º
V	2527.4(4) $Å^3$
D_c	1.619 g cm^{-3}
Z	2
Crystal Size	0.500x0.300x0.050 mm
Crystal Colour	colourless
Crystal Habit	shard
Temperature	150(2) Kelvin
λ(MoKα)	0.71073 Å
μ(MoKα)	0.997 mm^{-1}
T(TWINABS (SHELDRICK, 2007))$_{min,max}$	0.494, 0.951
$2\theta_{max}$	56.70º
hkl range	-11 13, -18 21, -22 19
N	11245
N_{obs}	6779(I > 2σ(I))
N_{var}	643
Residuals* *R*1(*F*), *wR*2(F^2)	0.0873, 0.2496
GoF(all)	1.035
Residual Extrema	-1.744, 3.257 e^- $Å^{-3}$

*$R1 = \Sigma||F_o| - |F_c||/\Sigma|F_o|$ for $F_o > 2\sigma(F_o)$; $wR2 = (\Sigma w(F_o^2 - F_c^2)^2/\Sigma(wF_c^2)^2)^{1/2}$ all reflections

$w=1/[\sigma^2(F_o^2)+(0.1383P)^2+0.0000P]$ where $P=(F_o^2+2F_c^2)/3$

Table B.32 Non-hydrogen bond lengths (Å) for [Cd**L**(NO_3)] (NO_3)·CH_3CH_2OH (**L** = **132**).

atom	atom	Distance	atom	atom	Distance
C(1)	C(2)	1.506(15)	C(1)	S(1)	1.836(12)
C(2)	N(1)	1.483(10)	C(3)	C(8)	1.378(14)
C(3)	C(4)	1.420(11)	C(3)	N(1)	1.450(12)
C(4)	C(5)	1.401(14)	C(4)	C(9)	1.506(13)
C(5)	C(6)	1.372(14)	C(6)	C(7)	1.368(14)
C(7)	C(8)	1.376(15)	C(9)	N(2)	1.469(13)
C(10)	N(2)	1.495(11)	C(10)	C(11)	1.511(14)
C(11)	N(3)	1.479(12)	C(12)	N(3)	1.471(13)
C(12)	C(13)	1.506(15)	C(13)	N(4)	1.502(12)
C(14)	N(4)	1.470(12)	C(14)	C(15)	1.535(13)
C(15)	C(16)	1.386(14)	C(15)	C(20)	1.414(14)
C(16)	C(17)	1.414(13)	C(16)	S(1)	1.786(9)
C(17)	C(18)	1.405(14)	C(18)	C(19)	1.398(16)
C(19)	C(20)	1.367(14)	C(21)	C(22)	1.526(15)
C(21)	S(2)	1.839(11)	C(22)	N(7)	1.473(11)
C(23)	C(28)	1.399(14)	C(23)	C(24)	1.412(13)
C(23)	N(7)	1.431(12)	C(24)	C(25)	1.396(14)
C(24)	C(29)	1.519(14)	C(25)	C(26)	1.385(14)
C(26)	C(27)	1.387(14)	C(27)	C(28)	1.390(14)
C(29)	N(8)	1.470(12)	C(30)	N(8)	1.496(12)
C(30)	C(31)	1.525(14)	C(31)	N(9)	1.510(12)
C(32)	N(9)	1.476(13)	C(32)	C(33)	1.523(15)
C(33)	N(10)	1.490(11)	C(34)	N(10)	1.484(12)
C(34)	C(35)	1.524(12)	C(35)	C(40)	1.352(15)
C(35)	C(36)	1.427(14)	C(36)	C(37)	1.406(14)
C(36)	S(2)	1.788(12)	C(37)	C(38)	1.384(16)
C(38)	C(39)	1.376(15)	C(39)	C(40)	1.422(14)
C(41)	O(13)	1.453(15)	C(41)	C(42)	1.511(19)
N(1)	Cd(1)	2.468(8)	N(2)	Cd(1)	2.358(7)
N(3)	Cd(1)	2.421(8)	N(4)	Cd(1)	2.449(8)
N(5)	O(3)	1.223(12)	N(5)	O(1)	1.252(11)
N(5)	O(2)	1.270(10)	N(6)	O(4)	1.216(11)
N(6)	O(6)	1.240(12)	N(6)	O(5)	1.266(12)
N(7)	Cd(2)	2.425(8)	N(8)	Cd(2)	2.389(7)
N(9)	Cd(2)	2.395(8)	N(10)	Cd(2)	2.404(8)
N(11)	O(9)	1.238(11)	N(11)	O(8)	1.261(10)
N(11)	O(7)	1.268(10)	N(12)	O(10)	1.235(12)
N(12)	O(11)	1.244(12)	N(12)	O(12)	1.264(12)
O(1)	Cd(1)	2.441(6)	O(2)	Cd(1)	2.526(7)
O(7)	Cd(2)	2.618(7)	O(8)	Cd(2)	2.400(7)
S(1)	Cd(1)	2.806(3)	S(2)	Cd(2)	2.891(2)

Symmetry Operators (1) x, y, z (2) -x, -y, -z

Table B.33 Non-hydrogen bond angles (º) for [Cd**L**(NO_3)] (NO_3)·CH_3CH_2OH (**L** = **132**).

atom	atom	atom	angle
C(2)	C(1)	S(1)	114.6(7)
N(1)	C(2)	C(1)	110.1(7)
C(8)	C(3)	C(4)	119.7(9)
C(8)	C(3)	N(1)	124.0(8)
C(4)	C(3)	N(1)	116.3(8)
C(5)	C(4)	C(3)	117.5(8)
C(5)	C(4)	C(9)	119.7(8)
C(3)	C(4)	C(9)	122.8(9)
C(6)	C(5)	C(4)	121.5(9)
C(7)	C(6)	C(5)	120.1(10)
C(6)	C(7)	C(8)	120.2(9)
C(7)	C(8)	C(3)	121.0(8)
N(2)	C(9)	C(4)	114.0(8)
N(2)	C(10)	C(11)	111.4(7)
N(3)	C(11)	C(10)	110.0(8)
N(3)	C(12)	C(13)	111.7(8)
N(4)	C(13)	C(12)	110.3(8)
N(4)	C(14)	C(15)	111.4(8)
C(16)	C(15)	C(20)	118.8(9)
C(16)	C(15)	C(14)	123.9(9)
C(20)	C(15)	C(14)	117.3(9)
C(15)	C(16)	C(17)	120.7(9)
C(15)	C(16)	S(1)	117.3(7)
C(17)	C(16)	S(1)	122.0(9)
C(18)	C(17)	C(16)	118.7(10)
C(19)	C(18)	C(17)	120.7(9)
C(20)	C(19)	C(18)	119.6(10)
C(19)	C(20)	C(15)	121.6(11)
C(22)	C(21)	S(2)	111.6(7)
N(7)	C(22)	C(21)	111.6(8)
C(28)	C(23)	C(24)	119.0(9)
C(28)	C(23)	N(7)	122.5(8)
C(24)	C(23)	N(7)	118.4(8)
C(25)	C(24)	C(23)	118.5(9)
C(25)	C(24)	C(29)	120.2(8)
C(23)	C(24)	C(29)	121.2(8)
C(26)	C(25)	C(24)	121.9(9)

C(25)	C(26)	C(27)	119.4(9)
C(26)	C(27)	C(28)	119.8(9)
C(27)	C(28)	C(23)	121.2(9)
N(8)	C(29)	C(24)	111.5(8)
N(8)	C(30)	C(31)	109.8(8)
N(9)	C(31)	C(30)	109.3(7)
N(9)	C(32)	C(33)	112.5(8)
N(10)	C(33)	C(32)	111.4(8)
N(10)	C(34)	C(35)	114.6(8)
C(40)	C(35)	C(36)	119.8(9)
C(40)	C(35)	C(34)	119.1(9)
C(36)	C(35)	C(34)	121.1(9)
C(37)	C(36)	C(35)	119.4(10)
C(37)	C(36)	S(2)	122.4(9)
C(35)	C(36)	S(2)	118.0(7)
C(38)	C(37)	C(36)	118.7(11)
C(39)	C(38)	C(37)	122.6(9)
C(38)	C(39)	C(40)	118.0(11)
C(35)	C(40)	C(39)	121.4(11)
O(13)	C(41)	C(42)	111.0(11)
C(3)	N(1)	C(2)	114.8(7)
C(3)	N(1)	Cd(1)	108.5(6)
C(2)	N(1)	Cd(1)	110.5(6)
C(9)	N(2)	C(10)	110.6(7)
C(9)	N(2)	Cd(1)	114.9(5)
C(10)	N(2)	Cd(1)	109.7(5)
C(12)	N(3)	C(11)	114.7(8)
C(12)	N(3)	Cd(1)	111.3(5)
C(11)	N(3)	Cd(1)	106.3(6)
C(14)	N(4)	C(13)	109.1(8)
C(14)	N(4)	Cd(1)	120.5(7)
C(13)	N(4)	Cd(1)	106.2(6)
O(3)	N(5)	O(1)	122.1(8)
O(3)	N(5)	O(2)	119.6(9)
O(1)	N(5)	O(2)	118.1(9)
O(4)	N(6)	O(6)	120.7(11)
O(4)	N(6)	O(5)	119.6(10)
O(6)	N(6)	O(5)	119.6(10)
C(23)	N(7)	C(22)	117.3(8)
C(23)	N(7)	Cd(2)	106.6(5)
C(22)	N(7)	Cd(2)	111.6(6)
C(29)	N(8)	C(30)	110.0(8)
C(29)	N(8)	Cd(2)	116.7(5)
C(30)	N(8)	Cd(2)	109.2(6)
C(32)	N(9)	C(31)	113.1(7)
C(32)	N(9)	Cd(2)	110.0(6)

C(31)	N(9)	Cd(2)	105.7(5)
C(34)	N(10)	C(33)	111.0(7)
C(34)	N(10)	Cd(2)	120.6(6)
C(33)	N(10)	Cd(2)	104.4(6)
O(9)	N(11)	O(8)	121.0(8)
O(9)	N(11)	O(7)	120.9(8)
O(8)	N(11)	O(7)	118.1(9)
O(10)	N(12)	O(11)	120.1(10)
O(10)	N(12)	O(12)	119.0(11)
O(11)	N(12)	O(12)	120.2(11)
N(5)	O(1)	Cd(1)	97.2(5)
N(5)	O(2)	Cd(1)	92.7(6)
N(11)	O(7)	Cd(2)	90.1(6)
N(11)	O(8)	Cd(2)	100.7(5)
C(16)	S(1)	C(1)	104.5(5)
C(16)	S(1)	Cd(1)	98.8(3)
C(1)	S(1)	Cd(1)	96.8(3)
C(36)	S(2)	C(21)	103.9(5)
C(36)	S(2)	Cd(2)	97.3(3)
C(21)	S(2)	Cd(2)	96.3(3)
N(2)	Cd(1)	N(3)	75.3(3)
N(2)	Cd(1)	O(1)	118.7(3)
N(3)	Cd(1)	O(1)	152.9(3)
N(2)	Cd(1)	N(4)	130.2(3)
N(3)	Cd(1)	N(4)	73.5(3)
O(1)	Cd(1)	N(4)	80.4(3)
N(2)	Cd(1)	N(1)	82.5(2)
N(3)	Cd(1)	N(1)	129.0(3)
O(1)	Cd(1)	N(1)	77.6(3)
N(4)	Cd(1)	N(1)	146.8(2)
N(2)	Cd(1)	O(2)	78.9(2)
N(3)	Cd(1)	O(2)	116.0(3)
O(1)	Cd(1)	O(2)	51.6(2)
N(4)	Cd(1)	O(2)	81.1(3)
N(1)	Cd(1)	O(2)	103.5(3)
N(2)	Cd(1)	S(1)	141.0(2)
N(3)	Cd(1)	S(1)	94.7(2)
O(1)	Cd(1)	S(1)	87.30(17)
N(4)	Cd(1)	S(1)	79.6(2)
N(1)	Cd(1)	S(1)	74.97(18)
O(2)	Cd(1)	S(1)	136.93(15)
N(8)	Cd(2)	N(9)	75.6(3)
N(8)	Cd(2)	O(8)	79.4(2)
N(9)	Cd(2)	O(8)	123.3(2)
N(8)	Cd(2)	N(10)	133.8(2)
N(9)	Cd(2)	N(10)	75.6(3)

O(8)	Cd(2)	N(10)	87.2(3)
N(8)	Cd(2)	N(7)	80.9(3)
N(9)	Cd(2)	N(7)	126.5(3)
O(8)	Cd(2)	N(7)	97.9(3)
N(10)	Cd(2)	N(7)	145.0(3)
N(8)	Cd(2)	O(7)	122.1(2)
N(9)	Cd(2)	O(7)	153.2(3)
O(8)	Cd(2)	O(7)	51.0(2)
N(10)	Cd(2)	O(7)	77.9(2)
N(7)	Cd(2)	O(7)	78.8(3)
N(8)	Cd(2)	S(2)	135.97(19)
N(9)	Cd(2)	S(2)	90.74(19)
O(8)	Cd(2)	S(2)	138.94(16)
N(10)	Cd(2)	S(2)	79.44(19)
N(7)	Cd(2)	S(2)	74.14(19)
O(7)	Cd(2)	S(2)	88.10(15)
Symmetry Operators	(1) x, y, z	(2) -x, -y, -z	

(iv) Ag(I)

Table B.34 Crystal data and a summary of data collection for [Ag**L**]PF_6 (**L** = **132**).

Formula of the Refinement Model	$C_{40}H_{56}Ag_2F_{12}N_8P_2S_2$
Model Molecular Weight	1218.73
Crystal System	monoclinic
Space Group	$P2_1/c$(#??)
a	26.2610(13) Å
b	9.0530(5) Å
c	22.2820(11) Å
β	115.043(2)º
V	4799.3(4) $Å^3$
D_C	1.687 g cm^{-3}
Z	4
Crystal Size	0.150x0.100x0.050 mm
Crystal Colour	yellow
Crystal Habit	shard
Temperature	150(2) Kelvin
λ(MoKα)	0.71073 Å
μ(MoKα)	1.056 mm^{-1}
$T(\text{SADABS})_{min,max}$	0.877, 0.949

$2\theta_{max}$	60.04º
hkl range	-36 36, -11 12, -31 30
N	56845
N_{ind}	13943(R_{merge} 0.0314)
N_{obs}	10849(I > 2σ(I))
N_{var}	619
Residuals* *R*1(*F*), *wR*2(F^2)	0.0328, 0.0777
GoF(all)	1.021
Residual Extrema	-0.743, 1.222 e^- $Å^{-3}$

*$R1 = \Sigma||F_o| - |F_c||/\Sigma|F_o|$ for $F_o > 2\sigma(F_o)$; $wR2 = (\Sigma w(F_o^2 - F_c^2)^2/\Sigma(wF_c^2)^2)^{1/2}$ all reflections

$w=1/[\sigma^2(F_o^2)+(0.0302P)^2+4.0210P]$ where $P=(F_o^2+2F_c^2)/3$

Table B.35 Non-hydrogen bond lengths (Å) for [Ag**L**]PF_6 (**L** = **132**).

---

atom	atom	Distance	atom	atom	Distance
C(1)	C(2)	1.522(3)	C(1)	S(1)	1.819(2)
C(2)	N(1)	1.470(3)	C(3)	C(8)	1.390(3)
C(3)	C(4)	1.412(3)	C(3)	N(1)	1.427(3)
C(4)	C(5)	1.397(3)	C(4)	C(9)	1.509(3)
C(5)	C(6)	1.388(3)	C(6)	C(7)	1.384(3)
C(7)	C(8)	1.399(3)	C(9)	N(2)	1.476(3)
C(10)	N(2)	1.480(3)	C(10)	C(11)	1.516(3)
C(11)	N(3)	1.472(3)	C(12)	N(3)	1.472(3)
C(12)	C(13)	1.527(3)	C(13)	N(4)	1.478(3)
C(14)	N(4)	1.479(3)	C(14)	C(15)	1.515(3)
C(15)	C(20)	1.398(3)	C(15)	C(16)	1.407(3)
C(16)	C(17)	1.402(3)	C(16)	S(1)	1.790(2)
C(17)	C(18)	1.391(3)	C(18)	C(19)	1.384(3)
C(19)	C(20)	1.385(3)	C(21)	C(22)	1.532(3)
C(21)	S(2)	1.812(2)	C(22)	N(5)	1.469(3)
C(23)	C(28)	1.395(3)	C(23)	C(24)	1.410(3)
C(23)	N(5)	1.451(3)	C(24)	C(25)	1.404(3)
C(24)	C(29)	1.505(3)	C(25)	C(26)	1.384(4)
C(26)	C(27)	1.386(4)	C(27)	C(28)	1.391(3)
C(29)	N(6)	1.481(3)	C(30)	N(6)	1.482(3)

C(30)	C(31)	1.517(4)	C(31)	N(7)	1.471(4)
C(32)	N(7)	1.467(4)	C(32)	C(33)	1.515(4)
C(33)	N(8)	1.484(3)	C(34)	N(8)	1.470(3)
C(34)	C(35)	1.511(3)	C(35)	C(40)	1.399(3)
C(35)	C(36)	1.408(3)	C(36)	C(37)	1.401(3)
C(36)	S(2)	1.790(2)	C(37)	C(38)	1.381(4)
C(38)	C(39)	1.391(4)	C(39)	C(40)	1.382(4)
N(1)	Ag(1)	2.6096(19)	N(2)	Ag(1)	2.3625(18)
N(3)	Ag(1)	2.5162(19)	N(4)	Ag(1)	2.3722(18)
N(5)	Ag(2)	2.5328(19)	N(6)	Ag(2)	2.391(2)
N(7)	Ag(2)	2.478(2)	N(8)	Ag(2)	2.357(2)
F(1)	P(1)	1.5873(16)	F(2)	P(1)	1.5995(16)
F(3)	P(1)	1.6033(16)	F(4)	P(1)	1.6006(16)
F(5)	P(1)	1.6055(16)	F(6)	P(1)	1.6014(15)
F(7)	P(2)	1.5856(16)	F(8)	P(2)	1.5955(17)
F(9)	P(2)	1.6114(16)	F(10)	P(2)	1.6039(16)
F(11)	P(2)	1.5905(19)	F(12)	P(2)	1.5873(18)
S(1)	Ag(1)	2.7044(6)	S(2)	Ag(2)	2.7717(6)

Symmetry Operators

(1) x, y, z (2) -x, y+1/2, -z+1/2 (3) -x, -y, -z
(4) x, -y-1/2, z-1/2

Table B.36 Non-hydrogen bond angles (º) for [Ag**L**]PF_6 (**L** = **132**).

atom	atom	atom	angle
C(2)	C(1)	S(1)	114.83(15)
N(1)	C(2)	C(1)	110.20(17)
C(8)	C(3)	C(4)	119.7(2)
C(8)	C(3)	N(1)	121.97(19)
C(4)	C(3)	N(1)	118.30(19)
C(5)	C(4)	C(3)	118.8(2)
C(5)	C(4)	C(9)	119.24(19)
C(3)	C(4)	C(9)	121.89(19)
C(6)	C(5)	C(4)	121.7(2)
C(7)	C(6)	C(5)	118.9(2)
C(6)	C(7)	C(8)	120.9(2)
C(3)	C(8)	C(7)	120.1(2)
N(2)	C(9)	C(4)	111.00(16)
N(2)	C(10)	C(11)	109.97(18)
N(3)	C(11)	C(10)	111.2(2)
N(3)	C(12)	C(13)	112.33(18)

N(4)	C(13)	C(12)	112.59(18)
N(4)	C(14)	C(15)	109.15(17)
C(20)	C(15)	C(16)	118.37(18)
C(20)	C(15)	C(14)	118.30(18)
C(16)	C(15)	C(14)	123.21(18)
C(17)	C(16)	C(15)	120.01(18)
C(17)	C(16)	S(1)	122.30(16)
C(15)	C(16)	S(1)	117.62(15)
C(18)	C(17)	C(16)	119.94(19)
C(19)	C(18)	C(17)	120.5(2)
C(18)	C(19)	C(20)	119.5(2)
C(19)	C(20)	C(15)	121.7(2)
C(22)	C(21)	S(2)	114.16(15)
N(5)	C(22)	C(21)	109.11(19)
C(28)	C(23)	C(24)	119.8(2)
C(28)	C(23)	N(5)	121.9(2)
C(24)	C(23)	N(5)	118.3(2)
C(25)	C(24)	C(23)	118.3(2)
C(25)	C(24)	C(29)	119.3(2)
C(23)	C(24)	C(29)	122.3(2)
C(26)	C(25)	C(24)	121.5(2)
C(25)	C(26)	C(27)	119.7(2)
C(26)	C(27)	C(28)	120.1(2)
C(27)	C(28)	C(23)	120.5(2)
N(6)	C(29)	C(24)	110.45(19)
N(6)	C(30)	C(31)	109.7(2)
N(7)	C(31)	C(30)	110.9(2)
N(7)	C(32)	C(33)	113.1(2)
N(8)	C(33)	C(32)	112.6(2)
N(8)	C(34)	C(35)	110.54(19)
C(40)	C(35)	C(36)	118.9(2)
C(40)	C(35)	C(34)	118.5(2)
C(36)	C(35)	C(34)	122.6(2)
C(37)	C(36)	C(35)	119.4(2)
C(37)	C(36)	S(2)	122.89(18)
C(35)	C(36)	S(2)	117.66(18)
C(38)	C(37)	C(36)	120.4(2)
C(37)	C(38)	C(39)	120.5(2)
C(40)	C(39)	C(38)	119.4(2)
C(39)	C(40)	C(35)	121.3(2)
C(3)	N(1)	C(2)	117.51(18)
C(3)	N(1)	Ag(1)	108.03(12)
C(2)	N(1)	Ag(1)	110.33(12)
C(9)	N(2)	C(10)	111.99(17)
C(9)	N(2)	Ag(1)	114.74(13)
C(10)	N(2)	Ag(1)	107.34(13)

C(11)	N(3)	C(12)	114.8(2)
C(11)	N(3)	Ag(1)	102.80(13)
C(12)	N(3)	Ag(1)	108.13(13)
C(13)	N(4)	C(14)	113.91(17)
C(13)	N(4)	Ag(1)	107.30(13)
C(14)	N(4)	Ag(1)	108.72(12)
C(23)	N(5)	C(22)	116.91(18)
C(23)	N(5)	Ag(2)	109.28(13)
C(22)	N(5)	Ag(2)	109.74(13)
C(29)	N(6)	C(30)	112.1(2)
C(29)	N(6)	Ag(2)	114.21(15)
C(30)	N(6)	Ag(2)	107.26(17)
C(32)	N(7)	C(31)	114.6(2)
C(32)	N(7)	Ag(2)	107.05(16)
C(31)	N(7)	Ag(2)	103.77(16)
C(34)	N(8)	C(33)	113.0(2)
C(34)	N(8)	Ag(2)	110.36(13)
C(33)	N(8)	Ag(2)	106.21(16)
F(1)	P(1)	F(2)	179.12(11)
F(1)	P(1)	F(4)	91.06(11)
F(2)	P(1)	F(4)	89.81(11)
F(1)	P(1)	F(6)	90.45(8)
F(2)	P(1)	F(6)	89.49(9)
F(4)	P(1)	F(6)	89.64(9)
F(1)	P(1)	F(3)	90.21(10)
F(2)	P(1)	F(3)	88.91(10)
F(4)	P(1)	F(3)	178.70(11)
F(6)	P(1)	F(3)	90.07(9)
F(1)	P(1)	F(5)	89.93(9)
F(2)	P(1)	F(5)	90.14(9)
F(4)	P(1)	F(5)	90.51(10)
F(6)	P(1)	F(5)	179.59(9)
F(3)	P(1)	F(5)	89.77(9)
F(7)	P(2)	F(12)	90.27(11)
F(7)	P(2)	F(11)	90.11(12)
F(12)	P(2)	F(11)	179.58(11)
F(7)	P(2)	F(8)	179.76(14)
F(12)	P(2)	F(8)	89.51(11)
F(11)	P(2)	F(8)	90.11(12)
F(7)	P(2)	F(10)	90.66(9)
F(12)	P(2)	F(10)	89.06(9)
F(11)	P(2)	F(10)	90.75(10)
F(8)	P(2)	F(10)	89.42(10)
F(7)	P(2)	F(9)	89.15(9)
F(12)	P(2)	F(9)	89.72(10)

F(11)	P(2)	F(9)	90.46(10)
F(8)	P(2)	F(9)	90.76(10)
F(10)	P(2)	F(9)	178.77(10)
C(16)	S(1)	C(1)	104.44(10)
C(16)	S(1)	Ag(1)	97.17(7)
C(1)	S(1)	Ag(1)	101.26(7)
C(36)	S(2)	C(21)	103.42(11)
C(36)	S(2)	Ag(2)	97.95(8)
C(21)	S(2)	Ag(2)	98.11(8)
N(2)	Ag(1)	N(4)	125.53(6)
N(2)	Ag(1)	N(3)	75.52(6)
N(4)	Ag(1)	N(3)	74.39(6)
N(2)	Ag(1)	N(1)	81.30(6)
N(4)	Ag(1)	N(1)	141.27(6)
N(3)	Ag(1)	N(1)	144.11(6)
N(2)	Ag(1)	S(1)	145.65(5)
N(4)	Ag(1)	S(1)	88.07(5)
N(3)	Ag(1)	S(1)	112.07(5)
N(1)	Ag(1)	S(1)	74.08(4)
N(8)	Ag(2)	N(6)	126.54(7)
N(8)	Ag(2)	N(7)	75.80(8)
N(6)	Ag(2)	N(7)	75.34(8)
N(8)	Ag(2)	N(5)	140.28(7)
N(6)	Ag(2)	N(5)	81.85(7)
N(7)	Ag(2)	N(5)	143.44(7)
N(8)	Ag(2)	S(2)	86.64(5)
N(6)	Ag(2)	S(2)	145.80(6)
N(7)	Ag(2)	S(2)	110.23(6)
N(5)	Ag(2)	S(2)	74.64(4)

Symmetry Operators

(1) x, y, z (2) -x, y+1/2, -z+1/2 (3) -x, -y, -z
(4) x, -y-1/2, z-1/2

Table B.37 Crystal data and a summary of data collection for [Ag**L**]PF_6 (**L** = **141**).

Formula of the Refinement Model	$C_{20}H_{27}AgF_6N_3OPS$
Model Molecular Weight	610.35
Crystal System	monoclinic
Space Group	$P2_1/n$(#14)
a	13.8017(16) Å
b	9.4378(11) Å
c	17.114(2) Å
β	90.106(7)º
V	2229.2(4) $Å^3$
D_c	1.819 g cm^{-3}
Z	4
Crystal Size	0.270x0.250x0.080 mm
Crystal Colour	colourless
Crystal Habit	plate
Temperature	150(2) Kelvin
λ(MoKα)	0.71073 Å
μ(MoKα)	1.139 mm^{-1}
T(SADABS)$_{min,max}$	0.788, 0.913
$2\theta_{max}$	60.00º
hkl range	-18 19, -13 13, -23 23
N	23629
N_{ind}	6424(R_{merge} 0.0397)
N_{obs}	5089(I > 2σ(I))
N_{var}	248
Residuals* $R1(F)$, $wR2(F^2)$	0.0378, 0.0978
GoF(all)	1.039
Residual Extrema	-0.756, 1.424 e^- $Å^{-3}$

*$R1 = \Sigma||F_o| - |F_c||/\Sigma|F_o|$ for $F_o > 2\sigma(F_o)$; $wR2 = (\Sigma w(F_o^2 - F_c^2)^2/\Sigma(wF_c^2)^2)^{1/2}$ all reflections

$w=1/[\sigma^2(F_o^2)+(0.0445P)^2+2.1962P]$ where $P=(F_o^2+2F_c^2)/3$

Table B.38 Non-hydrogen bond lengths (Å) for [Ag**L**]PF_6 (**L** = **141**).

atom	atom		Distance	atom	atom		Distance
C(1A)	C(2A)		1.479(15)	C(1A)	O(1A)		1.660(12)
C(2A)	N(1A)		1.435(10)	C(2B)	N(1B)		1.37(3)
C(2B)	C(1B)		1.57(5)	C(1B)	O(1B)		1.62(3)
C(3B)	C(4B)		1.3900	C(3B)	C(8B)		1.3900
C(3B)	N(1B)		1.5012(10)	C(4B)	C(5B)		1.3900
C(4B)	C(9B)		1.5012(10)	C(5B)	C(6B)		1.3900
C(6B)	C(7B)		1.3900	C(7B)	C(8B)		1.3900
C(8A)	C(7A)		1.3900	C(8A)	C(3A)		1.3900
C(7A)	C(6A)		1.3900	C(6A)	C(5A)		1.3900
C(5A)	C(4A)		1.3900	C(4A)	C(3A)		1.3900
C(4A)	C(9A)		1.421(10)	C(3A)	N(1A)		1.511(5)
C(9A)	N(2A)		1.384(12)	C(9B)	N(2B)		1.50(3)
C(10A)	C(11A)		1.447(12)	C(10A)	N(2A)		1.502(10)
C(10B)	N(2B)		1.52(3)	C(11A)	S(1)		1.799(8)
C(12A)	C(13A)		1.510(11)	C(12A)	S(1)		1.848(8)
C(13A)	N(3A)		1.439(11)	C(13B)	N(3B)		1.50(3)
C(14A)	C(15A)		1.368(9)	C(14A)	N(3A)		1.629(9)
C(15B)	C(16B)		1.3900	C(15B)	C(20B)		1.3900
C(16B)	C(17B)		1.3900	C(16B)	O(1B)		1.526(5)
C(17B)	C(18B)		1.3900	C(18B)	C(19B)		1.3900
C(19B)	C(20B)		1.3900	C(16A)	O(1A)		1.3133
C(16A)	C(17A)		1.3900	C(16A)	C(15A)		1.3900
C(17A)	C(18A)		1.3900	C(18A)	C(19A)		1.3900
C(19A)	C(20A)		1.3900	C(20A)	C(15A)		1.3900
N(1A)	Ag(1)		2.848(3)	N(1B)	Ag(1)		2.726(2)
N(2A)	Ag(1)		2.391(4)	N(2B)	Ag(1)		2.331(3)
N(3A)	Ag(1)		2.340(4)	N(3B)	Ag(1)		2.308(4)
O(1A)	Ag(1)		2.851(3)	O(1B)	Ag(1)		2.739(2)
F(1A)	P(1)		1.618(5)	F(2A)	P(1)		1.636(9)
F(3A)	P(1)		1.604(6)	F(4A)	P(1)		1.610(9)
F(5A)	P(1)		1.600(6)	F(6A)	P(1)		1.642(5)
F(1B)	F(2B)		1.39(3)	F(1B)	P(1)		1.48(2)
F(2B)	P(1)		1.39(3)	F(2B)	F(5B)		1.67(4)
F(3B)	F(4B)		1.48(4)	F(3B)	P(1)		1.59(3)
F(4B)	P(1)		1.48(3)	F(5B)	P(1)		1.57(3)
F(6B)	P(1)		1.43(3)	S(1)	Ag(1)	2	2.6294(7)
Ag(1)	S(1)	2_545	2.6294(7)				

Symmetry Operators

(1) x, y, z (2) -x+1/2, y+1/2, -z+1/2 (3) -x, -y, -z
(4) x-1/2, -y-1/2, z-1/2

Table B.39 Non-hydrogen bond angles (º) for [Ag**L**]PF_6 (**L** = **141**).

atom	atom	atom	angle
C(2A)	C(1A)	O(1A)	109.0(8)
N(1A)	C(2A)	C(1A)	100.8(8)
N(1B)	C(2B)	C(1B)	118(2)
C(2B)	C(1B)	O(1B)	83(2)
C(4B)	C(3B)	C(8B)	120.0
C(4B)	C(3B)	N(1B)	119.4(13)
C(8B)	C(3B)	N(1B)	120.5(13)
C(5B)	C(4B)	C(3B)	120.0
C(5B)	C(4B)	C(9B)	132.5(16)
C(3B)	C(4B)	C(9B)	106.9(16)
C(4B)	C(5B)	C(6B)	120.0
C(7B)	C(6B)	C(5B)	120.0
C(6B)	C(7B)	C(8B)	120.0
C(7B)	C(8B)	C(3B)	120.0
C(7A)	C(8A)	C(3A)	120.0
C(8A)	C(7A)	C(6A)	120.0
C(5A)	C(6A)	C(7A)	120.0
C(6A)	C(5A)	C(4A)	120.0
C(5A)	C(4A)	C(3A)	120.0
C(5A)	C(4A)	C(9A)	107.3(5)
C(3A)	C(4A)	C(9A)	132.4(5)
C(4A)	C(3A)	C(8A)	120.0
C(4A)	C(3A)	N(1A)	111.5(4)
C(8A)	C(3A)	N(1A)	128.5(4)
N(2A)	C(9A)	C(4A)	115.2(8)
N(2B)	C(9B)	C(4B)	122(2)
C(11A)	C(10A)	N(2A)	113.7(7)
C(10A)	C(11A)	S(1)	122.0(6)
C(13A)	C(12A)	S(1)	117.2(6)
N(3A)	C(13A)	C(12A)	111.9(7)
C(15A)	C(14A)	N(3A)	101.7(7)
C(16B)	C(15B)	C(20B)	120.0
C(17B)	C(16B)	C(15B)	120.0
C(17B)	C(16B)	O(1B)	122.6(3)
C(15B)	C(16B)	O(1B)	117.4(3)
C(16B)	C(17B)	C(18B)	120.0
C(19B)	C(18B)	C(17B)	120.0
C(18B)	C(19B)	C(20B)	120.0
C(19B)	C(20B)	C(15B)	120.0
O(1A)	C(16A)	C(17A)	124.9
O(1A)	C(16A)	C(15A)	114.4
C(17A)	C(16A)	C(15A)	120.0
C(16A)	C(17A)	C(18A)	120.0

C(19A)	C(18A)	C(17A)	120.0
C(20A)	C(19A)	C(18A)	120.0
C(19A)	C(20A)	C(15A)	120.0
C(14A)	C(15A)	C(20A)	113.8(5)
C(14A)	C(15A)	C(16A)	126.2(4)
C(20A)	C(15A)	C(16A)	120.0
C(2A)	N(1A)	C(3A)	108.8(5)
C(2A)	N(1A)	Ag(1)	106.7(4)
C(3A)	N(1A)	Ag(1)	98.2(3)
C(2B)	N(1B)	C(3B)	118.6(17)
C(2B)	N(1B)	Ag(1)	118.3(14)
C(3B)	N(1B)	Ag(1)	93.1(9)
C(9A)	N(2A)	C(10A)	116.1(6)
C(9A)	N(2A)	Ag(1)	113.1(4)
C(10A)	N(2A)	Ag(1)	109.9(4)
C(9B)	N(2B)	C(10B)	112.2(14)
C(9B)	N(2B)	Ag(1)	109.0(9)
C(10B)	N(2B)	Ag(1)	110.3(10)
C(13A)	N(3A)	C(14A)	105.0(5)
C(13A)	N(3A)	Ag(1)	112.6(5)
C(14A)	N(3A)	Ag(1)	107.4(3)
C(13B)	N(3B)	Ag(1)	113.9(9)
C(16A)	O(1A)	C(1A)	145.2(5)
C(16A)	O(1A)	Ag(1)	102.61(7)
C(1A)	O(1A)	Ag(1)	105.9(5)
C(16B)	O(1B)	C(1B)	85.9(12)
C(16B)	O(1B)	Ag(1)	95.9(2)
C(1B)	O(1B)	Ag(1)	109.1(13)
F(2B)	F(1B)	P(1)	58.0(16)
F(1B)	F(2B)	P(1)	64.4(14)
F(1B)	F(2B)	F(5B)	80.3(19)
P(1)	F(2B)	F(5B)	61.0(17)
F(4B)	F(3B)	P(1)	57.6(15)
P(1)	F(4B)	F(3B)	64.9(18)
P(1)	F(5B)	F(2B)	50.8(11)
F(2B)	P(1)	F(6B)	86.9(16)
F(2B)	P(1)	F(4B)	173(2)
F(6B)	P(1)	F(4B)	100(2)
F(2B)	P(1)	F(1B)	57.6(16)
F(6B)	P(1)	F(1B)	96.3(17)
F(4B)	P(1)	F(1B)	121.4(15)
F(2B)	P(1)	F(5B)	68.2(16)
F(6B)	P(1)	F(5B)	152.3(15)
F(4B)	P(1)	F(5B)	104.8(19)
F(1B)	P(1)	F(5B)	80.9(12)
F(2B)	P(1)	F(3B)	123.4(19)

F(6B)		P(1)	F(3B)		85.0(19)
F(4B)		P(1)	F(3B)		57.5(18)
F(1B)		P(1)	F(3B)		178(2)
F(5B)		P(1)	F(3B)		98.3(13)
F(5A)		P(1)	F(3A)		88.1(4)
F(5A)		P(1)	F(4A)		86.0(6)
F(3A)		P(1)	F(4A)		98.3(6)
F(5A)		P(1)	F(1A)		91.9(3)
F(3A)		P(1)	F(1A)		177.8(6)
F(4A)		P(1)	F(1A)		79.5(5)
F(5A)		P(1)	F(2A)		97.4(6)
F(3A)		P(1)	F(2A)		82.2(7)
F(4A)		P(1)	F(2A)		176.6(5)
F(1A)		P(1)	F(2A)		100.0(6)
F(4B)		P(1)	F(6A)		87.7(17)
F(1B)		P(1)	F(6A)		96.3(10)
F(5B)		P(1)	F(6A)		166.8(12)
F(3B)		P(1)	F(6A)		84.7(12)
F(5A)		P(1)	F(6A)		172.5(7)
F(3A)		P(1)	F(6A)		92.3(4)
F(4A)		P(1)	F(6A)		86.5(6)
F(1A)		P(1)	F(6A)		87.4(4)
F(2A)		P(1)	F(6A)		90.1(6)
C(11A)		S(1)	C(12A)		103.27(16)
C(11A)		S(1)	Ag(1)	2	95.5(2)
C(12A)		S(1)	Ag(1)	2	94.2(3)
N(3B)		Ag(1)	N(2B)		97.49(8)
N(3B)		Ag(1)	N(3A)		20.6
N(2B)		Ag(1)	N(3A)		111.93(9)
N(3B)		Ag(1)	N(2A)		111.32(8)
N(2B)		Ag(1)	N(2A)		19.4
N(3A)		Ag(1)	N(2A)		120.92(8)
N(3B)		Ag(1)	S(1)	2_545	130.10(12)
N(2B)		Ag(1)	S(1)	2_545	130.24(14)
N(3A)		Ag(1)	S(1)	2_545	111.45(11)
N(2A)		Ag(1)	S(1)	2_545	112.56(14)
N(3B)		Ag(1)	N(1B)		113.66(9)
N(2B)		Ag(1)	N(1B)		74.27(9)
N(3A)		Ag(1)	N(1B)		130.42(11)
N(2A)		Ag(1)	N(1B)		81.79(10)
S(1)	2_545	Ag(1)	N(1B)		95.07(8)
N(3B)		Ag(1)	O(1B)		74.24(9)
N(2B)		Ag(1)	O(1B)		114.81(8)
N(3A)		Ag(1)	O(1B)		82.08(11)
N(2A)		Ag(1)	O(1B)		130.49(10)
S(1)	2_545	Ag(1)	O(1B)		94.15(7)

N(1B)		Ag(1)	O(1B)	53.9
N(3B)		Ag(1)	O(1A)	76.53(10)
N(2B)		Ag(1)	O(1A)	124.81(8)
N(3A)		Ag(1)	O(1A)	80.80(11)
N(2A)		Ag(1)	O(1A)	139.51(10)
S(1)	2_545	Ag(1)	O(1A)	85.16(8)
N(1B)		Ag(1)	O(1A)	59.9
O(1B)		Ag(1)	O(1A)	10.3
N(3B)		Ag(1)	N(1A)	122.85(8)
N(2B)		Ag(1)	N(1A)	76.58(9)
N(3A)		Ag(1)	N(1A)	138.59(11)
N(2A)		Ag(1)	N(1A)	80.99(11)
S(1)	2_545	Ag(1)	N(1A)	86.64(8)
N(1B)		Ag(1)	N(1A)	9.5
O(1B)		Ag(1)	N(1A)	59.0
O(1A)		Ag(1)	N(1A)	63.3

Symmetry Operators

(1) x, y, z (2) -x+1/2, y+1/2, -z+1/2 (3) -x, -y, -z
(4) x-1/2, -y-1/2, z-1/2

Table B.40 Crystal data and a summary of data collection for [Ag**L**]PF_6·MeCN (L = **164**).

Formula of the Refinement Model	$C_{36}H_{41}AgF_6N_3PS_3$
Model Molecular Weight	864.74
Crystal System	Monoclinic
Space Group	$P2_1/c$(#14)
a	9.1249(14) Å
b	24.720(4) Å
c	16.670(3) Å
β	101.913(3)º
V	3679.3(10) $Å^3$
D_C	1.561 g cm^{-3}
Z	4
Crystal Size	0.348x0.158x0.120 mm
Crystal Colour	colourless

Crystal Habit	prism
Temperature	150(2) Kelvin
λ(MoKα)	0.71073 Å
μ(MoKα)	0.823 mm^{-1}
T(SADABS)$_{min,max}$	0.777, 0.906
$2\theta_{max}$	56.64°
hkl range	-12 12, -32 32, -22 21
N	36352
N_{ind}	8880(R_{merge} 0.0501)
N_{obs}	6610(I > 2σ(I))
N_{var}	452
Residuals* $R1(F)$, $wR2(F^2)$	0.0383, 0.0894
GoF(all)	1.016
Residual Extrema	-0.314, 0.608 e^- $Å^{-3}$

*$R1 = \Sigma||F_o| - |F_c||/\Sigma|F_o|$ for $F_o > 2\sigma(F_o)$; $wR2 = (\Sigma w(F_o^2 - F_c^2)^2/\Sigma(wF_c^2)^2)^{1/2}$ all reflections

$w=1/[\sigma^2(F_o^2)+(0.0406P)^2+1.5802P]$ where $P=(F_o^2+2F_c^2)/3$

Table B.41 Non-hydrogen bond lengths (Å) for [Ag**L**]PF_6·MeCN (L = **164**).

atom	atom	Distance	atom	atom	Distance
C(1)	C(2)	1.525(4)	C(1)	S(1)	1.808(3)
C(2)	N(1)	1.485(3)	C(3)	N(1)	1.500(3)
C(3)	C(4)	1.515(4)	C(4)	C(5)	1.394(4)
C(4)	C(9)	1.407(4)	C(5)	C(6)	1.385(4)
C(6)	C(7)	1.378(4)	C(7)	C(8)	1.389(4)
C(8)	C(9)	1.396(4)	C(9)	S(2)	1.777(3)
C(10)	C(11)	1.521(4)	C(10)	S(2)	1.815(3)
C(11)	S(3)	1.811(3)	C(12)	C(13)	1.388(4)
C(12)	C(17)	1.402(4)	C(12)	S(3)	1.786(3)
C(13)	C(14)	1.388(4)	C(14)	C(15)	1.375(4)
C(15)	C(16)	1.387(4)	C(16)	C(17)	1.394(4)
C(17)	C(18)	1.504(4)	C(18)	N(2)	1.486(3)
C(19)	N(2)	1.477(3)	C(19)	C(20)	1.530(4)
C(20)	S(1)	1.814(3)	C(21)	N(1)	1.493(3)

C(21)	C(22)	1.505(4)	C(22)	C(27)	1.386(4)
C(22)	C(23)	1.399(4)	C(23)	C(24)	1.382(5)
C(24)	C(25)	1.378(5)	C(25)	C(26)	1.383(5)
C(26)	C(27)	1.378(4)	C(28)	N(2)	1.486(3)
C(28)	C(29)	1.507(4)	C(29)	C(30)	1.389(4)
C(29)	C(34)	1.394(4)	C(30)	C(31)	1.387(4)
C(31)	C(32)	1.376(5)	C(32)	C(33)	1.379(4)
C(33)	C(34)	1.386(4)	C(35)	C(36)	1.436(6)
C(36)	N(3)	1.134(5)	N(1)	Ag(1)	2.387(2)
N(2)	Ag(1)	2.617(2)	F(1)	P(1)	1.562(2)
F(2)	P(1)	1.585(2)	F(3)	P(1)	1.582(2)
F(4)	P(1)	1.605(2)	F(5)	P(1)	1.592(2)
F(6)	P(1)	1.581(2)	S(1)	Ag(1)	2.5938(8)
S(2)	Ag(1)	2.8307(9)	S(3)	Ag(1)	2.5097(8)

Symmetry Operators

(1) x, y, z (2) -x, y+1/2, -z+1/2 (3) -x, -y, -z
(4) x, -y-1/2, z-1/2

Table B.42 Non-hydrogen bond angles (º) for [Ag**L**]PF_6·MeCN (L = **164**).

atom	atom	atom	angle
C(2)	C(1)	S(1)	115.9(2)
N(1)	C(2)	C(1)	115.9(2)
N(1)	C(3)	C(4)	113.3(2)
C(5)	C(4)	C(9)	118.2(2)
C(5)	C(4)	C(3)	118.9(2)
C(9)	C(4)	C(3)	122.9(2)
C(6)	C(5)	C(4)	121.4(3)
C(7)	C(6)	C(5)	120.2(3)
C(6)	C(7)	C(8)	119.7(3)
C(7)	C(8)	C(9)	120.5(3)
C(8)	C(9)	C(4)	120.0(2)
C(8)	C(9)	S(2)	121.2(2)
C(4)	C(9)	S(2)	118.7(2)
C(11)	C(10)	S(2)	117.18(19)
C(10)	C(11)	S(3)	117.95(19)

C(13)	C(12)	C(17)	120.8(2)
C(13)	C(12)	S(3)	122.2(2)
C(17)	C(12)	S(3)	116.9(2)
C(12)	C(13)	C(14)	120.2(3)
C(15)	C(14)	C(13)	119.9(3)
C(14)	C(15)	C(16)	119.8(3)
C(15)	C(16)	C(17)	121.7(3)
C(16)	C(17)	C(12)	117.5(3)
C(16)	C(17)	C(18)	119.2(3)
C(12)	C(17)	C(18)	123.2(2)
N(2)	C(18)	C(17)	114.9(2)
N(2)	C(19)	C(20)	113.1(2)
C(19)	C(20)	S(1)	110.83(19)
N(1)	C(21)	C(22)	114.9(2)
C(27)	C(22)	C(23)	118.1(3)
C(27)	C(22)	C(21)	122.2(3)
C(23)	C(22)	C(21)	119.6(3)
C(24)	C(23)	C(22)	120.7(3)
C(25)	C(24)	C(23)	120.1(3)
C(24)	C(25)	C(26)	120.1(3)
C(27)	C(26)	C(25)	119.7(3)
C(26)	C(27)	C(22)	121.4(3)
N(2)	C(28)	C(29)	116.1(2)
C(30)	C(29)	C(34)	118.3(3)
C(30)	C(29)	C(28)	120.9(3)
C(34)	C(29)	C(28)	120.7(3)
C(31)	C(30)	C(29)	120.8(3)
C(32)	C(31)	C(30)	120.0(3)
C(31)	C(32)	C(33)	120.2(3)
C(32)	C(33)	C(34)	119.8(3)
C(33)	C(34)	C(29)	120.9(3)
N(3)	C(36)	C(35)	179.1(5)
C(2)	N(1)	C(21)	107.5(2)
C(2)	N(1)	C(3)	109.9(2)
C(21)	N(1)	C(3)	109.9(2)
C(2)	N(1)	Ag(1)	103.59(15)
C(21)	N(1)	Ag(1)	114.25(17)
C(3)	N(1)	Ag(1)	111.40(15)
C(19)	N(2)	C(18)	111.3(2)
C(19)	N(2)	C(28)	112.5(2)
C(18)	N(2)	C(28)	109.9(2)
C(19)	N(2)	Ag(1)	107.05(15)
C(18)	N(2)	Ag(1)	110.65(15)
C(28)	N(2)	Ag(1)	105.28(15)
F(1)	P(1)	F(6)	90.20(14)
F(1)	P(1)	F(3)	91.54(16)

F(6)	P(1)	F(3)	89.57(12)
F(1)	P(1)	F(2)	178.55(15)
F(6)	P(1)	F(2)	90.83(13)
F(3)	P(1)	F(2)	89.49(14)
F(1)	P(1)	F(5)	89.89(15)
F(6)	P(1)	F(5)	91.62(12)
F(3)	P(1)	F(5)	178.14(14)
F(2)	P(1)	F(5)	89.06(14)
F(1)	P(1)	F(4)	89.83(14)
F(6)	P(1)	F(4)	179.62(12)
F(3)	P(1)	F(4)	90.05(12)
F(2)	P(1)	F(4)	89.14(13)
F(5)	P(1)	F(4)	88.76(11)
C(1)	S(1)	C(20)	103.83(13)
C(1)	S(1)	Ag(1)	96.58(9)
C(20)	S(1)	Ag(1)	99.96(9)
C(9)	S(2)	C(10)	105.20(13)
C(9)	S(2)	Ag(1)	95.64(9)
C(10)	S(2)	Ag(1)	96.93(9)
C(12)	S(3)	C(11)	105.14(13)
C(12)	S(3)	Ag(1)	102.23(9)
C(11)	S(3)	Ag(1)	103.98(9)
N(1)	Ag(1)	S(3)	141.78(5)
N(1)	Ag(1)	S(1)	82.22(6)
S(3)	Ag(1)	S(1)	134.39(2)
N(1)	Ag(1)	N(2)	122.22(7)
S(3)	Ag(1)	N(2)	83.23(5)
S(1)	Ag(1)	N(2)	77.20(5)
N(1)	Ag(1)	S(2)	86.15(5)
S(3)	Ag(1)	S(2)	83.17(2)
S(1)	Ag(1)	S(2)	91.02(2)
N(2)	Ag(1)	S(2)	146.53(5)

Symmetry Operators

(1) x, y, z (2) -x, y+1/2, -z+1/2 (3) -x, -y, -z

(4) x, -y-1/2, z-1/2

Table B.43 Crystal data and a summary of data collection for (**L**H_2)$(NO_3)_2$ (**L** = **137**).

Formula of the Refinement Model	$C_{20}H_{28.90}N_5O_6S_2Zn_{0.05}$
Model Molecular Weight	502.77
Crystal System	Triclinic
Space Group	$P\ \bar{1}$(#??)
a	8.3360(7) Å
b	11.2220(9) Å
c	13.4650(11) Å
α	92.0670(10)º
β	103.4500(10)º
γ	107.6510(10)º
V	1159.64(16) $Å^3$
D_c	1.440 g cm^{-3}
Z	2
Crystal Size	0.219x0.149x0.140 mm
Crystal Colour	yellow
Crystal Habit	shard
Temperature	150(2) Kelvin
λ(MoKα)	0.71073 Å
μ(MoKα)	0.327 mm^{-1}
$T(\text{SADABS})_{min,max}$	0.874, 0.962
$2\theta_{max}$	56.66º
hkl range	-10 10, -14 14, -17 17
N	11558
N_{ind}	5402(R_{merge} 0.0247)
N_{obs}	4444(I > 2σ(I))
N_{var}	310
Residuals* *R*1(*F*), *wR*2(F^2)	0.0439, 0.1165
GoF(all)	1.039
Residual Extrema	-0.422, 0.546 e^- $Å^{-3}$

*$R1 = \Sigma||F_o| - |F_c||/\Sigma|F_o|$ for $F_o > 2\sigma(F_o)$; $wR2 = (\Sigma w(F_o^2 - F_c^2)^2/\Sigma(wF_c^2)^2)^{1/2}$ all reflections

$w=1/[\sigma^2(F_o^2)+(0.0522P)^2+0.8900P]$ where $P=(F_o^2+2F_c^2)/3$

Table B.44 Non-hydrogen bond lengths (Å) for (**L**H_2)$(NO_3)_2$ (**L** = **137**).

atom	atom	Distance	atom	atom	Distance
C(1)	C(2)	1.533(3)	C(1)	S(1)	1.802(2)
C(2)	N(1)	1.454(3)	C(3)	C(4)	1.402(3)
C(3)	N(1)	1.409(3)	C(3)	C(8)	1.409(3)
C(4)	C(5)	1.391(3)	C(5)	C(6)	1.379(3)
C(6)	C(7)	1.389(3)	C(7)	C(8)	1.391(3)
C(8)	C(9)	1.512(3)	C(9)	N(2)	1.513(2)
C(10)	N(2)	1.493(2)	C(10)	C(11)	1.522(3)
C(11)	S(2)	1.8092(19)	C(12)	C(13)	1.520(3)
C(12)	S(2)	1.8181(19)	C(13)	N(3)	1.497(2)
C(14)	C(15)	1.503(3)	C(14)	N(3)	1.505(2)
C(15)	C(20)	1.393(3)	C(15)	C(16)	1.407(3)
C(16)	C(17)	1.400(3)	C(16)	S(1)	1.7687(19)
C(17)	C(18)	1.389(3)	C(18)	C(19)	1.377(3)
C(19)	C(20)	1.385(3)	N(4)	O(2)	1.235(2)
N(4)	O(1)	1.245(2)	N(4)	O(3)	1.263(2)
N(5)	O(5)	1.248(2)	N(5)	O(6)	1.251(2)
N(5)	O(4)	1.252(2)			

Symmetry Operators

(1) x, y, z (2) -x, -y, -z

Table B.45 Non-hydrogen bond angles (º) for (**L**H_2)$(NO_3)_2$ (**L** = **137**).

atom	atom	atom	angle
C(2)	C(1)	S(1)	109.05(15)
N(1)	C(2)	C(1)	109.86(18)
C(4)	C(3)	N(1)	122.53(18)
C(4)	C(3)	C(8)	118.33(18)
N(1)	C(3)	C(8)	119.13(18)
C(5)	C(4)	C(3)	121.0(2)
C(6)	C(5)	C(4)	120.6(2)
C(5)	C(6)	C(7)	118.81(19)
C(6)	C(7)	C(8)	121.86(19)
C(7)	C(8)	C(3)	119.35(18)
C(7)	C(8)	C(9)	118.25(18)

C(3)	C(8)	C(9)	122.39(17)
C(8)	C(9)	N(2)	111.93(15)
N(2)	C(10)	C(11)	111.68(15)
C(10)	C(11)	S(2)	110.75(13)
C(13)	C(12)	S(2)	112.90(14)
N(3)	C(13)	C(12)	113.71(15)
C(15)	C(14)	N(3)	109.33(15)
C(20)	C(15)	C(16)	119.49(18)
C(20)	C(15)	C(14)	118.89(18)
C(16)	C(15)	C(14)	121.60(17)
C(17)	C(16)	C(15)	118.87(18)
C(17)	C(16)	S(1)	124.54(16)
C(15)	C(16)	S(1)	116.56(14)
C(18)	C(17)	C(16)	120.07(19)
C(19)	C(18)	C(17)	121.09(19)
C(18)	C(19)	C(20)	119.17(19)
C(19)	C(20)	C(15)	121.13(19)
C(3)	N(1)	C(2)	118.65(18)
C(10)	N(2)	C(9)	114.14(14)
C(13)	N(3)	C(14)	116.35(14)
O(2)	N(4)	O(1)	120.90(17)
O(2)	N(4)	O(3)	120.65(16)
O(1)	N(4)	O(3)	118.44(16)
O(5)	N(5)	O(6)	119.90(18)
O(5)	N(5)	O(4)	119.90(19)
O(6)	N(5)	O(4)	120.19(18)
C(16)	S(1)	C(1)	102.67(10)
C(11)	S(2)	C(12)	98.53(9)

Symmetry Operators (1) x, y, z (2) -x, -y, -z

Appendix C

Modeling stability constants

Appendix C.1 Internal consistency check data

In the following tables, experimental data which is deemed imprecise is denoted by an asterisk (*), while the absence of experimental values for at least one of the metal complex pairs is indicated by a dash (-).

Table 4.2 $\log K_{\text{M-NNN}} - \log K_{\text{M-NON}}$

	100 - 101	**112 - 114**	**127 - 128**	**93 -94**	**138 - 142**	**132 - 136**	Average
Co(II)	*	-	*	-	5.1	-	*
Ni(II)	*	*	*	-	-	-	-
Cu(II)	7.7	*	7.8	*	6.3	5.4	6.8
Zn(II)	*	-	*	4.1	5.0	3.8	4.3
Cd(II)	3.4	3.4	3.2	2.1	2.5	2.5	2.85
Ag(I)	1.6	*	1.4	0.5	0.7	1.0	1.04
Pb(II)	2.6	*	3.3	2.7	3.1	3.3	3.0

Table 4.3 $\log K_{\text{M-NNN}} - \log K_{\text{M-NSN}}$

	100 - 102	**112 - 113**	**127 - 129**	**93 - 95**	**138 - 141**	**132 - 137**	Average
Co(II)	*	-	*	-	3.0	-	-
Ni(II)	4.5	-	-	-	-	-	-
Cu(II)	6.8	*	6.5	*	-	-	6.65
Zn(II)	*	*	*	3.0	3.2	3.8	3.33
Cd(II)	4.3	-	*	2.9	4.5	3.1	3.70
Ag(I)	0.1	*	-0.4	-0.5	-0.1	-0.7	-0.32
Pb(II)	3.6	*	*	3.5	4.2	3.8	3.78

Table 4.4 $\log K_{\text{M-NON}} - \log K_{\text{M-NSN}}$

	101 - 102	**114 - 113**	**128 - 129**	**94 -95**	**136 - 137**	**142 - 141**	Average
Co(II)	*	*	*	-	-1.8	-2.1	-1.95
Ni(II)	*	-	-	-	-1.7	-1.7	-1.7
Cu(II)	-0.9	-1.2	-1.3	0.0	-2.7	-1.9	-1.33
Zn(II)	*	-	*	-1.1	0.0	-1.8	-0.97
Cd(II)	0.9	-	*	0.8	0.6	2.0	1.08
Ag(I)	-1.5	-2.1	-1.8	*	-1.7	-0.8	-1.58
Pb(II)	1.0	*	*	0.8	0.5	1.1	0.85

Table 4.5 $2(\log K_{M\text{-}O} - \log K_{M\text{-}S})$

	100 - 112	**101 - 114**	**102 - 113**	Average
Co(II)	-	*	*	-
Ni(II)	0.5	*	-	-
Cu(II)	*	-0.4	-0.7	-0.55
Zn(II)	1.2	-	*	-
Cd(II)	0.9	0.9	-	0.90
Ag(I)	*	-3.2	-3.8	-3.5
Pb(II)	0.1	*	*	-

Table 4.6 $\log K_{M\text{-}O} - \log K_{M\text{-}S}$

	100 - 127	**101 - 128**	**102 - 129**	**127 - 112**	**128 - 114**	**129 - 113**	**138 - 132**	**141 - 137**	**142 - 136**	Av.
Co(II)	0.5	*	*	-	*	*	-	0.8	0.5	0.6
Ni(II)	*	*	-	*	*	-	-	-0.6	-0.6	-0.6
Cu(II)	0.3	0.4	0.0	*	-0.8	-0.7	*	-1.2	-0.4	-0.34
Zn(II)	0.5	*	*	0.7	-	*	1.8	1.8	0.6	1.08
Cd(II)	0.6	0.4	*	0.3	0.5	-	1.3	-0.1	1.3	0.61
Ag(I)	-2.1	-2.2	-2.5	*	-1.0	-1.3	-1.7	-2.3	-1.4	-1.81
Pb(II)	0.3	1.0	*	-0.2	*	*	0.3	-0.1	0.5	0.30

Table 4.7 $2(\log K_{M\text{-}O} - \log K_{M\text{-}N})$

	100 - 93	**101 -94**	**102 -95**	Average
Co(II)	-	-3.5	-	-
Ni(II)	-	-	-	-
Cu(II)	*	-8.0	-7.1	-7.55
Zn(II)	-4.4	*	*	-
Cd(II)	-3.4	-4.7	-4.8	-4.30
Ag(I)	-1.6	-2.7	-2.2	-2.17
Pb(II)	-1.3	-1.2	-1.4	-1.30

Table 4.8 $\log K_{M\text{-}O} - \log K_{M\text{-}N}$

	100 - 138	**138 - 93**	**127 - 132**	**141 - 95**	**142 - 94**	**Average**
Co(II)	-1.5	-	-	-	-2.9	-2.2
Ni(II)	-	-	-	-	-	-
Cu(II)	*	*	*	-3.3	-5.2	-4.25

Zn(II)	-2.3	-2.1	-1.0	-2.3	-3.0	-2.14
Cd(II)	-2.2	-1.2	-1.5	-2.8	-1.6	-1.86
Ag(I)	-1.1	-0.5	-0.8	-0.9	-0.7	-0.8
Pb(II)	-0.7	-0.6	-0.7	-1.3	-1.0	-0.86

Table 4.9 $2(\log K_{\text{M-S}} - \log K_{\text{M-N}})$

	112 – 93	**114 -94**	**113 -95**	**Average**
Co(II)	-	*	-	-
Ni(II)	-	-	-	-
Cu(II)	*	-7.6	-6.4	-7.0
Zn(II)	-5.6	-	*	-
Cd(II)	-4.3	-5.6	-	-4.95
Ag(I)	*	0.5	1.6	1.05
Pb(II)	-1.4	*	*	-

Table 4.10 $\log K_{\text{M-S}} - \log K_{\text{M-N}}$

	112 – 132	**132 - 93**	**127 - 138**	**136 - 94**	**113 - 137**	**Average**
Co(II)	-	-	-2.0	-3.4	*	-2.7
Ni(II)	-	-	-	-	-	-
Cu(II)	*	*	*	-4.8	-4.3	-4.55
Zn(II)	-1.7	-3.9	-2.8	-3.6	-0.9	-2.58
Cd(II)	-1.8	-2.5	-2.8	-2.9	-	-2.5
Ag(I)	*	1.2	1.0	0.7	0.2	0.78
Pb(II)	-0.5	-0.9	-1.0	-1.5	*	-0.98

Table 4.11 $\log K_{\text{M-O}} - \log K_{\text{M-S}} + 2\log K_{\text{M-N}}$

	128 -94	**129 -95**	**127 - 93**	**Average**
Co(II)	*	-	-	-
Ni(II)	-	-	-	-
Cu(II)	-8.4	-7.1	*	-7.75
Zn(II)	*	*	-4.9	-
Cd(II)	-5.1	*	-4.0	-4.55
Ag(I)	-0.5	0.3	0.5	0.1
Pb(II)	-2.2	*	-1.6	-1.9

Table 4.12 $\log K_{M\text{-}N} - \log K_{M\text{-}S} + 2\log K_{M\text{-}O}$

	132 - 100	**137 - 102**	**136 - 101**	**Average**
Co(II)	-	*	*	-
Ni(II)	-	2.3	*	-
Cu(II)	*	5.0	3.2	4.1
Zn(II)	0.5	*	*	-
Cd(II)	0.9	2.1	1.8	1.6
Ag(I)	2.8	3.6	3.4	3.27
Pb(II)	0.4	0.2	-0.3	0.1

Table 4.13 $\log K_{M\text{-}O} - \log K_{M\text{-}N} + 2\log K_{M\text{-}S}$

	138 - 112	**141 - 113**	**142 - 114**	**Average**
Co(II)	-	*	*	-
Ni(II)	-	-	*	-
Cu(II)	*	3.1	2.4	2.75
Zn(II)	3.5	*	-	-
Cd(II)	3.1	-	4.0	3.55
Ag(I)	*	-2.5	-1.2	-1.85
Pb(II)	-0.8	*	*	-

Appendix C.2

Calculated log *K*, observed log *K* and their differences

*Data from ligands excluded (see text) from the construction of the linear equations. Donor group contributions are shown at the beginning of each set of calculations for individual metals.

```
==================================================
==================================================
Co(II)

Donor group contributions

 -O-        -0.04
 -S-        -0.61
 -N-         2.12
-NNN-        7.57
-NON-        2.29
-NSN-        4.01


  Ligand       Calc          Obs           Diff
  OO/NNN       7.49          7.70          0.21
  OO/NON *     2.21          3.50          1.29
  OO/NSN *     3.93          3.30         -0.63
  SS/NNN *     6.35
  SS/NON *     1.07          3.50          2.43
  SS/NSN *     2.79          3.50          0.71
  OS/NON *     1.64          3.50          1.86
  OS/NSN *     3.36          3.50          0.14
  NN/NNN *    11.81
  NN/NON       6.53          7.00          0.47
  NN/NSN       8.25
  NO/NNN       9.65          9.18         -0.47
  OS/NNN       6.92          7.20          0.28
  NS/NNN       9.08
  SN/NSN       5.52          5.40         -0.12
  SN/NON       3.80          3.64         -0.16
  ON/NSN       6.09          6.20          0.11
  ON/NON       4.37          4.06         -0.31


==================================================
==================================================
Ni(II)

Donor group contributions

 -O-         0.35
 -S-         0.39
 -N-         2.31
-NNN-        9.01
```

-NON- 3.16
-NSN- 4.80

Ligand		Calc	Obs	Diff
OO/NNN		9.71	10.00	0.29
OO/NON	*	3.86	3.50	-0.36
OO/NSN		5.50	5.50	0.00
SS/NNN		9.79	9.50	-0.29
SS/NON	*	3.94	3.40	-0.54
SS/NSN	*	5.58		
OS/NON	*	3.90	3.50	-0.40
OS/NSN	*	5.54		
NN/NNN	*	13.63		
NN/NON	*	7.78		
NN/NSN	*	9.42		
NO/NNN	*	11.67		
OS/NNN	*	9.75	9.50	-0.25
NS/NNN	*	11.71		
SN/NSN		7.50	7.80	0.30
SN/NON		5.86	6.13	0.27
ON/NSN		7.46	7.15	-0.31
ON/NON		5.82	5.54	-0.28

==========
==========
Cu(II)

Donor group contributions

-O- 0.04
-S- 0.37
-N- 3.89
-NNN- 13.80
-NON- 5.96
-NSN- 7.29

Ligand		Calc	Obs	Diff
OO/NNN		13.88	14.20	0.32
OO/NON		6.04	6.50	0.46
OO/NSN		7.37	7.40	0.03
SS/NNN	*	14.54	15.60	1.06
SS/NON		6.70	6.90	0.20
SS/NSN		8.03	8.10	0.07
OS/NON		6.37	6.10	-0.27
OS/NSN		7.70	7.40	-0.30
NN/NNN	*	21.58	16.30	-5.28
NN/NON		13.74	14.50	0.76
NN/NSN		15.07	14.50	-0.57
NO/NNN	*	17.73	15.60	-2.13
OS/NNN		14.21	13.90	-0.31
NS/NNN	*	18.06	15.10	-2.96
SN/NSN		11.55	12.40	0.85
SN/NON		10.22	9.70	-0.52

ON/NSN	11.22	11.16	-0.06
ON/NON	9.89	9.26	-0.63

==========
==========
Zn(II)

Donor group contributions

-O-	-0.16
-S-	-0.98
-N-	2.13
-NNN-	7.89
-NON-	3.08
-NSN-	4.30

Ligand		Calc	Obs	Diff
OO/NNN		7.57	7.50	-0.07
OO/NON	*	2.76	3.50	0.74
OO/NSN	*	3.98	3.50	-0.48
SS/NNN		5.93	6.30	0.37
SS/NON		1.12		
SS/NSN	*	2.34	3.30	0.96
OS/NON	*	1.94	4.00	2.06
OS/NSN	*	3.16	4.00	0.84
NN/NNN		12.15	11.90	-0.25
NN/NON		7.34	7.80	0.46
NN/NSN		8.56	8.90	0.34
NO/NNN		9.86	9.80	-0.06
OS/NNN		6.75	7.00	0.25
NS/NNN		9.04	8.80	-0.24
SN/NSN		5.45	4.80	-0.65
SN/NON		4.23	4.16	-0.07
ON/NSN		6.27	6.59	0.32
ON/NON		5.05	4.66	-0.39

==========
==========
Cd(II)

Donor group contributions

-O-	0.22
-S-	-0.30
-N-	2.34
-NNN-	8.03
-NON-	5.18
-NSN-	4.20

Ligand	Calc	Obs	Diff
OO/NNN	8.47	8.70	0.23
OO/NON	5.62	5.30	-0.32
OO/NSN	4.64	4.40	-0.24
SS/NNN	7.43	7.80	0.37
SS/NON	4.58	4.40	-0.18
SS/NSN	3.60		
OS/NON	5.10	4.90	-0.20
OS/NSN *	4.12	4.00	-0.12
NN/NNN	12.71	12.10	-0.61
NN/NON	9.86	10.00	0.14
NN/NSN	8.88	9.20	0.32
NO/NNN	10.59	10.90	0.31
OS/NNN	7.95	8.10	0.15
NS/NNN	10.07	9.60	-0.47
SN/NSN	6.24	6.49	0.25
SN/NON	7.22	7.11	-0.11
ON/NSN	6.76	6.42	-0.34
ON/NON	7.74	8.40	0.66

==========
==========
Ag(I)

Donor group contributions

-O-	1.04
-S-	2.79
-N-	2.11
-NNN-	6.57
-NON-	5.38
-NSN-	6.88

Ligand	Calc	Obs	Diff
OO/NNN	8.65	8.70	0.05
OO/NON	7.46	7.10	-0.36
OO/NSN	8.96	8.60	-0.36
SS/NNN *	12.15	11.70	-0.45
SS/NON	10.96	10.30	-0.66
SS/NSN	12.46	12.40	-0.06
OS/NON	9.21	9.30	0.09
OS/NSN	10.71	11.10	0.39
NN/NNN	10.79	10.30	-0.49
NN/NON	9.60	9.80	0.20
NN/NSN	11.10	10.80	-0.30
NO/NNN	9.72	9.80	0.08
OS/NNN	10.40	10.75	0.35
NS/NNN	11.47	11.50	0.03
SN/NSN	11.78	12.21	0.43
SN/NON	10.28	10.45	0.17
ON/NSN	10.03	9.94	-0.09

ON/NON	8.53	9.11	0.58

==========
==========

Pb(II)

Donor group contributions

-O-	0.69
-S-	0.40
-N-	1.34
-NNN-	6.81
-NON-	3.74
-NSN-	2.95

Ligand	Calc	Obs	Diff
OO/NNN	8.19	8.10	-0.09
OO/NON	5.12	5.50	0.38
OO/NSN	4.33	4.50	0.17
SS/NNN	7.61	8.00	0.39
SS/NON *	4.54	3.00	-1.54
SS/NSN *	3.75	3.00	-0.75
OS/NON	4.83	4.50	-0.33
OS/NSN *	4.04	3.80	-0.24
NN/NNN	9.49	9.40	-0.09
NN/NON	6.42	6.70	0.28
NN/NSN	5.63	5.90	0.27
NO/NNN	8.84	8.80	-0.04
OS/NNN	7.90	7.80	-0.10
NS/NNN	8.55	8.50	-0.05
SN/NSN	4.69	4.66	-0.03
SN/NON	5.48	5.23	-0.25
ON/NSN	4.98	4.57	-0.41
ON/NON	5.77	5.67	-0.10

Appendix D

List of publications

Publications:

Synthesis and X-ray Structures of potentially pentadentate ligands incorporating non-symmetrically arranged N_4S-, N_3OS-, N_2O_2S- and N_2S_2O-heteroatoms
D. S. Baldwin, B. F. Bowden, P. A. Duckworth, L. F. Lindoy, B. J. McCool, G. V. Meehan, I. M. Vasilescu and S. B. Wild, *Aust. J. Chem.*, 2002, 597, "New Macrocyclic Ligands. XIV*

Metal ion recognition. Modelling the stability constants of some mixed-donor macrocyclic metal ion complexes-a simple model
K. R. Adam, D. S. Baldwin, L. F. Lindoy, G. V. Meehan, I. M. Vasilescu and G. Wei, *Inorg. Chim. Acta*, 2003, 352.

Rational ligand design for metal ion recognition. Synthesis of a N-benzylated N_2S_3-donor macrocycle for enhanced silver(I) discrimination
Ioana M. Vasilescu, David J. Bray, Jack K. Clegg, Leonard F. Lindoy, George V. Meehan and GangWei, *Dalton Trans.*, 2006**,** 5115–5117

Leonard F. Lindoy, George V. Meehan, Ioana M. Vasilescu, Hyun Jee Kim, Ji-Eun Lee, Shim Sung Lee, *Coord. Chem. Rev.*, 2009, in press.
doi:10.1016/j.ccr.2009.11.012